

Exotic pentaquark states and Chromomagnetic interaction

Hong-Tao An^{1,2,*}, Kan Chen^{1,2,3,4,†} and Xiang Liu^{1,2‡}

¹*School of Physical Science and Technology, Lanzhou University, Lanzhou 730000, China*

²*Research Center for Hadron and CSR Physics, Lanzhou University
and Institute of Modern Physics of CAS, Lanzhou 730000, China*

³*Center of High Energy Physics, Peking University, Beijing 100871, China*

⁴*School of Physics and State Key Laboratory of Nuclear Physics and Technology, Peking University, Beijing 100871, China*

(Dated: October 13, 2020)

In the framework of the modified chromo-magnetic interaction model, we perform a systematical study on the mass spectrums of the ground pentaquark states with $qqq\bar{Q}$, $qq\bar{Q}\bar{q}$, $QQQ\bar{Q}\bar{q}$, $QQ\bar{Q}\bar{Q}$, and $QQ\bar{Q}q\bar{Q}$, ($Q = c, b; q = n, s; n = u, d$) configurations. The isospin-color-spin wave functions satisfying Pauli principle for each type of ground pentaquark states are constructed. With the help of experimental data, we estimate their possible mass spectrums in two different schemes. Based on our results, we present a detailed analysis on the mass spectrums and decay behaviors for the discussed pentquark states. We hope that our study will be helpful to experimentally search for such types of the exotic pentaquark states in the future.

I. INTRODUCTION

The existence of the $qq\bar{q}\bar{q}$ tetraquarks and $qqqq\bar{q}$ pentaquarks are proposed by Gell-Mann and Zweig [1–3] at the birth of quark model in 1964. But until 2003, the evidence of exotic state $X(3872)$ was firstly reported by the Belle Collaboration [4–6]. After that, many exotic XYZ states were observed in experiment [7–19]. Among them, the charged charmonium-like or bottomonium-like states, the $Z(4430)$ [20–23], the $Z_c(4200)$ [22], the $Z_1(4050)$ [24], the $Z_2(4250)$ [24], the $Z_c(3900)$ [25–28], the $Z_c(3885)$ [29–31], the $Z_c(4020)$ [32, 33], the $Z_c(4025)$ [34, 35], the $Z_c(4032)$ [36], the $Z_b(10610)$ [37], and the $Z_b(10650)$ [37], are possible tetraquark candidates, they are also candidates for hidden flavor molecular states.

In 2003, another important observation is that BaBar Collaboration reported a narrow state $D_s(2317)$ decaying to $D_s^+\pi^0$ final states [38]. Later, CLEO collaboration [39] confirm the $D_s(2317)$ and observed another narrow resonance $D_s(2460)$ in $D_s^{*+}\pi^0$ final states. The masses of $D_s(2317)$ and $D_s(2460)$ deviate from quark model expectations [40] and their decay behaviors are unlike the conventional charmed mesons. Later, SELEX Collaboration reported a charm-strange meson $D_{sJ}^+(2632)$ [41]. However, $D_{sJ}^+(2632)$ was not confirmed later. Very recently, LHCb collaboration reported the discovery of two new exotic structures $X_0(2900)$ and $X_1(2900)$ [42, 43], this observation reignite the study of exotic charmed mesons [44–54].

In 2017, based on the prediction of Ref. [56], the LHCb Collaboration reported the observation of Ξ_{cc}^{++} in the $\Lambda_c^+K^-\pi^+\pi^+$ decay mode and its mass was determined to be $3621.40 \pm 0.72(\text{stat.}) \pm 0.27(\text{syst.}) \pm 0.14(\Lambda_c)$ MeV [57]. This observation motivates theorists to further study the

possible stable tetraquark state with $QQ\bar{q}\bar{q}$ configuration [59–63].

We are constantly reminded by the discovery of experiment that the present observed exotic tetraquark candidates might be just the tip of the iceberg. Very recently, the LHCb announced that they found a narrow structure at around 6.9 GeV with a global significance of more than 5σ , this state is considered as a possible candidate of fully-charm $QQ\bar{Q}\bar{Q}$ tetraquark state [64]. If such state exists, the tetraquarks with three heavy quarks may also exist. To our knowledge, the tetraquark states with $QQ\bar{Q}\bar{Q}$ configuration is only studied in the frame work of chromo-magnetic interaction model [65]. From the lesson of tetraquark states, we learn that systematical researches on different tetraquark systems are crucial to find them and to clarify their nature.

The story of pentaquarks can also trace back to 2003. The original observation is made by the LEPS group [66]. They found a narrow resonance signal at 1540 MeV with $S = +1$, called $\Theta^+(1540)$, whose quark component is $uudd\bar{s}$. Although further experimental reexamination did not confirm this state, it triggered a lot of theoretical and experimental works on pentaquark systems [67, 68]. In 2015, the LHCb Collaboration measured the $\Lambda_b^0 \rightarrow J/\psi K^-p$ decay process and observed two hidden-charm pentaquark-like resonances $P_c(4380)$ and $P_c(4450)$ in the $J/\psi p$ channel, which indicates that they have a minimal quark content of $uud\bar{c}\bar{c}$ [69, 70]. In 2019, the LHCb Collaboration announced the observation of three narrow peaks in the $J/\psi p$ invariant mass spectrum in the $\Lambda_b \rightarrow J/\psi K^-p$ decay process [71]. They found that the $P_c(4450)$ is actually composed of two substructures, $P_c(4440)$ and $P_c(4457)$ with 5.4σ significance. Moreover, they also reported a new state below the $\Sigma_c\bar{D}$ threshold, namely the $P_c(4312)$ with 7.3σ significance. The spin-parity of these three pentaquark states are consistent with the previous predictions of molecular states [72–74]. Along with the step of studying tetraquarks, we have reason to believe that these three molecular pentaquarks are just the beginning of pentaquark study.

* anht14@lzu.edu.cn

† chenk_10@pku.edu.cn

‡ xiangliu@lzu.edu.cn

With the development of experiment, more states possessing pentaquark-like structure would be observed in the near future. This stimulate us to further study different types of pentaquark states.

As a preliminary research to pentaquark systems, we adopt the Chromomagnetic Interaction (CMI) model to study the mass spectrums of pentaquarks. This model has been widely adopted to study the mass spectrums of multiquark systems [59, 65, 75–89]. In the CMI model, the masses of the ground state hadrons consist of the effective quark masses and the chromomagnetic interaction terms. The CMI model provide us a simple framework to handle multiquark problems. Despite its simple Hamiltonian, this model can catch the basic features of hadron spectrums, since the mass splittings between hadrons reflect the basic symmetries of their inner structures [90]. However, in such simply model, the effective mass term is not sufficient to describe the two-body color-electric effects for both meson and baryon systems simultaneously. Thus, Karliner et al. added a color-singlet binding energy term to compensate the color-electric effects for different hadron systems [91, 92]. In this work, we will also adopt this modification and mainly discuss the pentaquark mass spectrums obtained from this scheme. Besides, for comparison, we will also present the results obtained from the conventional CMI model.

From the lessons of tetraquark states, we have reason to believe that the heavy pentaquark systems with at least one constituent heavy quark are possible to exist. As presented in Ref. [93], before this work, we have systematically studied the $\bar{Q}Qqqq$ [75], $QQqq\bar{q}$ [76], $QQQq\bar{q}$ [77], and $\bar{Q}QQQq$ [78] pentaquark systems. Thus, in this work, we will study the rest of pentaquark systems including the $qqqq\bar{Q}$, $qqqQ\bar{q}$, $QQQQ\bar{q}$, $QQQQ\bar{Q}$, and $QQQq\bar{Q}$ pentaquarks. Among these pentaquark systems, most of them have explicit properties of exotic states, if such pentaquark exist, they could be easily identified once they were observed. Besides, there are also implicit pentaquark states in the $qqqQ\bar{q}$ system, such implicit pentaquark states act like the excited states of charmed/bottom baryons. At present, it is difficult to identify them both experimentally or theoretically. However, we will also give some basic features for these pentaquark states with our modified CMI model. We hope that our studies will be helpful to find these pentaquark states in future experiments.

This paper is organised as follows. In Sec. II, we introduce the modified Chromomagnetic Interaction model (CMI model). In Sec. III, we construct the symmetrically allowed isospin \otimes color \otimes spin wave functions for the $qqqq\bar{Q}$, $qqqQ\bar{q}$, $QQQQ\bar{q}$, $QQQQ\bar{Q}$, and $QQQq\bar{Q}$ pentaquark systems. In Sec. IV, we calculate the expressions of CMI Hamiltonian elements for the discussed pentaquark systems. In Sec. V, we determine the parameters used in the CMI model and in the modified CMI model. In Sec. VI, we present the mass spectrums and the mass splittings, possible strong decay channels, the relative partial decay widths, and the stability for all the

discussed pentaquark states. In Sec. VII, we give a short summary. Finally, we present some useful expressions in our appendixes in Sec. IX.

II. THE CHROMOMAGNETIC INTERACTION MODEL

The mass of the ground hadron state can be described by the effective Hamiltonian

$$H = \sum_i m_i + H_{\text{CMI}}, \quad (1)$$

$$H_{\text{CMI}} = - \sum_{i < j} C_{ij} \vec{\lambda}_i \cdot \vec{\lambda}_j \vec{\sigma}_i \cdot \vec{\sigma}_j, \quad (2)$$

where the H_{CMI} denotes the Hamiltonian of the chromomagnetic interaction [94]. m_i is the effective mass of the i -th constituent quark and C_{ij} denotes the effective coupling constant between the i -th quark and j -th quark. σ_i and λ_i are the Pauli matrices and the Gell-Mann matrices, respectively. Note that for antiquark, the λ_i should be replaced by $-\lambda_i^*$. The effective quark mass m_i and coupling constant C_{ij} can be determined from the experimental hadron masses. As an oversimplified model, the chromo-electric interaction and color confinement effect are also incorporated in the effective quark mass m_i .

Fitting the experimental data of hadron masses is a direct way to determine the effective masses of constituent quarks. However, as indicated in Ref. [59, 65, 75–82], the effective masses obtained in this way do not sufficiently incorporate the attractive interactions among quarks (antiquarks) in a specific hadron system. In most cases, the hadron masses are generally overestimated. Thus, in order to take such effective attractive interaction into account, we replace the sum of m_i term in Eq. (1) with $M_{\text{ref}} - \langle H_{\text{CMI}} \rangle_{\text{ref}}$. In this scheme, the mass of ground hadron can be written as

$$M = M_{\text{ref}} - \langle H_{\text{CMI}} \rangle_{\text{ref}} + \langle H_{\text{CMI}} \rangle, \quad (3)$$

where M_{ref} , $\langle H_{\text{CMI}} \rangle_{\text{ref}}$, and $\langle H_{\text{CMI}} \rangle$ are the physical mass of the reference system, the CMI eigenvalue for the reference system, and the CMI eigenvalue for the discussed multi-quark state, respectively. In this work, we label the method determining the mass of pentaquark states with hadron-hadron reference masses as the first scheme.

Obviously, in the first scheme, the problem of applying the overestimated constituent quark masses calculated from conventional hadrons to pentaquark systems [95] can be avoided.

Besides, in this work, we also introduce another scheme to estimate the masses of multiquark states. Note that in Eq. (1), the chromoelectric effects from the color interaction are implicitly included in the effective quark mass m_i . However, this treatment is not sufficient to describe the two-body color-electric effects in both meson

and baryon masses. Based on the above discussions, we generalized the chromomagnetic interaction model by introducing a chromoelectric term [83–85] to describe the Hamiltonian of a multiquark state

$$\begin{aligned} H &= \sum_i m_i + H_{\text{CEI}} + H_{\text{CMI}} \\ &= -\frac{3}{4} \sum_{i < j} m_{ij} V_{ij}^C - \sum_{i < j} v_{ij} V_{ij}^{\text{CMI}}. \end{aligned} \quad (4)$$

Here, $V_{ij}^C = \vec{\lambda}_i \cdot \vec{\lambda}_j$ and $V_{ij}^{\text{CMI}} = \vec{\lambda}_i \cdot \vec{\lambda}_j \vec{\sigma}_i \cdot \vec{\sigma}_j$ are the chromoelectric and chromomagnetic interaction between quarks, respectively. The parameters m_{ij} and v_{ij} can be extracted from the conventional hadrons. This scheme has been successfully applied to study the X(3872), Ξ_{cc} , and the pentaquarks with $qqqc\bar{c}$ ($q = u, d, s$) [83–85] configuration. This treatment is similar to Ref. [91, 92]. In their work, they introduce a color-singlet binding energy to describe the color-eletric effects. We label this way of determining the masses of multiquark states as the second scheme.

In this work, we mainly focus on the results of pentaquark mass spectrums obtained from the modified CMI model scheme. Besides, as a comparison, we will also present our results calculated from the meson-baryon threshold scheme.

III. SYMMETRY PROPERTIES OF THE $qqqq\bar{Q}$, $qqqQ\bar{q}$, $QQQQ\bar{q}$, $QQQQ\bar{Q}$, AND $QQQq\bar{Q}$ PENTAQUARK SYSTEMS

In this work, we study systematically the mass spectrums of the $qqqq\bar{Q}$, $qqqQ\bar{q}$, $QQQQ\bar{q}$, $QQQQ\bar{Q}$, and $QQQq\bar{Q}$ pentaquark systems. In order to calculate the mass spectrums of the above ground pentaquark systems, we need to exhaust all the possible spin and color wave functions of pentaquark states and combine them with the corresponding flavor wave functions. The constructed pentaquark wave functions should be constrained appropriately from Pauli principle. After that, we can use the obtained pentaquark wave functions to calculate the mass spectrums of the corresponding pentaquark subsystems.

The total wave function of pentaquark state can be described by the direct product of space, flavor, color, and spin wave functions

$$\psi_{\text{tot}} = \psi_{\text{space}} \otimes \psi_{\text{flavor}} \otimes \psi_{\text{color}} \otimes \psi_{\text{spin}}. \quad (5)$$

In this work, since we only consider the low-lying S -wave pentaquark states, the symmetrical constraint from spatial pentaquark wave function is trivial. Thus, the $\psi_{\text{flavor}} \otimes \psi_{\text{color}} \otimes \psi_{\text{spin}}$ wave functions of pentaquark states should be fully antisymmetric when exchanging identical quarks.

Note that the mass of s quark is heavier than that of the u, d quarks, leading to SU(3) flavor symmetry breaking effect. In our calculation, we will include this effect

TABLE I. All possible flavor combinations for the $qqqq\bar{Q}$, $qqqQ\bar{q}$, $QQQQ\bar{q}$, $QQQQ\bar{Q}$, and $QQQq\bar{Q}$ pentaquark systems. Here, $q = n, s$ ($n = u, d$) and $Q = c, b$.

$qqqq\bar{Q}$	$qqqQ\bar{q}$	$QQQQ\bar{q}$	$QQQQ\bar{Q}$	$QQQq\bar{Q}$
$nnnn\bar{c}$ (\bar{b})	$nncn\bar{n}$ (\bar{s})	$cccc\bar{n}$ (\bar{s})	$cccc\bar{c}$ (\bar{b})	$cccn\bar{c}$ (\bar{b})
$nnns\bar{c}$ (\bar{b})	$nnnb\bar{n}$ (\bar{s})	$cccb\bar{n}$ (\bar{s})	$cccb\bar{c}$ (\bar{b})	$cccs\bar{c}$ (\bar{b})
$nsss\bar{c}$ (\bar{b})	$nns\bar{c}\bar{n}$ (\bar{s})	$ccb\bar{n}$ (\bar{s})	$ccb\bar{c}$ (\bar{b})	$ccb\bar{n}\bar{c}$ (\bar{b})
$sssn\bar{c}$ (\bar{b})	$nnsc\bar{n}$ (\bar{s})	$bbbc\bar{n}$ (\bar{s})	$bbbc\bar{c}$ (\bar{b})	$ccbs\bar{c}$ (\bar{b})
$ssss\bar{c}$ (\bar{b})	$ssnc\bar{n}$ (\bar{s})	$bbbb\bar{n}$ (\bar{s})	$bbbb\bar{c}$ (\bar{b})	$bbcn\bar{c}$ (\bar{b})
	$ssnb\bar{n}$ (\bar{s})			$bbcs\bar{c}$ (\bar{b})
	$sssc\bar{n}$ (\bar{s})			$bbbn\bar{c}$ (\bar{b})
	$sssb\bar{n}$ (\bar{s})			$bbbs\bar{c}$ (\bar{b})

by distinguishing s quark from u, d quarks. More specifically, we only consider SU(2) flavor symmetry when constructing the flavor wave functions of pentaquark states, and take s quark as a flavor singlet.

In Table I, we list all the possible flavor combinations for the $qqqq\bar{Q}$, $qqqQ\bar{q}$, $QQQQ\bar{q}$, $QQQQ\bar{Q}$, and $QQQq\bar{Q}$ pentaquark systems. When checking the above pentaquark systems, we find that the $qqqq\bar{Q}$ and $qqqQ\bar{q}$ systems have more types of flavor combinations than that of the other pentaquark systems. Since we will consider SU(3) flavor symmetry breaking effect, the light quarks $n = u, d$ can be described by SU(2) isospin group, while s quark and heavy flavor quarks $Q = c, b$ are all treated as flavor singlet. Indeed, the flavor wave functions with different isospin for the $QQQQ\bar{q}$, $QQQQ\bar{Q}$, and $QQQq\bar{Q}$ pentaquark systems can be precisely reproduced from the $qqqq\bar{Q}$ and $qqqQ\bar{q}$ by appropriately exchanging $q \leftrightarrow Q$ ($\bar{q} \leftrightarrow \bar{Q}$) quarks. Thus, in the following discussion, we will briefly introduce the the isospin wave functions, color wave functions, and spin wave functions for the $qqqq\bar{Q}$ and $qqqQ\bar{q}$ pentaquark systems, separately.

A. Isospin, color, and spin wave functions

Firstly, we discuss the flavor wave functions for the $qqqq\bar{Q}$ and $qqqQ\bar{q}$ pentaquark systems. For the $qqqq\bar{Q}$ pentaquark system, as shown in Table I, the possible flavor combinations are the $nnnn\bar{c}$ (\bar{b}), $nnns\bar{c}$ (\bar{b}), $nsss\bar{c}$ (\bar{b}), and $ssss\bar{c}$ (\bar{b}). Similarly, as presented in Table I, the $qqqQ\bar{q}$ pentaquark system includes the $nncn\bar{n}$ (\bar{s}), $nnnb\bar{n}$ (\bar{s}), $nns\bar{c}\bar{n}$ (\bar{s}), $nnsb\bar{n}$ (\bar{s}), $ssnc\bar{n}$ (\bar{s}), $ssnb\bar{n}$ (\bar{s}), $sssc\bar{n}$ (\bar{s}), and $sssb\bar{n}$ (\bar{s}) flavor combinations.

Specifically, the $nnnn\bar{Q}$ pentaquark subsystem with isospin 2, 1, 0 can be represented by the Young tableau

as

$$\begin{aligned} & \square_I \otimes \square_I \otimes \square_I \otimes \square_I \\ = & \begin{array}{c} \square \end{array}_I \oplus \begin{array}{ccccc} \square & \square & \square & \square \end{array}_I \oplus \begin{array}{cccc} \square & \square & \square & \square \end{array}_I \oplus \\ & \begin{array}{ccc} \square & \square & \square \end{array}_I \oplus \begin{array}{cc} \square & \square \end{array}_I \oplus \begin{array}{cc} \square & \square \end{array}_I . \end{aligned} \quad (6)$$

For the $nnns\bar{c}$ (\bar{b}) ($I = 3/2, 1/2$) and $nnnQ\bar{n}$ (\bar{s}) ($I_{nnn} = 3/2, 1/2$) pentaquark subsystems, the direct product in flavor space represented in the Young tableau can be written as:

$$\begin{aligned} & \square_I \otimes \square_I \otimes \square_I \\ = & \begin{array}{c} \square \end{array}_I \oplus \begin{array}{ccc} \square & \square & \square \end{array}_I \oplus \begin{array}{cc} \square & \square \end{array}_I , \end{aligned} \quad (7)$$

For the $nnss\bar{c}$ (\bar{b}) ($I = 1, 0$) and $nnsQ\bar{n}$ (\bar{s}) ($I_{nn} = 1, 0$) pentaquark subsystems, one can easily obtain the direct product in terms of the Young tableau as

$$\square_I \otimes \square_I = \begin{array}{c} \square \end{array}_I \oplus \begin{array}{c} \square \end{array}_I . \quad (8)$$

For other pentaquarks in the $qqq\bar{Q}$ and $qqQ\bar{q}$ pentaquark systems, the Young tableau in isospin space have very naive expressions. Thus, we do not further list them here.

Next, we briefly introduce the color wave functions for all the discussed pentaquark systems. The color wave functions for pentaquark systems can be deduced from the following direct product

$$[3]_C \otimes [3]_C \otimes [3]_C \otimes [3]_C \otimes [\bar{3}]_C . \quad (9)$$

Based on Eq. (9), we can perform the direct product of the first four color triplets, then combine the results with the last anti-quark, which belongs to the anti-triplet in color space. For the first four quarks, we can construct the color triplet states with the direct product $[3]_C \otimes [3]_C \otimes [3]_C \otimes [3]_C$. The corresponding Young tableau $[2,1,1]$ can be written as

$$\begin{aligned} \begin{array}{c} 1 \\ 3 \\ 4 \end{array} &= \{(12)_6 (34)_{\bar{3}}\}_3 , \quad \begin{array}{c} 1 \\ 2 \\ 4 \end{array} = \{(12)_{\bar{3}} 34\}_3 , \\ \begin{array}{c} 1 \\ 2 \\ 3 \end{array} &= \{(123)_1 4\}_3 . \end{aligned} \quad (10)$$

Here, the subscript labels the irreducible representation of SU(3) group. Then, by combining the antitriplet from antiquark with the deduced three color triplets in Eq. (10), we obtain three color singlets for all the studied pentaquark systems and show them in Eqs. (114-116) of Appendix A.

Lastly, in spin space, the direct product of five fermions represented in terms of Young tableau can be written as

$$\begin{aligned} & \square_S \otimes \square_S \otimes \square_S \otimes \square_S \otimes \square_S \\ \rightarrow & \begin{array}{ccccc} \square & \square & \square & \square & \square \end{array}_S \oplus \begin{array}{ccccc} \square & \square & \square & \square & \square \end{array}_S \oplus \begin{array}{ccccc} \square & \square & \square & \square & \square \end{array}_S . \end{aligned} \quad (11)$$

The three obtained Young tableaus represent $S = 5/2$, $3/2$, and $1/2$ spin states, respectively.

B. Isospin \otimes Color \otimes Spin wave functions

With the above preparation, we can start to construct the total wave functions for the pentaquark states with $qqqq\bar{Q}$, $qqqQ\bar{q}$, $QQQQ\bar{Q}$, $QQQQ\bar{q}$, and $QQQq\bar{Q}$ configurations.

Here, we first discuss the wave functions of the pentaquark systems including four identical fermions. For such pentaquark systems, due to Pauli principle, the constructed isospin \otimes color \otimes spin wave functions should be fully antisymmetric when exchanging each pair of identical quarks.

To obtain the color \otimes spin bases for the quarks 1, 2, 3, and 4 [96], we need to combine the three color singlet bases presented in Eq. (10) with spin bases given in Eq. (11) by the outer product of the permutation group S_4 .

Following the method described in Ref. [96], when we discuss the symmetry property for the first four quarks 1, 2, 3, and 4, we also express the spin bases for Young tableau [4], [3,1], and [2,2] in Eq. (11) with the Young-Yamanouchi bases. All the possible Young-Yamanouchi bases obtained from the color \otimes spin coupling in Eqs. (13-17) are presented in Eq. (117) of Appendix B.

Now we need to appropriately combine the flavor wave functions with the color \otimes spin wave functions to construct the total wave functions of pentaquark states. A direct way to determine the coefficients in front of the flavor wave function is given by the following equation [97]

$$\begin{aligned} S([f']p'q'y'[f'']p''q''y''|[f]pqy) = \\ K([f']p'[f'']p''|[f]p)S([f'_p]q'y'[f''_p]q''y''|[f_p]qy) , \end{aligned} \quad (12)$$

where S in the left-hand (right-hand) side is a CG coefficient of S_n (S_{n-1}) and K is a matrix factorized from S_n [96, 98-100].

$$J = \frac{5}{2} : \begin{array}{c} \text{C} \\ \text{S} \end{array} \otimes \begin{array}{c} \text{C} \\ \text{S} \end{array} = \begin{array}{c} \text{C} \\ \text{S} \end{array}, \quad (13)$$

$$J = \frac{3}{2} : \begin{array}{c} \text{C} \\ \text{S} \end{array} \otimes \begin{array}{c} \text{C} \\ \text{S} \end{array} = \begin{array}{c} \text{C} \\ \text{S} \end{array} \oplus \begin{array}{c} \text{C} \\ \text{S} \end{array} \oplus \begin{array}{c} \text{C} \\ \text{S} \end{array} \oplus \begin{array}{c} \text{C} \\ \text{S} \end{array}, \quad (14)$$

$$J = \frac{5}{2} : \begin{array}{c} \text{C} \\ \text{S} \end{array} \otimes \begin{array}{c} \text{C} \\ \text{S} \end{array} = \begin{array}{c} \text{C} \\ \text{S} \end{array}, \quad (15)$$

$$J = \frac{1}{2} : \begin{array}{c} \text{C} \\ \text{S} \end{array} \otimes \begin{array}{c} \text{C} \\ \text{S} \end{array} = \begin{array}{c} \text{C} \\ \text{S} \end{array} \oplus \begin{array}{c} \text{C} \\ \text{S} \end{array} \oplus \begin{array}{c} \text{C} \\ \text{S} \end{array} \oplus \begin{array}{c} \text{C} \\ \text{S} \end{array}, \quad (16)$$

$$J = \frac{1}{2} : \begin{array}{c} \text{C} \\ \text{S} \end{array} \otimes \begin{array}{c} \text{C} \\ \text{S} \end{array} = \begin{array}{c} \text{C} \\ \text{S} \end{array} \oplus \begin{array}{c} \text{C} \\ \text{S} \end{array}, \quad (17)$$

Now we combine the Young tableaus representations of isospin states in Eqs. (6-8) with the Young tableaus representations of color \otimes spin in Eqs. (13-17), the obtained Young-Yamanouchi bases for the $nnnn\bar{Q}$, $nnns\bar{Q}$, $nsss\bar{Q}$, and $nnsQ\bar{q}$ pentaquark subsystems are presented in Appendix C, D, E, and F, respectively. Besides, since different pentaquark systems may share the same symmetry properties, we collect the studied $qqqq\bar{Q}$, $qqqQ\bar{q}$, $QQQQ\bar{q}$, $QQQQ\bar{Q}$, and $QQQq\bar{Q}$ pentaquark flavor configurations with the same symmetry properties in Table II. Moreover, the pentaquark systems sharing the same symmetry properties have the same CMI Hamiltonian expressions after we appropriately replacing constituent quark masses and coupling parameters. We will discuss this question further in the following analysis.

IV. THE HAMILTONIAN EXPRESSIONS

In the previous section, we have constructed all the possible wave functions for the $qqqq\bar{Q}$, $qqqQ\bar{q}$, $QQQQ\bar{q}$, $QQQQ\bar{Q}$, and $QQQq\bar{Q}$ pentaquark systems. Next, with the constructed wave functions, we can calculate the CMI matrices for the corresponding pentquark systems.

In Table III, we present values of the allowed isospin \otimes color \otimes spin bases for the $qqqq\bar{Q}$, $qqqQ\bar{q}$, $QQQQ\bar{q}$, $QQQQ\bar{Q}$, and $QQQq\bar{Q}$ pentaquark systems. We present the expressions of CMI Hamiltonians for the $nnnn\bar{Q}$ ($I = 2, 1, 0$) pentaquark states in Table IV. The expressions of CMI Hamiltonians for the $nnns\bar{Q}$ ($I = 3/2, 1/2$), $nsss\bar{Q}$ ($I = 1, 0$), and $nnsQ\bar{q}$ ($I_{nn} = 1, 0$) pentaquark states are

presented in Tables XXXVII, XXXVIII, and XXXIX of Appendix G, respectively.

As discussed in Sec. III, the wave functions for the $QQQQ\bar{q}$, $QQQq\bar{Q}$, and $QQQQ\bar{Q}$ pentaquark systems can be precisely obtained by appropriately exchanging the constituent quark components in the $qqqq\bar{Q}$ and $qqqQ\bar{q}$ pentaquark systems. Similarly, by exchanging the corresponding effective coupling constants, we can directly obtain the expressions of CMI matrices for the $QQQQ\bar{q}$, $QQQQ\bar{Q}$, and $QQQq\bar{Q}$ pentaquark systems from that of the $qqqq\bar{Q}$ and $qqqQ\bar{q}$ pentaquark systems. For example, the explicit forms of the CMI Hamiltonian for the $ssss\bar{Q}$ and $sssn\bar{Q}$ pentaquark subsystems are identical to that of the $nnnn\bar{Q}$ ($I = 2$) and $nnns\bar{Q}$ ($I = 3/2$) pentaquark subsystems after we appropriately replace the C_{ij} constants. To obtain the expressions of the CMI Hamiltonian for the $ssss\bar{Q}$ pentaquark subsystem, we can replace C_{nn} and $C_{n\bar{Q}}$ in the explicit form of the CMI Hamiltonian for the $nnnn\bar{Q}$ ($I = 2$) pentaquark subsystem with effective constants C_{ss} and $C_{s\bar{Q}}$, respectively. Similarity, to obtain the expressions of the CMI Hamiltonian for the $sssn\bar{Q}$ or $cccb\bar{Q}$ pentaquark subsystems, we need to replace the effective coupling constants C_{nn} , C_{ns} , $C_{n\bar{Q}}$, and $C_{s\bar{Q}}$ in the explicit form of CMI Hamiltonian for the $nnns\bar{Q}$ ($I = 3/2$) pentaquark subsystem with the C_{ss} , C_{ns} , $C_{s\bar{Q}}$, and $C_{n\bar{Q}}$ for the $sssn\bar{Q}$ pentaquark subsystem or C_{cc} , C_{cb} , $C_{c\bar{Q}}$, and $C_{b\bar{Q}}$ for the $cccb\bar{Q}$ pentaquark subsystem, respectively.

TABLE II. Pentaquark subsystems with the same symmetry properties among the studied $qqqq\bar{Q}$, $qqqQ\bar{q}$, $QQQQ\bar{q}$, $QQQQ\bar{Q}$, and $QQQq\bar{Q}$ pentaquark systems. Here, $q = n, s$ ($n = u, d$) and $Q = c, b$.

Subsystems	Isospin	Subsystems					
$nnnn\bar{Q}$	2	$ssss\bar{Q}$	$cccc\bar{q}$	$bbbb\bar{q}$	$cccc\bar{Q}$		
		$bbbb\bar{Q}$	$nnnn\bar{Q}$ ($I = 2$)				
	1	$nnnn\bar{Q}$ ($I = 1$)					
$nnns\bar{Q}$	0	$nnnn\bar{Q}$ ($I = 0$)					
	3/2	$sssn\bar{Q}$	$cccb\bar{q}$	$cccb\bar{Q}$	$cccq\bar{Q}$		
		$bbbc\bar{Q}$	$bbbc\bar{q}$	$bbbq\bar{Q}$	$sssQ\bar{q}$		
		$nnnQ\bar{q}$ ($I = 3/2$)					
$nsss\bar{Q}$	1/2	$nnnQ\bar{q}$ ($I = 1/2$)					
	1	$ccb\bar{Q}$	$ccb\bar{q}$	$nnss\bar{Q}$ ($I = 1$)			
	0	$nnss\bar{Q}$ ($I = 0$)					
$nnsQ\bar{q}$	1	$ccbq\bar{Q}$	$bbcq\bar{Q}$	$ssnQ\bar{q}$			
		$nnsQ\bar{q}$ ($I = 1$)					
	0	$nnsQ\bar{q}$ ($I = 0$)					

V. THE DETERMINATION OF PARAMETERS AND ESTIMATION STRATEGY

In Sec. IV, we present the explicit forms of CMI matrices for all the $qqqq\bar{Q}$, $qqqQ\bar{q}$, $QQQQ\bar{q}$, $QQQQ\bar{Q}$, and $QQQq\bar{Q}$ pentaquark systems. Before we perform numerical analysis to the above pentaquark systems, we need to determine the effective coupling constants in the expressions of CMI matrices for all the discussed pentaquark systems.

In this work, we use two schemes to estimate the masses of the $qqqq\bar{Q}$, $qqqQ\bar{q}$, $QQQQ\bar{q}$, $QQQQ\bar{Q}$, and $QQQq\bar{Q}$ pentaquark states. In both schemes, we need some typical hadron masses as input to fit the corresponding parameters. Thus, we collect the masses of these typical hadrons in Table V. Here, we need to emphasize that for some not-yet observed hadrons, we have introduced some theoretical results [40, 84] as our input. We denote the masses of these hadrons with parentheses in Table V.

Now we can fit the effective coupling parameters in the first and second schemes by applying Eqs. (1-2) and Eq. (4), respectively. The obtained parameters are presented in Table VI. Interested readers can refer to Ref. [84, 85, 93] for more details.

TABLE III. The multiplicities for the studied $qqqq\bar{Q}$, $qqqQ\bar{q}$, $QQQQ\bar{q}$, $QQQQ\bar{Q}$, and $QQQq\bar{Q}$ pentaquark systems. Here, $q = n, s$ ($n = u, d$) and $Q = c, b$. Isospin denotes the isospin of the first four quarks. M denotes the multiplicity of pentaquark state with flavor \otimes color \otimes spin wave function.

Flavor state	Isospin	Spin	M	Flavor state	Isospin	Spin	M		
$nnnn\bar{Q}$	2	5/2	0	$nnns\bar{Q}$	3/2	5/2	1		
		3/2	1				3/2		
		1/2	1				1/2		
$nnnn\bar{Q}$	1	5/2	1		1/2	5/2	1		
		3/2	2				3/2		
		1/2	2				1/2		
$sssn\bar{Q}$	0	5/2	0	$nnss\bar{Q}$	1	5/2	1		
		3/2	1				3/2		
		1/2	1				1/2		
$ssss\bar{Q}$	1/2	5/2	1	$nnnQ\bar{q}$	3/2	5/2	1		
		3/2	3				3/2		
		1/2	3				1/2		
$nnsQ\bar{q}$	0	5/2	0	$ssnQ\bar{q}$	1/2	5/2	1		
		3/2	1				3/2		
		1/2	1				1/2		
$nnsQ\bar{q}$	1	5/2	2	$ssnQ\bar{q}$	1/2	5/2	1		
		3/2	7				3/2		
		1/2	8				1/2		
$ssssQ\bar{q}$	0	5/2	1	$QQQQ\bar{q}$	0	5/2	2		
		3/2	5				3/2		
		1/2	7				1/2		
$ssssQ\bar{q}$	0	5/2	1	$QQQQ'\bar{q}$	0	5/2	0		
		3/2	3				3/2		
		1/2	3				1/2		
$QQQQ'\bar{q}$	0	5/2	1	$QQQ'Q'\bar{q}$	0	5/2	1		
		3/2	3				3/2		
		1/2	3				1/2		
$QQQQ\bar{Q}$	0	5/2	0	$QQQ'Q'\bar{Q}$	0	5/2	1		
		3/2	1				3/2		
		1/2	1				1/2		
$QQQ'Q'\bar{Q}$	0	5/2	1	$QQQq\bar{Q}$	0	5/2	1		
		3/2	4				3/2		
		1/2	4				1/2		
$QQQ'q\bar{Q}$	0	5/2	2						
		3/2	7						
		1/2	8						

VI. MASS SPECTRUMS AND DECAY BEHAVIORS

We can introduce the parameters collected in Table VI to calculate the discussed CMI matrices, the corresponding CMI matrices can be diagnosed and the eigenvalues as well as eigenvectors for the corresponding pentaquark systems can also be obtained. In the following, based on the two schemes proposed in Sec. II, we will discuss our results for the masses and decay behaviors of the $qqqq\bar{Q}$, $qqqQ\bar{q}$, $QQQQ\bar{q}$, $QQQQ\bar{Q}$, and $QQQq\bar{Q}$ pentaquark systems.

For the convenience of readers, we provide three reading index tables, i.e., Tables VII, VIII, and IX. These

TABLE IV. The expressions of CMI Hamiltonian for the $nnnn\bar{Q}$ ($n = u, d$; $Q = c, b$) subsystem. The I (S) represents the isospin (spin) of pentaquark states.

I	S	The CMI Hamiltonian
$I = 2$	$S = 3/2$	$\frac{56}{3}C_{nn} - \frac{16}{3}C_{n\bar{Q}}$
	$S = 1/2$	$\frac{56}{3}C_{nn} + \frac{32}{3}C_{n\bar{Q}}$
$I = 1$	$S = 5/2$	$8C_{nn} + \frac{16}{3}C_{n\bar{Q}}$
	$S = 3/2$	$\begin{pmatrix} 8C_{nn} - 8C_{n\bar{Q}} & 4\sqrt{10}C_{n\bar{Q}} \\ 4\sqrt{10}C_{n\bar{Q}} & \frac{8}{3}C_{nn} - \frac{4}{3}C_{n\bar{Q}} \end{pmatrix}$
	$S = 1/2$	$\begin{pmatrix} \frac{8}{3}C_{nn} + \frac{8}{3}C_{n\bar{Q}} & 8C_{n\bar{Q}} \\ 8C_{n\bar{Q}} & 0 \end{pmatrix}$
	$S = 3/2$	$-\frac{16}{3}C_{nn} + \frac{20}{3}C_{n\bar{Q}}$
$I = 0$	$S = 1/2$	$-\frac{16}{3}C_{nn} - \frac{40}{3}C_{n\bar{Q}}$

three tables can help us to find the corresponding information on the masses and decay behaviors for each pentaquark states in the $qqq\bar{Q}$, $qqqQ\bar{q}$, $QQQ\bar{Q}\bar{q}$, $QQQQ\bar{Q}$, and $QQQq\bar{Q}$ pentaquark systems.

A. The $qqq\bar{Q}$ pentaquark states

We first discuss the $qqq\bar{Q}$ pentaquark system. Obviously, the pentaquarks with $qqq\bar{Q}$ configuration are explicitly exotic states.

For such pentaquark states, M. Genovese et al. discuss systematically their stability in the framework of chiral constituent quark model and find that the $qqq\bar{Q}$ pentaquark states are not bound, with energies above the lowest dissociation thresholds into baryon and meson final states [102]. However, it is shown [103] that in the $m_Q \rightarrow \infty$ limit, $qqqq = uuds$, $ddus$, and $ssud$ are in the $SU(3)_F$ limit, and with the assumptions that the strength of the chromomagnetic term is the same as that of the ordinary baryons, the $qqq\bar{Q}$ pentaquark state is bounded and lying about 150 MeV below the $\bar{Q}q + qqq$ meson-baryon threshold. This possible pentaquark is studied in the Fermilab experiment [104, 105], but no decisive conclusion was found. Moreover, the weak decay properties for the stable states in $qqq\bar{Q}$ pentaquark system are discussed in Ref. [106]. The existence of $qqq\bar{Q}$ pentaquark states is still an open question.

As presented in Table I, the $qqq\bar{Q}$ pentaquark system includes the states with $nnnn\bar{c}$ (\bar{b}), $nnns\bar{c}$ (\bar{b}), $nnss\bar{c}$ (\bar{b}), $sssn\bar{c}$ (\bar{b}), and $ssss\bar{c}$ (\bar{b}) flavor combinations.

As shown in Table II, according to symmetry properties, we can divide the $qqq\bar{Q}$ pentaquark system into three groups: (1) the $nnnn\bar{Q}$ and $ssss\bar{Q}$ pentaquark subsystems, (2) the $nnns\bar{Q}$ and $sssn\bar{Q}$ pentaquark subsystems, (3) the $nnss\bar{Q}$ pentaquark subsystem. In the following, we will discuss the mass spectrums and strong decay properties of $qqq\bar{Q}$ pentaquark system group by group.

TABLE V. The masses of ground conventional hadrons in units of MeV [101]. The adopted masses of not-yet-observed baryons in parentheses are taken from Ref. [84]. Besides, the mass value of B_c^* is taken from [40].

hadrons	$I(J^P)$	Mass	hadrons	$I(J^P)$	Mass
π	$1(0^-)$	139.6	N	$1/2(1/2^+)$	938.3
η	$0(0^-)$	547.9	Δ	$3/2(3/2^+)$	1232.0
η'	$0(0^-)$	957.8	Λ	$0(1/2^+)$	1115.7
ρ	$1(1^-)$	775.3	Σ	$1(1/2^+)$	1192.6
ω	$0(1^-)$	782.7	Σ^*	$1(3/2^+)$	1382.8
K	$1/2(0^-)$	493.7	Ξ	$1/2(1/2^+)$	1314.9
K^*	$1/2(1^-)$	891.8	Ξ^*	$1/2(3/2^+)$	1531.8
ϕ	$0(1^-)$	1019.5	Ω	$0(3/2^+)$	1672.5
D	$1/2(0^-)$	1869.6	Λ_c	$0(1/2^+)$	2286.5
D^*	$1/2(1^-)$	2010.3	Σ_c	$1(1/2^+)$	2454.0
D_s	$0(0^-)$	1968.3	Σ_c^*	$1(3/2^+)$	2518.4
D_s^*	$0(1^-)$	2112.2	Ξ_c	$1/2(1/2^+)$	2467.9
B	$1/2(0^-)$	5279.3	Ξ'_c	$1/2(1/2^+)$	2577.4
B^*	$1/2(1^-)$	5324.7	Ξ_c^*	$1/2(3/2^+)$	2645.5
B_s	$0(0^-)$	5366.8	Ω_c	$0(1/2^+)$	2695.2
B_s^*	$0(1^-)$	5415.4	Ω_c^*	$0(3/2^+)$	2765.9
η_c	$0(0^-)$	2983.9	Λ_b	$0(1/2^+)$	5619.6
J/ψ	$0(1^-)$	3096.9	Σ_b	$1(1/2^+)$	5811.3
η_b	$0(0^-)$	9399.0	Σ_b^*	$1(3/2^+)$	5832.1
Υ	$0(1^-)$	9460.3	Ξ_b	$1/2(1/2^+)$	5794.5
B_c	$0(0^-)$	6274.9	Ξ'_b	$1/2(1/2^+)$	5935.0
B_c^*	$0(1^-)$ (6338.0)		Ξ_b^*	$1/2(3/2^+)$	5955.3
Ξ_{cc}	$1/2(1/2^+)$	3621.4	Ω_b	$0(1/2^+)$	6046.1
Ξ_{cc}^*	$1/2(3/2^+)$ (3696.1)		Ω_b^*	$0(3/2^+)$ (6054.8)	
Ω_{cc}	$0(1/2^+)$ (3731.8)		Ξ_{bb}	$1/2(1/2^+)$ (10168.9)	
Ω_{cc}^*	$0(3/2^+)$ (3802.4)		Ξ_{bb}^*	$1/2(3/2^+)$ (10188.8)	
Ξ_{cb}	$1/2(1/2^+)$ (6922.3)		Ω_{bb}	$0(1/2^+)$ (10259.0)	
Ξ'_{cb}	$1/2(1/2^+)$ (6947.9)		Ω_{bb}^*	$0(3/2^+)$ (10267.5)	
Ξ_{cb}^*	$1/2(3/2^+)$ (6973.2)		Ω_{ccb}	$0(1/2^+)$ (7990.3)	
Ω_{cb}	$0(1/2^+)$ (7010.7)		Ω_{ccb}^*	$0(3/2^+)$ (8021.8)	
Ω'_{cb}	$0(1/2^+)$ (7047.0)		Ω_{cbb}	$0(1/2^+)$ (11165.0)	
Ω_{cb}^*	$0(3/2^+)$ (7065.7)		Ω_{cbb}^*	$0(3/2^+)$ (11196.4)	
Ω_{ccc}	$0(3/2^+)$ (4785.6)		Ω_{bbb}	$0(3/2^+)$ (14309.7)	

1. The $nnnn\bar{Q}$ and $ssss\bar{Q}$ pentaquark states

We first discuss the $nnnn\bar{c}$ (\bar{b}) and $ssss\bar{c}$ (\bar{b}) pentaquark subsystems. For the $nnnn\bar{c}$ (\bar{b}) pentaquark subsystem, the first four quarks can be described by the $SU(2)$ isospin group. The isospin quantum numbers for such pentaquark subsystem are $I = 2, 1$, and 0 . By substituting the related parameters collected in Table VI, we obtain the numerical results of CMI matrices for the $nnnn\bar{c}$ (\bar{b}) subsystem and we present them in Table IV. The mass splittings of the $nnnn\bar{c}$ (\bar{b}) pentaquark states can be calculated by diagnosing the numerical CMI matrices.

If we replace all the n (u, d) quark components with the s quark components in the $nnnn\bar{Q}$ pentaquark subsystem, we have the $ssss\bar{c}$ (\bar{b}) pentaquark subsystem. Note that the first four strange quarks are identical, the expressions of CMI matrix is simply $I = 2$ case for the $nnnn\bar{Q}$ pentaquark states presented in Table IV, where

TABLE VI. Coupling parameters obtained from the first and second schemes. All results are in units of MeV.

The first scheme:							
C_{nn}	C_{ns}	C_{ss}	C_{nc}	$C_{n\bar{n}}$	$C_{n\bar{s}}$	$C_{s\bar{s}}$	$C_{n\bar{c}}$
18.4	12.1	6.5	4.0	29.8	18.7	10.5	6.6
C_{sc}	C_{nb}	C_{sb}	C_{cb}	$C_{s\bar{c}}$	$C_{n\bar{b}}$	$C_{s\bar{b}}$	$C_{c\bar{b}}$
4.5	1.3	1.2	2.0	6.7	2.1	2.3	3.3
	C_{cc}	C_{bb}		$C_{c\bar{c}}$	$C_{b\bar{b}}$		
				3.3	1.8	5.3	2.9

The second scheme:							
m_{nn}	m_{ns}	m_{ss}	m_{nc}	$m_{n\bar{n}}$	$m_{n\bar{s}}$	$m_{s\bar{s}}$	$m_{n\bar{c}}$
182.2	226.7	262.3	520.0	154.0	198.6	234.1	493.3
v_{nn}	v_{ns}	v_{ss}	v_{nc}	$v_{n\bar{n}}$	$v_{n\bar{s}}$	$v_{s\bar{s}}$	$v_{n\bar{c}}$
19.1	13.3	12.2	3.9	29.9	18.7	15.6	6.6
m_{sc}	m_{nb}	m_{sb}	m_{cb}	$m_{s\bar{c}}$	$m_{n\bar{b}}$	$m_{s\bar{b}}$	$m_{c\bar{b}}$
545.9	1353.1	1373.7	1604.0	519.0	1328.3	1350.8	1580.6
v_{sc}	v_{nb}	v_{sb}	v_{cb}	$v_{s\bar{c}}$	$v_{n\bar{b}}$	$v_{s\bar{b}}$	$v_{c\bar{b}}$
4.4	1.2	0.5	2.0	6.7	2.1	2.3	2.9
m_{cc}	m_{bb}	v_{cc}	v_{bb}	$m_{c\bar{c}}$	$m_{b\bar{b}}$	$v_{c\bar{c}}$	$v_{b\bar{b}}$
792.9	2382.4	3.5	1.9	767.1	2361.2	5.3	2.9

TABLE VII. The list of figures for the mass spectrums of the $qqqq\bar{Q}$, $qqqQ\bar{q}$, $QQQQ\bar{q}$, $QQQQ\bar{Q}$, and $QQQq\bar{Q}$ pentaquark systems.

Figures	System	subsystems
Fig.1	$qqqq\bar{Q}$	$nnnn\bar{c} \ ssss\bar{c} \ nnn\bar{s} \ sss\bar{s} \ nnss\bar{c}$ $nnnn\bar{b} \ ssss\bar{b} \ nnn\bar{s} \ sss\bar{s} \ nnss\bar{b}$
Fig.2	$qqqQ\bar{q}$	$nnnc\bar{n} \ nnn\bar{b} \ sssc\bar{n} \ sss\bar{b}$ $nnnc\bar{s} \ nnn\bar{s} \ sssc\bar{s} \ sss\bar{s}$
Fig.3		$nns\bar{c} \ nns\bar{b} \ ssnc\bar{n} \ ssnb\bar{n}$
Fig.4		$nns\bar{s} \ nns\bar{s} \ ssnc\bar{s} \ ssnb\bar{s}$
Fig.5	$QQQQ\bar{q}$	$cccc\bar{n} \ bbbb\bar{n} \ cccb\bar{n} \ bbbc\bar{n} \ cccb\bar{n}$ $cccc\bar{s} \ bbbb\bar{s} \ cccb\bar{s} \ bbbc\bar{s} \ cccb\bar{s}$
Fig.6	$QQQQ\bar{Q}$	$cccc\bar{c} \ bbbb\bar{c} \ cccb\bar{c} \ bbbc\bar{c} \ cccb\bar{c}$ $cccc\bar{b} \ bbbb\bar{b} \ cccb\bar{b} \ bbbc\bar{b} \ cccb\bar{b}$
Fig.7	$QQQq\bar{Q}$	$cccn\bar{c} \ cccs\bar{c} \ ccbn\bar{c} \ ccbs\bar{c}$ $cccn\bar{b} \ cccs\bar{b} \ ccbn\bar{b} \ ccbs\bar{b}$
Fig.8		$bbbn\bar{c} \ bbs\bar{c} \ bbcn\bar{c} \ bcsc\bar{c}$ $bbbn\bar{b} \ bbs\bar{b} \ bbcn\bar{b} \ bcsc\bar{b}$

the coupling parameters C_{nn} and $C_{n\bar{Q}}$ should be replaced by C_{ss} and $C_{s\bar{Q}}$, respectively.

The eigenvalues and the mass spectrums for the $nnnn\bar{c}$ (\bar{b}) and $ssss\bar{c}$ (\bar{b}) pentaquark states calculated in the first and second schemes are presented in Table X. In the first scheme, the possible combinations of meson-baryon systems for the $nnnn\bar{c}$ (\bar{b}) and $ssss\bar{c}$ (\bar{b}) subsystems are the $\Delta+\bar{D}$ ($\Delta+B$) and $D_s+\Omega$ ($B_s+\Omega$), respectively. The masses of pentaquark states with $nnnn\bar{c}$ (\bar{b}) and $ssss\bar{c}$ (\bar{b}) flavor configurations can be obtained by substituting the reference masses of the corresponding mesons and

TABLE VIII. The list of tables for the mass spectrums of the $qqqq\bar{Q}$, $qqqQ\bar{q}$, $QQQQ\bar{q}$, $QQQQ\bar{Q}$, and $QQQq\bar{Q}$ pentaquark systems.

Tables	System	subsystems
Table X		$nnnn\bar{c} \ ssss\bar{c} \ nnn\bar{n} \ sss\bar{s}$
Table XIV	$qqqq\bar{Q}$	$nnns\bar{c} \ sssn\bar{c} \ nnss\bar{c}$ $nnns\bar{b} \ sssn\bar{b} \ nnss\bar{b}$
Table XVI	$qqqQ\bar{q}$	$nnnc\bar{n} \ sssc\bar{n} \ nnnb\bar{n} \ sssb\bar{n}$ $nnnc\bar{s} \ sssc\bar{s} \ nnnb\bar{s} \ sssb\bar{s}$
Table XIX		$nns\bar{c}\bar{n} \ ssbc\bar{n} \ nnsb\bar{n} \ ssnb\bar{n}$
Table XX		$nns\bar{s}\bar{s} \ ssbc\bar{s} \ nnsb\bar{s} \ ssnb\bar{s}$
Table XXV	$QQQQ\bar{q}$	$cccc\bar{n} \ bbbb\bar{n} \ cccb\bar{n} \ bbbc\bar{n} \ cccb\bar{n}$ $cccc\bar{s} \ bbbb\bar{s} \ cccb\bar{s} \ bbbc\bar{s} \ cccb\bar{s}$
Table XXVIII	$QQQQ\bar{Q}$	$cccc\bar{c} \ bbbb\bar{c} \ cccb\bar{c} \ bbbc\bar{c} \ cccb\bar{c}$ $cccc\bar{b} \ bbbb\bar{b} \ cccb\bar{b} \ bbbc\bar{b} \ cccb\bar{b}$
Table XXX	$qqqQ\bar{q}$	$cccn\bar{c} \ cccs\bar{c} \ ccbn\bar{c} \ ccbs\bar{c}$ $cccn\bar{b} \ cccs\bar{b} \ ccbn\bar{b} \ ccbs\bar{b}$
Table XXXI		$bbbn\bar{c} \ bbs\bar{c} \ bbcn\bar{c} \ bcsc\bar{c}$ $bbbn\bar{b} \ bbs\bar{b} \ bbcn\bar{b} \ bcsc\bar{b}$

TABLE IX. The list of tables for the relative partial decay widths of the $qqqq\bar{Q}$, $qqqQ\bar{q}$, $QQQQ\bar{q}$, $QQQQ\bar{Q}$, and $QQQq\bar{Q}$ pentaquark systems.

Tables	System	subsystems
Table XIII		$nnnn\bar{c} \ ssss\bar{c} \ nnn\bar{n} \ sss\bar{s}$
Table XV	$qqqq\bar{Q}$	$nnns\bar{c} \ sssn\bar{c} \ nnss\bar{c}$ $nnns\bar{b} \ sssn\bar{b} \ nnss\bar{b}$
Table XVII		$nnnc\bar{n} \ nnn\bar{n} \ sssc\bar{n} \ sss\bar{n}$
Table XVIII		$nnnc\bar{s} \ nnn\bar{s} \ sssc\bar{s} \ sss\bar{s}$
Table XXI	$qqqQ\bar{Q}$	$nns\bar{c}\bar{n} \ ssnc\bar{n}$
Table XXII		$nns\bar{b}\bar{n} \ ssnb\bar{n}$
Table XXIII		$nns\bar{c}\bar{s} \ ssnc\bar{s}$
Table XXIV		$nns\bar{s}\bar{s} \ ssnb\bar{s}$
Table XXVI	$QQQQ\bar{q}$	$cccc\bar{n} \ cccs\bar{n} \ cccb\bar{n} \ bbbc\bar{n} \ bbbn\bar{n}$ $cccc\bar{s} \ cccs\bar{s} \ cccb\bar{s} \ bbbc\bar{s} \ bbbn\bar{s}$
Table XXIX	$QQQQ\bar{Q}$	$cccc\bar{c} \ cccs\bar{c} \ cccb\bar{c} \ bbbc\bar{c} \ bbbn\bar{c}$ $cccc\bar{b} \ cccs\bar{b} \ cccb\bar{b} \ bbbc\bar{b} \ bbbn\bar{b}$
Table XXXII	$QQQq\bar{Q}$	$cccn\bar{c} \ cccs\bar{c} \ bbbn\bar{c} \ bbs\bar{c}$ $cccn\bar{b} \ cccs\bar{b} \ bbbn\bar{b} \ bbs\bar{b}$
Table XXXIII		$bbcs\bar{c} \ bbs\bar{c}$
Table XXXIV		$ccbn\bar{c} \ ccbn\bar{b} \ ccbs\bar{c}$
Table XXXV		$ccbn\bar{b} \ bbcn\bar{c} \ bbcn\bar{b}$

baryons into Eq. (3). The results listed in the fourth column of Table X are calculated from the second scheme by introducing the modified CMI model in Eq. (4).

Based on the $nnnn\bar{c}$ (\bar{b}) and $ssss\bar{c}$ (\bar{b}) pentaquark masses obtained from the second scheme in Table IV, we plot the mass spectrums for the $nnnn\bar{c}$, $nnnn\bar{b}$, $ssss\bar{c}$, and $ssss\bar{b}$ pentaquark states in Fig. 1 (a-d), respectively. Besides, by rearranging the five constituent quark components, we also illustrate the possible thresholds of de-

TABLE X. The estimated masses for the $nnnn\bar{Q}$ and $ssss\bar{Q}$ ($n = u, d$; $Q = c, b$) subsystems in units of MeV. The values in the second column are eigenvalues obtained with the CMI Hamiltonian in Eq. (2). The masses in the third and fourth columns are obtained with meson-baryon thresholds in Eq. (3) and the modified CMI model in Eq. (4), respectively.

$nnnn\bar{c}$			$nnnn\bar{b}$					
$I(J^P)$	Eigenvalue	$(\bar{D}\Delta)$	Mass	$I(J^P)$	Eigenvalue	$(B\Delta)$	Mass	
$2(\frac{3}{2}^-)$	307.7	3369.4	3381.4	$2(\frac{3}{2}^-)$	332.3	6730.0	6745.6	
$2(\frac{1}{2}^-)$	414.9	3476.6	3487.4	$2(\frac{1}{2}^-)$	365.9	6763.6	6779.5	
$1(\frac{5}{2}^-)$	182.9	3244.6	3248.5	$1(\frac{5}{2}^-)$	158.4	6556.1	6564.6	
$1(\frac{3}{2}^-)$	$\begin{pmatrix} 155.7 \\ -22.0 \end{pmatrix}$	$\begin{pmatrix} 3217.4 \\ 3039.7 \end{pmatrix}$	$\begin{pmatrix} 3220.0 \\ 3042.7 \end{pmatrix}$	$1(\frac{3}{2}^-)$	$\begin{pmatrix} 138.1 \\ 38.6 \end{pmatrix}$	$\begin{pmatrix} 6535.8 \\ 6436.3 \end{pmatrix}$	$\begin{pmatrix} 6543.9 \\ 6441.2 \end{pmatrix}$	
$1(\frac{1}{2}^-)$	$\begin{pmatrix} 96.7 \\ -29.7 \end{pmatrix}$	$\begin{pmatrix} 3158.4 \\ 3032.0 \end{pmatrix}$	$\begin{pmatrix} 3157.9 \\ 3031.7 \end{pmatrix}$	$1(\frac{1}{2}^-)$	$\begin{pmatrix} 59.4 \\ -4.8 \end{pmatrix}$	$\begin{pmatrix} 6457.1 \\ 6393.0 \end{pmatrix}$	$\begin{pmatrix} 6461.9 \\ 6395.9 \end{pmatrix}$	
$0(\frac{3}{2}^-)$	-53.5	3008.2	3002.9	$0(\frac{3}{2}^-)$	-84.1	6313.6	6313.0	
$0(\frac{1}{2}^-)$	-187.5	2874.2	2870.4	$0(\frac{1}{2}^-)$	-126.1	6271.6	6270.6	
$ssss\bar{c}$			$ssss\bar{b}$					
$I(J^P)$	Eigenvalue	$(\bar{D}_s\Omega)$	Mass	$I(J^P)$	Eigenvalue	$(B_s\Omega)$	Mass	
$0(\frac{3}{2}^-)$	85.6	3781.6	3842.1	$0(\frac{3}{2}^-)$	109.1	7133.3	7193.0	
$0(\frac{1}{2}^-)$	192.8	3888.8	3949.9	$0(\frac{1}{2}^-)$	145.9	7170.1	7229.4	

decay patterns for the $nnnn\bar{c}$ (\bar{b}) and $ssss\bar{c}$ (\bar{b}) pentaquark states in Fig. 1.

Due to the constraint from Pauli Principle, the ground pentaquark states $nnnn\bar{Q}$ with quantum number $I(J^P) = 2(5/2^-)$, $0(5/2^-)$ and $ssss\bar{Q}$ pentaquark state with quantum number $J^P = 5/2^-$ do not exist. From Fig. 1 (a-b), we can see that in the $nnnn\bar{c}$ (\bar{b}) subsystem, the pentaquark states with the lowest and the highest masses have $J^P = 1/2^-$. Besides, by labelling pentaquark states for $I = 2, 1$, and 0 with green, red, and black lines, respectively, we can easily find that the $I = 0$ states generally have lower masses than that of the $I = 1$ $nnnn\bar{c}$ (\bar{b}) pentaquark states. In addition, the masses of $I = 1$ pentaquark states are lower than the masses of the $I = 2$ pentaquark states, our results indicate that the $nnnn\bar{c}$ (\bar{b}) states carrying lower isospin quantum number are expected to form more compact $nnnn\bar{c}$ (\bar{b}) pentaquark structures and thus have lower masses.

Now we discuss the possible decay patterns for the $nnnn\bar{c}$ (\bar{b}) and $ssss\bar{c}$ (\bar{b}) pentaquark states. Possible reference meson-baryon systems for $nnnn\bar{c}$ (\bar{b}) and $ssss\bar{c}$ (\bar{b}) pentaquark states can be obtained by rearranging their constituent quarks and regroup them into meson-baryon systems. As shown in Fig. 1 (a-d), the reference meson-baryon systems for the $nnnn\bar{c}$ (\bar{b}) pentaquark states are the $\Delta\bar{D}^*$ (ΔB^*), $\Delta\bar{D}$ (ΔB), $N\bar{D}^*$ ($N B^*$), and $N\bar{D}$ ($N B$), while the reference meson-baryon systems for $ssss\bar{c}$ (\bar{b}) are $\Omega\bar{D}_s^*$ (ΩB_s^*) and $\Omega\bar{D}_s$ (ΩB_s).

In Fig. 1, we label the spin (isospin) of the baryon-meson states with superscript (subscript). When the spin (isospin) of an initial pentaquark state is equal to the number in the superscript (subscript) of a baryon-meson state, then the pentaquark state can decay into that baryon-meson channel through S -wave. Besides, since all the $ssss\bar{Q}$ pentaquark states have isospin 0, we

do not label the isospin of $ssss\bar{c}$ (\bar{b}) pentaquark states in the diagrams (c-d) of Fig. 1.

If we only consider the pentaquark decay through S -wave strong decay channels, from Fig. 1, we can see that all the $nnnn\bar{Q}$ and $ssss\bar{Q}$ pentaquark states are higher than the lowest thresholds of the corresponding strong decay channels. Indicating that there exists no stable pentaquark state with $nnnn\bar{Q}$ and $ssss\bar{Q}$ configurations.

Indeed, the stability of $nnnn\bar{Q}$ pentaquark state has been discussed for a long time. Especially, in Ref. [107], Jaffe and Wilczek find that the Θ^+ [66] could be a bound state with two spin-0 ud diquarks in P -wave attached with an \bar{s} antiquark. Thus, they made a simple mass estimation and suggest that the states analog to the $\Theta^+(1540)$, in which the \bar{s} is replaced by a heavy antiquark, may also bound. They denote the states with flavour structures $(ud)(ud)\bar{c}$ and $(ud)(ud)\bar{b}$ as Θ_c and Θ_b states, respectively. They predict their masses as $m_{\Theta_c} \simeq 2710$ MeV and $m_{\Theta_b} \simeq 6050$ MeV, lying 100 MeV and 165 MeV below the strong decay thresholds of pD^- and nB^+ , respectively. Based on the conclusion of Ref. [107], Ref. [108] suggests that the P -wave $I(J^P) = 0(3/2^+)$ Θ_Q^* could also be stable with respect to strong interaction and can decay into $\Theta_Q\gamma$ final state. Similarly, Yongseok OH et al. investigate the pentaquark (P) exotic baryons as soliton-antiflavored heavy mesons bound states by considering the chiral symmetry and heavy quark symmetry. Their results support the existence of the loosely bound non-strange P-baryon(s) ($nnnn\bar{c}$ and $nnnn\bar{b}$) [109]. Moreover, for these subsystems, Woosung Park et al. present systematically the results of the corresponding binding energies (defined as the difference between the hyperfine interaction of the pentaquark against its lowest threshold values) in Table IV of Ref. [110]. Until now, this topic is still an open issue. In the following,

we discuss the possible decay behaviors for the $nnnn\bar{Q}$ and $ssss\bar{Q}$ pentaquark states in the framework of modified CMI model.

The eigenvectors calculated from CMI matrices will also provide important information for the decay properties of the corresponding pentaquark states. The overlap for the pentaquark with a specific baryon \otimes meson state can be calculated by transforming the eigenvectors of the pentaquark states into the baryon \otimes meson configuration. Since the $8 \otimes 8$ component inside a pentaquark should be described by the gluon exchange interaction, thus, in this work, we still focus on the pentaquark states decay into the $1 \otimes 1$ meson \otimes baryon component, i.e., the so called “Okubo-Zweig-Iizuka-superallowed” decays.

For the two body decay via L -wave process, the expression describing partial decay width can be parameterized as [85]

$$\Gamma_i = \gamma_i \alpha \frac{k^{2L+1}}{m^{2L}} \cdot |c_i|^2, \quad (18)$$

where α is an effective coupling constant, γ_i should be fixed by the decay dynamics, m is the mass of the initial state, k is the momentum of the final states in the rest frame, and c_i is the coefficient related to the corresponding meson-baryon component. For one particular pentaquark state, in order to calculate the relative branching fractions between different strong decay channels, we need to determine the coefficients c_i and γ_i . As shown in Eq. (18), for each decay mode, the decay width is proportional to the square of c_i , this quantity can be calculated from the corresponding eigenvector. Such approximation have already been applied in Refs. [87, 88]. The γ_i depends on the spatial wave functions of initial and final states, this parameter is not the same for different decay processes. In the heavy quark limit, the spatial wave functions of the ground S -wave pseudoscalar and vector meson are the same. As a rough estimation, for the two body strong decay processes of $nnnn\bar{c}$ (\bar{b}) and $ssss\bar{c}$ (\bar{b}) pentaquark states, we introduce the following approximations

$$\gamma_{\Delta\bar{D}} = \gamma_{\Delta\bar{D}^*}, \quad \gamma_{N\bar{D}} = \gamma_{N\bar{D}^*}, \quad (19)$$

$$\gamma_{\Delta B} = \gamma_{\Delta B^*}, \quad \gamma_{NB} = \gamma_{NB^*}, \quad (20)$$

and

$$\gamma_{\Omega\bar{D}_s} = \gamma_{\Omega\bar{D}_s^*}, \quad \gamma_{\Omega B_s} = \gamma_{\Omega B_s^*}. \quad (21)$$

Using the eigenvectors obtained from $nnnn\bar{c}$ (\bar{b}) and $ssss\bar{c}$ (\bar{b}) in Table XI, we calculate the values of $k \cdot |c_i|^2$ for different decay channels and present them in Table XII.

As emphasised in the above discussion, for a particular pentaquark state, we are only interested in its relative partial decay widths between different decay modes. We present our results of relative partial decay widths

for different decay modes in Table XIII for $nnnn\bar{Q}$ and $ssss\bar{Q}$ pentaquark states, respectively. Here, we use the notation $P_{\text{content}}(\text{Mass}, I, J^P)$ to label a specific pentaquark state. Besides, for a particular pentaquark state, we chose one mode as the reference decay channel and set the corresponding decay width as “1” unit, then the relative partial decay widths for the other channels can be quantitatively determined. Meanwhile, we use “ \times ” to label the corresponding decay channel is forbidden for this pentaquark. In addition, “0.0” is used to denote that the pentaquark can decay into this channel, but it has a very small relative decay width.

Here, we mainly discuss the decay behavior of $nnnn\bar{c}$ pentaquark states, one can perform very similar discussions on the decay behaviors of the $nnnn\bar{b}$, $ssss\bar{c}$, and $ssss\bar{b}$ pentaquark states.

From Table XIII and the diagram (a) of Fig. 1, we find that the $P_{n^4\bar{c}}(3487.4, 2, 1/2^-)$ state can only decay into $\Delta\bar{D}^*$ final states, while the $P_{n^4\bar{c}}(3381.4, 2, 3/2^-)$ state has two decay channels, i.e., decaying into $\Delta\bar{D}^*$ and $\Delta\bar{D}$ final states. The ratio of relative decay widths between $\Delta\bar{D}^*$ and $\Delta\bar{D}$ mode is

$$\Gamma_{\Delta\bar{D}^*} : \Gamma_{\Delta\bar{D}} = 1 : 0.9, \quad (22)$$

i.e., both the $\Delta\bar{D}^*$ and $\Delta\bar{D}$ are dominant decay channels for the $P_{n^4\bar{c}}(3381.4, 2, 3/2^-)$ pentaquark.

Due to the conservation of angular momentum, the $P_{n^4\bar{c}}(3248.5, 1, 5/2^-)$ state can decay into $\Delta\bar{D}^*$ via S -wave. The $P_{n^4\bar{c}}(3220.0, 1, 3/2^-)$ state can decay into $\Delta\bar{D}$ and $N\bar{D}^*$ final states. As presented in Tables XI and XIII, although the $\Delta\bar{D}^*$ has the largest eigenvector component, this mode is kinematically forbidden. The $P_{n^4\bar{c}}(3042.7, 1, 3/2^-)$ state can only decay into $N\bar{D}^*$ channel, due to small eigenvector component, this state is expected to be a narrow state.

For the two $I(J^P) = 1(1/2^-)$ states: $P_{n^4\bar{c}}(3157.9, 1, 1/2^-)$ and $P_{n^4\bar{c}}(3031.7, 1, 1/2^-)$, we obtain the following relative ratios of decay width

$$\Gamma_{N\bar{D}^*} : \Gamma_{N\bar{D}} = 1 : 0.1, \quad (23)$$

and

$$\Gamma_{N\bar{D}^*} : \Gamma_{N\bar{D}} = 1 : 2.0, \quad (24)$$

respectively. The dominant decay mode for the $P_{n^4\bar{c}}(3002.9, 1, 1/2^-)$ state is $N\bar{D}^*$. Besides, the $I(J^P) = 0(3/2^-)$ states $P_{n^4\bar{c}}(3002.9, 0, 3/2^-)$ and the $I(J^P) = 0(1/2^-)$ state $P_{n^4\bar{c}}(2870.4, 0, 1/2^-)$ can only decay into $N\bar{D}^*$ and $N\bar{D}$ channels, respectively.

Since the $nnnn\bar{c}$ pentaquark states have no constituent light antiquarks and have 4 valance light quarks, if such state could be observed in its two body strong decay pattern, this state must be a $nnnn\bar{c}$ pentaquark state. This property holds for all the $qqqq\bar{Q}$ pentaquark states.

In addition, for the $nnnn\bar{b}$ subsystem, the LHCb collaboration have tried to find the pentaquark signal in the $P_{B^0p}^+(uudd\bar{b}) \rightarrow J/\psi K^+\pi^-p$ weak decay mode via

TABLE XI. The eigenvectors of the $nnnn\bar{c}$, $nnnn\bar{b}$, $ssss\bar{c}$, and $ssss\bar{b}$ pentaquark states. The masses are all in units of MeV.

$I(J^P)$	Mass	$nnn \otimes n\bar{c}$				$nnn \otimes n\bar{b}$			
		$\Delta\bar{D}^*$	$\Delta\bar{D}$	$N\bar{D}^*$	$N\bar{D}$	ΔB^*	ΔB	NB^*	NB
$2(\frac{3}{2}^-)$	3381.4	0.456	-0.354			6745.6	0.456	-0.354	
$2(\frac{1}{2}^-)$	3487.4	-0.577				6779.5	-0.577		
$1(\frac{5}{2}^-)$	3248.5	0.707				6564.6	0.707		
$1(\frac{3}{2}^-)$	3220.0	-0.618	-0.450	0.168		6543.9	-0.540	-0.442	-0.078
	3042.7	-0.099	0.613	0.235		6441.2	-0.322	0.492	0.278
$1(\frac{1}{2}^-)$	3157.9	0.507		0.334	0.100	6461.9	0.556	0.255	0.174
	3031.7	0.276		0.311	-0.339	6395.9	0.154	0.379	-0.308
$0(\frac{3}{2}^-)$	3002.9			0.577		6313.0			0.577
$0(\frac{1}{2}^-)$	2870.4			-0.289	-0.500	6270.6			-0.289 -0.500
$sss \otimes s\bar{c}$									
Mass	$\Omega\bar{D}_s^*$	$\Omega\bar{D}_s$	$sss \otimes s\bar{b}$				$\Delta B_s^* \Delta B_s$		
							ΔB_s^*	ΔB_s	
$0(\frac{3}{2}^-)$	3842.1	0.456	-0.354				7193.0	0.456	-0.354
$0(\frac{1}{2}^-)$	3949.9	-0.577					7229.4	-0.577	

TABLE XII. The values of $k \cdot |c_i|^2$ for the $nnnn\bar{c}$, $nnnn\bar{b}$, $ssss\bar{c}$, and $ssss\bar{b}$ pentaquark states. The masses are all in units of MeV.

$I(J^P)$	Mass	$nnn \otimes n\bar{c}$				$nnn \otimes n\bar{b}$			
		$\Delta\bar{D}^*$	$\Delta\bar{D}$	$N\bar{D}^*$	$N\bar{D}$	ΔB^*	ΔB	NB^*	NB
$2(\frac{3}{2}^-)$	3381.4	97.1	82.9			6745.6	131.0	88.3	
$2(\frac{1}{2}^-)$	3487.4	208.4				6779.5	228.8		
$1(\frac{5}{2}^-)$	3248.5	48.7				6564.6	62.9		
$1(\frac{3}{2}^-)$	3212.0	\times	85.9	17.2		6543.9	\times	50.1	4.3
	3042.7	\times	\times	19.4		6441.2	\times	\times	42.6
$1(\frac{1}{2}^-)$	3157.9	\times		59.3	6.9	6461.9	\times		30.7 19.7
	3031.7	\times		32.0	62.5	6395.9	\times		67.8 52.2
$0(\frac{3}{2}^-)$	3002.9			88.4		6313.0			94.9
$0(\frac{1}{2}^-)$	2870.4			\times	70.4	6270.6			9.21 73.4
$sss \otimes s\bar{c}$									
Mass	$\Omega\bar{D}_s^*$	$\Omega\bar{D}_s$	$sss \otimes s\bar{b}$				$\Delta B_s^* \Delta B_s$		
							ΔB_s^*	ΔB_s	
$0(\frac{3}{2}^-)$	3842.1	68.3	76.8				7193.0	108.8	79.5
$0(\frac{1}{2}^-)$	3949.9	187.0					7229.4	202.7	

the $b \rightarrow c\bar{s}s$ transition. Their search window for $nnnn\bar{b}$ pentaquark is 4668–6220 MeV. However, no evidence for such state is found [111]. According to the diagram (b) of Fig. 1, we suggest that the LHCb collaboration can check the $nnnn\bar{b}$ pentaquark signal in the 6200–6900 MeV search window.

2. The $nnns\bar{Q}$ and $sssn\bar{Q}$ pentaquark states

Now we discuss the $nnns\bar{c}$ (\bar{b}) and $sssn\bar{c}$ (\bar{b}) pentaquark subsystems. Firstly, according to Table II, the symmetry properties of the $nnns\bar{c}$ (\bar{b}) pentaquark states with isospin $I = 3/2$ is identical to that of the $sssn\bar{c}$ (\bar{b}) pentaquark states. By interchanging the n and s quarks, the expressions of CMI matrices for the $sssn\bar{c}$ (\bar{b}) pen-

taquark states can be obtained from Table XXXVII of Appendix G.

In Table XIV, we present the mass spectrums for the $nnns\bar{c}$ (\bar{b}) and $sssn\bar{c}$ (\bar{b}) pentaquark states calculated in two schemes. In the first scheme, we use two types of meson-baryon reference systems to estimate the masses of $nnns\bar{c}$ (\bar{b}) and $sssn\bar{c}$ (\bar{b}) states. Specifically, the masses of $nnns\bar{c}$ (\bar{b}) are estimated with reference systems $\bar{D}_s + \Delta$ ($B_s + \Delta$) and $\bar{D} + \Sigma$ ($B + \Sigma$), while the masses of $sssn\bar{c}$ (\bar{b}) are estimated with reference system $\bar{D}_s + \Xi$ ($B_s + \Xi$) and $\bar{D} + \Omega$ ($B + \Omega$). The results are presented in the third and fourth columns of Table XIV.

From Table XIV, we can see that the predictions calculated from the two reference systems differ by about 100 MeV for both $nnns\bar{Q}$ and $sssn\bar{Q}$ pentaquark states. Here, we need to emphasize that as a rough estimation,

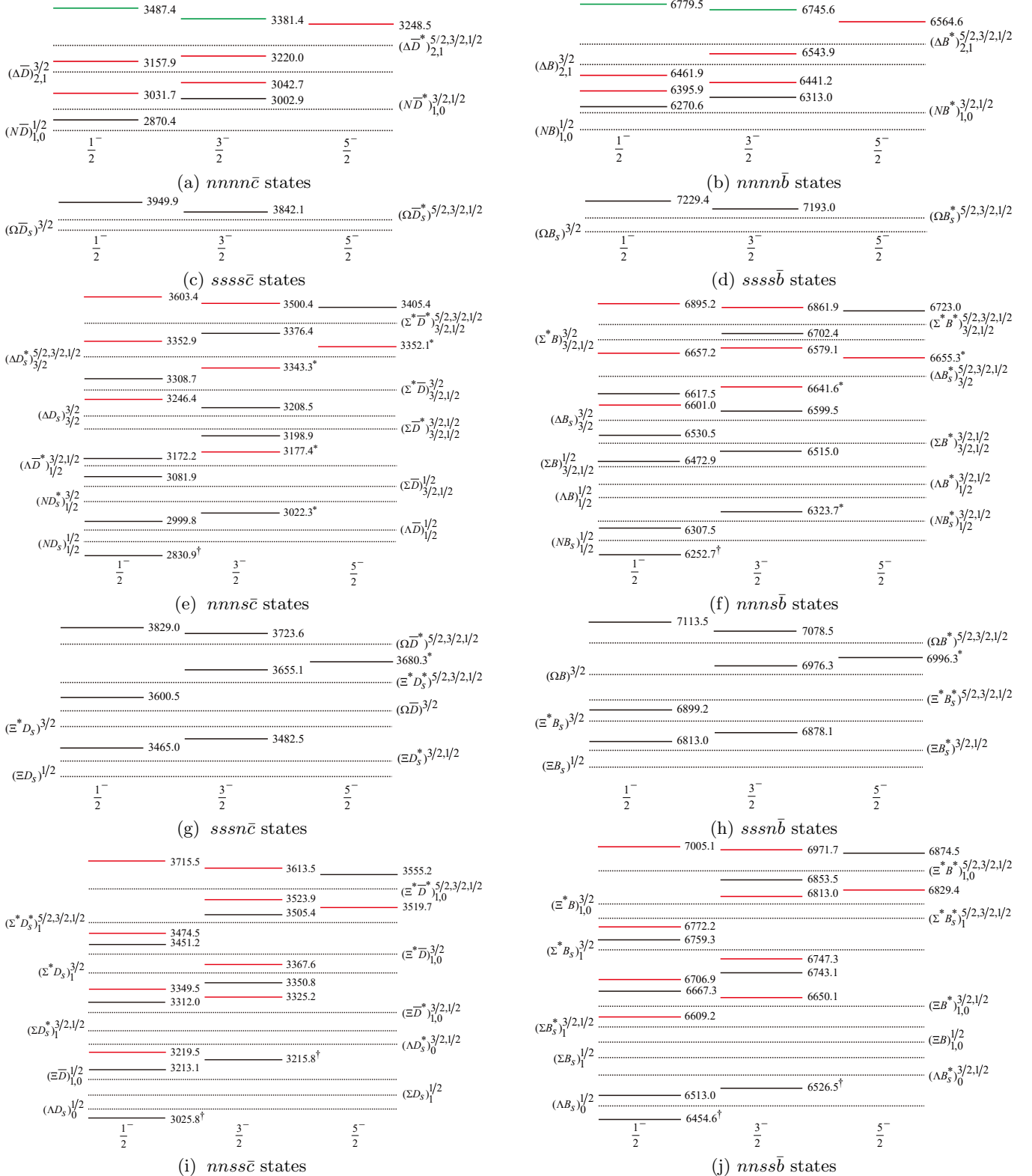


FIG. 1. Relative positions (units: MeV) for the $nnnn\bar{c}$, $nnnn\bar{b}$, $ssss\bar{c}$, $ssss\bar{b}$, $nnns\bar{c}$, $nnns\bar{b}$, $sssn\bar{c}$, $sssn\bar{b}$, $nnss\bar{c}$, and $nnss\bar{b}$ pentaquark states labeled with solid lines. In the $nnnn\bar{c}$, $nnnn\bar{b}$, $nnns\bar{c}$, and $nnns\bar{b}$ subsystems, the green, red, and black lines represent the pentaquark states with $I = 2$, $I = 1$, and $I = 0$, respectively. In the $nnns\bar{c}$ and $nnns\bar{b}$ subsystems, the red and black lines represent the pentaquark states with $I = 3/2$ and $I = 1/2$, respectively. The dotted lines denote various baryon-meson thresholds. When the spin (isospin) of an initial pentaquark state is equal to a number in the superscript (subscript) of a baryon-meson state, its decay into that baryon-meson channel through S -wave is allowed by the angular momentum (isospin) conservation. The scattering states and stable states in the modified CMI model are marked with “*” and “†”, respectively.

TABLE XIII. The relative partial widths for the $nnnn\bar{c}$, $nnnn\bar{b}$, $ssss\bar{c}$, and $ssss\bar{b}$ pentaquark states. For each pentaquark state, we choose one channel as a reference channel, and the relative partial widths for the other channels are obtained in units of the reference channel. The masses are all in units of MeV.

$I(J^P)$	Mass	$nnn \otimes n\bar{c}$				$nnn \otimes n\bar{b}$			
		$\Delta\bar{D}^*$	$\Delta\bar{D}$	$N\bar{D}^*$	$N\bar{D}$	ΔB^*	ΔB	NB^*	NB
$2(\frac{3}{2}^-)$	3381.4	1	0.9			6745.6	1	0.7	
$2(\frac{1}{2}^-)$	3487.4	1				6779.5	1		
$1(\frac{5}{2}^-)$	3248.5	1				6564.6	1		
$1(\frac{3}{2}^-)$	3220.0	\times	1	1		6543.9	\times	1	1
	3042.7	\times	\times	1		6441.2	\times	\times	1
$1(\frac{1}{2}^-)$	3157.9	\times		1	0.1	6461.9	\times	1	0.6
	3031.7	\times		1	2.0	6395.9	\times	1	0.8
$0(\frac{3}{2}^-)$	3002.9			1		6313.0			1
$0(\frac{1}{2}^-)$	2870.4		\times	1		6270.6			1
		$sss \otimes s\bar{c}$			$sss \otimes s\bar{b}$				
		Mass	$\Omega\bar{D}_s^*$	$\Omega\bar{D}_s$	Mass	ΩB_s^*	ΩB_s		
$0(\frac{3}{2}^-)$	3842.1	1	1.1		7193.0	1	0.7		
$0(\frac{1}{2}^-)$	3949.9	1			7229.4	1			

the dynamics and contributions from other terms in conventional meson and baryon potential are not elaborately considered [76] in this model. However, if one pentaquark state were observed, its partner states may be searched for with the relative positions presented in Table XIV. Such a study can be used to test our calculation. Meanwhile, we also calculate the mass spectrums of $nnns\bar{Q}$ and $sssn\bar{Q}$ in the modified CMI model (Eq. (4)) and present them in the fifth column of Table XIV.

Based on the results obtained from the modified CMI model in Table XIV, we plot the mass spectrums of the $nnns\bar{c}$, $nnns\bar{b}$, $sssn\bar{c}$, and $sssn\bar{b}$ subsystems in diagrams (e)-(h) of Fig. 1, respectively. The thresholds of relevant baryon-meson systems are also presented.

Besides the mass spectrums of the $nnns\bar{Q}$ and $sssn\bar{Q}$ subsystems, we need to extract the corresponding eigenvectors to discuss their two-body strong decay properties. The overlap for pentaquark state with a particular baryon \otimes meson basis is obtained by transforming the eigenvectors of the $nnns\bar{Q}$ pentaquark states into the $nnn \otimes s\bar{Q}$ and $nns \otimes n\bar{Q}$ bases. The eigenvectors obtained from the modified CMI model are presented in Table XL of Appendix H.

According to Table XL, we find that for the $nnns\bar{c}$ pentaquark subsystem, the $P_{n^3\bar{s}\bar{c}}(3352.1, 3/2, 5/2^-)$ state couples completely to the ΔD_s^* system, this state can be regarded as a purely $\Delta\bar{D}_s^*$ scattering state. Therefore, the $P_{n^3\bar{s}\bar{c}}(3352.1, 3/2, 5/2^-)$ state may have a broad width and is just a part of the continuum. Moreover, the $P_{n^3\bar{s}\bar{c}}(3343.3, 3/2, 3/2^-)$, $P_{n^3\bar{s}\bar{c}}(3177.4, 3/2, 3/2^-)$, and $P_{n^3\bar{s}\bar{c}}(3022.3, 1/2, 3/2^-)$ states couple almost completely to the $\Delta\bar{D}_s^*$, $\Delta\bar{D}_s$, and $N\bar{D}_s^*$ baryon-meson systems, respectively. They should be considered as the scatter-

ing states and have little chance to be found in experiment. In the following discussion, for the candidates of scattering states, we label them with “*” in all the relevant Tables and Figures. Besides, we find that the $P_{n^3\bar{s}\bar{c}}(2999.8, 1/2, 3/2^-)$ has 87.9% of $N\bar{D}_s^*$ component, and the $P_{n^3\bar{s}\bar{c}}(2830.9, 1/2, 1/2^-)$ has more than 85% of $N\bar{D}_s$ component. For such states, however, we still can not rule out the possibilities that they are genuine pentaquark states. Similarly, the candidates of scattering states in the $nnns\bar{b}$, $sssn\bar{c}$, and $sssn\bar{b}$ pentaquark subsystems are also labelled with “*” in Tables XV, XL, XLI, and Fig. 1.

After identifying the scattering states from the calculated $nnns\bar{Q}$ and $sssn\bar{Q}$ subsystems, the remaining states can be regarded as the genuine pentaquark states. In the following, we discuss the strong decay properties of these genuine pentaquarks.

From diagrams (e)-(h) of Fig. 1, we find that the $nnns\bar{c}$ (\bar{b}) subsystem has 10 possible strong decay channels, including $\Sigma^*\bar{D}^*$ (Σ^*B^*), ΔD_s^* (ΔB_s^*), $\Sigma^*\bar{D}$ (ΣB), ΔD_s (ΔB_s), $\Sigma\bar{D}^*$ (ΣB^*), $\Lambda\bar{D}^*$ (ΛB^*), $\Sigma\bar{D}$ (ΣB), $N\bar{D}_s^*$ (NB_s^*), $\Lambda\bar{D}$ (ΛB), and $N\bar{D}_s$ (NB_s). If one observed a state in these decay channels, this state would be a good candidate of $nnns\bar{Q}$ ($Q = c, b$) pentaquark state. Besides, for the $sssn\bar{c}$ and $sssn\bar{b}$ subsystems, they both have 6 possible rearrangement decay channels.

In Fig. 1, we find that the lowest $I(J^P) = 1/2(1/2^-)$ and $I(J^P) = 1/2(3/2^-)$ $nnns\bar{Q}$ states are all below the lowest allowed strong decay channels. However, from Table XL, we find that the lowest $I(J^P) = 1/2(3/2^-)$ $nnns\bar{c}$ (\bar{b}) state has quite large fraction of $N\bar{D}_s^*$ (NB_s^*) component. Thus, it is more reasonable to take this state as a scattering state. For the lowest $I(J^P) = 1/2(1/2^-)$ $nnns\bar{c}$ (\bar{b}) state, we consider it as a stable state, although it also has relatively large fraction of the color-singlet component. In Ref. [112], C Gignoux et al. also found that the states $P^0 = \bar{c}uds$ and $P^- = \bar{c}ddus$ with spin $1/2$ and their beauty analogs are very likely to be stable multiquarks. Similarly, possible stable pentaquark configurations $\bar{Q}sqqq$ were also proposed in Ref. [113]. In addition, the mass of $T_s(nnns\bar{c}, I = 1/2)$ is estimated to be $m_{T_s} \simeq 2580$ MeV in Ref. [106]. For $T_s \rightarrow D_s p$, the sum of the D_s and proton masses is 2910 MeV, i.e. the state is below the lowest meson-baryon threshold about 330 MeV. For the $R_s(nnns\bar{b}, I = 1/2)$, they have the prediction $m_{R_s} \simeq 5920$ MeV, which is 390 MeV less than the threshold of $B_s p$. Meanwhile, they find that there is no stable pentaquark in the $sssn\bar{Q}$ pentaquark subsystem.

Moreover, the $\bar{K}\bar{D}N$ three-body system with $I = 1/2$ has the minimal quark component with $uuds\bar{c}$ or $udds\bar{c}$. In Ref. [114], they find that such three-body system may form a bound state and act like a explicit “ $uuds\bar{c}$ ” pentaquark.

To extract more information about the decay behavior of $nnns\bar{Q}$ and $sssn\bar{Q}$ pentaquark states, we use the eigenvectors (see Table XL of Appendix H) to calculate $k \cdot |c_i|^2$ for each decay process and present them in Table XLI of Appendix H.

TABLE XIV. The estimated masses for the $nnns\bar{Q}$, $sssn\bar{Q}$, and $nnss\bar{Q}$ ($n = u, d$; $Q = c, b$) subsystems in units of MeV. The values in the second column are eigenvalues obtained with the CMI Hamiltonian in Eq. (2). The masses in the third, fourth, and fifth columns are obtained with two kinds of meson-baryon thresholds in Eq. (3) and the modified CMI model in Eq. (4), respectively.

$nnns\bar{c}$					$nnns\bar{b}$				
$I(J^P)$	Eigenvalue	$(\bar{D}_s\Delta)$	$(\bar{D}\Sigma)$	Mass	$I(J^P)$	Eigenvalue	$(B_s\Delta)$	$(B\Sigma)$	Mass
$\frac{3}{2}(\frac{5}{2}^-)$	182.9 (252.0)	3343.2 (3412.3)	3432.4 (3501.5)	3352.1 (3500.4)	$\frac{3}{2}(\frac{5}{2}^-)$	159.5 (276.2)	6648.0 (6764.7)	6745.0 (6861.7)	6655.3 (6861.9)
$\frac{3}{2}(\frac{3}{2}^-)$	169.9 -0.4	3330.2 (3159.9)	3419.4 (3249.1)	3343.3 (3177.4)	$\frac{3}{2}(\frac{3}{2}^-)$	142.0 68.4	6630.5 (6557.0)	6727.5 (6654.0)	6641.6 (6579.1)
$\frac{3}{2}(\frac{1}{2}^-)$	359.1 139.1 23.7	3519.4 (3299.4)	3608.6 (3388.6)	3603.2 (3353.0)	$\frac{3}{2}(\frac{1}{2}^-)$	310.5 98.5 52.8	6799.0 (6587.1) (6541.3)	6896.0 (6684.1) (6638.3)	6895.2 (6657.2) (6601.0)
$\frac{1}{2}(\frac{5}{2}^-)$	146.9 (122.3)	3307.2 (3282.6)	3396.4 (3371.8)	3405.4 (3376.4)	$\frac{1}{2}(\frac{5}{2}^-)$	122.3 (102.9)	6610.8 (6591.4)	6707.8 (6688.4)	6723.1 (6702.4)
$\frac{1}{2}(\frac{3}{2}^-)$	-31.8 -52.1 -146.8	3128.5 (3108.2)	3217.7 (3197.4)	3208.5 (3198.8)	$\frac{1}{2}(\frac{3}{2}^-)$	9.6 -62.4 -175.8	6498.1 (6426.1) (6312.7)	6595.1 (6523.1) (6409.7)	6599.5 (6515.0) (6323.7)
$\frac{1}{2}(\frac{1}{2}^-)$	67.9 -58.3 -146.7 -179.5 -349.1	3228.3 (3102.1)	3317.5 (3191.3)	3308.7 (3172.2)	$\frac{1}{2}(\frac{1}{2}^-)$	31.0 -33.5 -104.6 -195.2 -254.9	6519.5 (6455.0) (6383.9) (6293.3) (6233.6)	6616.5 (6552.0) (6480.9) (6390.3) (6330.6)	6617.1 (6530.5) (6472.9) (6307.5) (6252.7)
$sssn\bar{c}$					$sssn\bar{b}$				
$I(J^P)$	Eigenvalue	$(\bar{D}_s\Xi)$	$(\bar{D}\Omega)$	Mass	$I(J^P)$	Eigenvalue	$(B_s\Xi)$	$(B\Omega)$	Mass
$\frac{1}{2}(\frac{5}{2}^-)$	87.7 (140.9)	3593.1 (3646.3)	3685.1 (3738.3)	3680.3 (3723.6)	$\frac{1}{2}(\frac{5}{2}^-)$	63.2 (164.6)	6896.7 (6998.1)	6996.6 (7098.0)	6996.3 (7078.5)
$\frac{1}{2}(\frac{3}{2}^-)$	71.2 -100.1	3576.5 (3405.3)	3668.6 (3497.3)	3655.1 (3482.5)	$\frac{1}{2}(\frac{3}{2}^-)$	46.4 -32.1	6879.9 (6801.4)	6979.8 (6901.3)	6976.3 (6878.1)
$\frac{1}{2}(\frac{1}{2}^-)$	248.0 31.4 -90.8	3753.3 (3536.8)	3845.4 (3628.8)	3829.0 (3600.5)	$\frac{1}{2}(\frac{1}{2}^-)$	200.5 -6.3 -65.5	7034.1 (6827.2) (6768.0)	7133.9 (6927.1) (6867.9)	7113.5 (6899.2) (6813.0)
$nnss\bar{c}$					$nnss\bar{b}$				
$I(J^P)$	Eigenvalue	$(\bar{D}_s\Sigma)$	$(\bar{D}\Xi)$	Mass	$I(J^P)$	Eigenvalue	$(B_s\Sigma)$	$(B\Xi)$	Mass
$1(\frac{5}{2}^-)$	135.2 (196.4)	3483.2 (3544.4)	3541.9 (3603.1)	3519.7 (3613.5)	$1(\frac{5}{2}^-)$	111.2 (220.3)	6787.5 (6896.4)	6853.9 (6963.0)	6829.4 (6971.7)
$1(\frac{3}{2}^-)$	120.4 -20.8 -50.8	3468.5 (3327.2)	3527.1 (3385.9)	3505.4 (3367.6)	$1(\frac{3}{2}^-)$	94.0 18.3 -51.4	6770.3 (6694.5) (6624.9)	6836.7 (6761.0) (6691.3)	6813.0 (6747.3) (6650.1)
$1(\frac{1}{2}^-)$	303.4 85.0 -33.6 -155.3	3651.5 (3433.1)	3710.1 (3491.7)	3715.5 (3474.4)	$1(\frac{1}{2}^-)$	255.4 46.1 -6.4 -95.5	6931.7 (6722.3) (6669.9) (6580.8)	6998.1 (6788.8) (6736.3) (6647.2)	7005.1 (6772.2) (6706.9) (6609.2)
$0(\frac{5}{2}^-)$	57.6 (89.0)	3405.6 (3437.0)	3464.3 (3495.7)	3555.2 (3523.9)	$0(\frac{5}{2}^-)$	69.6 (68.1)	6745.9 (6744.3)	6812.3 (6810.8)	6874.5 (6853.5)
$0(\frac{3}{2}^-)$	-83.1 -168.0 38.7	3264.9 (3180.0)	3323.6 (3238.7)	3350.8 (3215.8)	$0(\frac{3}{2}^-)$	-20.1 -197.0 1.9	6656.2 (6479.3) (6678.2)	6722.6 (6545.7) (6744.6)	6743.1 (6526.5) (6759.3)
$0(\frac{1}{2}^-)$	-87.1 -170.6 -365.9	3260.9 (3177.4)	3319.6 (3236.1)	3312.0 (3213.1)	$0(\frac{1}{2}^-)$	-62.7 -207.8 -268.0	6613.5 (6468.4) (6408.3)	6680.0 (6534.9) (6474.7)	6667.3 (6513.0) (6454.6)

In the heavy quark limit, the spatial wave functions of the ground pseudoscalar and vector meson are the same. Similarly, the Σ (Ξ) and Σ^* (Ξ^*) have the same spatial wave function. Thus, for each of the $nnns\bar{Q}$ and $sssn\bar{Q}$ pentaquark state, we use the following approximations

$$\gamma_{\Delta\bar{D}_s} = \gamma_{\Delta\bar{D}_s^*}, \quad \gamma_{N\bar{D}_s} = \gamma_{N\bar{D}_s^*}, \quad (25)$$

$$\gamma_{\Delta B_s} = \gamma_{\Delta B_s^*}, \quad \gamma_{N B_s} = \gamma_{N B_s^*}, \quad (26)$$

$$\gamma_{\Sigma^*\bar{D}} = \gamma_{\Sigma^*\bar{D}^*} \approx \gamma_{\Sigma\bar{D}^*} = \gamma_{\Sigma\bar{D}}, \quad \gamma_{\Lambda\bar{D}} = \gamma_{\Lambda\bar{D}^*}, \quad (27)$$

$$\gamma_{\Sigma^*B} = \gamma_{\Sigma^*B^*} \approx \gamma_{\Sigma B^*} = \gamma_{\Sigma B}, \quad \gamma_{\Lambda B^*} = \gamma_{\Lambda B}, \quad (28)$$

for $nnns\bar{Q}$ pentaquark states, and

$$\gamma_{\Omega\bar{D}} = \gamma_{\Omega\bar{D}^*}, \quad \gamma_{\Omega B} = \gamma_{\Omega B^*}, \quad (29)$$

$$\gamma_{\Xi^*\bar{D}_s} = \gamma_{\Xi^*\bar{D}_s^*} \approx \gamma_{\Xi\bar{D}_s^*} = \gamma_{\Xi\bar{D}_s}, \quad (30)$$

$$\gamma_{\Xi^*B_s} = \gamma_{\Xi^*B_s^*} \approx \gamma_{\Xi B_s^*} = \gamma_{\Xi B_s}, \quad (31)$$

for $sssn\bar{Q}$ pentaquark states.

With the above relations, we calculate the relative partial decay widths for $nnns\bar{Q}$ and $sssn\bar{Q}$ pentaquark states and present them in Table XV. Similarly, we mainly discuss the decay behavior of the $nnns\bar{c}$ pentaquark subsystem.

For the $I(J^P) = 1/2(5/2^-)$ state, the $P_{n^3\bar{s}\bar{c}}(3405.4, 1/2, 5/2^-)$ can decay into $\Sigma_c^*\bar{D}^*$ final states via S -wave. Besides, the decay widths for $P_{n^3\bar{s}\bar{c}}(3405.4, 1/2, 5/2^-)$ into other higher partial wave channels are suppressed.

Other pentaquark states all have two types of decay mode: $nnn - s\bar{c}$ and $nns - n\bar{c}$. As the only genuine pentaquark state with quantum number $I(J^P) = 3/2(3/2^-)$, the $P_{n^3\bar{s}\bar{c}}(3500.4, 3/2, 3/2^-)$ has two $nnn - s\bar{c}$ decay channels, namely $\Delta\bar{D}_s$ and $\Delta\bar{D}_s^*$. The corresponding relative partial decay widths are

$$\Gamma_{\Delta\bar{D}_s^*} : \Gamma_{\Delta\bar{D}_s} = 1 : 1.9, \quad (32)$$

On the other hand, as shown in Table XV, the $P_{n^3\bar{s}\bar{c}}(3500.4, 3/2, 3/2^-)$ state also has three $nns - n\bar{c}$ decay modes. Their relative partial decay widths are

$$\Gamma_{\Sigma^*\bar{D}^*} : \Gamma_{\Sigma^*\bar{D}} : \Gamma_{\Sigma\bar{D}^*} = 20.5 : 15.6 : 1. \quad (33)$$

Our results suggest that the $\Sigma^*\bar{D}$ and $\Sigma^*\bar{D}^*$ are the dominant decay modes for the $P_{n^3\bar{s}\bar{c}}(3500.4, 3/2, 3/2^-)$ state.

Moreover, for the $nnn - s\bar{c}$ decay mode, the three genuine $I(J^P) = 1/2(3/2^-)$ pentaquark states have only one allowed decay channel $N\bar{D}_s^*$. While for the $nns - n\bar{c}$ decay mode, the three $I(J^P) = 1/2(3/2^-)$ pentaquark states can decay freely to the $\Lambda\bar{D}^*$ final states. Note that the spatial wave function of Λ baryon is different from that of the Σ and Σ^* baryons, we can not directly calculate

the ratios of relative partial decay widths between the decay channels with Λ and Σ (Σ^*) in the final states. For the $P_{n^3\bar{s}\bar{c}}(3208.5, 1/2, 3/2^-)$ and $P_{n^3\bar{s}\bar{c}}(3198.9, 1/2, 3/2^-)$ states, they have the same quantum numbers and similar masses, but we can use the allowed decay channels to distinguish them. As presented in Table XV, the $P_{n^3\bar{s}\bar{c}}(3208.5, 1/2, 3/2^-)$ can decay into the $\Sigma\bar{D}^*$, while this channel is forbidden for the $P_{n^3\bar{s}\bar{c}}(3198.9, 1/2, 3/2^-)$. Besides, the relative partial decay width ratio for the $P_{n^3\bar{s}\bar{c}}(3376.4, 1/2, 3/2^-)$ is

$$\Gamma_{\Sigma^*\bar{D}} : \Gamma_{\Sigma\bar{D}^*} = 10.1 : 1. \quad (34)$$

Thus, the dominant decay channel for $P_{n^3\bar{s}\bar{c}}(3376.4, 1/2, 3/2^-)$ is the $\Sigma^*\bar{D}$ channel in $nns - n\bar{c}$ decay mode.

For the five $I(J^P) = 1/2(1/2^-)$ pentaquark states, all of them can be considered as genuine pentaquark states. The lowest state $P_{n^3\bar{s}\bar{c}}(2830.9, 1/2, 1/2^-)$ is expected to be a stable pentaquark state. For the $P_{n^3\bar{s}\bar{c}}(3308.7, 1/2, 1/2^-)$ state, we find

$$\Gamma_{N\bar{D}_s^*} : \Gamma_{N\bar{D}_s} = 1 : 0.1, \quad (35)$$

and

$$\Gamma_{\Sigma\bar{D}^*} : \Gamma_{\Sigma\bar{D}} = 1 : 0.1, \quad \Gamma_{\Lambda\bar{D}^*} : \Gamma_{\Lambda\bar{D}} = 1 : 0.2. \quad (36)$$

Similarly, for the $P_{n^3\bar{s}\bar{c}}(3172.2, 1/2, 1/2^-)$ and $P_{n^3\bar{s}\bar{c}}(3081.9, 1/2, 1/2^-)$ states, we have:

$$\Gamma_{N\bar{D}_s^*} : \Gamma_{N\bar{D}_s} = 1 : 2.3, \quad \Gamma_{\Lambda\bar{D}^*} : \Gamma_{\Lambda\bar{D}} = 1 : 2.0, \quad (37)$$

and

$$\Gamma_{N\bar{D}_s^*} : \Gamma_{N\bar{D}_s} = 1 : 4.3, \quad (38)$$

respectively. Meanwhile, they both decay into $\Sigma\bar{D}$ channel in the $nns - n\bar{c}$ decay mode. These two pentaquark states may have broad widths since they can decay freely to many strong decay channels.

3. The $nnss\bar{Q}$ pentaquark states

For the $nnss\bar{Q}$ ($Q = c, b$) pentaquark subsystem, the isospin of the first two light quarks can couple to $I = 0, 1$. The expressions of CMI Hamiltonian for the $nnss\bar{Q}$ subsystem are collected in Tables XXXVII and XXXVIII of Appendix G. By substituting the corresponding parameters from Table VI, we obtain the mass spectrums for the $nnss\bar{c}$ (\bar{b}) pentaquark states and present them in Table XIV.

The constituent quarks in the $nnss\bar{Q}$ subsystem can regroup into $s\bar{Q} \otimes nns$ and $n\bar{Q} \otimes ssn$ meson-baryon decay modes. Thus, for $nnss\bar{c}$ (\bar{b}) pentaquark states, we use two types of meson-baryon reference systems to estimate their masses, i.e., $\bar{D}_s + \Sigma$ ($B_s + \Sigma$) and $\bar{D} + \Xi$ ($B + \Xi$). We present the corresponding results in the third and fourth columns of Table XIV. Meanwhile, we also obtain the

TABLE XV. The relative partial decay widths for the $nnns\bar{c}$, $nnns\bar{b}$, $sssn\bar{c}$, $sssn\bar{b}$, $nnss\bar{c}$, and $nnss\bar{b}$ pentaquark states. For each pentaquark state, we choose one channel as a reference channel, and the relative partial decay widths for the other channels are obtained in units of the reference channel. The masses are all in units of MeV. The scattering states and stable states in the modified CMI model are marked with “*” and “†”, respectively.

		$nnn \otimes s\bar{c}$				$nns \otimes n\bar{c}$						$nnn \otimes s\bar{b}$				$nns \otimes n\bar{b}$			
$I(J^P)$	Mass	$\Delta\bar{D}_s^*$	$\Delta\bar{D}_s$	$\Sigma^*\bar{D}^*$	$\Sigma^*\bar{D}$	$\Sigma\bar{D}^*$	$\Sigma\bar{D}$	$\Lambda\bar{D}^*$	$\Lambda\bar{D}$	Mass	ΔB_s^*	ΔB_s	Σ^*B^*	Σ^*B	ΣB^*	ΣB	ΛB^*	ΛB	
$\frac{3}{2}(\frac{5}{2}^-)$	3352.1*	1		\times						6655.3*	1		\times						
$\frac{3}{2}(\frac{3}{2}^-)$	3500.4	1	1.9	20.5	15.6	1				6861.9	1	0.8	25.9	16.9	1				
	3343.3*	\times	1	\times	0.3	1				6641.6*	\times	1	\times	\times	1				
	3177.4*	\times	\times	\times	\times	\times				6579.1	\times	\times	\times	\times	1				
$\frac{3}{2}(\frac{1}{2}^-)$	3603.2	1		223.9		1	1			6895.2	1		147.8		1	1.9			
	3352.9	1			\times	1	0.008			6657.2	1		\times	1	0.1				
	3246.4	\times				\times	1	4.5		6601.0	\times		\times	1	\times				
	$N\bar{D}_s^*$		$N\bar{D}_s$								NB_s^*		NB_s						
$\frac{1}{2}(\frac{5}{2}^-)$	3405.4			1						6723.1			1						
$\frac{1}{2}(\frac{3}{2}^-)$	3376.4	1		\times	10.1	1				6702.4	1		\times	87.2	1		1		
	3208.5	1		\times	\times	1				6599.5	1		\times	\times	1		1		
	3198.9	1		\times	\times	\times				6515.0	1		\times	\times	\times	1			
	3022.3*	\times		\times	\times	\times				6323.7*	\times		\times	\times	\times	\times			
$\frac{1}{2}(\frac{1}{2}^-)$	3308.7	1	0.1	\times		1	0.1	1	0.2	6617.5	1	0.6	\times		1	0.5	1	1.0	
	3172.2	1	2.3	\times		\times	1	1	2.6	6530.5	1	0.6	\times		1	0.5	1	0.9	
	3081.9	1	4.3	\times		\times	1	\times	1	6472.9	1	28.0	\times		\times	1	1	2.7	
	2999.8	\times	1	\times		\times	\times	\times	1	6307.5	\times	1	\times	\times	\times	\times	\times	\times	
	2830.9 [†]	\times	\times	\times		\times	\times	\times	\times	6252.7 [†]	\times	\times	\times	\times	\times	\times	\times	\times	
			$sss \otimes n\bar{c}$				$ssn \otimes s\bar{c}$						$sss \otimes n\bar{b}$				$ssn \otimes s\bar{b}$		
$I(J^P)$	Mass	$\Omega\bar{D}^*$	$\Omega\bar{D}$	$\Xi^*\bar{D}_s^*$	$\Xi^*\bar{D}_s$	$\Xi\bar{D}_s^*$	$\Xi\bar{D}_s$			Mass	ΩB^*	ΩB	$\Xi^*B_s^*$	Ξ^*B_s	ΞB_s^*	ΞB_s			
$\frac{1}{2}(\frac{5}{2}^-)$	3680.3*	\times		1						6996.3*	\times		1						
$\frac{1}{2}(\frac{3}{2}^-)$	3723.6	1	0.6	14.8	19.8	1				7078.5	1	0.6	28.9	22.1	1				
	3655.1	\times	1	0.6	0.03	1				6976.3	\times	1	0.7	0.4	1				
	3482.5	\times	\times	\times	\times	1				6878.1	\times	\times	\times	\times	1				
$\frac{1}{2}(\frac{1}{2}^-)$	3829.0	1		352.8		1	1.2			7113.5	1		230.0		1	2.3			
	3600.5	\times		\times		1	0.2			6899.2	\times		\times	1	0.7				
	3465.0	\times		\times		1	2.3			6813.0	\times		\times	1	0.7				
			$nns \otimes s\bar{c}$				$ssn \otimes n\bar{c}$						$nns \otimes s\bar{b}$				$ssn \otimes n\bar{b}$		
$I(J^P)$	Mass	$\Sigma^*\bar{D}_s^*$	$\Sigma^*\bar{D}_s$	$\Sigma\bar{D}_s^*$	$\Sigma\bar{D}_s$	$\Xi^*\bar{D}^*$	$\Xi^*\bar{D}$	$\Xi\bar{D}^*$	$\Xi\bar{D}$	Mass	$\Sigma^*B_s^*$	Σ^*B_s	ΣB_s^*	ΣB_s	Ξ^*B^*	Ξ^*B	ΞB^*	ΞB	
$1(\frac{5}{2}^-)$	3519.7	1				\times				6829.4	1						\times		
$1(\frac{3}{2}^-)$	3613.5	20.9	35.0	1		11.4	7.6	1		6971.7	20.9	35.0	1			15.4	9.7	1	
	3505.4	3.7	0.1	1		\times	0.6	1		6813.0	3.7	0.1	1			\times	0.4	1	
	3367.2	\times	0.4	1		\times	\times	1		6747.3	\times	0.4	1			\times	\times	1	
	3325.2	\times	\times	1		\times	\times	\times		6650.1	\times	\times	1			\times	\times	1	
$1(\frac{1}{2}^-)$	3715.5	217.7		1	0.9	143.8		1	1.6	7005.1	217.7		1	0.9	109.8		1	2.3	
	3474.5	\times		1	0.05	\times		1	0.2	6772.2	\times		1	0.05	\times		1	0.8	
	3349.5	\times		1	1.5	\times		1	4.6	6706.9	\times		1	1.5	\times		1	1.2	
	3219.5	\times		\times	1	\times		\times	1	6609.2	\times		\times	1	\times		\times	1	
			$\Lambda\bar{D}_s^*$				$\Lambda\bar{D}_s$						ΛB_s^*						
$0(\frac{5}{2}^-)$	3555.2			1						6874.5						1			
$0(\frac{3}{2}^-)$	3523.9	1				\times	7.5	1		6853.5	1					\times	17.4	1	
	3350.8	1				\times	\times	1		6743.1	1					\times	\times	1	
	3215.8 [†]	\times				\times	\times	\times		6526.5 [†]	\times					\times	\times		
$0(\frac{1}{2}^-)$	3451.2	1	0.2			\times		1	0.2	6759.3	1	0.2				\times	1	0.9	
	3312.0	1	3.2			\times		\times	1	6667.3	1	3.2				\times	1	0.8	
	3213.1	\times	1			\times		\times	1	6513.0	\times	1				\times	\times		
	3025.8 [†]	\times	\times			\times		\times	\times	6454.6 [†]	\times	\times				\times	\times		

mass spectrums of the $n n s s \bar{c}$ (\bar{b}) pentaquark subsystem with the modified CMI model in Eq. (4) and present them in the fifth column of Table XIV.

Here, we use the same procedure introduced in Sec. VIA 1 to calculate the overlap for a particular $n n s s \bar{Q}$ pentaquark state with the corresponding baryon \otimes meson bases. The eigenvectors are obtained under the $n n s \otimes s \bar{Q}$ and $s s n \otimes n \bar{Q}$ color singlet bases. We present the corresponding results in Table XL of Appendix H.

From Table XL, we find that there is no definite scattering states in the $n n s s \bar{Q}$ subsystem. The $P_{n^2 s^2 \bar{c}}(3555.2, 0, 5/2^-)$ and $P_{n^2 s^2 \bar{b}}(6874.5, 0, 5/2^-)$ both have more than 80% of $\Xi^* \bar{D}^*$ and $\Xi^* B^*$ components, respectively. However, we still cannot rule out the possibility that they are genuine pentaquark states.

Based on the results of mass spectrums obtained from the modified CMI model in Table XIV, we plot the mass spectrums of the $n n s s \bar{c}$ and $n n s s \bar{b}$ pentaquark subsystems in Fig. 1, the relevant thresholds of possible decay patterns are also labelled in the diagrams (i)-(j) of Fig. 1. When checking the diagram (i)-(j) of Fig. 1, we find that the $n n s s \bar{c}$ (\bar{b}) subsystem has 10 possible rearrangement decay channels, including $\Xi^* \bar{D}^*$ ($\Xi^* B^*$), $\Sigma^* D_s^*$ ($\Sigma^* B_s^*$), $\Xi^* \bar{D}$ ($\Xi^* B$), $\Sigma^* D_s$ ($\Sigma^* B_s$), $\Xi \bar{D}^*$ (ΞB^*), $\Sigma^* D_s^*$ ($\Sigma^* B_s^*$), ΛD_s^* (ΛB_s^*), $\Xi \bar{D}$ (ΞB), $\Sigma^* D_s$ ($\Sigma^* B_s$), and ΛD_s (ΛB_s). Especially, We find that the lowest $I(J^P) = 0(1/2^-)$ and $I(J^P) = 0(3/2^-)$ $n n s s \bar{Q}$ pentaquark states are below all allowed strong decay channels in the $n n s s \bar{Q}$ pentaquark subsystem. Thus, in our model, they should be considered as good stable pentaquark states. Our results is consistent with a pioneer CMI model calculation in Ref. [112]. Moreover, based on a antiquark-diquark-diquark model, Ref. [106] predict that the masses of stable pentaquark states $n n s s \bar{c}$ and $n n s s \bar{b}$ are $m_{T_{ss}}(n n s s \bar{c}, I=0) \simeq 2770$ MeV and $m_{R_{ss}}(n n s s \bar{b}, I=0) \simeq 6100$ MeV, respectively.

To achieve a quantitative understanding of S -wave strong decay behaviors for $n n s s \bar{Q}$ pentaquark states, we use Eq. (18) to calculate roughly the relative decay widths for all $n n s s \bar{Q}$ pentaquark states. The eigenvectors (see Table XL) are used to calculate the value of $k \cdot |c_i|^2$ for the corresponding decay processes of each $n n s s \bar{Q}$ pentaquark state and present them in Table XLI of Appendix H. Besides, the following approximations are applied to determine the parameter γ_i

$$\gamma_{\Sigma^* \bar{D}_s^*} = \gamma_{\Sigma^* \bar{D}_s} \approx \gamma_{\Sigma \bar{D}_s^*} = \gamma_{\Sigma \bar{D}_s}, \quad \gamma_{\Lambda \bar{D}_s} = \gamma_{\Lambda \bar{D}_s^*}, \quad (39)$$

and

$$\gamma_{\Xi^* \bar{D}^*} = \gamma_{\Xi^* \bar{D}} = \gamma_{\Xi \bar{D}^*} = \gamma_{\Xi \bar{D}}. \quad (40)$$

Similar approximations can also be applied to the $n n s s \bar{b}$ pentaquark states, i.e.,

$$\gamma_{\Sigma^* B_s^*} = \gamma_{\Sigma^* B_s} \approx \gamma_{\Sigma B_s^*} = \gamma_{\Sigma D_s}, \quad \gamma_{\Lambda B_s} = \gamma_{\Lambda B_s^*}, \quad (41)$$

and

$$\gamma_{\Xi^* B^*} = \gamma_{\Xi^* B} = \gamma_{\Xi B^*} = \gamma_{\Xi B}. \quad (42)$$

The calculated relative partial decay widths are listed in Table XV.

The mass spectrum and decay behavior of the $n n s s \bar{b}$ pentaquark subsystem is very similar to that of the $n n s s \bar{c}$ pentaquark subsystem. We also present the relative partial decay widths for $n n s s \bar{b}$ pentaquark states in Table XV. The corresponding eigenvectors, values of $k \cdot |c_i|^2$ are presented in Tables XL and XLI of Appendix H, respectively.

For convenience, we mainly discuss the decay behaviors of $n n s s \bar{c}$ pentaquark states, one can perform similar discussion on the $n n s s \bar{b}$ pentaquark subsystem. For the $n n s s \bar{c}$ pentaquark states with $I = 1$, the mass of $P_{n^2 s^2 \bar{c}}(3519.7, 1, 5/2^-)$ is below $\Xi^* \bar{D}_s^*$ threshold, this state can only decay into $\Sigma^* \bar{D}_s^*$ final states. In addition, this state should have a narrow width due to its small phase space.

The lowest $I(J^P) = 1(3/2^-)$ state $P_{n^2 s^2 \bar{c}}(3325.2, 1, 3/2^-)$ can only decay into $\Sigma \bar{D}_s^*$ final states, in our calculation, this pentaquark state is also considered as a narrow state. However, note that $P_{n^2 s^2 \bar{c}}(3325.2, 1, 3/2^-)$ is slightly above the threshold of $\Sigma \bar{D}_s^*$ channel, considering the uncertainty of parameters introduced in our modified CMI model, we still can not rule out the probability that the $P_{n^2 s^2 \bar{c}}(3325.2, 1, 3/2^-)$ might be a stable state.

For other $I(J^P) = 1(3/2^-)$ $n n s s \bar{c}$ pentaquark states, the $P_{n^2 s^2 \bar{c}}(3613.5, 1, 3/2^-)$ has

$$\Gamma_{\Sigma^* \bar{D}_s^*} : \Gamma_{\Sigma^* \bar{D}_s} : \Gamma_{\Sigma \bar{D}_s^*} = 20.9 : 35.0 : 1, \quad (43)$$

and

$$\Gamma_{\Xi^* \bar{D}^*} : \Gamma_{\Xi^* \bar{D}} : \Gamma_{\Xi \bar{D}^*} = 11.4 : 7.6 : 1. \quad (44)$$

Thus, the dominant decay channels for the $P_{n^2 s^2 \bar{c}}(3613.5, 1, 3/2^-)$ are $\Sigma^* \bar{D}_s$ and $\Sigma^* \bar{D}_s^*$ in $n n s - s \bar{c}$ decay mode. Similarly, in $n n s - n \bar{c}$ decay mode, the dominant decay channels are $\Xi^* \bar{D}^*$ and $\Xi^* \bar{D}$. In addition, the $P_{n^2 s^2 \bar{c}}(3505.4, 1, 3/2^-)$ and $P_{n^2 s^2 \bar{c}}(3367.2, 1, 3/2^-)$ have various two-body strong decay channels, they are expected to be broad states.

For the $n n s s \bar{c}$ pentaquark states with $I(J^P) = 1(1/2^-)$, they all have several two-body strong decay channels. Especially, the $P_{n^2 s^2 \bar{c}}(3715.5, 1, 1/2^-)$ has two dominant decay channels, i.e., $\Sigma^* \bar{D}_s^*$ and $\Xi^* \bar{D}^*$, the widths of these two channels are much larger than that of $\Sigma \bar{D}_s$, $\Sigma \bar{D}_s^*$, $\Xi \bar{D}^*$, and $\Xi \bar{D}$ channels.

For the $n n s s \bar{c}$ pentaquark states with $I = 0$, the $P_{n^2 s^2 \bar{c}}(3555.2, 0, 5/2^-)$ can only decay into $\Xi^* \bar{D}_s^*$ via S -wave. The angular momentum conservation suppress the rate of $P_{n^2 s^2 \bar{c}}(3555.2, 0, 5/2^-)$ decay via higher partial waves. This state only have $n n s - s \bar{c}$ decay mode. For the states with $I(J^P) = 0(3/2^-)$, they can only decay into $\Lambda \bar{D}_s$ channel in $n n s - s \bar{c}$ mode. In $s s n - n \bar{c}$ decay mode, for the $P_{n^2 s^2 \bar{c}}(3523.9, 0, 3/2^-)$ state, we have

$$\Gamma_{\Xi^* \bar{D}^*} : \Gamma_{\Xi^* \bar{D}} : \Gamma_{\Xi \bar{D}^*} = 0 : 7.5 : 1, \quad (45)$$

suggesting that the relative partial decay width of $\Xi^* \bar{D}$ channel is much larger than that of the $\Xi \bar{D}^*$ channel.

The $P_{n^2s^2\bar{c}}(3350.8, 0, 3/2^-)$ state can decay into $\Sigma^*\bar{D}_s^*$ and $\Xi\bar{D}^*$ channels for $ssn-n\bar{c}$ and $snn-s\bar{c}$ decay modes, respectively. In addition, in the modified CMI model, we also find a stable state $P_{n^2s^2\bar{c}}(3215.8, 0, 3/2^-)$, which is below all possible strong decay channels.

For $I(J^P) = 0(1/2^-)$ $nnss\bar{c}$ pentaquark states, the lowest $I(J^P) = 0(1/2^-)$ state is expected to be a stable state. For the $P_{n^2s^2\bar{c}}(3312.0, 0, 1/2^-)$ state, we find that

$$\Gamma_{\Lambda\bar{D}_s^*} : \Gamma_{\Lambda\bar{D}_s} = 1 : 3.2, \quad (46)$$

and for the $P_{n^2s^2\bar{c}}(3451.2, 0, 1/2^-)$ state, we have

$$\Gamma_{\Lambda\bar{D}_s^*} : \Gamma_{\Lambda\bar{D}_s} = 1 : 0.2, \quad (47)$$

and

$$\Gamma_{\Xi\bar{D}^*} : \Gamma_{\Xi\bar{D}} = 1 : 0.2. \quad (48)$$

B. The $qqqQ\bar{q}$ pentaquark states

In this subsection, we study the pentaquark system with $qqqQ\bar{q}$ configuration. As shown in Table I, this pentaquark system includes $nnnc\bar{n}$ (\bar{s}), $nnnb\bar{n}$ (\bar{s}), $nnsc\bar{n}$ (\bar{s}), $nnsb\bar{n}$ (\bar{s}), $ssnc\bar{n}$ (\bar{s}), $ssnb\bar{n}$ (\bar{s}), $sssc\bar{n}$ (\bar{s}), and $sssb\bar{n}$ (\bar{s}) flavor configurations.

As shown in Table II, the $qqqQ\bar{q}$ pentaquark system can be divided into two groups according to its symmetry property: (1) the $nnnQ\bar{n}$ (\bar{s}) and $sssQ\bar{n}$ (\bar{s}) pentaquark subsystems, (2) the $nnsQ\bar{n}$ (\bar{s}) and $ssnQ\bar{n}$ (\bar{s}) pentaquark subsystems. Especially, among the above $qqqQ\bar{q}$ pentaquark subsystems, the subsystems with $nnnQ\bar{s}$, $sssQ\bar{n}$, $nnnQ\bar{n}$ ($I = 2$), $nnsQ\bar{n}$ ($I = 3/2$), and $ssnQ\bar{n}$ ($I = 1$) flavor combinations have explicit pentaquark states. In such subsystems, the light quarks and antiquark can not annihilate. If such pentaquark states could be observed in experiment, their exotic nature can be easily identified. On the contrary, the pentaquark subsystems with $nnnQ\bar{n}$ ($I = 1, 0$), $sssQ\bar{s}$, $nnsQ\bar{n}$ ($I = 1/2$), $nnsQ\bar{s}$, $ssnQ\bar{n}$ ($I = 1$), and $ssnQ\bar{s}$ flavor combinations are implicit pentaquark subsystems, the mixing between exotic five quark component with three quark component make it difficult for experiment to identify them. This is very similar to the case of $D_{s0}^*(2317)$ and $D_{s1}(2460)$.

In the following, we study the mass spectrums and strong decay properties for all the $qqqQ\bar{q}$ pentaquark subsystems group by group.

1. The $nnnQ\bar{q}$ and $sssQ\bar{q}$ pentaquark states

Firstly, we discuss the $nnnQ\bar{n}$ (\bar{s}) and $sssQ\bar{n}$ (\bar{s}) pentaquark subsystems. The symmetry properties of the $nnnQ\bar{n}$ (\bar{s}) pentaquark subsystem are identical to that of the $nnnsQ$ pentaquark subsystem. Thus, we can directly obtain the numerical CMI matrices by appropriately substituting the relevant parameters in Table VI to the expressions of CMI Hamiltonian in Table XXXVII

of Appendix G. Additionally, according to Table II, the expressions of the CMI Hamiltonian for the $sssQ\bar{n}$ (\bar{s}) pentaquark subsystem can be obtained from that of the $nnnQ\bar{n}$ (\bar{s}) subsystem in $I_{nnn} = 3/2$ case, where I_{nnn} denotes the isospin of the three n quarks in the $nnnQ\bar{n}$ pentaquark subsystem.

In the threshold scheme, we use two types of meson-baryon reference systems to estimate the masses of $nnnQ\bar{q}$ and $sssQ\bar{q}$ pentaquark states. The corresponding pentaquark masses are presented in the third and fourth columns of Table XVI. For the $nnnc(b)\bar{n}$ subsystems, the two different types of meson-baryon reference systems are $D + \Delta$ ($B + \Delta$) and $\pi + \Sigma_c$ ($\pi + \Sigma_b$). Similarly, two types of meson-baryon reference systems for the $sssc\bar{n}$, $sssb\bar{n}$, $nnnc\bar{s}$, $nnnb\bar{s}$, $sssc\bar{s}$, and $sssb\bar{s}$ pentaquark subsystems are $D + \Omega$ ($K + \Omega_c$), $B + \Omega$ ($K + \Omega_b$), $D_s + \Delta$ ($K + \Sigma_c$), $B_s + \Delta$ ($K + \Sigma_b$), $D_s + \Omega$ ($\phi + \Omega_c$), and $B_s + \Omega$ ($\phi + \Omega_b$), respectively. The obtained masses calculated from the above reference systems for $nnnQ\bar{q}$ and $sssQ\bar{q}$ pentaquark states are presented in Table XVI. Meanwhile, we also get the mass spectrums of the $nnnQ\bar{q}$ and $sssQ\bar{q}$ pentaquark subsystems in the modified CMI model in Eq. (4) and show them in the fifth column of Table XVI. Based on the results listed in the fifth column of Table XVI, we plot the mass spectrums of the $nnnQ\bar{q}$ and $sssQ\bar{q}$ pentaquark subsystems in the diagrams (a)-(h) of Fig. 2. The corresponding meson-baryon thresholds are also illustrated.

For the $nnnc(b)\bar{n}$ subsystems with $I_{nnn} = 3/2$ and $I_{nnn} = 1/2$, the isospin of antiquark can couple to I_{nnn} and the total isospin of $nnnQ\bar{n}$ pentaquark states can be $I = 2, 1$, and 0 . Note that the symmetry property of $nnnQ\bar{n}$ pentaquark subsystem is determined from the first three identical quarks. Thus, the mass spectrums of $nnnQ\bar{n}$ pentaquark subsystem are identical for $I = 2$ and 1 in $I_{nnn}=3/2$ case. Similarly, we obtain identical mass spectrums for $I = 1$ and $I = 0$ $nnnQ\bar{n}$ pentaquark subsystem in the $I_{nnn} = 1/2$ case.

Besides the mass spectrum, we also calculate the overlaps for a particular $nnnQ\bar{q}$ ($sssQ\bar{q}$) pentaquark state with several baryon \otimes meson bases. For $nnnQ\bar{q}$ pentaquark states, we need to transform the eigenvectors of the $nnnQ\bar{q}$ pentaquark states into the $nnn \otimes Q\bar{q}$ and $nnQ \otimes n\bar{q}$ bases. Similarly, for the $sssQ\bar{q}$ pentaquark states, the corresponding eigenvectors are transformed into $sss \otimes Q\bar{q}$ and $ssQ \otimes s\bar{q}$ bases. The fractions of the relevant overlap are presented in Table XLII of Appendix H.

From Table XLII, we find that the $P_{n^3c\bar{n}}(3248.5, 3/2, 5/2^-)$, $P_{n^3c\bar{n}}(3294.6, 1/2, 5/2^-)$, $P_{n^3b\bar{n}}(6564.6, 3/2, 5/2^-)$, $P_{n^3b\bar{n}}(6612.8, 1/2, 5/2^-)$, $P_{s^3c\bar{n}}(3680.3, 1/2, 5/2^-)$, $P_{s^3c\bar{n}}(6996.3, 1/2, 5/2^-)$, $P_{n^3c\bar{s}}(3352.0, 3/2, 5/2^-)$, $P_{n^3c\bar{s}}(3414.9, 1/2, 5/2^-)$, $P_{n^3b\bar{s}}(6655.3, 3/2, 5/2^-)$, $P_{n^3b\bar{s}}(6734.8, 1/2, 5/2^-)$, $P_{s^3c\bar{s}}(3783.8, 0, 5/2^-)$, and $P_{s^3c\bar{s}}(7087.1, 0, 5/2^-)$ should be identified as scattering states. We label them with “*” in Table XLII. Thus, we have distinguished all the scattering states from the calculated $nnnQ\bar{q}$ and $sssQ\bar{q}$ pentaquark subsystems.

TABLE XVI. The estimated masses for the $nnnQ\bar{q}$ and $sssQ\bar{q}$ ($n = u, d$; $Q = c, b$) subsystems in units of MeV. The values in the second column are eigenvalues obtained with the CMI Hamiltonian in Eq. (2). The masses in the third, fourth, and fifth columns are obtained with two kinds of meson-baryon thresholds in Eq. (3) and the modified CMI model in Eq. (4), respectively.

$nnnc\bar{n}$ ($I_{nnn} = \frac{3}{2}, I = 2, 1$)				$nnnb\bar{n}$ ($I_{nnn} = \frac{3}{2}, I = 2, 1$)					
J^P	Eigenvalue	$(D\Delta)$	$(\pi\Sigma_c)$	Mass	J^P	Eigenvalue	$(B\Delta)$	$(\pi\Sigma_b)$	Mass
$\frac{5}{2}^-$	182.4	3243.2	3232.5	3248.5	$\frac{5}{2}^-$	158.4	6557.0	6541.6	6564.6
$\frac{3}{2}^-$	$\begin{pmatrix} 333.6 \\ 111.2 \\ -127.2 \end{pmatrix}$	$\begin{pmatrix} 3394.4 \\ 3172.0 \\ 2933.6 \end{pmatrix}$	$\begin{pmatrix} 3383.7 \\ 3161.3 \\ 2922.9 \end{pmatrix}$	$\begin{pmatrix} 3399.7 \\ 3176.6 \\ 2937.5 \end{pmatrix}$	$\frac{3}{2}^-$	339.0	6737.6	6722.2	6741.3
$\frac{1}{2}^-$	$\begin{pmatrix} 494.8 \\ 358.7 \\ -122.2 \end{pmatrix}$	$\begin{pmatrix} 3555.6 \\ 3419.5 \\ 2938.6 \end{pmatrix}$	$\begin{pmatrix} 3544.9 \\ 3408.8 \\ 2927.9 \end{pmatrix}$	$\begin{pmatrix} 3560.0 \\ 3425.0 \\ 2943.1 \end{pmatrix}$	$\frac{1}{2}^-$	483.3	6881.9	6866.5	6880.1
						350.4	6749.0	6733.6	6753.0
						-114.5	6284.1	6268.7	6285.6
$nnnc\bar{n}$ ($I_{nnn} = \frac{1}{2}, I = 0, 1$)				$nnnb\bar{n}$ ($I_{nnn} = \frac{1}{2}, I = 0, 1$)					
J^P	Eigenvalue	$(D\Omega)$	$(K\Omega_c)$	Mass	J^P	Eigenvalue	$(B\Omega)$	$(K\Omega_b)$	Mass
$\frac{5}{2}^-$	235.2	3296.0	3285.3	3294.6	$\frac{5}{2}^-$	222.0	6620.6	6605.2	6612.8
$\frac{3}{2}^-$	$\begin{pmatrix} 247.7 \\ 178.8 \\ -48.3 \\ -516.6 \end{pmatrix}$	$\begin{pmatrix} 3308.5 \\ 3239.6 \\ 3012.5 \\ 2544.2 \end{pmatrix}$	$\begin{pmatrix} 3297.8 \\ 3228.9 \\ 3001.8 \\ 2533.5 \end{pmatrix}$	$\begin{pmatrix} 3305.8 \\ 3239.1 \\ 3007.6 \\ 2539.8 \end{pmatrix}$	$\frac{3}{2}^-$	234.7	6633.3	6617.9	6624.1
$\frac{1}{2}^-$	$\begin{pmatrix} 223.1 \\ 57.7 \\ -115.9 \\ -423.9 \\ -611.45 \end{pmatrix}$	$\begin{pmatrix} 3284.0 \\ 3118.5 \\ 2944.9 \\ 2636.9 \\ 2449.3 \end{pmatrix}$	$\begin{pmatrix} 3273.3 \\ 3107.8 \\ 2934.2 \\ 2626.2 \\ 2438.6 \end{pmatrix}$	$\begin{pmatrix} 3281.2 \\ 3114.3 \\ 2939.4 \\ 2631.4 \\ 2445.9 \end{pmatrix}$	$\frac{1}{2}^-$	225.9	6624.5	6609.1	6615.6
						59.5	6458.1	6442.7	6452.1
						-85.1	6313.5	6298.1	6308.8
						-422.3	5976.3	5960.9	5968.0
						-565.6	5833.1	5817.7	5824.7
$sssc\bar{n}$ ($I = \frac{1}{2}$)				$sssb\bar{n}$ ($I = \frac{1}{2}$)					
J^P	Eigenvalue	$(D\Omega)$	$(K\Omega_c)$	Mass	J^P	Eigenvalue	$(B\Omega)$	$(K\Omega_b)$	Mass
$\frac{5}{2}^-$	87.7	3783.7	3777.1	3680.3	$\frac{5}{2}^-$	63.2	6996.8	6897.7	6996.3
$\frac{3}{2}^-$	$\begin{pmatrix} 115.2 \\ 51.0 \\ -93.1 \end{pmatrix}$	$\begin{pmatrix} 3811.2 \\ 3747.0 \\ 3602.9 \end{pmatrix}$	$\begin{pmatrix} 3804.6 \\ 3740.3 \\ 3596.3 \end{pmatrix}$	$\begin{pmatrix} 3741.4 \\ 3613.0 \\ 3431.9 \end{pmatrix}$	$\frac{3}{2}^-$	167.0	7100.6	7001.5	7075.5
$\frac{1}{2}^-$	$\begin{pmatrix} 205.5 \\ 117.3 \\ -56.2 \end{pmatrix}$	$\begin{pmatrix} 3901.5 \\ 3813.3 \\ 3639.8 \end{pmatrix}$	$\begin{pmatrix} 3894.9 \\ 3806.7 \\ 3633.2 \end{pmatrix}$	$\begin{pmatrix} 3837.6 \\ 3749.8 \\ 3434.8 \end{pmatrix}$	$\frac{1}{2}^-$	37.2	6970.8	6871.6	6966.9
						-117.3	6816.3	6717.2	6769.8
						253.9	7187.5	7088.4	7114.5
						177.6	7111.2	7012.1	7086.1
						-118.9	6814.7	6715.6	6772.6
$nnnc\bar{s}$ ($I = \frac{3}{2}$)				$nnnb\bar{s}$ ($I = \frac{3}{2}$)					
J^P	Eigenvalue	$(D_s\Delta)$	$(K\Sigma_c)$	Mass	J^P	Eigenvalue	$(B_s\Delta)$	$(K\Sigma_b)$	Mass
$\frac{5}{2}^-$	182.9	3343.9	3409.5	3352.9	$\frac{5}{2}^-$	159.5	6648.7	6719.2	6655.3
$\frac{3}{2}^-$	$\begin{pmatrix} 68.5 \\ 125.5 \\ -40.5 \end{pmatrix}$	$\begin{pmatrix} 3429.5 \\ 3286.5 \\ 3120.5 \end{pmatrix}$	$\begin{pmatrix} 3495.1 \\ 3352.1 \\ 3186.1 \end{pmatrix}$	$\begin{pmatrix} 3482.1 \\ 3309.4 \\ 3151.7 \end{pmatrix}$	$\frac{3}{2}^-$	272.4	6761.6	6832.1	6816.9
$\frac{1}{2}^-$	$\begin{pmatrix} 389.6 \\ 286.1 \\ -17.8 \end{pmatrix}$	$\begin{pmatrix} 3550.6 \\ 3447.1 \\ 3143.2 \end{pmatrix}$	$\begin{pmatrix} 3616.2 \\ 3512.7 \\ 3208.8 \end{pmatrix}$	$\begin{pmatrix} 3635.8 \\ 3497.7 \\ 3199.0 \end{pmatrix}$	$\frac{1}{2}^-$	131.9	6621.1	6691.6	6630.5
						-10.0	6479.2	6549.7	6524.6
						373.0	6862.2	6932.7	6957.4
						283.4	6772.6	6843.1	6824.8
						-9.8	6479.4	6549.9	6531.4
$nnnc\bar{s}$ ($I = \frac{1}{2}$)				$nnnb\bar{s}$ ($I = \frac{1}{2}$)					
J^P	Eigenvalue	$(D_s\Delta)$	$(K\Sigma_c)$	Mass	J^P	Eigenvalue	$(B_s\Delta)$	$(K\Sigma_b)$	Mass
$\frac{5}{2}^-$	168.5	3329.5	3395.1	3414.9	$\frac{5}{2}^-$	155.3	6644.5	6715.0	6734.8
$\frac{3}{2}^-$	$\begin{pmatrix} 162.9 \\ 107.5 \\ -68.1 \\ -317.8 \end{pmatrix}$	$\begin{pmatrix} 3323.9 \\ 3268.5 \\ 3092.9 \\ 2843.2 \end{pmatrix}$	$\begin{pmatrix} 3389.5 \\ 3334.1 \\ 3158.5 \\ 2908.8 \end{pmatrix}$	$\begin{pmatrix} 3407.2 \\ 3354.4 \\ 3113.8 \\ 2906.1 \end{pmatrix}$	$\frac{3}{2}^-$	148.9	6638.1	6708.6	6727.3
$\frac{1}{2}^-$	$\begin{pmatrix} 134.0 \\ -1.9 \\ -124.5 \\ -297.2 \end{pmatrix}$	$\begin{pmatrix} 3295.0 \\ 3159.1 \\ 3036.5 \\ 2863.8 \end{pmatrix}$	$\begin{pmatrix} 3360.6 \\ 3224.7 \\ 3102.1 \\ 2929.4 \end{pmatrix}$	$\begin{pmatrix} 3376.8 \\ 3204.4 \\ 3068.8 \\ 2907.5 \end{pmatrix}$	$\frac{1}{2}^-$	133.0	6622.2	6692.7	6712.3
						-80.2	6409.0	6479.5	6432.8
						-338.3	6150.9	6221.4	6213.6
						135.3	6624.5	6695.0	6713.1
						1.6	6490.8	6561.3	6539.0
						-102.3	6386.9	6457.4	6415.3
						-297.0	6192.2	6262.7	6230.4
						-371.8	6117.4	6187.9	6174.4
$sssc\bar{s}$ ($I = 0$)				$sssb\bar{s}$ ($I = 0$)					
J^P	Eigenvalue	$(D_s\Omega)$	$(\phi\Omega_c)$	Mass	J^P	Eigenvalue	$(B_s\Omega)$	$(\phi\Omega_b)$	Mass
$\frac{5}{2}^-$	87.7	3783.7	3777.1	3783.8	$\frac{5}{2}^-$	64.3	7088.5	7069.3	7087.1
$\frac{3}{2}^-$	$\begin{pmatrix} 115.2 \\ 51.0 \\ -93.1 \end{pmatrix}$	$\begin{pmatrix} 3811.2 \\ 3747.0 \\ 3602.9 \end{pmatrix}$	$\begin{pmatrix} 3804.6 \\ 3740.3 \\ 3596.3 \end{pmatrix}$	$\begin{pmatrix} 3842.3 \\ 3731.9 \\ 3574.0 \end{pmatrix}$	$\frac{3}{2}^-$	118.0	7142.2	7123.1	7167.1
$\frac{1}{2}^-$	$\begin{pmatrix} 205.5 \\ 117.3 \\ -56.2 \end{pmatrix}$	$\begin{pmatrix} 3901.5 \\ 3813.3 \\ 3639.8 \end{pmatrix}$	$\begin{pmatrix} 3894.9 \\ 3806.7 \\ 3633.2 \end{pmatrix}$	$\begin{pmatrix} 3948.9 \\ 3853.6 \\ 3597.0 \end{pmatrix}$	$\frac{1}{2}^-$	38.5	7062.7	7043.6	7056.9
						-44.6	6979.6	6960.5	6925.1
						173.5	7197.7	7178.5	7231.8
						127.2	7151.4	7132.3	7178.0
						-41.4	6982.9	6963.7	6931.3

TABLE XVII. The relative partial decay widths for the $nnnc\bar{n}$, $nnnb\bar{n}$, $sssc\bar{n}$, and $sssb\bar{n}$ pentaquark states. For each pentaquark state, we choose one channel as a reference channel, and the relative partial decay widths for the other channels are obtained in units of the reference channel. The masses are all in units of MeV. The scattering states and stable states in the modified CMI model are marked with “*” and “†”, respectively.

		$nnn \otimes c\bar{n}$				$nnc \otimes n\bar{n}$				$sss \otimes c\bar{n}$		$ssc \otimes s\bar{n}$						
$I[J^P]$	Mass	ΔD^*	ΔD	ND^*	ND	$\Sigma_c^*\rho(\omega)$	$\Sigma_c\rho(\omega)$	$\Sigma_c^*\pi(\eta)$	$\Sigma_c\pi(\eta)$	$\Lambda_c\rho(\omega)$	$\Lambda_c\pi(\eta)$	Mass	ΩD^*	ΩD	$\Omega_c^*K^*$	$\Omega_c K^*$	Ω_c^*K	$\Omega_c K$
$2(1)[\frac{5}{2}^-]$	3248.5*	1				x						3680.3*	x		1			
$2(1)[\frac{3}{2}^-]$	3399.7	2.7	1			2.5	1		1			3741.4	3.8	1	1.6	1		1
	3176.6	x	1			x	x		1			3613.0	x	1	x	1		1
	2937.5	x	x			x	x		1			3431.9	x	x	x	x		1
$2(1)[\frac{1}{2}^-]$	3560.0	1				5.5	1			1		3837.6	1		50.4	1		1
	3425.0	1				0.04	1			1		3749.8	1		0.04	1		1
	2943.1	x				x	x		1			3434.8	x	x	x	x		1
$0(1)[\frac{5}{2}^-]$	3294.6*					1												
$0(1)[\frac{3}{2}^-]$	3305.8					1	262	1	1			x						
	3239.1*					1	x	1	1			x						
	3007.6*					1	x	x	1			x						
	2539.8 [†]					x	x	x	x			x						
$0(1)[\frac{1}{2}^-]$	3281.2	3.1	1			x	1			1	1	1						
	3114.3	7.4	1			x	x			1	1	1						
	2939.4	x	1			x	x			1	1	1						
	2631.4	x	x			x	x			1	x	1						
	2445.9	x	x			x	x			x	x	1						
		$nnn \otimes b\bar{n}$				$nnb \otimes n\bar{n}$				$sss \otimes b\bar{n}$		$ssb \otimes s\bar{n}$						
$I[J^P]$	Mass	ΔB^*	ΔB	NB^*	NB	$\Sigma_b^*\rho(\omega)$	$\Sigma_b\rho(\omega)$	$\Sigma_b^*\pi(\eta)$	$\Sigma_b\pi(\eta)$	$\Lambda_b\rho(\omega)$	$\Lambda_b\pi(\eta)$	Mass	ΩB^*	ΩB	$\Omega_b^*K^*$	$\Omega_b K^*$	Ω_b^*K	$\Omega_b K$
$2(1)[\frac{5}{2}^-]$	6564.6*	1				x						6996.3*	0		1			
$2(1)[\frac{3}{2}^-]$	6741.3	2.0	1			3.9	1	1				7075.5	2.9	1	2.8	1		1
	6537.6*	x	1			x	1	1				6966.9	x	1	0.6	1		1
	6288.5	x	x			x	x	1				6769.8	x	x	x	x		1
$2(1)[\frac{1}{2}^-]$	6880.1	1				2.7	1		1			7114.5	1		3.9	1		1
	6753.0	1				0.25	1		1			7086.1	1		0.1	1		1
	6285.6	x				x	x		1			6772.6	x	x	x	x		1
$0(1)[\frac{5}{2}^-]$	6612.8*					1												
$0(1)[\frac{3}{2}^-]$	6624.1					1	78.0	1	1			x						
	6595.8*					1	x	1	1			x						
	6331.8*					1	x	x	1			x						
	5853.0 [†]					x	x	x	x			x						
$0(1)[\frac{1}{2}^-]$	6615.6	0.1	1	0.33	1				1	1	1							
	6452.1	4.3	1	x	x				1	x	1							
	6308.8	0.2	1	x	x				1	x	1							
	5968.0	x	x	x	x				1	x	1							
	5824.7	x	x	x	x				x	x	1							

Next, we start to discuss the genuine pentaquark states with $nnnQ\bar{q}$ and $sssQ\bar{q}$ configurations.

From Fig. 2, we can see that the $nnnc\bar{s}$ and $nnnb\bar{s}$ subsystems both have 10 possible two-body strong decay channels. Meanwhile, the $sssc\bar{n}$ and $sssb\bar{n}$ subsystems both have 6 possible decay channels. Due to all the $nnnQ\bar{s}$ and $sssQ\bar{n}$ ($Q = c, b$) pentaquark states are explicitly exotic states, if a state can be observed experimentally with such decay patterns, this state would be a good candidate of pentaquark state.

There are 16 and 8 possible quark rearrangement decay channels for the $nnnc(b)\bar{n}$ and $sssc(b)\bar{s}$ pentaquark subsystems, respectively. Different from the $nnnQ\bar{s}$ and $sssQ\bar{n}$ subsystems, the $nnnc(b)\bar{n}$ ($I = 1, 0$) and $sssc(b)\bar{s}$ states are like the excited $\Sigma_{c(b)}$ ($\Lambda_{c(b)}$) and $\Omega_{c(b)}$ states. To identify them, we need to carefully take into account the effect of the mixing between three quark and five quark components, this is still a difficult task due to the complexity of heavy baryon spectrum. An exception is that the $nnnQ\bar{n}$ pentaquark states with $I = 2$ is an ex-

TABLE XVIII. The relative partial decay widths for the $nnnc\bar{s}$, $nnnb\bar{s}$, $sssc\bar{s}$, and $sssb\bar{s}$ pentaquark states. For each pentaquark state, we choose one channel as a reference channel, and the relative partial decay widths for the other channels are obtained in units of the reference channel. The masses are all in units of MeV. The stable states in the modified CMI model are marked with “ \dagger ”.

$nnnc\bar{s}$		$nnn \otimes c\bar{s}$				$nnc \otimes n\bar{s}$				$sssc\bar{s}$		$sss \otimes c\bar{s}$		$ssc \otimes s\bar{s}$				
$I(J^P)$	Mass	ΔD_s^*	ΔD_s	ND_s^*	ND_s	$\Sigma_c^* K^*$	$\Sigma_c K^*$	$\Sigma_c^* K$	$\Sigma_c K$	$\Lambda_c K^*$	$\Lambda_c K$	Mass	ΩD_s^*	ΩD_s	$\Omega_c^* \phi$	$\Omega_c \phi$	$\Omega_c^* \eta'$	$\Omega_c \eta'$
$\frac{3}{2}(\frac{5}{2}^-)$	3352.0*	1				\times						3783.8*	\times		\times			
$\frac{3}{2}(\frac{3}{2}^-)$	3482.1	2.2	1			2.7	1		1			3842.3	3.3	1	1.7	1		1
	3309.4	\times	1			\times	\times		1			3731.9	\times	1	\times	1		1
	3151.7	\times	\times			\times	\times		1			3574.0	\times	\times	\times	\times	1	
$\frac{3}{2}(\frac{1}{2}^-)$	3635.8	1				5.8	1			1		3948.9	1		23.6	1		1
	3497.7	1				0.04	1			1		3853.6	1		0.01	1		1
	3199.0	\times				\times	\times		1			3597.0	\times	\times	\times	\times	1	
$\frac{1}{2}(\frac{5}{2}^-)$	3414.9*					1												
$\frac{1}{2}(\frac{3}{2}^-)$	3407.2					1	\times	1		1		\times						
	3354.4					1	\times	1		1		\times						
	3113.8					1	\times	\times		1		\times						
	2906.1 †					\times	\times	\times		\times		\times						
$\frac{1}{2}(\frac{1}{2}^-)$	3376.8	4.0	1			\times	1			1		1	1					
	3204.4	5.9	1			\times	\times			1		\times	1					
	3068.8	0.2	1			\times	\times			1		\times	1					
	2907.5	\times	1			\times	\times			\times		\times	1					
	2779.5 †	\times	\times			\times	\times			\times		\times	\times					
$nnnb\bar{s}$		$NNN \otimes b\bar{s}$				$nnb \otimes n\bar{s}$				$sssb\bar{s}$		$sss \otimes b\bar{s}$		$ssb \otimes s\bar{s}$				
$I(J^P)$	Mass	ΔB_s^*	ΔB_s	NB_s^*	NB_s	$\Sigma_b^* K^*$	$\Sigma_b K^*$	$\Sigma_b^* K$	$\Sigma_b K$	$\Lambda_b K^*$	$\Lambda_b K$	Mass	ΩB_s^*	ΩB_s	$\Omega_b^* \phi$	$\Omega_b \phi$	$\Omega_b^* \eta'$	$\Omega_b \eta'$
$\frac{3}{2}(\frac{5}{2}^-)$	6655.3*	1				\times						7087.1*	\times		1			
$\frac{3}{2}(\frac{3}{2}^-)$	6816.9	1.9	1			4.0	1		1			7167.1	2.9	1	2.9	1		1
	6630.5	\times	1			\times	\times		1			7056.9	\times	1	\times	1		1
	6524.6	\times	\times			\times	\times		1			6925.1	\times	\times	\times	\times	1	
$\frac{3}{2}(\frac{1}{2}^-)$	6957.4	1				2.7	1			1		7231.8	1		2.9	1		1
	6824.8	1				0.3	1			1		7178.0	1		0.2	1		1
	6531.4	\times				\times	\times		1			6931.3	\times	\times	\times	\times	1	
$\frac{1}{2}(\frac{5}{2}^-)$	6734.8*					1												
$\frac{1}{2}(\frac{3}{2}^-)$	6727.3					1	1.4	1		1		\times						
	6712.3					1	\times	1		1		\times						
	6432.8					1	\times	\times		1		\times						
	6213.6 †					\times	\times	\times		\times		\times						
$\frac{1}{2}(\frac{1}{2}^-)$	6713.1	0.2	1			\times	1			1		1	1					
	6539.0	4.0	1			\times	\times			1		1	1					
	6415.3	0.3	1			\times	\times			1		\times	1					
	6230.4	\times	\times			\times	\times			\times		\times	1					
	6174.4	\times	\times			\times	\times			\times		\times	\times					

plicitly exotic state, if such states exist, they can be easily identified.

In Fig. 2, we find that the lowest $I(J^P) = 1/2$ ($1/2^-$) $nnnc\bar{s}$, $I(J^P) = 1/2(3/2^-)$ $nnnQ\bar{s}$, and $I(J^P) = 0(1)[3/2^-]$ $nnnQ\bar{n}$ states are all below their possible quark rearrangement decay channels. Thus, in the modified CMI model, the $P_{n^3c\bar{n}}$ (2539.8, 0(1), $3/2^-$), $P_{n^3b\bar{n}}$ (5853.0, 0(1), $3/2^-$), $P_{n^3c\bar{s}}$ (2779.5, $1/2$, $1/2^-$), $P_{n^3c\bar{s}}$ (2906.1, $1/2$, $3/2^-$), and $P_{n^3b\bar{s}}$ (6213.6, $1/2$, $3/2^-$) can be considered as stable pentaquark states. Meanwhile, the other $nnnQ\bar{q}$ and $sssQ\bar{q}$ pentaquark states all have two-body strong decay channels.

To have a quantitative description to the two-body strong decay behaviors for $nnnQ\bar{q}$ and $sssQ\bar{q}$ pentaquark states, we use the obtained eigenvectors to calculate the relative partial decay widths for all $nnnQ\bar{q}$ and $sssQ\bar{q}$ pentaquark states and present them in Tables XVII and XVIII.

As shown in Tables XVII and XVIII, the final states of two-body strong decay for $nnnQ\bar{q}$ and $sssQ\bar{q}$ pentaquark states includes π , η , and K mesons. Here, to avoid the complexity of flavor octet-singlet mixing and the chiral anomaly, we use the following partially conserved axial

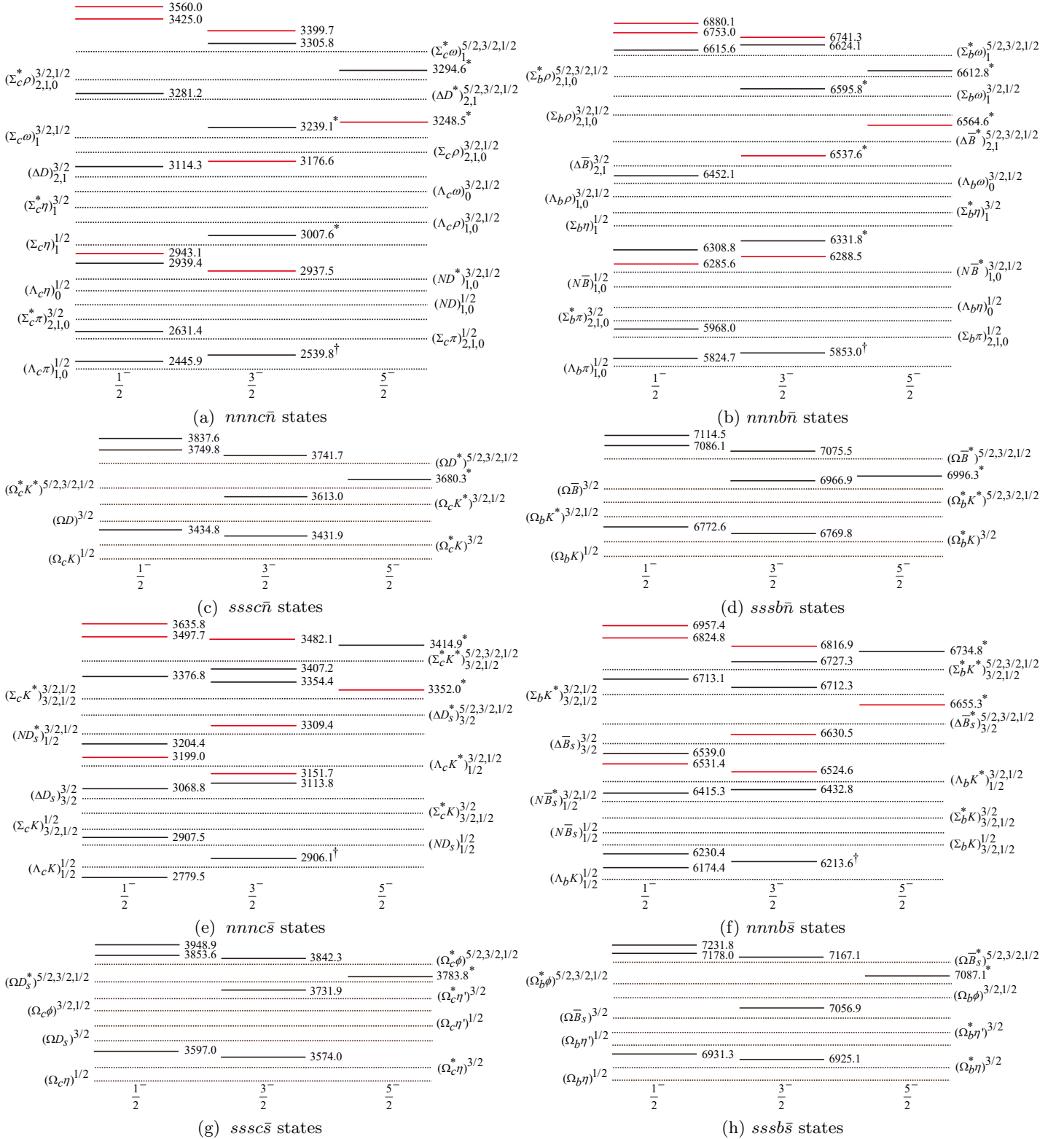


FIG. 2. Relative positions (units: MeV) for the $nnnc\bar{n}$, $nnnb\bar{n}$, $sssc\bar{n}$, $sssb\bar{n}$, $nnnc\bar{s}$, $nnnb\bar{s}$, $sssc\bar{s}$, and $sssb\bar{s}$ pentaquark states labeled with solid lines. In the $nnnc\bar{n}$, $nnnb\bar{n}$, $nnnc\bar{s}$, and $nnnb\bar{s}$ subsystems, the red and black lines represent the pentaquark states with $I_{nnn} = 3/2$ and $I_{nnn} = 1/2$, respectively. The dotted lines denote various baryon-meson thresholds. When the spin (isospin) of an initial pentaquark state is equal to a number in the superscript (subscript) of a baryon-meson state, its decay into that baryon-meson channel through S -wave is allowed by the angular momentum (isospin) conservation. The scattering states and stable states in the modified CMI model are marked with “ $*$ ” and “ \dagger ”, respectively.

current result [115]

$$\begin{aligned} M_{\eta_{n\bar{n}}}^2(1S_0) &\simeq M_\pi^2, \\ M_{\eta_{s\bar{s}}}^2(1S_0) &\simeq 2M_K^2 - M_\pi^2, \end{aligned} \quad (49)$$

i.e., we adopt $M_{\eta_{s\bar{s}}} = 628.2$ MeV and $M_{\eta_{n\bar{n}}} = 139.6$ MeV in our calculation.

Besides, unlike the heavy mesons and baryons with singlet heavy quark, the spatial wave functions for π and K mesons are different from that of the ρ and K^* mesons. Thus, the relation $\gamma_{\Sigma_c^* K} \approx \gamma_{\Sigma_c^* K^*}$ may not hold. Thus, for $nnnQ\bar{q}$ pentaquark states we apply the following relations

$$\gamma_{\Delta D^*} = \gamma_{\Delta D}, \quad \gamma_{\Delta D_s^*} = \gamma_{\Delta D_s}, \quad (50)$$

$$\gamma_{ND^*} = \gamma_{ND}, \quad \gamma_{ND_s^*} = \gamma_{ND_s}, \quad (51)$$

$$\gamma_{\Delta B} = \gamma_{\Delta B^*}, \quad \gamma_{\Delta B_s} = \gamma_{\Delta B_s^*}, \quad (52)$$

$$\gamma_{NB^*} = \gamma_{NB}, \quad \gamma_{NB_s^*} = \gamma_{NB_s}, \quad (53)$$

$$\gamma_{\Sigma_c^* \rho} = \gamma_{\Sigma_c \rho}, \quad \gamma_{\Sigma_c^* K^*} = \gamma_{\Sigma_c K^*}, \quad (54)$$

$$\gamma_{\Sigma_b^* \rho} = \gamma_{\Sigma_b \rho}, \quad \gamma_{\Sigma_b^* K^*} = \gamma_{\Sigma_b K^*}, \quad (55)$$

respectively. And for each $sssQ\bar{q}$ pentaquark state, we have

$$\gamma_{\Omega D} = \gamma_{\Omega D^*}, \quad \gamma_{\Omega D_s} = \gamma_{\Omega D_s^*}, \quad (56)$$

$$\gamma_{\Omega B} = \gamma_{\Omega B^*}, \quad \gamma_{\Omega B_s} = \gamma_{\Omega B_s^*}, \quad (57)$$

$$\gamma_{\Omega_c^* \phi} = \gamma_{\Omega_c \phi}, \quad \gamma_{\Omega_b^* \phi} = \gamma_{\Omega_b \phi}, \quad (58)$$

$$\gamma_{\Omega_c^* K^*} = \gamma_{\Omega_c K^*}, \quad \gamma_{\Omega_b^* K^*} = \gamma_{\Omega_b K^*}. \quad (59)$$

The calculated relative partial decay widths are listed in Tables XVII and XVIII.

Here, we firstly discuss the decay behavior of $nnnc\bar{n}$ pentaquark states. The corresponding relative partial decay widths can be found in Table XVII. If the isospin for the first three n quarks is $I_{nnn} = 3/2$, then the total isospin for $nnnc\bar{n}$ pentaquark states are $I = 2, 1$. The $I = 2$ $nnnc\bar{n}$ pentaquark states may decay into ΔD^* and ΔD channels in $nnn - c\bar{n}$ decay mode. Meanwhile, due to isospin conservation, they can also decay into $\Sigma_c^* \rho$, $\Sigma_c^* \pi$, $\Sigma_c \rho$ and $\Sigma_c \pi$ in $nnc - n\bar{n}$ final states. Similar to the $I = 2$ $nnnc\bar{n}$ pentaquark states, the $I = 1$ ($I_{nnn} = 3/2$) $nnnc\bar{n}$ pentaquark states can also decay into ΔD^* and ΔD channels in $nnn - c\bar{n}$ decay mode. Meanwhile, they can also decay into $\Sigma_c^* \rho$, $\Sigma_c^* \pi$, $\Sigma_c \rho$, $\Sigma_c \pi$, $\Sigma_c^* \omega$, $\Sigma_c^* \eta_{n\bar{n}}$, $\Sigma_c \omega$, and $\Sigma_c \eta_{n\bar{n}}$ channels in $nnc - n\bar{n}$ decay mode.

Another case for $nnnc\bar{n}$ pentaquark states is that the isospin of the first three n quarks I_{nnn} is $1/2$, then the total isospin of $nnnc\bar{n}$ pentaquark states are $I = 1$ and $I = 0$. The $I = 0$ $nnnc\bar{n}$ pentaquark states may decay into ND^* and ND channels in $nnn - c\bar{n}$ decay mode. They can also decay into $\Sigma_c^* \rho$, $\Sigma_c^* \pi$, $\Sigma_c \rho$, $\Sigma_c \pi$, $\Lambda_c \omega$, and $\Lambda_c \eta_{n\bar{n}}$ channels in $nnc - n\bar{n}$ decay mode. For the $I = 1$ ($I_{nnn} = 1/2$) $nnnc\bar{n}$ pentaquark states, they can decay into ND^* and ND channels in $nnn - c\bar{n}$ decay mode, and decay to $\Sigma_c^* \rho$, $\Sigma_c^* \pi$, $\Sigma_c \rho$, $\Sigma_c \pi$, $\Sigma_c^* \omega$, $\Sigma_c^* \eta_{n\bar{n}}$, $\Sigma_c \omega$, $\Sigma_c \eta_{n\bar{n}}$, $\Lambda_c \rho$, and $\Lambda_c \pi$ channels in $nnc - n\bar{n}$ decay mode.

The mass of ω and $\eta_{n\bar{n}}$ mesons are closed to that of the ρ and π mesons. As an approximation, we adopt $m_\rho \approx m_\omega$ and $m_{\eta_{n\bar{n}}} \approx m_\pi$. In this case, we only need to calculate the relative decay widths with ρ and π in the $nnc - n\bar{n}$ final states. The relative decay widths with ω and $\eta_{n\bar{n}}$ in the final states have the same numerical values as that of the ρ and π cases. Thus, in Table XVII, we use only one column to show the relative partial decay widths with ρ , π or ω , $\eta_{n\bar{n}}$ in the final states.

Next, we mainly discuss the decay behaviors of $nnnc\bar{s}$ pentaquark states. From Table XVII, we find that the lowest $I(J^P) = 1/2(1/2^-)$ state, $P_{n^3 c\bar{s}}(2779.5, 1/2, 1/2^-)$ have no strong decay channels and it should be a stable state. While the lowest $I(J^P) = 3/2(1/2^-)$ state $P_{n^3 c\bar{s}}(3199.0, 3/2, 1/2^-)$ can decay into $\Sigma_c K$. And the $P_{n^3 c\bar{s}}(3151.7, 3/2, 3/2^-)$ can only decay to $\Sigma_c^* K$ channel. Other $nnnc\bar{s}$ pentaquark states all have $nnn - c\bar{s}$ and $nnc - n\bar{s}$ strong decay modes.

For the other two $I(J^P) = 3/2(3/2^-)$ states, In $nnn - s\bar{c}$ decay mode, the $P_{n^3 s\bar{c}}(3309.4, 3/2, 3/2^-)$ has only one decay channel, i.e., ΔD_s , and it has $\Sigma_c^* K$ channel in $nnc - n\bar{s}$ decay mode. The $P_{n^3 s\bar{c}}(3482.1, 3/2, 3/2^-)$ can decay into ΔD_s^* , ΔD_s , $\Sigma_c^* K^*$, $\Sigma^* K^*$, and $\Sigma_c^* K$ channel. The relative partial decay width ratio between ΔD_s^* and ΔD_s is

$$\Gamma_{\Delta D_s^*} : \Gamma_{\Delta D_s} = 2.2 : 1, \quad (60)$$

which indicates that the partial decay width of the ΔD_s^* channel is larger than that of the ΔD_s in $nnn - c\bar{s}$ decay mode. On the other hand, the relative partial decay width ratio between $\Sigma_c^* K^*$ and $\Sigma_c^* K$ is

$$\Gamma_{\Sigma_c^* K^*} : \Gamma_{\Sigma_c^* K} = 2.7 : 1. \quad (61)$$

in $nnc - n\bar{s}$ decay mode.

For the four $I(J^P) = 1/2(3/2^-)$ states, though some of these pentaquark states are higher than the threshold of $\Lambda_c K^*$, the overlap of the four pentaquark states with the $\Lambda_c K^*$ basis is close to 0, although the spin and isospin quantum numbers are allowed. Thus, the $I(J^P) = 1/2(3/2^-)$ pentaquark states can not decay into $\Lambda_c K^*$ channel. Similar situations also appear in $I_{nnn}(J^P) = 1/2(3/2^-)$ $nnnQ\bar{n}$ and $I(J^P) = 1/2(3/2^-)$ $nnnb\bar{s}$ pentaquark states.

For the other two $I(J^P) = 3/2(1/2^-)$ pentaquark state, they only decay into ΔD_s in $nnn - c\bar{s}$ decay mode. For $nnc - n\bar{s}$ decay mode, we find

$$\Gamma_{\Sigma_c^* K^*} : \Gamma_{\Sigma_c^* K} = 5.8 : 1, \quad (62)$$

and

$$\Gamma_{\Sigma_c^* K^*} : \Gamma_{\Sigma_c^* K} = 0.04 : 1. \quad (63)$$

We also present relative decay widths for other $nnnQ\bar{q}$ and $sssQ\bar{q}$ pentaquark subsystems in Tables XVII and XVIII. Especially, we need to mention that for the $nnnb\bar{n}$ pentaquark subsystem, the LHCb collaboration also tried to find the relevant peak in the $P_{\Lambda_b^0 \pi^+}^+(udd\bar{b}) \rightarrow J/\psi K^- \pi^+ p$ and $P_{\Lambda_b^0 \pi^-}^-(udd\bar{b}) \rightarrow J/\psi K^- \pi^- p$ weak decay modes in search window 4668-5760 MeV, but no evidence for such pentaquark was found [111].

2. The $nnsQ\bar{q}$ and $ssnQ\bar{q}$ pentaquark states

The $nnsQ\bar{q}$ and $ssnQ\bar{q}$ pentaquark states are implicit exotic states. Such pentaquark states are like the excited $\Xi_Q^{(\prime)}$ (Λ_Q , Σ_Q) and Ω_Q ($\Xi_Q^{(\prime)}$) baryon states. The included subsystems are $nnsc(b)\bar{n}$, $nnsc(b)\bar{s}$, $ssnc(b)\bar{n}$ and $ssnc(b)\bar{s}$. According to Table II, the forms of CMI Hamiltonian for the $ssnQ\bar{n}$ (\bar{s}) subsystem are similar to the expressions of CMI Hamiltonian for the $nnsQ\bar{n}$ (\bar{s}) subsystem in $I_{nn} = 1$ case. Thus, we use the CMI Hamiltonian in Tables XXXVIII and XXXIX of Appendix G, and substitute the appropriate parameters collected in Table VI to obtain the mass spectrums of the $nnsQ\bar{n}$ (\bar{s}) and $ssnQ\bar{n}$ (\bar{s}) pentaquark subsystems.

We also use two schemes to estimate the mass spectrums of the $nnsQ\bar{q}$ and $ssnQ\bar{q}$ subsystems. In the first scheme, we use three types of baryon-meson reference systems to estimate the masses of the $nnsQ\bar{q}$ and $ssnQ\bar{q}$ states. For example, the reference systems for the $nnsc(b)\bar{n}$ system are $\pi + \Xi_c$ ($\pi + \Xi_b$), $K + \Sigma_c$ ($K + \Sigma_b$), and $D + \Sigma$ ($\bar{B} + \Sigma$). The baryon-meson reference systems for the $nnsc(b)\bar{s}$, $ssnc(b)\bar{n}$, and $ssnc(b)\bar{s}$ subsystems can be listed by way of analog. Finally, we present the corresponding $nnsQ\bar{q}$ and $ssnQ\bar{q}$ pentaquark masses in the third, fourth, and fifth columns of Tables XIX and XX. The results calculated from the modified CMI model (Eq. (4)) are also shown in the sixth column of Tables XIX and XX.

Based on the results listed in the sixth column, we plot the mass spectrums of the $nnsc\bar{n}$, $nnsb\bar{n}$, $ssnc\bar{n}$, $ssnb\bar{n}$, $nnsc\bar{s}$, $nnsb\bar{s}$, $ssnc\bar{s}$, and $ssnb\bar{s}$ subsystems in the diagrams (a)-(d) of Figs. 3 and 4. The thresholds of relevant quark rearrangement decay patterns are also presented in Figs. 3 and 4.

In addition, to calculate the relative partial decay widths for $nnsQ\bar{q}$ pentaquark states, we need to transform the corresponding eigenvectors into the $nns \otimes Q\bar{q}$, $nnQ \otimes s\bar{q}$, and $nsQ \otimes n\bar{q}$ bases. Similarly, for the $ssnQ\bar{q}$ pentaquark states, their eigenvectors should be transformed into the $ssn \otimes Q\bar{q}$, $ssQ \otimes n\bar{q}$, and $nsQ \otimes s\bar{q}$ bases. The obtained overlaps for $nnsQ\bar{q}$ and $ssnQ\bar{q}$ pentaquark states with baryon \otimes meson bases are presented in Tables XLIII, XLIV, XLV, and XLVI of Appendix H, respectively. The obtained relative partial decay widths

for $nnsQ\bar{q}$ and $ssnQ\bar{q}$ pentaquark subsystems are presented in Tables XXI, XXII, XXIII, and XXIV, respectively.

Here, we mainly focus on the mass spectrum and decay behavior of the $nnsc\bar{n}$ pentaquark subsystem. The $nnsb\bar{n}$, $nnsc\bar{s}$, and $nnsb\bar{s}$ subsystems can be analysed in a similar way. According to Table XLIII, we find that the $P_{n^2sc\bar{n}}(3408.1, 3/2(1/2), 5/2^-)$ couples completely to $\Sigma_b^* K^*$ channel, this state can be considered as a $\Sigma_b^* K^*$ scattering state. Moreover, the $P_{n^2sc\bar{n}}(3356.7, 3/2(1/2), 3/2^-)$ and $P_{n^2sc\bar{n}}(3223.9, 3/2(1/2), 3/2^-)$ states should also be identified as scattering states. We label them with “*” in Tables XXI, XLIII, and the diagram (a) of Fig. 3.

After identify the scattering states, other states in $nnsc\bar{n}$ pentaquark subsystem can be regarded as genuine $nnsc\bar{n}$ pentaquark states. From the diagram (a) of Fig. 3, we can see that the $nnsc\bar{n}$ subsystem has 26 possible rearrangement decay channels.

If the isospin for the first two quarks is $I_{nn} = 1$, the total isospin for $nnsc\bar{n}$ pentaquark states can be $I = 3/2$ or $I = 1/2$. In $I = 3/2$ case, the $nnsc\bar{n}$ pentaquark states may decay into $\Sigma^* D^*$, $\Sigma^* D$, ΣD^* , and ΣD channels in $nns - c\bar{n}$ decay mode. Besides, they can also decay into $\Sigma_c^* K^*$, $\Sigma_c K^*$, $\Sigma_c^* K$, and $\Sigma_c K$ channels in $nnc - s\bar{n}$ decay mode. Meanwhile, these states can also decay into $\Xi_c^* \rho$, $\Xi_c^* \pi$, $\Xi_c' \rho$, $\Xi_c' \pi$, $\Xi_c \rho$, and $\Xi_c \pi$ channels in $nsc - n\bar{n}$ decay mode. For the $I = 1/2$ ($I_{nn} = 1$) $nnsc\bar{n}$ pentaquark states, they have the same decay channels with that of the $I = 3/2$ $nnsc\bar{n}$ pentaquark states in $nns - c\bar{n}$ and $nnc - s\bar{n}$ decay modes. However, in $nsc - n\bar{n}$ decay mode, the $I = 1/2$ ($I_{nn} = 1$) $nnsc\bar{n}$ pentaquark states also can decay into $\Xi_c^* \omega$, $\Xi_c^* \eta_{n\bar{n}}$, $\Xi_c' \omega$, $\Xi_c' \eta_{n\bar{n}}$, $\Xi_c \omega$, and $\Xi_c \eta_{n\bar{n}}$.

If the isospin for the first two quarks is $I_{nn} = 0$, then the total isospin of $nnsc\bar{n}$ pentaquark states is $I = 1/2$. The $I = 1/2$ ($I_{nn} = 0$) $nnsc\bar{n}$ pentaquark states may decay into ΛD^* and ΛD channels in $nns - c\bar{n}$ decay mode. Moreover, they can decay into $\Lambda_c^* K$ and $\Lambda_c K$ channels in $nnc - s\bar{n}$ mode. In $nsc - n\bar{n}$ decay mode, the allowed decay channels are the same as that of the $I = 1/2$ ($I_{nn} = 1$) $nnsc\bar{n}$ pentaquark states. Lastly, we notice that since we only consider the so called “Okubo-Zweig-Iizuka-superallowed” decay channels, the $I = 1/2$ ($I_{nn} = 1$) $nnsc\bar{n}$ pentaquark states can not decay into ΛD^* , ΛD channels in $nns - c\bar{n}$ decay mode, or $\Lambda_c^* K$ and $\Lambda_c K$ channels in $nnc - s\bar{n}$ decay mode, though such processes are isospin allowed. Similarly, we also notice that the $I = 1/2$ ($I_{nn} = 0$) $nnsc\bar{n}$ pentaquark states can not decay into $\Sigma^* D^*$, $\Sigma^* D$, ΣD^* , ΣD channels in $nns - c\bar{n}$ decay mode and $\Sigma_c^* K^*$, $\Sigma_c K^*$, $\Sigma_c^* K$, $\Sigma_c K$ channels in $nnc - s\bar{n}$ decay mode.

The $nnsc\bar{n}$ pentaquark states are like the excited Ξ_c baryons, and they share very close energy range with the excited Ξ_c baryons. Thus, to identify the nature of such pentaquark in experiment is very difficult. It is hard to distinguish whether the observed state is a conventional baryon or a pentaquark state if its isospin quantum number is 1/2. However, the observed state

TABLE XIX. The estimated masses for the $nnsQ\bar{n}$ and $ssnQ\bar{n}$ ($n = u, d$; $Q = c, b$) subsystems in units of MeV. The values in the second column are eigenvalues that are obtained with the CMI Hamiltonian in Eq. (2). The masses in the third, fourth, and fifth columns are determined with meson-baryon thresholds in Eq. (3). The masses in the sixth column are determined with the modified CMI model in Eq. (4).

$nns\bar{n}$ ($I_{nn} = 1, I = \frac{1}{2}, \frac{3}{2}$)					$nnsb\bar{n}$ ($I_{nn} = 1, I = \frac{1}{2}, \frac{3}{2}$)						
J^P	Eigenvalue	$(\pi\Xi_c)$	$(K\Sigma_c)$	$(D\Sigma)$	Mass	J^P	Eigenvalue	$(\pi\Xi_b)$	$(K\Sigma_b)$	$(B\Sigma)$	Mass
$\frac{5}{2}^-$	(198.0)	(3379.1)	(3424.6)	(3436.2)	(3408.1)	$\frac{5}{2}^-$	(181.8)	(6689.5)	(6813.4)	(6757.6)	(6730.5)
	(139.1)	(3320.2)	(3365.7)	(3377.3)	(3397.2)		(117.3)	(6625.0)	(6748.9)	(6693.1)	(6702.3)
	(289.6)	(3470.7)	(3516.2)	(3527.8)	(3515.6)		(291.6)	(6799.3)	(6923.2)	(6867.4)	(6853.5)
	(226.1)	(3407.2)	(3452.7)	(3464.3)	(3452.3)		(218.2)	(6725.9)	(6849.8)	(6794.0)	(6766.3)
	(141.6)	(3322.7)	(3368.2)	(3379.8)	(3356.7)		(164.4)	(6682.1)	(6796.0)	(6740.2)	(6709.4)
	(76.5)	(3257.6)	(3303.1)	(3314.7)	(3326.3)		(91.8)	(6599.5)	(6723.4)	(6667.6)	(6682.1)
	(6.9)	(3188.0)	(3233.5)	(3245.1)	(3223.8)		(-2.1)	(6505.6)	(6629.5)	(6573.7)	(6546.9)
	(-122.3)	(3058.8)	(3104.3)	(3115.9)	(3126.1)		(-106.8)	(6400.9)	(6524.8)	(6469.0)	(6474.1)
	(-379.3)	(2801.8)	(2847.3)	(2858.9)	(2832.0)		(-398.3)	(6109.4)	(6233.3)	(6233.3)	(6138.4)
	(421.1)	(3602.2)	(3647.7)	(3659.3)	(3641.4)		(406.2)	(6913.9)	(7037.8)	(6982.0)	(6947.7)
$\frac{3}{2}^-$	(302.0)	(3483.2)	(3528.7)	(3540.3)	(3535.5)	$\frac{3}{2}^-$	(300.4)	(6808.1)	(6932.0)	(6876.2)	(6865.8)
	(217.7)	(3398.8)	(3444.3)	(3455.9)	(3433.6)		(214.3)	(6722.1)	(6846.0)	(6790.2)	(6761.0)
	(80.0)	(3261.1)	(3306.6)	(3318.2)	(3321.2)		(83.1)	(6590.8)	(6714.8)	(6658.9)	(6664.8)
	(-49.9)	(3131.2)	(3176.7)	(3188.3)	(3165.4)		(-23.0)	(6484.7)	(6608.7)	(6552.8)	(6522.7)
	(-130.8)	(3050.3)	(3095.8)	(3107.4)	(3112.7)		(-114.1)	(6393.6)	(6517.6)	(6461.7)	(6468.0)
	(-379.4)	(2801.7)	(2847.2)	(2858.8)	(2817.7)		(-382.8)	(6124.9)	(6248.8)	(6193.0)	(6316.3)
	(-478.2)	(2703.0)	(2748.5)	(2760.1)	(2737.6)		(-426.8)	(6080.9)	(6204.8)	(6149.0)	(6117.0)
	$nns\bar{n}$ ($I_{nn} = 0, I = \frac{1}{2}$)					$nnsb\bar{n}$ ($I_{nn} = 0, I = \frac{1}{2}$)					
$\frac{5}{2}^-$	222.9	3404.0	3449.5	3461.1	3427.3	$\frac{5}{2}^-$	208.1	6715.8	6839.7	6783.9	6731.7
	(212.5)	(3394.6)	(3440.1)	(3451.7)	(3416.4)		(199.1)	(6706.8)	(6830.7)	(6774.9)	(6723.8)
	(155.3)	(3336.4)	(3381.9)	(3393.5)	(3361.3)		(184.2)	(6691.9)	(6815.8)	(6760.0)	(6713.3)
	(2.6)	(3183.7)	(3229.2)	(3240.8)	(3192.8)		(0.1)	(6507.9)	(6631.8)	(6576.0)	(6510.0)
	(-75.5)	(3105.6)	(3151.1)	(3162.7)	(3174.0)		(-86.7)	(6421.0)	(6544.9)	(6489.1)	(6506.9)
	(-534.9)	(2646.2)	(2691.7)	(2703.3)	(2666.1)		(-555.4)	(5952.3)	(5952.3)	(6020.4)	(5966.2)
	(181.9)	(3363.0)	(3408.5)	(3420.1)	(3387.5)		(183.1)	(6690.8)	(6814.7)	(6758.9)	(6708.9)
	(41.4)	(3222.5)	(3268.0)	(3279.6)	(3248.0)		(44.9)	(6552.6)	(6676.5)	(6620.7)	(6578.7)
	(-3.6)	(3177.5)	(3223.0)	(3234.6)	(3188.9)		(-1.3)	(6506.4)	(6630.3)	(6574.5)	(6512.2)
	(-128.7)	(3052.4)	(3097.9)	(3109.5)	(3114.5)		(-106.1)	(6401.6)	(6525.5)	(6469.7)	(6481.9)
$\frac{1}{2}^-$	(-340.8)	(2840.3)	(2885.8)	(2897.4)	(2905.5)	$\frac{1}{2}^-$	(-333.0)	(6174.7)	(6298.6)	(6242.8)	(6251.3)
	(-628.7)	(2552.4)	(2597.9)	(2609.5)	(2574.9)		(-582.8)	(5924.9)	(6048.8)	(5993.0)	(5945.1)
	(-784.1)	(2397.0)	(2442.5)	(2454.1)	(2404.5)		(-783.9)	(5723.9)	(5847.8)	(5792.0)	(5726.5)
$ssn\bar{n}$ ($I = 0, 1$)					$ssnb\bar{n}$ ($I = 0, 1$)						
J^P	Eigenvalue	$(K\Xi_c)$	$(\pi\Omega_c)$	$D\Xi$	Mass	J^P	Eigenvalue	$(K\Xi_b)$	$(\pi\Omega_b)$	$B\Xi$	Mass
$\frac{5}{2}^-$	(200.9)	(3558.5)	(3543.2)	(3602.8)	(3547.2)	$\frac{5}{2}^-$	(183.9)	(6868.1)	(6841.9)	(6923.7)	(6866.1)
	(111.4)	(3469.0)	(3453.6)	(3513.3)	(3538.5)		(88.3)	(6772.5)	(6746.3)	(6828.1)	(6829.7)
	(231.0)	(3588.6)	(3573.2)	(3632.9)	(3628.3)		(232.5)	(6916.7)	(6890.5)	(6972.2)	(6965.5)
	(180.8)	(3538.4)	(3523.1)	(3582.7)	(3541.8)		(172.5)	(6856.7)	(6830.4)	(6912.2)	(6841.5)
	(123.1)	(3480.7)	(3465.3)	(3525.0)	(3483.8)		(149.9)	(6834.1)	(6807.9)	(6889.6)	(6835.0)
	(50.7)	(3408.3)	(3393.0)	(3452.6)	(3468.7)		(62.5)	(6746.7)	(6720.4)	(6802.2)	(6818.8)
	(-35.8)	(3321.8)	(3306.5)	(3366.1)	(3372.5)		(-45.8)	(6638.4)	(6612.2)	(6693.9)	(6699.3)
	(-131.8)	(3225.8)	(3210.5)	(3270.1)	(3285.3)		(-112.4)	(6571.8)	(6545.6)	(6627.3)	(6628.5)
	(-476.7)	(2880.9)	(2865.5)	(2925.2)	(2865.1)		(-497.5)	(6186.7)	(6160.4)	(6242.2)	(6154.2)
	(348.7)	(3706.4)	(3691.0)	(3750.7)	(3734.5)		(330.2)	(7014.2)	(6988.0)	(7069.8)	(7026.3)
$\frac{3}{2}^-$	(240.2)	(3597.8)	(3582.5)	(3642.2)	(3643.0)	$\frac{3}{2}^-$	(241.3)	(6925.5)	(6899.2)	(6981.0)	(6976.7)
	(151.3)	(3508.9)	(3493.5)	(3553.2)	(3519.6)		(148.1)	(6832.3)	(6806.1)	(6887.9)	(6830.4)
	(40.9)	(3398.5)	(3383.2)	(3442.8)	(3413.1)		(47.6)	(6731.8)	(6705.6)	(6787.3)	(6746.5)
	(-82.6)	(3275.0)	(3259.7)	(3319.3)	(3316.4)		(-64.1)	(6620.1)	(6593.8)	(6675.6)	(6672.1)
	(-136.4)	(3221.2)	(3205.9)	(3265.5)	(3274.6)		(-119.5)	(6564.8)	(6538.5)	(6620.3)	(6625.9)
	(-290.9)	(3066.4)	(3051.4)	(3111.1)	(3114.0)		(-280.3)	(6403.9)	(6377.7)	(6459.5)	(6455.6)
	(-570.4)	(2787.2)	(2771.8)	(2831.5)	(2776.2)		(-523.1)	(6161.1)	(6134.8)	(6216.6)	(6140.2)

would be a good $nns\bar{c}\bar{n}$ pentaquark candidate if the state carries explicitly exotic quantum number $I = 3/2$.

According to the diagram (a) of Fig. 3, we find that the two lowest $I(J^P) = 1/2(1/2^-)$ $P_{n^2\bar{s}\bar{n}}$ (2404.5, 1/2, 1/2 $^-$) and $P_{n^2\bar{s}\bar{n}}$ (2574.9, 1/2, 1/2 $^-$) as well as the lowest $I(J^P) = 1/2(3/2^-)$ $P_{n^2\bar{s}\bar{n}}$ (2666.1, 1/2, 3/2 $^-$) states have no strong decay channels and should be considered as stable states. We mark them with “+” in Fig. 3 and Tables XXI and XLIII. Other pentaquark subsystems also have similar properties.

Now we calculate the relative partial decay widths for the $nns\bar{c}\bar{n}$ pentaquark subsystem. For $nns\bar{c}\bar{n}$ subsystem, We need to apply the following relations

$$\gamma_{\Sigma^* D^*} = \gamma_{\Sigma^* D} \approx \gamma_{\Sigma D^*} = \gamma_{\Sigma D}, \quad (64)$$

$$\gamma_{\Sigma_c^* K^*} = \gamma_{\Sigma_c K^*}, \quad \gamma_{\Sigma_c K} = \gamma_{\Sigma_c^* K}, \quad (65)$$

$$\gamma_{\Xi_c^* \rho} = \gamma_{\Xi_c' \rho} \approx \gamma_{\Xi_c \rho}, \quad \gamma_{\Xi_c \pi} \approx \gamma_{\Xi_c^* \pi} = \gamma_{\Xi_c' \pi}, \quad (66)$$

$$\gamma_{\Xi_c^* \omega} = \gamma_{\Xi_c' \omega} \approx \gamma_{\Xi_c \omega}, \quad \gamma_{\Xi_c \eta_{n\bar{n}}} \approx \gamma_{\Xi_c^* \eta_{n\bar{n}}} = \gamma_{\Xi_c' \eta_{n\bar{n}}}. \quad (67)$$

Moreover, since the mass of ω and $\eta_{n\bar{n}}$ is closed to the mass of ρ and π . For convenience, we further adopt the approximation $m_\omega \approx m_\rho$ and $m_{\eta_{nn}} \approx m_\pi$. The calculated relative partial decay widths for the $nns\bar{c}\bar{n}$ pentaquark subsystem are presented in Table XXI.

For the $nns\bar{c}\bar{n}$ pentaquark states with $I_{nn} = 0$, the total isospin is 1/2. From Table XXI, we find that the $P_{n^2\bar{s}\bar{n}}$ (3427.3, 1/2, 5/2 $^-$) can only decay into $\Xi_c^* \rho$ and $\Xi_c^* \omega$ channels due to angular momentum conservation. Except the $P_{n^2\bar{s}\bar{n}}$ (3427.3, 1/2, 5/2 $^-$), the other $nns\bar{c}\bar{n}$ pentaquark states with $I_{nn} = 0$ all have three different decay modes: $nns - c\bar{n}$, $nnc - s\bar{n}$, and $nsc - n\bar{n}$.

For the five $I(J^P) = 1/2(3/2^-)$ states, the lowest $P_{n^2\bar{s}\bar{n}}$ (2666.1, 1/2, 3/2 $^-$) state is a stable state. Due to angular momentum conservation law, the other two states can only decay into ΛD^* and $\Lambda_c K^*$ final states in $nns - c\bar{n}$ and $nnc - s\bar{n}$ decay modes, respectively. In the $nsc - n\bar{n}$ decay mode, we have relative partial decay width ratios for the $P_{n^2\bar{s}\bar{n}}$ (3416.4, 1/2, 3/2 $^-$) and $P_{n^2\bar{s}\bar{n}}$ (3361.3, 1/2, 3/2 $^-$),

$$\Gamma_{\Xi_c' \rho(\omega)} : \Gamma_{\Xi_c \rho(\omega)} = 0.3 : 1, \quad (68)$$

and

$$\Gamma_{\Xi_c' \rho(\omega)} : \Gamma_{\Xi_c \rho(\omega)} = 3.3 : 1, \quad (69)$$

respectively.

For $I(J^P) = 1/2(1/2^-)$ states, the lowest two states are below all allowed decay channels, thus they are stable states. Others $I(J^P) = 1/2(1/2^-)$ states all have many different decay channels in different decay modes. For example, for the $P_{n^2\bar{s}\bar{n}}$ (2905.4, 1/2, 1/2 $^-$) state, it can decay to $\Lambda_c K$, $\Xi' \pi$ ($\eta_{n\bar{n}}$), and $\Xi \pi$ ($\eta_{n\bar{n}}$). Meanwhile, we have

$$\Gamma_{\Xi' \pi(\eta_{n\bar{n}})} : \Gamma_{\Xi \pi(\eta_{n\bar{n}})} = 0.14 : 1. \quad (70)$$

When the isospin of the first two light quarks is $I_{nn} = 1$, the mass spectrums of $nns\bar{c}\bar{n}$ for $I = 1/2$ and $I = 3/2$ are degenerate. The only $I[J^P] = 3/2(1/2)[5/2^-]$ state $P_{n^2\bar{s}\bar{n}}$ (3397.3, 3/2(1/2), 5/2 $^-$) can only decay into $\Sigma^* D^*$ final state.

The lowest $I(J^P) = 3/2(3/2^-)$ state $P_{n^2\bar{s}\bar{n}}$ (2832.0, 3/2, 3/2 $^-$) has only one decay channel $\Xi_c \pi$. Meanwhile, the lowest $I(J^P) = 1/2(3/2^-)$ state $P_{n^2\bar{s}\bar{n}}$ (2832.0, 1/2, 3/2 $^-$) has $\Xi_c \pi$ and $\Xi_c \eta_{n\bar{n}}$ decay channels, these two states are expected to be narrow. Other $I(J^P) = 3/2(1/2)[3/2^-]$ states all have several decay channels. For example, for the $P_{n^2\bar{s}\bar{n}}$ (3326.1, 3/2(1/2), 3/2 $^-$), we find

$$\Gamma_{\Sigma D^*} : \Gamma_{\Sigma D} = 1018 : 1, \quad (71)$$

our results suggest that the ΣD^* in $nns - c\bar{n}$ decay mode is the most important decay channel for the $P_{n^2\bar{s}\bar{n}}$ (3326.1, 3/2(1/2), 3/2 $^-$) pentaquark state. For $I[J^P] = 3/2(1/2)[1/2^-]$ states, except the lowest two states, they all have many different decay channels and are expected to be broad states.

For other $nnsQ\bar{q}$ and $ssnQ\bar{q}$ pentaquark subsystems, their corresponding relative partial decay widths can be found in Tables XXI, XXII, XXIII, and XXIV, respectively.

C. The $QQQ\bar{Q}$ pentaquark states

In this section, we discuss the pentaquark states with $QQQ\bar{Q}$ configuration. The pentaquark states consist of four heavy quarks is dominantly bounded by the gluon exchange interaction, and can hardly be considered as molecular states. If such pentaquark states could be observed in experiment, its pentaquark state nature could be easily identified.

Obviously, by appropriately exchanging $q \leftrightarrow Q$ ($\bar{q} \leftrightarrow \bar{Q}$) quarks, the $QQQ\bar{Q}$ is like a mirror structure of $qqq\bar{Q}\bar{Q}$. As shown in Table I, such configuration includes the $cccc\bar{n}$ (\bar{s}), $cccb\bar{n}$ (\bar{s}), $ccb\bar{b}\bar{n}$ (\bar{s}), $bbbc\bar{n}$ (\bar{s}), and $bbbb\bar{n}$ (\bar{s}) pentaquark subsystems.

In the following discussion, we will divide the $QQQ\bar{Q}$ pentaquark system into three groups of subsystems according to their symmetry properties, i.e., (1) the $cccc\bar{q}$ and $bbbb\bar{q}$ pentaquark subsystems, (2) the $cccb\bar{q}$ and $bbbc\bar{q}$ pentaquark subsystems, (3) the $ccb\bar{b}\bar{q}$ pentaquark subsystem. In the following, we study the mass spectrums and decay properties in the $QQQ\bar{Q}$ pentaquark system.

1. The $cccc\bar{q}$ and $bbbb\bar{q}$ pentaquark states

We first discuss the $cccc\bar{n}$ (\bar{s}) and $bbbb\bar{n}$ (\bar{s}) pentaquark subsystems. The symmetry properties of the $cccc\bar{n}$ (\bar{s}) and $bbbb\bar{n}$ (\bar{s}) pentaquark subsystems are identical to that of the $ssss\bar{Q}$ pentaquark states. According to Table II, the expressions of CMI Hamiltonian for the $cccc\bar{n}$ (\bar{s})

TABLE XX. The estimated masses for the $nnsQ\bar{s}$ and $ssnQ\bar{s}$ ($n = u, d$; $Q = c, b$) subsystems in units of MeV. The values in the second column are eigenvalues that are obtained with the CMI Hamiltonian in Eq. (2). The masses in the third, fourth, and fifth columns are determined with meson-baryon thresholds in Eq. (3). The masses in the sixth column are determined with the modified CMI model in Eq. (4).

$nns\bar{s}$ ($I = 1$)					$nnsb\bar{s}$ ($I = 1$)						
J^P	Eigenvalue	$(K\Xi_c)$	$(\phi\Sigma_c)$	$(D_s\Sigma)$	Mass	J^P	Eigenvalue	$(K\Xi_b)$	$(\phi\Sigma_b)$	$(B_s\Sigma)$	Mass
$\frac{5}{2}^-$	(160.1)	(3517.7)	(3557.3)	(3498.5)	(3534.2)	$\frac{5}{2}^-$	(138.4)	(6822.6)	(6868.7)	(6801.8)	(6858.8)
	(124.4)	(3482.0)	(3521.6)	(3462.8)	(3501.5)		(107.6)	(6791.8)	(6837.9)	(6771.0)	(6714.4)
	(222.2)	(3579.8)	(3619.4)	(3560.6)	(3600.3)		(224.7)	(6908.9)	(6955.0)	(6888.1)	(6903.1)
	(157.5)	(3515.1)	(3554.7)	(3495.9)	(3550.1)		(143.6)	(6827.8)	(6873.9)	(6807.0)	(6873.5)
	(99.4)	(3457.0)	(3496.6)	(3437.8)	(3482.5)		(115.8)	(6800.0)	(6846.1)	(6779.2)	(6843.4)
	(79.0)	(3436.6)	(3476.2)	(3417.4)	(3450.9)		(87.3)	(6771.5)	(6817.6)	(6750.7)	(6691.8)
	(-9.4)	(3348.2)	(3387.8)	(3329.0)	(3324.7)		(3.0)	(6687.2)	(6733.3)	(6666.4)	(6614.1)
	(-56.2)	(3301.4)	(3341.0)	(3282.2)	(3296.9)		(-42.1)	(6642.1)	(6688.2)	(6621.3)	(6575.7)
	(-210.2)	(3147.4)	(3187.0)	(3128.2)	(3112.3)		(-229.8)	(6454.4)	(6500.5)	(6433.6)	(6396.7)
	(326.4)	(3684.0)	(3723.6)	(3664.8)	(3729.8)		(305.2)	(6989.4)	(7035.5)	(6968.6)	(7049.6)
$\frac{3}{2}^-$	(230.8)	(3588.5)	(3628.1)	(3569.3)	(3614.9)	$\frac{3}{2}^-$	(233.4)	(6917.6)	(6963.7)	(6896.8)	(6910.5)
	(140.8)	(3498.4)	(3538.0)	(3479.2)	(3530.4)		(136.5)	(6820.7)	(6866.8)	(6799.9)	(6867.0)
	(26.8)	(3384.4)	(3424.0)	(3365.2)	(3403.7)		(30.2)	(6714.4)	(6760.5)	(6693.6)	(6708.1)
	(-14.1)	(3343.5)	(3383.1)	(3324.3)	(3331.4)		(-2.2)	(6682.0)	(6728.1)	(6661.2)	(6622.6)
	(-87.6)	(3270.0)	(3309.6)	(3250.8)	(3269.2)		(-60.5)	(6623.7)	(6669.8)	(6602.9)	(6560.6)
	(-242.2)	(3115.4)	(3155.0)	(3096.2)	(3104.8)		(-246.7)	(6437.5)	(6483.6)	(6416.7)	(6382.2)
	(-326.8)	(3030.8)	(3070.4)	(3011.6)	(2996.9)		(-266.6)	(6417.6)	(6463.7)	(6396.8)	(6354.1)
	$nns\bar{s}$ ($I = 0$)					$nnsb\bar{s}$ ($I = 0$)					
$\frac{5}{2}^-$	154.3	3511.9	3551.5	3492.7	3546.7	$\frac{5}{2}^-$	139.6	6823.8	6869.9	6803.0	6864.0
	(136.3)	(3493.9)	(3533.5)	(3474.7)	(3531.3)		(127.2)	(6811.4)	(6857.5)	(6790.6)	(6855.3)
	(81.0)	(3438.6)	(3478.2)	(3419.4)	(3478.1)		(103.6)	(6787.8)	(6833.9)	(6767.0)	(6839.0)
	(-56.7)	(3300.9)	(3340.5)	(3281.7)	(3300.8)		(-63.3)	(6620.9)	(6667.0)	(6600.1)	(6633.6)
	(-107.9)	(3249.7)	(3289.3)	(3230.5)	(3277.2)		(-113.9)	(6570.3)	(6616.4)	(6549.5)	(6544.8)
	(-334.9)	(3022.7)	(3062.3)	(3003.5)	(3043.1)		(-356.0)	(6328.2)	(6374.3)	(6307.4)	(6316.0)
	(100.2)	(3457.8)	(3497.4)	(3438.6)	(3498.4)		(99.0)	(6783.2)	(6829.3)	(6762.4)	(6833.4)
	(-14.6)	(3343.0)	(3382.6)	(3323.8)	(3343.4)		(-8.1)	(6676.1)	(6722.2)	(6655.3)	(6646.5)
	(-73.5)	(3284.1)	(3323.7)	(3264.9)	(3299.8)		(-69.0)	(6615.2)	(6661.3)	(6594.4)	(6636.4)
	(-134.3)	(3223.3)	(3262.9)	(3204.1)	(3232.1)		(-126.3)	(6557.9)	(6604.0)	(6537.1)	(6528.8)
$\frac{1}{2}^-$	(-253.3)	(3104.4)	(3144.0)	(3085.2)	(3084.1)	$\frac{1}{2}^-$	(-239.2)	(6445.0)	(6491.1)	(6424.2)	(6365.2)
	(-437.4)	(2920.2)	(2959.8)	(2901.0)	(2929.5)		(-385.2)	(6299.0)	(6345.1)	(6278.2)	(6281.0)
	(-557.6)	(2800.0)	(2839.6)	(2780.8)	(2780.9)		(-557.2)	(6127.0)	(6173.1)	(6106.2)	(6116.0)
$ssn\bar{s}$ ($I = 1/2$)					$ssnb\bar{s}$ ($I = 1/2$)						
J^P	Eigenvalue	$(\phi\Xi_c)$	$(K\Omega_c)$	$(D_s\Xi)$	Mass	J^P	Eigenvalue	$(\phi\Xi_b)$	$(K\Omega_b)$	$(B_s\Xi)$	Mass
$\frac{5}{2}^-$	(143.0)	(3671.2)	(3661.8)	(3645.1)	(3666.8)	$\frac{5}{2}^-$	(124.1)	(6978.9)	(6958.6)	(6954.5)	(6972.5)
	(107.0)	(3635.2)	(3625.8)	(3609.1)	(3644.5)		(86.4)	(6941.2)	(6920.8)	(6916.7)	(6937.8)
	(170.2)	(3698.4)	(3689.0)	(3672.3)	(3718.9)		(172.4)	(7027.2)	(7006.9)	(7002.7)	(7047.1)
	(122.2)	(3650.4)	(3641.0)	(3624.4)	(3660.4)		(111.5)	(6966.3)	(6946.0)	(6741.8)	(6959.9)
	(66.8)	(3595.0)	(3585.6)	(3568.9)	(3606.2)		(81.7)	(6936.5)	(6916.1)	(6912.0)	(6953.1)
	(56.7)	(3584.9)	(3575.5)	(3558.9)	(3589.5)		(61.3)	(6916.1)	(6896.7)	(6891.6)	(6916.6)
	(-50.5)	(3477.7)	(3468.3)	(3451.6)	(3470.5)		(-24.5)	(6830.3)	(6809.9)	(6805.8)	(6798.3)
	(-76.4)	(3451.8)	(3442.4)	(3425.8)	(3438.1)		(-72.5)	(6782.4)	(6762.0)	(6757.9)	(6784.7)
	(-289.2)	(3239.0)	(3229.6)	(3213.0)	(3208.3)		(-310.1)	(6544.7)	(6524.4)	(6520.3)	(6496.8)
	(265.1)	(3793.3)	(3783.9)	(3767.2)	(3834.0)		(238.9)	(7093.7)	(7073.4)	(7069.2)	(7130.0)
$\frac{3}{2}^-$	(174.2)	(3702.4)	(3693.0)	(3676.4)	(3733.4)	$\frac{3}{2}^-$	(181.3)	(7036.1)	(7015.8)	(7011.6)	(7057.6)
	(83.3)	(3611.5)	(3602.1)	(3585.5)	(3636.0)		(78.6)	(6933.4)	(6913.1)	(6909.0)	(6950.4)
	(-8.0)	(3520.2)	(3510.7)	(3494.1)	(3512.7)		(0.3)	(6855.1)	(6834.8)	(6830.6)	(6837.6)
	(-37.5)	(3490.7)	(3481.3)	(3464.6)	(3466.1)		(-24.4)	(6830.4)	(6810.1)	(6805.9)	(6801.1)
	(-102.7)	(3425.5)	(3416.0)	(3399.4)	(3414.1)		(-94.0)	(6760.8)	(6740.4)	(6736.3)	(6759.4)
	(-213.6)	(3314.6)	(3305.2)	(3288.6)	(3271.8)		(-193.7)	(6661.1)	(6640.8)	(6636.7)	(6608.4)
$\frac{1}{2}^-$	(-390.6)	(3137.7)	(3128.2)	(3111.6)	(3102.6)	$\frac{1}{2}^-$	(-337.9)	(6516.9)	(6496.6)	(6492.5)	(6477.4)

and $bbbb\bar{n}$ (\bar{s}) pentaquark subsystems are the same as that of the $nnnn\bar{c}$ (\bar{b}) ($I = 2$) pentaquark subsystem by appropriately replacing the constituent quarks.

Substituting the appropriate parameters into the $cccc\bar{n}$ (\bar{s}) and $bbbb\bar{n}$ (\bar{s}) CMI Hamiltonians and diagonalizing them, the corresponding mass spectrums for $cccc\bar{q}$ and $bbbb\bar{q}$ pentaquark subsystems can be obtained and we present them in Table XXV. Our results for the mass spectrums of $cccc\bar{n}$ (\bar{s}) and $bbbb\bar{n}$ (\bar{s}) pentaquark subsystems are calculated in two schemes. In the first scheme, the only combination of meson-baryon reference systems are $(\Omega_{ccc}) + (D)$, $(\Omega_{ccc}) + (D_s)$, $(\Omega_{bbb}) + (\bar{B})$, and $(\Omega_{bbb}) + (\bar{B}_s)$ for the $cccc\bar{n}$, $cccc\bar{s}$, $bbbb\bar{n}$, and $bbbb\bar{s}$ subsystems, respectively. The obtained eigenvalues and results calculated from Eq. (3) are presented in the second and third columns of Table XXV, respectively. Meanwhile, the results calculated from the modified CMI model in Eq. (4) are presented in the fifth column of Table XXV.

Based on the results listed in the fifth column, we plot the mass spectrums of the $cccc\bar{n}$, $cccc\bar{s}$, $bbbb\bar{n}$, and $bbbb\bar{s}$ subsystems in the diagrams (a)-(d) of Fig. 5, respectively. Note that due to the constraint from Pauli principle, the ground $J^P = 5/2^-$ pentaquark state with $cccc\bar{q}$ and $bbbb\bar{q}$ can not exist. In addition, we also present the thresholds for relevant quark rearrangement decay patterns in Fig. 5.

Based on the obtained $cccc\bar{q}$ and $bbbb\bar{q}$ pentaquark spectrums, we can discuss the possible decay patterns by considering different rearrangement of quarks in the corresponding pentaquark states. The observation of possible decay patterns for $cccc\bar{q}$ and $bbbb\bar{q}$ pentaquark states is a direct way to prove the existence of the $QQQQ\bar{q}$ pentaquark states. From the diagrams (a)-(d) of Fig. 5, we find that all the $cccc\bar{q}$ and $bbbb\bar{q}$ pentaquark states have strong decay channels, indicating that in the modified CMI model, no stable $cccc\bar{q}$ and $bbbb\bar{q}$ pentaquark exists.

Besides the mass spectrums, the calculated eigenvectors can also give us valuable information about the overlap for a $cccc\bar{q}$ or a $bbbb\bar{q}$ pentaquark state with a particular baryon \otimes meson component. Here, the overlaps of different baryon \otimes meson components for $cccc\bar{q}$ and $bbbb\bar{q}$ pentaquark states are collected in Table XLVII of Appendix H. According to Table XLVII, we can infer that all the $cccc\bar{q}$ and $bbbb\bar{q}$ states are genuine pentaquark states. Meanwhile, using the results of eigenvectors in Table XLVII, the relative partial decay widths can also be calculated and we present them in Table XXVI.

Similarly, according to heavy quark symmetry, we use the following parameters

$$\gamma_{\Omega_{ccc}D^*} = \gamma_{\Omega_{ccc}D}, \quad \gamma_{\Omega_{ccc}D_s^*} = \gamma_{\Omega_{ccc}D_s}, \quad (72)$$

and

$$\gamma_{\Omega_{ccc}B^*} = \gamma_{\Omega_{ccc}B}, \quad \gamma_{\Omega_{ccc}B_s^*} = \gamma_{\Omega_{ccc}B_s}, \quad (73)$$

for $cccc\bar{q}$ and $bbbb\bar{q}$ pentaquark subsystems, respectively.

Based on Eqs. 18, 72, and 73, we can calculate relative partial decay widths for the $cccc\bar{q}$ and $bbbb\bar{q}$

pentaquark subsystems. Due to small phase spaces, the $P_{c^4\bar{n}}(6761.4, 1/2, 3/2^-)$ and $P_{c^4\bar{s}}(6863.7, 0, 3/2^-)$ can only decay into $\Omega_{ccc}D$ and $\Omega_{ccc}D_s$ final states, respectively. While for the two $J^P = 3/2^-$ $bbbb\bar{q}$ pentaquark states, the $P_{b^4\bar{n}}(19647.2, 1/2, 3/2^-)$ and $P_{b^4\bar{s}}(19736.2, 0, 3/2^-)$, we find

$$\Gamma_{\Omega_{bbb}B^*} : \Gamma_{\Omega_{bbb}B} = 1 : 1.3, \quad (74)$$

and

$$\Gamma_{\Omega_{bbb}B_s^*} : \Gamma_{\Omega_{bbb}B_s} = 1 : 1.4, \quad (75)$$

respectively.

2. The $cccb\bar{q}$ and $bbbc\bar{q}$ pentaquark states

Now we discuss the $cccb\bar{q}$ and $bbbc\bar{q}$ pentaquark subsystems. The $cccb\bar{q}$ and $bbbc\bar{q}$ pentaquark subsystems include three identical heavy quarks. Note that for the $cccb\bar{n}$ (\bar{s}) and $bbbc\bar{n}$ (\bar{s}) pentaquark states, the CMI Hamiltonian expressions can be directly obtained from Table XXXVII of Appendix G by appropriately replacing the flavor of constituent quarks. Thus, the mass spectrums as well as eigenvectors for the $cccb\bar{n}$ (\bar{s}) and $bbbc\bar{n}$ (\bar{s}) subsystems can also be calculated by substituting the relevant parameters collected in Table VI.

The masses of $cccb\bar{n}$ (\bar{s}) and $bbbc\bar{n}$ (\bar{s}) pentaquark states can be determined in two schemes. In the first scheme, we can exhaust two types of baryon-meson reference systems. Specifically, we can use the $\Omega_{ccc} + B$ (B_s) and $\Omega_{ccb} + D$ (D_s) as reference systems to estimate the mass of the $cccb\bar{n}$ (\bar{s}) pentaquark subsystem. Similarly, the meson-baryon reference systems $\Omega_{bbb} + D$ (D_s) and $\Omega_{bbc} + B$ (B_s) are used to calculate the mass of the $bbbc\bar{n}$ (\bar{s}) pentaquark subsystem. The obtained eigenvalues and masses of $cccb\bar{n}$ (\bar{s}) and $bbbc\bar{n}$ (\bar{s}) pentaquark states calculated from two types of reference systems are presented in the third and fourth columns of Table XXV, respectively. Moreover, the results calculated from the modified CMI model are also shown in the fifth column of Table XXV. Based on the results listed in the fifth column, we plot the mass spectrums and relevant quark rearrangement decay patterns for the $cccb\bar{n}$, $cccb\bar{s}$, $bbbc\bar{n}$, and $bbbc\bar{s}$ subsystems in the diagrams (e)-(h) of Fig. 5, respectively.

According to the modified CMI model, we can obtain the overlaps for $bbbc\bar{n}$ and $bbbc\bar{s}$ pentaquark states with different baryon \otimes meson bases, the results are shown in Table XLVII of Appendix H.

In the following, we only concentrate on the $cccb\bar{n}$ pentaquark subsystem, one can perform similar discussions on the $cccb\bar{s}$, $bbbc\bar{n}$, and $bbbc\bar{s}$ pentaquark subsystems.

From Table XLVII, we find that the $J^P = 5/2^-$ $QQQQ'\bar{q}$ pentaquark state has only one component $\Omega_{QQQ}B^{(*)}$ ($D^{(*)}$), such pentaquark states can be regarded as a scattering state and unlikely to be found in any experiment. Thus, from our analysis, there is no $J^P = 5/2^-$ ground state $cccb\bar{q}$ and $bbbc\bar{q}$ pentaquark

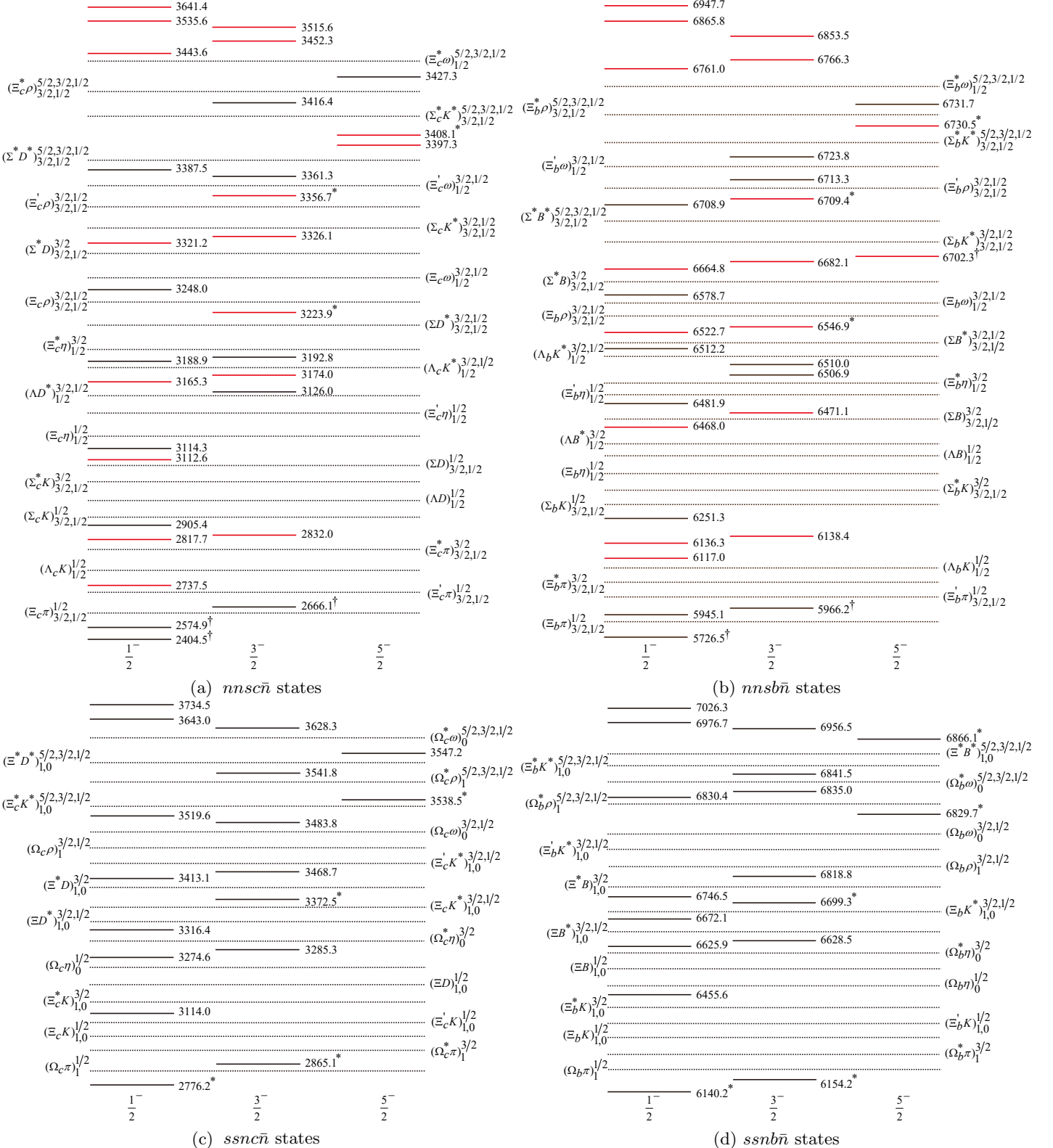


FIG. 3. Relative positions (units: MeV) for the $nnsc\bar{n}$, $nnsb\bar{n}$, $ssnc\bar{n}$, and $ssnb\bar{n}$ pentaquark states labeled with solid lines. In the $nnsc\bar{n}$ and $nnsb\bar{n}$ subsystems, the red and black lines represent the pentaquark states with $I = 3/2, 1/2$ ($I_{nn} = 1$) and $I = 1/2$ ($I_{nn} = 0$), respectively. The dotted lines denote various baryon-meson thresholds. When the spin (isospin) of an initial pentaquark state is equal to a number in the superscript (subscript) of a baryon-meson state, its decay into that baryon-meson channel through S -wave is allowed by the angular momentum (isospin) conservation. The scattering states and stable states in the modified CMI model are marked with “ $*$ ” and “ \dagger ”, respectively.

states. Moreover, for the $P_{c^3b\bar{n}}(10117.6, 1/2, 3/2^-)$, $P_{c^3b\bar{n}}(10078.2, 1/2, 3/2^-)$, and $P_{c^3b\bar{n}}(10134.4, 1/2, 1/2^-)$ states, they strongly couple to the $\Omega_{ccc}\bar{B}^*$, $\Omega_{ccc}\bar{B}$, and $\Omega_{ccc}\bar{B}^*$ bases, respectively. In our calculation, these three pentaquarks are also scattering states. Thus, we label them with “*” in Tables XXVI, XLVII, and Fig. 5. After identifying the above scattering states, the rest of the $QQQQ'\bar{q}$ pentaquark states can be safely considered as the genuine pentaquark states.

For $cccb\bar{n}$ pentaquark states, they have two types of decay modes: $ccb - b\bar{n}$ and $ccb - c\bar{n}$. Meanwhile, from heavy quark symmetry, we have

$$\gamma_{\Omega_{ccc}B^*} = \gamma_{\Omega_{ccc}B}, \quad (76)$$

and

$$\gamma_{\Omega_{ccb}^*D^*} = \gamma_{\Omega_{ccb}^*D} = \gamma_{\Omega_{ccb}D^*} = \gamma_{\Omega_{ccb}D}. \quad (77)$$

Based on Table XLVII, we obtain relative partial decay widths for $cccb\bar{n}$ pentaquark states and present them in Table XXVI. According to Table XXVI, we can see that the $P_{c^3b\bar{n}}(9961.3, 1/2, 3/2^-)$ and $P_{c^3b\bar{n}}(9945.5, 1/2, 1/2^-)$ states only decay into Ω_{ccb}^*D and $\Omega_{ccb}D$ final states, respectively. For the $P_{c^3b\bar{n}}(10061.5, 1/2, 1/2^-)$ states, we have its relative partial decay width ratios as

$$\Gamma_{\Omega_{ccb}^*D^*} : \Gamma_{\Omega_{ccb}D^*} : \Gamma_{\Omega_{ccb}D} = 24 : 24 : 1, \quad (78)$$

suggesting that the partial decay width of the $\Omega_{ccb}^*D^*$ channel is nearly equal to that of the $\Omega_{ccb}D^*$ channel. Note that if a state would be observed in the decay pattern $\Omega_{ccb}^*D^*$, Ω_{ccb}^*D , $\Omega_{ccb}D^*$, and $\Omega_{ccb}D$, it is a good candidate of a $cccb\bar{n}$ pentaquark state. For the $cccb\bar{s}$, $bbbc\bar{n}$, and $bbbc\bar{s}$ pentaquark subsystems, the relevant results are also given in Tables XLVII, XXVI, and Fig. 5.

3. The $ccbb\bar{q}$ pentaquark states

The last group of the $QQQQ\bar{q}$ system is the pentaquark states with the $ccbb\bar{n}$ (\bar{s}) configuration. The $ccbb\bar{q}$ (\bar{b}) pentaquark states has two pairs of identical heavy quarks, i.e., cc pair and bb pair. When we construct the wave functions of $ccbb\bar{q}$ pentaquark states, the Pauli principle should be satisfied simultaneously for these two pairs of heavy quarks.

According to Table II, the expressions of CMI Hamiltonians for $ccbb\bar{q}$ subsystem are similar to that of the $nnss\bar{c}$ (\bar{b}) ($I = 1$) pentaquark subsystem. Thus, we can obtain the mass spectrums of the $ccbb\bar{n}$ (\bar{s}) pentaquark subsystem with the help of the CMI Hamiltonian for $nnss\bar{Q}$ ($I = 1$) pentaquark states.

We can also determine the mass spectrums of $ccbb\bar{n}$ (\bar{s}) pentaquark subsystem in two scheme. In the first scheme, there are two types of meson-baryon reference systems for the $ccbb\bar{n}$ (s) pentaquark subsystem, i.e., the $\Omega_{ccb} + B$ ($\Omega_{ccb} + B_s$) and $\Omega_{ccb} + D$ ($\Omega_{ccb} + D_s$). Moreover,

the results calculated from the modified CMI model are also presented in the fifth column of Table XXV.

Based on the results obtained from the modified CMI model, we plot the mass spectrums and possible decay patterns via rearrangement of constituent quarks in $ccbb\bar{n}$ and $ccbb\bar{s}$ pentaquark states in the diagrams (i)-(j) of Fig. 5. According to Fig. 5, we find that all $ccbb\bar{n}$ and $ccbb\bar{s}$ pentaquark states have strong decay channels. i.e., from the modified CMI model analysis, there is no stable pentaquark state in $ccbb\bar{n}$ and $ccbb\bar{s}$ pentaquark subsystems.

Meanwhile, based on the obtained eigenvectors of the modified CMI model, the overlaps for $ccbb\bar{q}$ pentaquark states with particular baryon \otimes meson bases are presented in Table XLVII. From Table XLVII, we can safely treat all the $ccbb\bar{q}$ pentaquark states as genuine pentaquark states. Here, we need to consider $ccb - b\bar{q}$ and $cbb - c\bar{q}$ decay modes. To calculate the strong decay widths of the $ccbb\bar{n}$ and $ccbb\bar{s}$ pentaquark subsystems, we can use the following approximations

$$\gamma_{\Omega_{ccb}^*D^*} = \gamma_{\Omega_{ccb}^*D} = \gamma_{\Omega_{ccb}D^*} = \gamma_{\Omega_{ccb}D}, \quad (79)$$

$$\gamma_{\Omega_{ccb}^*B^*} = \gamma_{\Omega_{ccb}^*B} = \gamma_{\Omega_{ccb}B^*} = \gamma_{\Omega_{ccb}B}, \quad (80)$$

$$\gamma_{\Omega_{ccb}^*D_s^*} = \gamma_{\Omega_{ccb}^*D_s} = \gamma_{\Omega_{ccb}D_s^*} = \gamma_{\Omega_{ccb}D_s}, \quad (81)$$

$$\gamma_{\Omega_{ccb}^*B_s^*} = \gamma_{\Omega_{ccb}^*B_s} = \gamma_{\Omega_{ccb}B_s^*} = \gamma_{\Omega_{ccb}B_s}. \quad (82)$$

By introducing the above relations, the relative partial decay widths for $ccbb\bar{n}$ ($ccbb\bar{s}$) pentaquark states can be obtained and we present them in Table XXVI.

To discuss the strong decay behaviors of the $ccbb\bar{q}$ pentaquark states, we mainly focus on the relative partial decay widths of the $ccbb\bar{n}$ subsystem, the $ccbb\bar{s}$ subsystem can be analyzed in a similar way.

From Table XXVI, we find that the $J^P = 5/2^-$, the lowest $J^P = 3/2^-$, and the lowest $J^P = 1/2^-$ states can only decay into $\Omega_{ccb}^*D^*$, Ω_{ccb}^*D , and $\Omega_{ccb}D$, respectively. The most important decay channel for the $P_{c^2b^2\bar{n}}(13382.7, 1/2, 3/2^-)$ is Ω_{ccb}^*D channel in $bbc - c\bar{n}$ decay mode. The highest $J^P = 3/2^-$ state $P_{c^2b^2\bar{n}}(13413.9, 1/2, 1/2^-)$ have many different decay channels and this state is expected to be broad. For the $P_{c^2b^2\bar{n}}(13382.7, 1/2, 3/2^-)$, we have

$$\gamma_{\Omega_{ccb}^*D^*} : \gamma_{\Omega_{ccb}^*D} : \gamma_{\Omega_{ccb}D^*} = 1.7 : 18.7 : 1, \quad (83)$$

and

$$\gamma_{\Omega_{ccb}^*B^*} : \gamma_{\Omega_{ccb}^*B} : \gamma_{\Omega_{ccb}B^*} = 0.04 : 0.004 : 1. \quad (84)$$

Obviously, its dominant decay modes in $cbb - c\bar{n}$ and $ccb - b\bar{n}$ sectors are Ω_{ccb}^*D and $\Omega_{ccb}B^*$ channels, respectively. For the $P_{c^2b^2\bar{n}}(13413.9, 1/2, 1/2^-)$, we have

$$\gamma_{\Omega_{ccb}^*D^*} : \gamma_{\Omega_{ccb}D^*} : \gamma_{\Omega_{ccb}D} = 12 : 3.7 : 1, \quad (85)$$

and

$$\gamma_{\Omega_{ccb}^*B^*} : \gamma_{\Omega_{ccb}B^*} : \gamma_{\Omega_{ccb}B} = 1.1 : 0.7 : 1. \quad (86)$$

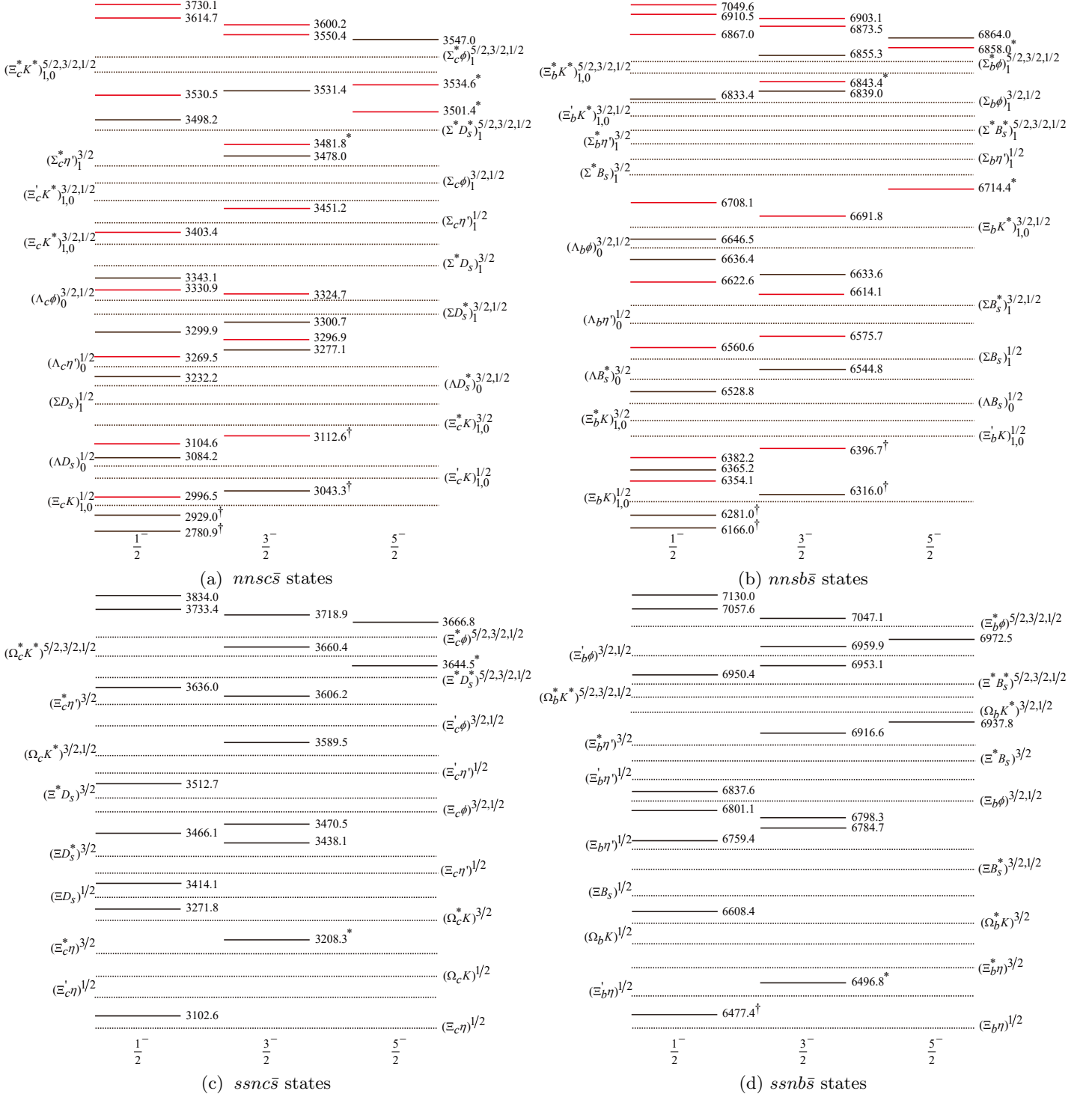


FIG. 4. Relative positions (units: MeV) for the $nnsc\bar{s}$, $nnsb\bar{s}$, $ssnc\bar{s}$, and $ssnb\bar{s}$ pentaquark states labeled with solid lines. In the $nnsc\bar{s}$ and $nnsb\bar{s}$ subsystems, the red and black lines represent the pentaquark states with $I = 1$ and $I = 0$, respectively. The dotted lines denote various baryon-meson thresholds. When the spin (isospin) of an initial pentaquark state is equal to a number in the superscript (subscript) of a baryon-meson state, its decay into that baryon-meson channel through S -wave is allowed by the angular momentum (isospin) conservation. The scattering states and stable states are marked with “*” and “†”, respectively.

Other three $J^P = 3/2^-$ and three $J^P = 1/2^-$ states only have $c\bar{b} - c\bar{n}$ decay mode. The numerical results for relative partial decay widths are presented in Table XXVI. Although they also have large coefficient in their corresponding eigenvectors, their $ccb - bn$ decay mode are strongly suppressed by the corresponding phase space. One can obtain very similar conclusion on $ccb\bar{s}$ subsystem according to Table XXVI.

D. The $QQQQ\bar{Q}$ pentaquark states

Recently, the LHCb Collaboration has found a peak in the $J/\psi J/\psi$ invariant mass spectrum and a width of about 80 MeV structure near 6.9 GeV/ c^2 was observed [64]. This observation revitalized the studies on fully heavy multiquark states [116–124]. If one replace the J/ψ meson with a fully heavy charmed baryon, we obtain a fully heavy charmed pentaquark candidate. In this subsection, we study the pentaquark system with fully heavy quarks $QQQQ\bar{Q}$.

Similar to the $QQQQ\bar{q}$ pentaquark systems, the $QQQQ\bar{Q}$ pentaquark systems can be divided into three groups according to their symmetry properties, i.e., (1) the $cccc\bar{Q}$ and $bbbb\bar{Q}$ pentaquark subsystems, (2) the $cccb\bar{Q}$ and $bbbc\bar{Q}$ pentaquark subsystems, (3) the $ccb\bar{b}$ pentaquark subsystem. In the following, we study the mass spectrums and decay properties for the $QQQQ\bar{Q}$ pentaquark system group by group.

1. The $cccc\bar{Q}$ and $bbbb\bar{Q}$ pentaquark states

Here, we first discuss the fully heavy pentaquark states with $cccc\bar{c}$ (\bar{b}) and $bbbb\bar{c}$ (\bar{b}) flavor combinations. Note that the symmetrical properties of the $cccc\bar{c}$ (\bar{b}) and $bbbb\bar{c}$ (\bar{b}) pentaquark subsystems are the same as that of the $ssss\bar{Q}$ pentaquark subsystem. Thus, according to Table II, the forms of CMI Hamiltonian for $cccc\bar{c}$ (\bar{b}) and $bbbb\bar{c}$ (\bar{b}) subsystems can be obtained with the help of the CMI Hamiltonians for the $nnnn\bar{c}$ (b) ($I = 2$) subsystem.

By substituting the parameters for the effective mass of heavy quarks and the coupling constants listed in Table VI, we present the mass spectrums for $QQQQ\bar{Q}$ pentaquark system in Table XXVIII.

Firstly, for the $cccc\bar{Q}$ and $bbbb\bar{Q}$ penatquark subsystems, there is only one type of reference system in the first scheme. Here, the reference baryon-meson systems ($\Omega_{ccc} + (\eta_c)$, ($\Omega_{ccc} + (B_c)$, ($\Omega_{bbb} + (B_c)$, and ($\Omega_{bbb} + (\eta_b)$ are used to estimate the mass spectrums of $cccc\bar{c}$, $cccc\bar{b}$, $bbbb\bar{c}$, and $bbbb\bar{b}$ pentaquark subsystems, respectively. The calculated eigenvalues, pentaquark masses obtained from the first scheme in Eq. (3), and masses obtained from the second scheme in Eq. (4) are presented in the second, third, and fifth columns of Table XXVIII, respectively. Meanwhile, based on the values listed in the fifth column of Table XXVIII, we plot the mass spectrums of

the $cccc\bar{c}$, $cccc\bar{b}$, $bbbb\bar{c}$, and $bbbb\bar{b}$ subsystems in the diagrams (a)-(d) of Fig. 6. In addition, the thresholds for all possible strong decay channels via the rearrangement of $QQQQ\bar{Q}$ constituent quarks are also illustrated in Fig. 6.

Based on the mass spectrums of all the $QQQQ\bar{Q}$ pentaquark system, we discuss their corresponding strong decay behaviors. Note that due to the constraint from Pauli principle, there is no ground pentaquark state with quantum number $J^P = 5/2^-$ in the $cccc\bar{Q}$ and $bbbb\bar{Q}$ penatquark subsystems. From Table XXVIII, we find that all the $cccc\bar{Q}$ and $bbbb\bar{Q}$ pentaquark states are higher than the thresholds of the lowest possible meson-baryon systems. Thus, in our model, no stable pentaquark state exists in the $cccc\bar{Q}$ and $bbbb\bar{Q}$ pentaquark subsystems.

We use the modified CMI model to calculate the overlaps for $cccc\bar{Q}$ ($bbbb\bar{Q}$) pentaquark states with baryon \otimes meson bases and present the results in Table XLVIII of Appendix H.

In order to calculate the relative partial decay widths of $cccc\bar{Q}$ and $bbbb\bar{Q}$ pentaquark states, for each $cccc\bar{Q}$ and $bbbb\bar{Q}$ pentaquark subsystems, we apply the following relations

$$\gamma_{\Omega_{ccc}J/\psi} = \gamma_{\Omega_{ccc}\eta_c}, \quad \gamma_{\Omega_{ccc}B_c^*} = \gamma_{\Omega_{ccc}B_c}, \quad (87)$$

and

$$\gamma_{\Omega_{ccc}B_c^*} = \gamma_{\Omega_{ccc}B_c}, \quad \gamma_{\Omega_{ccc}\Upsilon} = \gamma_{\Omega_{ccc}\eta_b}. \quad (88)$$

Based on Eqs. 18, 87, and 88, we obtain the relative partial decay widths for the $cccc\bar{Q}$ and $bbbb\bar{Q}$ pentaquark states and present them in Table XXIX. Because of the angular conservation law, the $J^P = 1/2^-$ $cccc\bar{c}$ ($bbbb\bar{b}$) pentaquark state can only decay into $\Omega_{ccc}J/\psi$ ($\Omega_{bbb}\Upsilon$). In addition, For the $P_{b^4\bar{c}}(20651.7, 0, 3/2^-)$ and $P_{b^4\bar{b}}(23774.8, 0, 3/2^-)$, we find

$$\Gamma_{\Omega_{bbb}B_c^*} : \Gamma_{\Omega_{bbb}B_c} = 0.4 : 1, \quad (89)$$

and

$$\Gamma_{\Omega_{bbb}\Upsilon} : \Gamma_{\Omega_{bbb}\eta_b} = 0.45 : 1, \quad (90)$$

respectively.

2. The $cccb\bar{Q}$ and $bbbc\bar{Q}$ pentaquark states

Next, we discuss the $cccb\bar{c}$ (\bar{b}) and $bbbc\bar{c}$ (\bar{b}) pentaquark states. Since the first three quarks for $cccb\bar{Q}$ and $bbbc\bar{Q}$ pentaquark system are identical, we can use the expressions of CMI Hamiltonian in Table XXXVII of Appendix G to calculate the mass spectrums of the $cccb\bar{c}$ (\bar{b}) and $bbbc\bar{c}$ (\bar{b}) pentaquark states.

We get the mass spectrums for the $cccb\bar{Q}$ and $bbbc\bar{Q}$ pentaquark subsystems under two different schemes and present the corresponding results in Table XXVIII. The overlaps for $QQQQ\bar{Q}$ pentaquark states with baryon \otimes meson bases are calculated and are presented in Table

TABLE XXI. The relative partial decay widths for the $nns\bar{c}\bar{n}$ and $ssn\bar{c}\bar{n}$ pentaquark states. For each pentaquark state, we choose one channel as a reference channel, and the relative partial decay widths for the other channels are obtained in units of the reference channel. The masses are all in units of MeV. The scattering states and stable states in the modified CMI model are marked with “*” and “†”, respectively.

$nns\bar{c}\bar{n}(I_{nn} = 1)$		$nns \otimes c\bar{n}$				$nnc \otimes s\bar{n}$				$nsc \otimes n\bar{n}$					
$I[J^P]$	Mass	$\Sigma^* D^*$	$\Sigma^* D$	ΣD^*	ΣD	$\Sigma_c^* K^*$	$\Sigma_c K^*$	$\Sigma_c^* K$	$\Sigma_c K$	$\Xi_c^* \rho(\omega)$	$\Xi_c' \rho(\omega)$	$\Xi_c \rho(\omega)$	$\Xi_c^* \pi(\eta)$	$\Xi_c' \pi(\eta)$	$\Xi_c \pi(\eta)$
$\frac{3}{2}(\frac{1}{2})[\frac{5}{2}^-]$	3408.1*	1				x				x					
	3397.3	1				x				x					
$\frac{3}{2}(\frac{1}{2})[\frac{3}{2}^-]$	3515.6	3	1	0.016		1.5	1	1		13.8	5.5	1		1	
	3452.3	1.8	1	12.7		22	1	1		0.3	x	1		1	
	3356.7*	x	1	0.7		x	1	1		x	0.9	1		1	
	3326.1	x	1018	1		x	x	1		x	x	1		1	
	3223.9*	x	x	1		x	x	1		x	x	x		1	
	3126.0	x	x	x		x	x	1		x	x	x		1	
	2832.0	x	x	x		x	x	x		x	x	x		1	
$\frac{3}{2}(\frac{1}{2})[\frac{1}{2}^-]$	3641.4	690	1	1	8.5	1			1	688	70	1		1.4	1
	3535.6	337	1	1	0.0	1			1	0.2	81	1		1.8	1
	3433.6	0.35	4	1	0.8	1			1	0.09	0.15	1		0.001	1
	3321.2	x	8.5	1	x	x			1	x	x	1		0.0	1
	3165.3	x	x	1	x	x			1	x	x	x		1	1
	3112.6	x	x	1	x	x			1	x	x	x		26	1
	2817.7	x	x	x	x	x			x	x	x	x		0.09	1
	2737.5	x	x	x	x	x			x	x	x	x		1.5	1
$nns\bar{c}\bar{n}(I_{nn} = 0)$		ΛD^*	ΛD			$\Lambda_c K^*$	$\Lambda_c K$			$\Xi_c^* \rho(\omega)$	$\Xi_c' \rho(\omega)$	$\Xi_c \rho(\omega)$	$\Xi_c^* \pi(\eta)$	$\Xi_c' \pi(\eta)$	$\Xi_c \pi(\eta)$
$\frac{1}{2}[\frac{5}{2}^-]$	3427.3									1					
$\frac{1}{2}[\frac{3}{2}^-]$	3416.4	1				1				x	0.3	1		1	
	3361.3	1				1				x	3.3	1		1	
	3192.8	1				1				x	x	x		1	
	3174.0	1				x				x	x	x		1	
	2666.1†	x				x				x	x	x		x	
$\frac{1}{2}[\frac{1}{2}^-]$	3387.5	5.5	1			1	1			x	0.6	1		4.4	1
	3248.0	9.3	1			1	1			x	x	1		0.07	1
	3188.9	2.6	1			1	1			x	x	x		24	1
	3114.3	x	1			x	1			x	x	x		2.2	1
	2905.4	x	x			x	1			x	x	x		0.14	1
	2574.9†	x	x			x	x			x	x	x		x	x
	2404.5†	x	x			x	x			x	x	x		x	x
$ssn\bar{c}\bar{n}$		$ssn \otimes c\bar{n}$				$ssc \otimes n\bar{n}$				$nsc \otimes s\bar{n}$					
$I[J^P]$	Mass	$\Xi^* D^*$	$\Xi^* D$	ΞD^*	ΞD	$\Omega_c^* \rho(\omega)$	$\Omega_c \rho(\omega)$	$\Omega_c^* \pi(\eta)$	$\Omega_c \pi(\eta)$	$\Xi_c^* K^*$	$\Xi_c' K^*$	$\Xi_c K^*$	$\Xi_c^* K$	$\Xi_c' K$	$\Xi_c K$
$1(0)[\frac{5}{2}]$	3547.2	1				1				1					
	3538.5*	x				x				1					
$1(0)[\frac{3}{2}]$	3628.3	88	25	1		1.9	1	1		94.5	52.5	1		1	
	3541.8	x	1	163		5	1	1		1	0.1	5.5		1	
	3483.8	x	14	1		x	1	1		x	0.6	1		1	
	3468.7	x	64	1		x	x	1		x	x	1		1	
	3372.5*	x	x	1		x	x	1		x	x	1		1	
	3285.3	x	x	x		x	x	1		x	x	x		1	
	2865.1*	x	x	x		x	x	x		x	x	x		x	
$1(0)[\frac{1}{2}]$	3734.5	264.5	0.0	1	20.5	1			1	20.1	1	0.007		0.008	1
	3643.0	265.7	1	0.7	1	81.6			1	2.1	197	1		117	1
	3519.6	x	10.3	1	x	1			1	x	0.08	1		1	1
	3413.1	x	12.6	1	x	x			1	x	x	1		0.1	1
	3316.4	x	x	1	x	x			1	x	x	x		4	1
	3274.6	x	x	x	x	x			1	x	x	x		8	1
	3114.0	x	x	x	x	x			1	x	x	x		x	1
	2776.2*	x	x	x	x	x			x	x	x	x		x	x

XLVIII of Appendix H. In addition, based on the values listed in the fifth column of Table XXVIII, we plot the mass spectrums and all possible decay channels of the $cccb\bar{c}$, $cccb\bar{b}$, $bbbc\bar{c}$, and $bbbc\bar{b}$ pentaquark subsystems in the diagrams (e)-(h) of Fig. 6, respectively.

The overlaps for fully heavy pentaquark states with baryon \otimes meson bases are collected in Table XLVIII. Here, we mainly focus on the properties of $cccb\bar{b}$ pentaquark subsystem, the $cccb\bar{c}$, $bbbc\bar{c}$, and $bbbc\bar{b}$ pentaquark subsystems can be analyzed from Tables XXVIII, XXIX, XLVIII ,and Fig. 6 in a similar way.

Based on the eigenvectors listed in Table XLVIII, we label all the scattering states with “*” in Tables XXIX, XLVIII and Fig. 6. Here, the rearrangement of constituent quarks for such pentaquark states leads to two types of decay modes: $ccc - b\bar{b}$ and $ccb - c\bar{b}$. We can use the following approximations

$$\gamma_{\Omega_{ccc}\Upsilon} = \gamma_{\Omega_{ccc}\eta_b}, \quad (91)$$

and

$$\gamma_{\Omega_{ccb}^* B_c^*} = \gamma_{\Omega_{ccb}^* B_c} = \gamma_{\Omega_{ccb} B_c^*} = \gamma_{\Omega_{ccb} B_c}, \quad (92)$$

to estimate the relative partial decay widths and present them in Table XXIX, in which we find

$$\Gamma_{\Omega_{ccc}\Upsilon} : \Gamma_{\Omega_{ccc}\eta_b} = 0.1 : 1, \quad (93)$$

and

$$\Gamma_{\Omega_{ccb}^* B_c^*} : \Gamma_{\Omega_{ccb}^* B_c} : \Gamma_{\Omega_{ccb} B_c^*} = 3.3 : 3.7 : 1, \quad (94)$$

for the $P_{c^3b\bar{b}}(14372.6, 0, 3/2^-)$ state. Thus, for this pentaquark state, the relative partial decay width of $\Omega_{ccc}\Upsilon$ channel is much larger than that of the $\Omega_{ccb}\eta_b$ channel in the $ccc - b\bar{b}$ decay mode. Meanwhile, in the $ccc - b\bar{b}$ decay mode, the partial decay width of the $\Omega_{ccb}^* B_c^*$ is nearly equal to that of the $\Omega_{ccb}^* B_c$.

For the two $J^P = 1/2^-$ genius pentaquark states, they can both decay into $\Omega_{ccc}\Upsilon$ final states. We find

$$\Gamma_{\Omega_{ccb}^* B_c^*} : \Gamma_{\Omega_{ccb} B_c^*} : \Gamma_{\Omega_{ccb} B_c} = 31 : 4 : 1, \quad (95)$$

and

$$\Gamma_{\Omega_{ccb} B_c^*} : \Gamma_{\Omega_{ccb} B_c} = 2.1 : 1, \quad (96)$$

for the $P_{c^3b\bar{b}}(14411.0, 0, 1/2^-)$ and $P_{c^3b\bar{b}}(14356.9, 0, 1/2^-)$, respectively.

3. The $ccbb\bar{Q}$ pentaquark states

Now, we discuss the last group of the $QQQQ\bar{Q}$ system, the $ccbb\bar{c}$ (\bar{b}) subsystem. The symmetry property for $ccbb\bar{c}$ (\bar{b}) pentaquark subsystem is identical to that of the $ccbb\bar{n}$ (\bar{s}) pentaquark subsystem, i.e., there are two pairs of identical heavy quarks.

According to Table II, the forms of CMI Hamiltonian for the $ccbb\bar{Q}$ subsystem are similar to that of the $nnss\bar{c}$

(\bar{b}) ($I = 1$) pentaquark subsystem. By appropriately replace the constituent quarks, we can introduce the expressions of CMI Hamiltonian in Table XXXVII of Appendix G to calculate the mass spectrums of the $ccbb\bar{c}$ (\bar{b}) pentaquark states. We present the results of the mass spectrums for the $ccbb\bar{Q}$ subsystem obtained from two schemes in Table XXVIII. Moreover, the overlaps for $ccbb\bar{Q}$ pentaquark states with a specific baryon \otimes meson basis are calculated according to the modified CMI model (Eq. (4)), we present them in Table XLVIII of Appendix H. In addition, based on the results listed in the fifth column of Table XXVIII, we also plot the mass spectrum and relevant quark rearrangement decay patterns of the $ccbb\bar{Q}$ pentaquark subsystem in the diagrams (i)-(j) of Fig. 6.

Based on Table XLVIII, we label all the scattering states in $ccbb\bar{Q}$ subsystem with “*”. We can see that all states in the $ccbb\bar{c}$ and $ccbb\bar{b}$ subsystems are genuine pentaquark states.

For the $ccbb\bar{Q}$ subsystem, the rearrangement of constituent heavy quarks leads to $ccc - b\bar{Q}$ and $ccb - c\bar{Q}$ decay modes. To calculate the relative partial decay widths for the $ccbb\bar{c}$ subsystem, we use the following approximations

$$\gamma_{\Omega_{ccb}^* J/\psi} = \gamma_{\Omega_{ccb}^* \eta_c} = \gamma_{\Omega_{ccb} J/\psi} = \gamma_{\Omega_{ccb} \eta_c}, \quad (97)$$

$$\gamma_{\Omega_{ccb}^* B_c^*} = \gamma_{\Omega_{ccb}^* B_c} = \gamma_{\Omega_{ccb} B_c^*} = \gamma_{\Omega_{ccb} B_c}. \quad (98)$$

And for the $ccbb\bar{b}$ pentaquark subsystem, we have

$$\gamma_{\Omega_{ccb}^* B_c^*} = \gamma_{\Omega_{ccb}^* B_c} = \gamma_{\Omega_{ccb} B_c^*} = \gamma_{\Omega_{ccb} B_c}, \quad (99)$$

and

$$\gamma_{\Omega_{ccb}^* \Upsilon} = \gamma_{\Omega_{ccb}^* \eta_b} = \gamma_{\Omega_{ccb} \Upsilon} = \gamma_{\Omega_{ccb} \eta_b}. \quad (100)$$

With the above preparation, we present the relative partial decay widths for the $ccbb\bar{c}$ and $ccbb\bar{b}$ subsystems in Table XXIX.

Here, we contrate on the $ccbb\bar{b}$ subsystem and one can perform similar analysis to the $ccbb\bar{c}$ pentaquark states. According to the diagram (j) of Fig. 6, we find that the $P_{c^2b^2\bar{b}}(17476.5, 0, 5/2^-)$ do not have S wave strong decay channels, but it can decay into $\Omega_{ccb}\eta_b$ and $\Omega_{ccb} B_c$ final states via D -wave. This state should be a narrow state in the modified CMI model.

For the $J^P = 3/2^-$ $ccbb\bar{b}$ pentaquark states, we find that the lowest $P_{c^2b^2\bar{b}}(17416.2, 0, 3/2^-)$ state lies below all the allowed strong decay channels, which is a good candidate of stable pentaquark state. The heaviest $J^P = 3/2^-$ state $P_{c^2b^2\bar{b}}(17554.2, 0, 3/2^-)$ dominantly decay into $\Omega_{ccb}^* \eta_b$ in $ccb - bb$ mode. The $\Omega_{ccb}^* \eta_b$ channel would be an important decay mode to search for $J^P = 3/2^-$ $ccbb\bar{b}$ pentaquark states experimentally. The lowest two $J^P = 1/2^-$ states $P_{c^2b^2\bar{b}}(17404.9, 0, 1/2^-)$ and $P_{c^2b^2\bar{b}}(17437.4, 0, 1/2^-)$ can only decay into $\Omega_{ccb}\eta_b$ final states. Due to the small phase spaces, they should be two narrow states. The other two $J^P = 1/2^-$ states $P_{c^2b^2\bar{b}}(17575.8, 0, 1/2^-)$

TABLE XXII. The relative partial decay widths for the $nnsb\bar{n}$ and $ssnb\bar{n}$ pentaquark states. For each pentaquark state, we choose one channel as a reference channel, and the relative partial decay widths for the other channels are obtained in units of the reference channel. The masses are all in units of MeV. The scattering states and stable states in the modified CMI model are marked with “*” and “†”, respectively.

J^P	Mass	$nns \otimes b\bar{n}$				$nnb \otimes s\bar{n}$			$nsb \otimes n\bar{n}$						
		$\Sigma^* B^*$	$\Sigma^* B$	ΣB^*	ΣB	$\Sigma_b^* K^*$	$\Sigma_b^* K$	$\Sigma_b K^*$	$\Sigma_b K$	$\Xi_b^* \rho(\omega)$	$\Xi_b' \rho(\omega)$	$\Xi_b \rho(\omega)$	$\Xi_b^* \pi(\eta)$	$\Xi_b' \pi(\eta)$	$\Xi_b \pi(\eta)$
$\frac{5}{2}^-$	6730.5*	1				1				1					
	6702.3†	×				×				×					
$\frac{3}{2}^-$	6853.5	80	37	1		3.7	1	1		55	16	1		1	
	6766.3	0.25	0.05	1		10.2	1	1		0.36	0.03	1		1	
	6709.4*	40.8	316	1		×	1	1		×	×	1		1	
	6682.1	×	1500	1		×	×	1		×	×	1		1	
	6546.9*	×	×	1		×	×	1		×	×	1		1	
	6474.1	×	×	×		×	×	1		×	×	1		1	
	6138.4	×	×	×		×	×	×		×	×	1			
$\frac{1}{2}^-$	6947.7	53		1	1	3	1		1	2.8	1	0.0		0.3	1
	6865.8	223		0.6	1	0.2	1		1	8	36	1		300	1
	6761.0	0.65		0.05	1	0.5	1		1	0.1	0.2	1		0.3	1
	6664.8	×		4.5	1	×	×		1	×	×	1		×	1
	6522.7	×		0.08	1	×	×		1	×	×	1		0.008	1
	6468.0	×		×	×	×	×		1	×	×	1		430	1
	6136.3	×		×	×	×	×		1	×	1	1		0.025	1
	6117.0	×		×	×	1	1		1	1	1	1		4.7	1
		ΛB^*	ΛB			$\Lambda_b K^*$	$\Lambda_b K$			$\Xi_b^* \rho(\omega)$	$\Xi_b' \rho(\omega)$	$\Xi_b \rho(\omega)$	$\Xi_b^* \pi(\eta)$	$\Xi_b' \pi(\eta)$	$\Xi_b \pi(\eta)$
$\frac{5}{2}^-$	6731.7									1					
$\frac{3}{2}^-$	6723.8	1				1				1	4.4	1		1	
	6713.3	1				1				1	0.5	1		1	
	6510.0	1				1				1	1	1		1	
	6506.9	1				1				1	1	1		1	
	5966.2†	×				1				1	1	1		1	
$\frac{1}{2}^-$	6708.9	1	4			1	1			1	1	1		97.5	1
	6578.7	1	0.2			1	1			1	1	1		0.02	1
	6512.2	1	14			1	1			1	1	1		3.8	1
	6481.9	1	5.7			1	1			1	1	1		13	1
	6251.3	×	×			1	1			1	1	1		0.01	1
	5945.1	×	×			1	1			1	1	1		1	
	5726.5†	×	×			1	1			1	1	1		1	
		$ssn \otimes b\bar{n}$				$ssb \otimes n\bar{n}$				$nsb \otimes s\bar{n}$					
J^P	Mass	$ssn \otimes b\bar{n}$				$ssb \otimes n\bar{n}$			$nsb \otimes s\bar{n}$						
		$\Xi^* B^*$	$\Xi^* B$	ΞB^*	ΞB	$\Omega_b^* \rho(\omega)$	$\Omega_b^* \rho(\omega)$	$\Omega_b^* \pi(\eta)$	$\Omega_b \pi(\eta)$	$\Xi_b^* K^*$	$\Xi_b' K^*$	$\Xi_b K^*$	$\Xi_b^* K$	$\Xi_b' K$	$\Xi_b K$
$\frac{5}{2}^-$	6866.1*	1				1				1					
	6829.7*	×				1				1					
$\frac{3}{2}^-$	6965.5	59	24	1		2.9	1	1		833	254	1		1	
	6841.5	×	62	1		0.4	1	1		1	19	1		1	
	6835.0	×	8	1		9	1	1		1	1	28.5		1	
	6818.8	×	566	1		1	1	1		1	1	1		1	
	6699.3*	×	1			1	1	1		1	1	1		1	
	6628.5	×	1			1	1	1		1	1	1		1	
	6154.2*	×	1			1	1	1		1	1	1		1	
$\frac{1}{2}^-$	7026.3	22	1.2	1		3	1		1	3.3	1	0.0		0.001	1
	6976.7	165	0.7	1		0.16	1		1	30	200	1		288	1
	6830.4	×	0.9	1		0.12	1		1	1	20		42		1
	6746.5	×	7.7	1		1	1		1	1	1		1		37
	6672.1	×	0.12	1		1	1		1	1	1		8.5		1
	6625.9	×	1			1	1		1	1	1		250		1
	6455.6	×	1			1	1		1	1	1		1		1
	6140.2*	×	1			1	1		1	1	1		1		1

and $P_{c^2 b^2 \bar{b}}(17496.6, 0, 1/2^-)$ mainly decay into $\Omega_{ccb}^* \Upsilon$ in $ccb - bb$ decay mode. This decay channel is crucial to find $J^P = 1/2^- cccb\bar{b}$ pentaquark states.

E. The $QQQq\bar{Q}$ pentaquark states

Lastly, we discuss the pentaquark system with $QQQq\bar{Q}$ configuration. By exchanging the $q \leftrightarrow Q$ ($\bar{q} \leftrightarrow \bar{Q}$), we can see that the $QQQq\bar{Q}$ configuration is like a mirror structure of the $qqqQ\bar{q}$ configuration. As listed in Table I, such configuration includes the states with $cccn\bar{c}$ (\bar{b}), $cccs\bar{c}$ (\bar{b}), $ccbn\bar{c}$ (\bar{b}), $cbs\bar{c}$ (\bar{b}), $bbn\bar{c}$ (\bar{b}), $bbcs\bar{c}$ (\bar{b}), $bbn\bar{c}$ (\bar{b}), and $bbbs\bar{c}$ (\bar{b}) flavor combinations. Obviously, the isospin of such pentaquark states only depend on the flavor of the light constituent quark.

As shown in Table II, due to different symmetric properties among various flavor combinations in $QQQq\bar{Q}$ pentaquark system, we can divide the $QQQq\bar{Q}$ pentaquark system into two groups, i.e., (1) the $cccq\bar{Q}$ and $bbbq\bar{Q}$ pentaquark subsystems, (2) the $ccbq\bar{Q}$ and $bcbq\bar{Q}$ pentaquark subsystems.

1. The $cccq\bar{Q}$ and $bbbq\bar{Q}$ pentaquark states

We first discuss the $cccq\bar{c}$ (\bar{b}) and $bbbq\bar{c}$ (\bar{b}) pentaquark subsystems. Firstly, the restrictions from Pauli principle for the $cccq\bar{c}$ (\bar{b}) pentaquark states are identical to that of the $sssQ\bar{q}$ pentaquark states. More specifically, according to Table II, the CMI Hamiltonians for the $cccq\bar{c}$ (\bar{b}) and $bbbq\bar{c}$ (\bar{b}) pentaquark subsystems can be directly obtained with the help of the CMI Hamiltonian for $nnnQ\bar{n}$ (\bar{s}) ($I_{nnn} = 3/2$) pentaquark states.

We can use two types of meson-baryon reference systems to estimate the mass spectrums of the $cccq\bar{c}$ (\bar{b}) and $bbbq\bar{c}$ (\bar{b}) pentaquark subsystems. For example, the masses of the $bbn\bar{c}$ pentaquark states can be estimated by using the $\Omega_{bbb}D$ and $\Xi_{bb}B_c$ reference systems. Similarly, we can exhaust all the possible meson-baryon reference systems for the $bbbn\bar{b}$, $bbbs\bar{c}$ (\bar{b}), and $cccq\bar{c}$ (\bar{b}) subsystems by way of analog. The obtained eigenvalues and masses calculated from two difference reference systems in Eq. (3) for all the $QQQq\bar{Q}$ pentaquark subsystems are presented in the second, third, and fourth columns of Tables XXX and XXXI, respectively. In addition, the results calculated from the modified CMI model in Eq. (4) are also presented in the sixth column of Tables XXX and XXXI. Based on the results listed in the sixth column of Tables XXX and XXXI, we plot the mass spectrums of the $cccn\bar{c}$, $cccn\bar{b}$, $cccs\bar{c}$, $cccs\bar{b}$, $bbn\bar{c}$, $bbn\bar{b}$, $bbbs\bar{c}$, and $bbbs\bar{b}$ subsystems in the diagrams (a)-(d) of Figs. 7 and 8, respectively. The thresholds for different meson-baryon reference systems are also illustrated in Figs. 7 and 8.

According to the modified CMI model, we can obtain the overlaps for a particular $QQQq\bar{Q}$ pentaquark state with several baryon \otimes meson bases, the results are listed in Table XLIX of Appendix H.

Now, we mainly focus on the $bbbn\bar{c}$ pentaquark subsystem and one can perform similar discussion on other $cccq\bar{Q}$ and $bbbq\bar{Q}$ subsystems. From Table XLIX, we find that the $P_{b^3 n\bar{c}}(16318.2, 1/2, 5/2^-)$, $P_{b^3 n\bar{c}}(16317.8, 1/2, 3/2^-)$, $P_{c^3 n\bar{c}}(16175.8, 1/2, 3/2^-)$, and $P_{c^3 n\bar{c}}(16314.8, 1/2, 1/2^-)$ states have significant $\Omega_{bbb}D^*$, $\Omega_{bbb}D^*$, $\Omega_{ccc}D$, and $\Omega_{bbb}D^*$ components, respectively. These states should be identified as scattering states and can not be found in experiment. Moreover, since the $J^P = 5/2^-$ state has significant $\Omega_{QQQ}D^*$ (B^*) or $\Omega_{QQQ}D_s^*$ (B_s^*) components, they should also be identified as scattering states. Thus, in the modified CMI model, there is no $J^P = 5/2^-$ ground state for the $cccq\bar{Q}$ and $bbbq\bar{Q}$ pentaquark subsystems. We label all the scattering states for $QQQq\bar{Q}$ system with “*” in Tables XXXII, XLIX, and Figs. 7, 8. After identify the scattering states in $bbbn\bar{c}$ subsystem, only three genuine $bbbn\bar{c}$ pentaquark states left.

For $bbbn\bar{c}$ pentaquark states, we can apply the following approximations to calculate the corresponding relative decay widths

$$\gamma_{\Omega_{bbb}D^*} = \gamma_{\Omega_{bbb}D}, \quad (101)$$

and

$$\gamma_{\Xi_{bb}^* B_c^*} = \gamma_{\Xi_{bb} B_c} = \gamma_{\Xi_{bb} B_c^*} = \gamma_{\Xi_{bb} B_c}. \quad (102)$$

Thus, based on the overlaps for $bbbn\bar{c}$ pentaquark states with the corresponding baryon \otimes meson bases listed in Table XLIX, we obtain the relative partial decay widths for $bbbn\bar{c}$ pentaquark states and show them in Table XXXII.

According to Table XXXII, we find that the three genuine pentaquark states all have two type of decay modes, i.e., $bbb - n\bar{c}$ and $bbn - b\bar{c}$. For the $P_{b^3 n\bar{c}}(16583.0, 1/2, 1/2^-)$ and $P_{b^3 n\bar{c}}(16535.5, 1/2, 1/2^-)$, in $bbb - n\bar{c}$ mode, they both can decay into $\Omega_{bbb}^* D^*$ final states and have comparable decay widths. While in $bbn - b\bar{c}$ mode, we obtain

$$\Gamma_{\Xi_{bb}^* B_c^*} : \Gamma_{\Xi_{bb} B_c^*} : \Gamma_{\Xi_{bb} B_c} = 18.4 : 2.1 : 1, \quad (103)$$

and

$$\Gamma_{\Xi_{bb}^* B_c^*} : \Gamma_{\Xi_{bb} B_c} : \Gamma_{\Xi_{bb} B_c^*} = 0.03 : 1.6 : 1. \quad (104)$$

Our results suggest that the $\Xi_{bb}^* B_c^*$ is the dominant decay channel for the $P_{b^3 n\bar{c}}(16583.0, 1/2, 1/2^-)$.

For the only genuine $J^P = 3/2^- bbbn\bar{c}$ pentaquark state, the $P_{b^3 n\bar{c}}(16538.8, 3/2, 1/2^-)$, we find

$$\Gamma_{\Omega_{bbb}^* D^*} : \Gamma_{\Omega_{bbb} D} = 0.6 : 1, \quad (105)$$

and

$$\Gamma_{\Xi_{bb}^* B_c^*} : \Gamma_{\Xi_{bb} B_c} : \Gamma_{\Xi_{bb} B_c^*} = 3.2 : 4.1 : 1, \quad (106)$$

in $bbb - n\bar{c}$ and $bbn - b\bar{c}$ decay modes, respectively. If such pentaquark state exist, the $\Omega_{bbb}D^*$, $\Omega_{bbb}D$, $\Xi_{bb}^* B_c^*$, and $\Xi_{bb} B_c^*$ decay channels should all contribute considerable widths.

TABLE XXIII. The relative partial decay widths for the $nns c\bar{s}$ and $ssnc\bar{s}$ pentaquark states. For each pentaquark state, we choose one channel as a reference channel, and the relative partial decay widths for the other channels are obtained in units of the reference channel. The masses are all in units of MeV. The scattering states and stable states in the modified CMI model are marked with “*” and “†”, respectively.

$I = 1$ J^P	$nns \otimes c\bar{s}$				$nnc \otimes s\bar{s}$				$nsc \otimes n\bar{s}$					
	$\Sigma^* D_s^*$	$\Sigma^* D_s$	ΣD_s^*	ΣD_s	$\Sigma_c^* \phi$	$\Sigma_c \phi$	$\Sigma_c^* \eta'$	$\Sigma_c \eta'$	$\Xi_c^* K^*$	$\Xi_c' K^*$	$\Xi_c K^*$	$\Xi_c^* K$	$\Xi_c' K$	$\Xi_c K$
$\frac{5}{2}^-$	3534.6*	1				\times				\times				
	3501.4*	1				\times				\times				
$\frac{3}{2}^-$	3600.2	2.6	1	0.002		1.1	1	1		11.6	4	1	1	
	3550.4	1.4	0.35	1		15.4	1	0.22		18.4	1	99	1	
	3481.8*	\times	2.4	1		\times	1	1		\times	1.1	1	1	
	3451.2	\times	850	1		\times	\times	\times		\times	\times	1	1	
	3324.7	\times	\times	1		\times	\times	\times		\times	\times	\times	1	
	3296.9	\times	\times	\times		\times	\times	\times		\times	\times	\times	1	
	3112.6†	\times	\times	\times		\times	\times	\times		\times	\times	\times	\times	
$\frac{1}{2}^-$	3730.1	1518		0.45	7.9	1			1	8.9	1	0.01		1.6 1
	3614.7	888.4		0.84	1	319.6			1	1.1	100	1		21 1
	3530.5	0.7		4.8	1	\times	1		1	\times	1	7.7		0.02 1
	3403.4	\times		7.7	1	\times	\times		\times	\times	\times	1		1 293
	3330.9	\times		0.007	1	\times	\times		\times	\times	\times	\times		514 1
	3269.5	\times		\times	1	\times	\times		\times	\times	\times	\times		0.9 1
	3104.6	\times		\times	\times	\times	\times		\times	\times	\times	\times		1 13.6
	2996.5	\times		\times	\times	\times	\times		\times	\times	\times	\times		\times 1
$I = 0$	ΛD_s^*	ΛD_s			$\Lambda_c \phi$	$\Lambda_c \eta'$			$\Xi_c^* K^*$	$\Xi_c' K^*$	$\Xi_c K^*$	$\Xi_c^* K$	$\Xi_c' K$	$\Xi_c K$
$\frac{5}{2}^-$	3547.0									1				
$\frac{3}{2}^-$	3531.4	1				1				\times	1	1.8	1	
	3478.0	1				1				\times	2.7	1	1	
	3300.7	1				\times				\times	\times	\times	1	
	3277.1	1				\times				\times	\times	\times	1	
	3043.3†	\times				\times				\times	\times	\times	\times	
$\frac{1}{2}^-$	3498.2	7.5	1			1	1			\times	1	1.7		1 0.23
	3343.1	7.2	1			1	1			\times	\times	\times		1 31.3
	3299.9	26	1			\times	1			\times	\times	\times		6.4 1
	3232.2	1	9			\times	\times			\times	\times	\times		3 1
	3084.2	\times	1			\times	\times			\times	\times	\times		1 3.5
	2929.0†	\times	\times			\times	\times			\times	\times	\times		\times \times
	2780.9†	\times	\times			\times	\times			\times	\times	\times		\times \times
$ssn \otimes c\bar{s}$														
J^P	$\Xi^* D_s^*$	$\Xi^* D_s$	ΞD_s^*	ΞD_s	$\Omega_c^* K^*$	$\Omega_c K^*$	$\Omega_c^* K$	$\Omega_c K$	$\Xi_c^* \phi$	$\Xi_c' \phi$	$\Xi_c \phi$	$\Xi_c^* \eta'$	$\Xi_c' \eta'$	$\Xi_c \eta'$
$\frac{5}{2}^-$	3666.8	1				1				1				
	3644.5*	1				\times				\times				
$\frac{3}{2}^-$	3718.9	287	92	1		2.2	1	1		352	208	1	1	
	3660.4	0.06	1	15		6.7	1	1		\times	1	32	1	
	3606.2	\times	15	1		\times	1	1		\times	5.8	1	1	
	3589.5	\times	38	1		\times	1	1		\times	\times	1	1	
	3470.5	\times	\times	1		\times	\times	1		\times	\times	\times	1	
	3438.1	\times	\times	1		\times	\times	1		\times	\times	\times	1	
	3208.3*	\times	\times	\times		\times	\times	\times		\times	\times	\times	\times	
$\frac{1}{2}^-$	3834.0	544		0.2	1	14	1		1	14	1	0.0		100 1
	3733.4	1450		1.4	1	1	566		1	\times	1	0.0		0.15 1
	3636.0	\times		15	1	\times	1		1	\times	1	13		1 1
	3512.7	\times		20	1	\times	\times		1	\times	\times	1		1 16.5
	3466.1	\times		0.05	1	\times	\times		1	\times	\times	\times		243 1
	3414.1	\times		\times	1	\times	\times		1	\times	\times	\times		1 61
	3271.8	\times		\times	\times	\times	\times		1	\times	\times	\times		1 44
	3102.6	\times		\times	\times	\times	\times		\times	\times	\times	\times		\times 1

2. The $ccbq\bar{Q}$ and $bbcq\bar{Q}$ pentaquark states

For the $ccbq\bar{c}$ (\bar{b}) and $bbcq\bar{c}$ (\bar{b}) pentaquark subsystems, the first two quarks are identical. According to Table II, the expressions of CMI Hamiltonian for the $ccbq\bar{c}$ (\bar{b}) and $bbcq\bar{c}$ (\bar{b}) pentaquark subsystems can be easily obtained from the CMI Hamiltonians of the $nnsQ\bar{n}$ (\bar{s}) ($I_{nn} = 1$) subsystem.

Therefore, we use the expressions of CMI Hamiltonian in Table XXXIX of Appendix G, and replace the relevant parameters collected in Table VI to get the mass spectrums of the $ccbq\bar{c}$ (\bar{b}) and $bbcq\bar{c}$ (\bar{b}) pentaquark subsystems.

To estimate the mass spectrums of the $ccbn\bar{c}$ (\bar{b}), $ccbs\bar{c}$ (\bar{b}), $bbcn\bar{c}$ (\bar{b}), and $bbcs\bar{c}$ (\bar{b}) pentaquark subsystems, the rearrangement of constituent quarks allows three kinds of meson-baryon reference systems for each type of pentaquark subsystem. For example, we can use $\Omega_{ccb}B_s$, $\Omega_{cc}\eta_b$, and $\Omega_{cb}^*B_c$ as three different reference systems to estimate the masses of $ccbs\bar{b}$ pentaquark states. The three kinds of meson-baryon reference systems for $ccbs\bar{c}$ (\bar{b}), $ccbn\bar{c}$ (\bar{b}), $bbcn\bar{c}$ (\bar{b}), and $bbcs\bar{c}$ (\bar{b}) can be listed by way of analogy.

Here, the obtained eigenvalues and results calculated from the reference systems in Eq. (3) are presented in the second, third, fourth and fifth columns of Tables XXX and XXXI, respectively. Moreover, the masses calculated from the modified CMI model [Eq. (4)] are also given in the sixth column of Tables XXX and XXXI for the $ccbq\bar{Q}$ and $bbcq\bar{Q}$ subsystems, respectively. Based on the values listed in the sixth column, we plot the mass spectrums and the thresholds of possible meson-baryon reference systems for the $ccbn\bar{c}$, $ccbn\bar{b}$, $ccbs\bar{c}$, $ccbs\bar{b}$, $bbcn\bar{c}$, $bbcn\bar{b}$, $bbcs\bar{c}$, and $bbcs\bar{b}$ subsystems in the diagrams (a)-(d) of Figs. 7 and 8, respectively.

According to the modified CMI model, the overlaps for $ccbq\bar{Q}$ and $bbcq\bar{Q}$ pentaquark states with baryon \otimes meson bases are calculated and presented in Tables L, LI, and LII of Appendix H.

We identify the scattering states from the $ccbq\bar{Q}$ and $bbcq\bar{Q}$ pentaquark subsystems and label them with “*” in relevant Tables and Figs. 7, 8. Other states for the $ccbq\bar{Q}$ and $bbcq\bar{Q}$ pentaquark subsystems are considered as genuine $ccbq\bar{Q}$ and $bbcq\bar{Q}$ pentaquark states, respectively. Besides, from the diagrams (e)-(h) of Figs. 7 and 8, we find that some pentaquark states are below all the allowed two-body strong decay channels in the modified CMI model, they are considered as stable pentaquark states and we label them with “†” in Figs. 7 and 8.

Now, we mainly discuss the $ccbs\bar{b}$ pentaquark subsystem and one can perform similar analysis to the $ccbs\bar{c}$, $ccbn\bar{b}$, $ccbn\bar{c}$, $bbcs\bar{b}$, $bbcs\bar{c}$, $bbcn\bar{b}$, and $bbcn\bar{c}$ pentaquark subsystems.

In Table LI, we find that the two $J^P = 5/2^-$ states $P_{c^2bs\bar{b}}(13457.4, 0, 5/2^-)$ and $P_{c^2bs\bar{b}}(13262.7, 0, 5/2^-)$ couple almost completely to the $\Omega_{ccb}^*B_s^*$ and $\Omega_{cc}^*\Upsilon$ baryon \otimes meson bases, respectively. They should be considered as scattering states. Similarly, the

$P_{c^2bs\bar{b}}(13460.1, 0, 3/2^-)$, $P_{c^2bs\bar{b}}(13262.3, 0, 3/2^-)$, and $P_{c^2bs\bar{b}}(13199.0, 0, 3/2^-)$ states should also be regarded as scattering states in our modified CMI model. On the contrary, the lowest $J^P = 3/2^-$ state $P_{c^2bs\bar{b}}(13191.3, 0, 3/2^-)$ is a good candidate of stable $cccs\bar{b}$ pentaquark state. Besides, the lowest $J^P = 1/2^-$ state $P_{c^2bs\bar{b}}(13127.8, 0, 1/2^-)$, couples almost completely to $\Omega_{cc}^*\Upsilon$ baryon \otimes meson basis, we consider this state as a scattering state. For each pentaquark states in the $ccbs\bar{b}$ subsystem, we use the following approximations

$$\gamma_{\Omega_{ccb}^*B_s^*} = \gamma_{\Omega_{ccb}^*B_s} = \gamma_{\Omega_{ccb}B_s^*} = \gamma_{\Omega_{ccb}B_s}, \quad (107)$$

$$\gamma_{\Omega_{cc}^*\Upsilon} = \gamma_{\Omega_{cc}^*\eta_b} = \gamma_{\Omega_{cc}\Upsilon} = \gamma_{\Omega_{cc}\eta_b}, \quad (108)$$

and

$$\gamma_{\Omega_{cb}^*B_c^*} = \gamma_{\Omega_{cb}^*B_c} = \gamma_{\Omega'_{cb}B_c^*} = \gamma_{\Omega'_{cb}B_c} \approx \gamma_{\Omega_{cb}B_c^*} = \gamma_{\Omega_{cb}B_c}. \quad (109)$$

Thus, based on the overlaps between $ccbs\bar{b}$ pentaquark states and baryon \otimes meson bases collected in Table LI, we obtain the relative partial decay widths and present them in Table XXXV.

According to Table XXXV, we find that the $P_{c^2bs\bar{b}}(13189.3, 0, 1/2^-)$ state can only decay into $\Omega_{cc}\eta_b$ final states. Besides, due to small phase shift, it might be a narrow state. For the $P_{c^2bs\bar{b}}(13257.9, 0, 1/2^-)$ state, it can decay only via $ccs - bb$ decay mode and we obtain

$$\Gamma_{\Omega_{cc}\Upsilon} : \Gamma_{\Omega_{cc}\eta_b} = 1 : 6.8, \quad (110)$$

indicating that the relative partial decay width of $\Omega_{cc}\Upsilon$ channel is smaller than that of $\Omega_{cc}\eta_b$ channel. Other genuine pentaquark states in the $ccbs\bar{b}$ subsystem all have more than one decay modes. They can decay freely to many decay channels and should be relatively broad. For example, for the $P_{c^2bs\bar{b}}(13441.4, 0, 3/2^-)$, we have

$$\Gamma_{\Omega_{ccb}^*B_s^*} : \Gamma_{\Omega_{ccb}^*B_s} : \Gamma_{\Omega_{ccb}B_s^*} = 0.9 : 16 : 1, \quad (111)$$

$$\Gamma_{\Omega_{cc}^*\Upsilon} : \Gamma_{\Omega_{cc}^*\eta_b} : \Gamma_{\Omega_{cc}\Upsilon} = 240 : 1 : 0.002, \quad (112)$$

and

$$\Gamma_{\Omega_{cb}^*B_c^*} : \Gamma_{\Omega_{cb}^*B_c} : \Gamma_{\Omega'_{cb}B_c^*} : \Gamma_{\Omega_{cb}B_c^*} = 1.1 : 0.1 : 7.6 : 1, \quad (113)$$

in $ccb - s\bar{b}$, $ccs - b\bar{b}$ and $cbs - c\bar{b}$ decay modes, respectively. Thus, the dominant decay channels are $\Omega_{cc}^*B_c^*$, $\Omega_{ccb}^*B_s$, and $\Omega'_{cb}B_c^*$ in $ccs - b\bar{b}$, $ccb - s\bar{b}$, and $cbs - c\bar{b}$ decay modes, respectively. We present our results for other $ccbq\bar{Q}$ and $bbcq\bar{Q}$ pentaquark subsystems in Tables XXXIV, XXXV, and XXXIII. One can perform similar discussions on these pentaquark subsystems, which we do not present them further.

VII. SUMMARY

New discoveries for exotic multiquark candidates are constantly being made experimentally [4, 20–39, 41–43, 64]. The lessons from the study of tetraquark candidates and the observation of the $P_c(4312)$, $P_c(4440)$, and

TABLE XXIV. The relative partial decay widths for the $nnsb\bar{s}$ and $ssnb\bar{s}$ pentaquark states. For each pentaquark state, we choose one channel as a reference channel, and the relative partial decay widths for the other channels are obtained in units of the reference channel. The masses are all in units of MeV. The scattering states and stable states in the modified CMI model are marked with “*” and “†”, respectively.

$I = 1$ J^P Mass	$nns \otimes b\bar{s}$				$nnb \otimes s\bar{s}$				$nsb \otimes n\bar{s}$					
	$\Sigma^* B_s^*$	$\Sigma^* B_s$	ΣB_s^*	ΣB_s	$\Sigma_b^* \phi$	$\Sigma_b \phi$	$\Sigma_b^* \eta'$	$\Sigma_b \eta'$	$\Xi_b^* K^*$	$\Xi_c' K^*$	$\Xi_b K^*$	$\Xi_b^* K$	$\Xi_c' K$	$\Xi_b K$
$\frac{5}{2}^-$ 6858.8*	1				1				1					
6714.4*	x				x				x					
$\frac{3}{2}^-$ 6903.1	1.7	1	0.008		3	1	1		8.8	2.1	1	1		
6873.5	1.4	1	0.57		39.3	1	1		1	0.01	7	1		
6843.4*	5	1	0.04		x	1	1		x	3.5	1	1		
6691.8	x	x	1		x	x	x		x	x	1	1		
6614.1	x	x	1		x	x	x		x	x	x	1		
6575.7	x	x	x		x	x	x		x	x	x	1		
6396.7†	x	x	x		x	x	x		x	x	x	x		
$\frac{1}{2}^-$ 7049.6	18.3		1	0.44	2.5	1		1	1586	1	0.0	6	1	
6910.5	376.5		1	0.75	1	4.7		1	1	1.5	22.8	1	0.0	
6867.0	6.7		0.003	1	1	2.7		1	1	1.5	22.8	9.6	1	
6708.1	x		3.5	1	x	x		x	x	x	1	1	2079	
6622.6	x		0.02	1	x	x		x	x	x	x	1124	1	
6560.6	x		x	1	x	x		x	x	x	x	18.6	1	
6382.2	x		x	x	x	x		x	x	x	x	x	1	
6354.1	x		x	x	x	x		x	x	x	x	x	1	
$I = 0$	ΛB_s^*	ΛB_s			$\Lambda_b \phi$	$\Lambda_b \eta'$			$\Xi_b^* K^*$	$\Xi_c' K^*$	$\Xi_b K^*$	$\Xi_b^* K$	$\Xi_c' K$	$\Xi_b K$
$\frac{5}{2}^-$ 6864.0									1					
$\frac{3}{2}^-$ 6855.3	1					1			8	26.5	1	1		
6839.0	1					1			x	1	2	1		
6633.6	1					1			x	x	x	1		
6544.8	1					1			x	x	x	1		
6316.0†	x					x			x	x	x	x		
$\frac{1}{2}^-$ 6833.4	1	2				1	1		x	1	2.3	1	0.01	
6646.5	4	1				1	1		x	x	x	1	78.6	
6636.4	1.1	1				1	1		x	x	x	1	0.15	
6528.8	x	1				1	1		x	x	x	101	1	
6365.2	x	x				x	x		x	x	x	x	1	
6281.0†	x	x				x	x		x	x	x	x	x	
6116.0†	x	x				x	x		x	x	x	x	x	
$ssn \otimes b\bar{s}$														
J^P Mass	$\Xi^* B_s^*$	$\Xi^* B_s$	ΞB_s^*	ΞB_s	$\Omega_b^* K^*$	$\Omega_b K^*$	$\Omega_b^* K$	$\Omega_b K$	$\Xi_b^* \phi$	$\Xi_b' \phi$	$\Xi_b \phi$	$\Xi_b^* \eta'$	$\Xi_b' \eta'$	$\Xi_b \eta'$
$\frac{5}{2}^-$ 6972.5	1				1				x					
6937.8	x				x				x					
$\frac{3}{2}^-$ 7047.1	123.5	48	1		3	1	1		3.2	1	0.005	1		
6959.9	5	16	1		1	1	1		x	0.8	1	1		
6953.1	1	5.8	0.001		0.6	1	1		x	x	1	1		
6916.6	x	1	x		x	x	1		x	x	1	1		
6798.3	x	x	1		x	x	1		x	x	x	1		
6784.7	x	x	1		x	x	1		x	x	x	1		
6496.8*	x	x	x		x	x	x		x	x	x	x		
$\frac{1}{2}^-$ 7130.0	18		2.4	1	2.7	1		1	2.9	1	0.0	170	1	
7057.6	335		0.7	1	1	4.3		1	0.6	2.5	1	2200	1	
6950.4	0.1		3.5	1	1	2.8		1	x	x	1	37.5	1	
6837.6	x		7	1	x	x		1	x	x	1	1	28.8	
6801.1	x		1.1	1	x	x		1	x	x	x	1	0.0	
6759.4	x		1	6.3	x	x		1	x	x	x	1	1.7	
6608.4	x		x	x	x	x		1	x	x	x	1	820	
6477.4†	x		x	x	x	x		x	x	x	x	x	x	

TABLE XXV. The estimated masses for the $QQQQ\bar{q}$ ($q = n, s$; $n = u, d$; $Q = c, b$) system in units of MeV. The values in the second column are eigenvalues obtained with the CMI Hamiltonian in Eq. (2). The masses in the third and fourth columns are determined with relevant thresholds in Eq. (3). The masses in the fifth column are determined with the modified CMI model in Eq. (4).

$cccc\bar{n}$			$cccc\bar{s}$						
J^P	Eigenvalue	$(D\Omega_{ccc})$	Mass	J^P	Eigenvalue	$(D_s\Omega_{ccc})$	Mass		
$\frac{3}{2}^-$	26.4	6760.9	6761.4	$\frac{3}{2}^-$	25.9	6860.6	6863.7		
$\frac{1}{2}^-$	132.0	6866.5	6867.4	$\frac{1}{2}^-$	133.1	6967.8	6971.5		
$bbbb\bar{n}$			$bbbb\bar{s}$						
J^P	Eigenvalue	$(B\Omega_{bbb})$	Mass	J^P	Eigenvalue	$(B_s\Omega_{bbb})$	Mass		
$\frac{3}{2}^-$	22.4	19630.8	19647.2	$\frac{3}{2}^-$	21.3	19720.3	19736.2		
$\frac{1}{2}^-$	56.0	19664.4	19681.1	$\frac{1}{2}^-$	58.1	19757.1	19772.6		
$cccb\bar{n}$			$cccb\bar{s}$						
J^P	Eigenvalue	$(B\Omega_{ccc})$	$(D\Omega_{ccb})$	Mass	J^P	Eigenvalue	$(B_s\Omega_{ccc})$	$(D_s\Omega_{ccb})$	Mass
$\frac{5}{2}^-$	37.6	10109.9	9815.7	10110.3	$\frac{5}{2}^-$	38.7	10201.6	9917.0	10201.0
$\frac{3}{2}^-$	$\begin{pmatrix} 65.3 \\ 22.0 \\ -40.6 \end{pmatrix}$	$\begin{pmatrix} 10137.6 \\ 10094.3 \\ 10031.7 \end{pmatrix}$	$\begin{pmatrix} 9843.4 \\ 9800.2 \\ 9737.5 \end{pmatrix}$	$\begin{pmatrix} 10117.6 \\ 10078.2 \\ 9961.3 \end{pmatrix}$	$\frac{3}{2}^-$	$\begin{pmatrix} 65.9 \\ 21.3 \\ -43.1 \end{pmatrix}$	$\begin{pmatrix} 10228.8 \\ 10184.2 \\ 10119.8 \end{pmatrix}$	$\begin{pmatrix} 9944.2 \\ 9899.7 \\ 9835.2 \end{pmatrix}$	$\begin{pmatrix} 10209.5 \\ 10167.7 \\ 10062.0 \end{pmatrix}$
$\frac{1}{2}^-$	$\begin{pmatrix} 110.4 \\ 68.0 \\ -41.3 \end{pmatrix}$	$\begin{pmatrix} 10182.7 \\ 10140.3 \\ 10031.0 \end{pmatrix}$	$\begin{pmatrix} 9888.6 \\ 9846.1 \\ 9736.8 \end{pmatrix}$	$\begin{pmatrix} 10134.4 \\ 10061.5 \\ 9945.5 \end{pmatrix}$	$\frac{1}{2}^-$	$\begin{pmatrix} 111.6 \\ 69.1 \\ -41.7 \end{pmatrix}$	$\begin{pmatrix} 10274.5 \\ 10232.0 \\ 10121.2 \end{pmatrix}$	$\begin{pmatrix} 9990.0 \\ 9947.5 \\ 9836.6 \end{pmatrix}$	$\begin{pmatrix} 10228.3 \\ 10166.1 \\ 10047.1 \end{pmatrix}$
$bbbc\bar{n}$			$bbbc\bar{s}$						
J^P	Eigenvalue	$(D\Omega_{bbb})$	$(B\Omega_{bbc})$	Mass	J^P	Eigenvalue	$(D_s\Omega_{bbb})$	$(B_s\Omega_{bbc})$	Mass
$\frac{5}{2}^-$	49.6	16320.2	16544.2	16318.2	$\frac{5}{2}^-$	50.1	16420.9	16635.4	16421.8
$\frac{3}{2}^-$	$\begin{pmatrix} 49.6 \\ 16.6 \\ -94.5 \end{pmatrix}$	$\begin{pmatrix} 1630.2 \\ 16287.2 \\ 16176.1 \end{pmatrix}$	$\begin{pmatrix} 16544.2 \\ 16511.2 \\ 16400.1 \end{pmatrix}$	$\begin{pmatrix} 16537.8 \\ 16318.2 \\ 16175.9 \end{pmatrix}$	$\frac{3}{2}^-$	$\begin{pmatrix} 50.2 \\ 16.1 \\ -94.4 \end{pmatrix}$	$\begin{pmatrix} 16421.0 \\ 16386.9 \\ 16274.4 \end{pmatrix}$	$\begin{pmatrix} 16635.5 \\ 16601.3 \\ 16488.8 \end{pmatrix}$	$\begin{pmatrix} 16625.6 \\ 16421.8 \\ 16276.8 \end{pmatrix}$
$\frac{1}{2}^-$	$\begin{pmatrix} 72.2 \\ 30.3 \\ -7.5 \end{pmatrix}$	$\begin{pmatrix} 16342.8 \\ 16300.9 \\ 16263.1 \end{pmatrix}$	$\begin{pmatrix} 16566.9 \\ 16525.0 \\ 16487.1 \end{pmatrix}$	$\begin{pmatrix} 16573.5 \\ 16522.8 \\ 16315.2 \end{pmatrix}$	$\frac{1}{2}^-$	$\begin{pmatrix} 74.0 \\ 31.8 \\ -8.7 \end{pmatrix}$	$\begin{pmatrix} 16444.8 \\ 16402.6 \\ 16362.1 \end{pmatrix}$	$\begin{pmatrix} 16659.2 \\ 16617.0 \\ 16576.6 \end{pmatrix}$	$\begin{pmatrix} 16663.2 \\ 16611.2 \\ 16418.3 \end{pmatrix}$
$ccbb\bar{n}$			$ccbb\bar{s}$						
J^P	Eigenvalue	$(B\Omega_{ccb})$	$(D\Omega_{bbc})$	Mass	J^P	Eigenvalue	$(B_s\Omega_{ccb})$	$(D_s\Omega_{bbc})$	Mass
$\frac{5}{2}^-$	42.1	13358.1	13199.0	13244.0	$\frac{5}{2}^-$	42.9	13449.5	13300.0	13341.1
$\frac{3}{2}^-$	$\begin{pmatrix} 61.2 \\ 24.3 \\ 11.3 \\ -70.4 \end{pmatrix}$	$\begin{pmatrix} 13377.2 \\ 13340.2 \\ 13327.3 \\ 13245.5 \end{pmatrix}$	$\begin{pmatrix} 13218.1 \\ 13181.1 \\ 13168.2 \\ 13086.4 \end{pmatrix}$	$\begin{pmatrix} 13382.7 \\ 13231.0 \\ 13220.5 \\ 13099.6 \end{pmatrix}$	$\frac{3}{2}^-$	$\begin{pmatrix} 61.7 \\ 24.1 \\ 12.0 \\ -72.6 \end{pmatrix}$	$\begin{pmatrix} 13468.3 \\ 13430.6 \\ 13418.5 \\ 13334.0 \end{pmatrix}$	$\begin{pmatrix} 13318.8 \\ 13281.1 \\ 13269.0 \\ 13184.5 \end{pmatrix}$	$\begin{pmatrix} 13469.5 \\ 13329.2 \\ 13319.3 \\ 13200.3 \end{pmatrix}$
$\frac{1}{2}^-$	$\begin{pmatrix} 90.3 \\ 44.8 \\ -5.4 \\ -84.4 \end{pmatrix}$	$\begin{pmatrix} 13406.2 \\ 13360.7 \\ 13310.5 \\ 13231.5 \end{pmatrix}$	$\begin{pmatrix} 13247.1 \\ 13201.6 \\ 13151.4 \\ 13072.4 \end{pmatrix}$	$\begin{pmatrix} 13413.9 \\ 13241.7 \\ 13211.5 \\ 13086.1 \end{pmatrix}$	$\frac{1}{2}^-$	$\begin{pmatrix} 91.7 \\ 46.3 \\ -7.3 \\ -85.6 \end{pmatrix}$	$\begin{pmatrix} 13498.3 \\ 13452.8 \\ 13399.3 \\ 13321.0 \end{pmatrix}$	$\begin{pmatrix} 13348.8 \\ 13303.3 \\ 13249.8 \\ 13171.5 \end{pmatrix}$	$\begin{pmatrix} 13501.8 \\ 13343.3 \\ 13307.0 \\ 13186.7 \end{pmatrix}$

$P_c(4457)$ states achieved by the LHCb Collaboration [71] give us strong confidence to study the mass spectrums of the $qqqq\bar{Q}$, $qqqQ\bar{q}$, $QQQQ\bar{q}$, $QQQQ\bar{Q}$, and $QQQq\bar{Q}$ pentaquark systems within the framework of CMI model.

In this work, by including the flavor SU(3) breaking effect, we firstly construct the isospin-color-spin wave functions based on the SU(2) and SU(3) symmetry and Pauli Principle. Then we extract the effective coupling con-

stants from the conventional hadrons. After that, we systematically calculate the chromomagnetic interaction Hamiltonian for the discussed pentaquark states and obtain the corresponding mass spectrums. As a modification to the CMI model, the effect of chromoelectric interaction is added in the modified CMI model. In this work, we mainly discussed the results of mass spectrums for the $qqqq\bar{Q}$, $qqqQ\bar{q}$, $QQQQ\bar{q}$, $QQQQ\bar{Q}$, and $QQQq\bar{Q}$ pen-

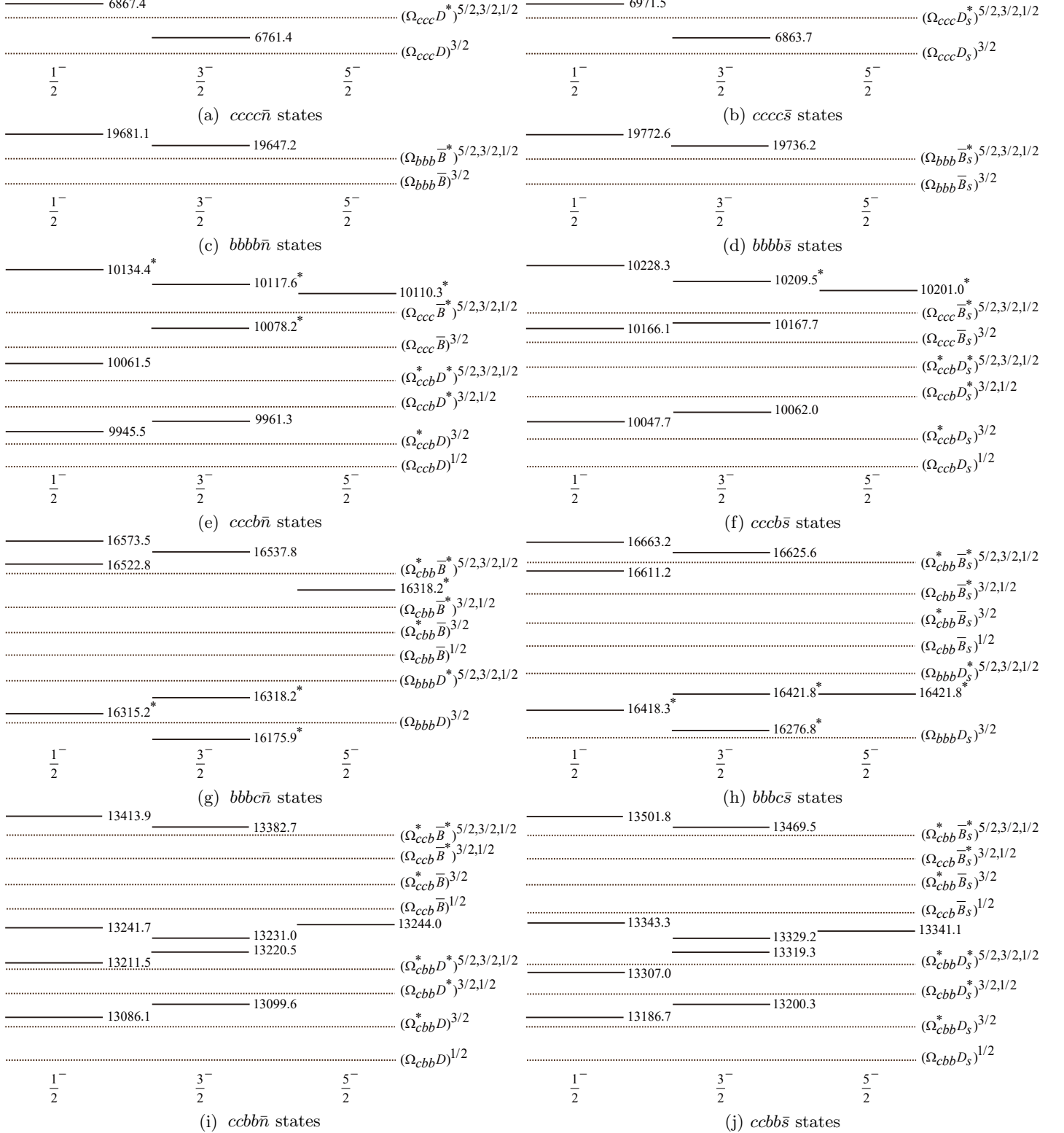


FIG. 5. Relative positions (units: MeV) for the $cccc\bar{n}$, $cccs\bar{s}$, $bbbb\bar{n}$, $bbbb\bar{s}$, $cccb\bar{n}$, $bbbc\bar{n}$, $bbbc\bar{s}$, $ccbb\bar{n}$, and $ccbb\bar{s}$ pentaquark states labeled with solid lines. The dotted lines denote various baryon-meson thresholds. When the spin of an initial pentaquark state is equal to a number in the superscript of a baryon-meson state, its decay into that baryon-meson channel through S -wave is allowed by the angular momentum conservation. The scattering states in the modified CMI model are marked with “*”.

taquark systems obtained from the modified CMI model. The results from the CMI model are presented for comparison. Besides the eigenvalues, we also provide the eigenvectors to extract useful information about the decay properties for the studied pentaquark systems. Finally, we analyze the stability, possible quark rearrangement decay channels and relative partial decay widths for all the $qqqq\bar{Q}$, $qqqQ\bar{q}$, $QQQQ\bar{Q}$, $QQQQ\bar{q}$, and $QQQq\bar{Q}$ pentaquark states.

Among the studied pentaquark subsystems, the $nnnn\bar{Q}$, $nnns\bar{Q}$, $nnss\bar{Q}$, $sssn\bar{Q}$, and $ssss\bar{Q}$ in $qqqq\bar{Q}$ system, the $nnnQ\bar{s}$, $nnnQ\bar{n}$ ($I = 2$), $nnsQ\bar{n}$ ($I = 3/2$), $ssnQ\bar{n}$ ($I = 1$), and $sssQ\bar{n}$ in $qqqQ\bar{q}$ system, the $cccc\bar{b}$ and $bbbb\bar{c}$ in $QQQQ\bar{Q}$ system, the $cccc\bar{q}$, $cccb\bar{q}$, $cbb\bar{q}$, $bbc\bar{q}$, and $bbb\bar{q}$ in $QQQQ\bar{q}$ system, the $ccc\bar{b}$ and $bbb\bar{q}$ in $QQQq\bar{Q}$ ($Q = c, b; q = n, s; n = u, d$) system are explicitly exotic states, they can be easily identified as exotic pentaquark states if they were observed in experiment. Besides, the $cccc\bar{c}$, $ccb\bar{Q}$, $ccb\bar{Q}$, $bbc\bar{Q}$, and $bbb\bar{b}$ in $QQQQ\bar{Q}$ system, the $ccc\bar{c}$, $ccb\bar{Q}$, $bbc\bar{Q}$, and $bbb\bar{b}$ in $QQQq\bar{Q}$ ($Q = c, b; q = n, s; n = u, d$) system are implicitly exotic states, they can be regarded as the excited heavy baryons by exciting one pair of $c\bar{c}$ or $b\bar{b}$, thus, they can also be easily identified as exotic baryons because of their large masses. Other pentaquark states including the $nnnQ\bar{n}$ ($I = 1, 0$), $nnsQ\bar{n}$ ($I = 1/2$), $nnsQ\bar{s}$, $ssnQ\bar{n}$ ($I = 0$), $ssnQ\bar{s}$, and $sssQ\bar{s}$ in $qqqQ\bar{q}$ ($Q = c, b; q = n, s; n = u, d$) system are all implicitly exotic states and in the mass range of excited baryons, so they can hardly be identified. However, we also present their mass spectrums and decay properties in this work.

From the obtained Tables and Figs for the $qqqq\bar{Q}$, $qqqQ\bar{q}$, $QQQQ\bar{Q}$, $QQQQ\bar{q}$, and $QQQq\bar{Q}$ pentaquark systems, we find some stable candidates in the modified CMI model, we collect them in Table XXVII. However, due to the uncertainty of the modified CMI model, not all of them are truly stable states, further dynamical calculations may help us to clarify their natures. Especially, some stable states are closed to the meson-baryon thresholds of the lowest strong decay channels, if the mass deviations in the modified CMI model are larger than the difference between the pentaquark states and the corresponding meson-baryon thresholds, these states can no longer be considered as stable pentaquark states. On the contrary, some unstable states, which are a little higher than the meson-baryon thresholds of lowest strong decay channels, also have possibilities to become stable states. Meanwhile, the whole mass spectrum has a slight shift or down due to the mass deviation of constituent quarks. While the mass gaps between different pentaquark states are relatively stable, if one pentaquark states are observed in experiment, we can use these mass gaps to predict their corresponding multiplets.

For the $qqqq\bar{Q}$ ($Q = c, b; q = n, s; n = u, d$) pentaquark system, due to the constraint from symmetry, there is no ground $I(J^P) = 0(5/2^-)$, $I(J^P) = 2(5/2^-)$ $nnnn\bar{Q}$ state, and $J^P = 5/2^-$ $ssss\bar{Q}$ state in the $nnnn\bar{Q}$ and $ssss\bar{Q}$ subsystems. Meanwhile, for $I(J^P) = 3/2(5/2^-)$

$nnns\bar{Q}$ states and $I(J^P) = 1/2(5/2^-)$ $sssn\bar{Q}$ states, all of them are scattering state since they only have $1 \otimes 1$ components. Besides, in the modified CMI model, there is no stable $nnnn\bar{Q}$, $ssss\bar{Q}$, and $sssn\bar{Q}$ pentaquark states. This conclusion is consistent with Ref. [110]. Moreover, according to our calculated results on $nnnb$ subsystem, we suggest that the LHCb collaboration could change the search window from 4600-6220 MeV to 6200-6900 MeV to search for the $nnnn\bar{b}$ ($I = 0$) and $nnns\bar{b}$ ($I = 1/2$) pentaquark states via the $b \rightarrow c\bar{c}s$ transition in the $J/\psi K^+ \pi^- p$ and $J/\psi \phi p$ [111] final states. In the $nnns\bar{Q}$ subsystems, we found that the lowest $I(J^P) = 1/2(1/2^-)$ $nnns\bar{Q}$ pentaquark state are all below the lowest allowed strong decay channels and are good stable pentaquark candidates. This conclusion has already been proposed in Ref. [110, 112, 113]. In the $nnss\bar{Q}$ subsystem, we suggest that the lowest $I(J^P) = 0(1/2^-)$ and $I(J^P) = 0(3/2^-)$ $nnss\bar{Q}$ state are stable states, though our results are higher than the predictions from Ref. [106] about 300 MeV.

In the $qqqQ\bar{q}$ pentaquark system, there is no ground $I_{nnn}(J^P) = 3/2(5/2^-)$ $nnnQ\bar{q}$ state and $J^P = 5/2^-$ $sssQ\bar{q}$ state. The states with such quantum numbers and flavor configurations are more likely to be scattering states. For the $nnnQ\bar{n}$ subsystem with $I_{nnn} = 3/2(1/2)$, we get the same mass spectrums for the pentaquark subsystems with the total isospin $I = 2, 1$ ($1, 0$). This is due to the fact that the symmetry property of $nnnQ\bar{n}$ subsystem do not depend on the antiquark [75]. This behavior is also appear in the $nnsQ\bar{n}$ and $ssnQ\bar{n}$ subsystems. For the $nnnb\bar{n}$ subsystem, in our modified CMI model, we find that the lowest $I[J^P] = 0(1)[3/2^-]$ state is a good candidate of stable pentaquark state and suggest that the LHCb collaboration could change the search window in around 5800 MeV [111]. In addition, to analysis the decay behavior of $qqqQ\bar{q}$ pentaquark system, we adopt the partially conserved axial current result $M_{\eta_{ss}} = 628.2$ MeV and $M_{\eta_{n\bar{n}}} = 139.6$ MeV [115] to perform our calculation.

The $QQQQ\bar{q}$ and $QQQQ\bar{Q}$ systems have the same symmetry properties. Firstly, due to the constraint from Pauli principle, there exists no ground $J^P = 5/2^-$ $cccc\bar{Q}$, $cccc\bar{q}$, $bbbb\bar{Q}$, and $bbbb\bar{q}$ pentaquark state. Meanwhile, there is no the ground $J^P = 5/2^-$ $ccb\bar{q}$ (\bar{Q}) and $bbc\bar{q}$ (\bar{Q}) state since such states are identified as scattering states in the modified CMI model. Similar to the fully-heavy $QQ\bar{Q}\bar{Q}$ tetraquark system [64], the $QQQQ\bar{q}$ and $QQQQ\bar{Q}$ systems consist of four or five heavy quarks are dominantly bounded by the gluon exchange interaction, and can hardly be considered as molecular states. Meanwhile, although all the $QQQq\bar{q}$ states are explicitly exotic states, we find that in our modified CMI model, no stable $QQQq\bar{q}$ pentaquark state exists. Besides, some states with lower masses in $QQQQ\bar{q}$ system are only slightly higher than the lowest allowed decay channels, they can be considered as narrow pentaquark states, and have opportunities to be found in future experiment. On the other hand, if our results under the

TABLE XXVI. The relative partial decay widths for the $cccc\bar{n}$, $cccc\bar{s}$, $bbbb\bar{n}$, $bbbb\bar{s}$, $cccb\bar{n}$, $cccb\bar{s}$, $bbbc\bar{n}$, $bbbc\bar{s}$, $ccb\bar{n}$, and $ccb\bar{s}$ pentaquark states. For each pentaquark state, we choose one channel as a reference channel, and the relative partial decay widths for the other channels are obtained in units of the reference channel. The masses are all in units of MeV. The scattering states in the modified CMI model are marked with “*”.

J^P	Mass	$ccc \otimes c\bar{n}$		$ccc \otimes c\bar{s}$			$bbb \otimes b\bar{n}$		$bbb \otimes b\bar{s}$					
		$\Omega_{ccc}D^*$	$\Omega_{ccc}D$	Mass	$\Omega_{ccc}D_s^*$	$\Omega_{ccc}D_s$	Mass	$\Omega_{bbb}B^*$	$\Omega_{bbb}B$					
$(\frac{3}{2}^-)$	6761.4	\times	1	6863.7	\times	1		19647.2	1	1.3	19736.2	1	1.4	
	6867.4	1		6971.5	1			19681.1	1		19772.6	1		
		$ccc \otimes b\bar{n}$		$ccb \otimes c\bar{n}$			$ccc \otimes b\bar{s}$		$ccb \otimes c\bar{s}$					
J^P	Mass	$\Omega_{ccc}B^*$	$\Omega_{ccc}B$	$\Omega_{ccb}D^*$	$\Omega_{ccb}D$	$\Omega_{ccb}D_s^*$	$\Omega_{ccb}D_s$	Mass	$\Omega_{ccc}B_s^*$	$\Omega_{ccc}B_s$	$\Omega_{ccb}D_s^*$	$\Omega_{ccb}D_s$	$\Omega_{ccb}D_s^*$	$\Omega_{ccb}D_s$
$\frac{5}{2}^-$	10110.3*	\times		1				10201.0*	1		1			
$\frac{3}{2}^-$	10117.6*	9.4	1	0.6	0.4	1		10209.5*	8.7	1	0.7	0.34	1	
	10078.2*	\times	1	2.8	0.02	1		10167.7	\times	1	3.0	0.1	1	
$\frac{1}{2}^-$	9961.3	\times	\times	\times	1	\times		10062.0	\times	\times	\times	1	\times	
	10134.4*	1		4.7		1.9	1	10228.3	1		7.1		2.2	1
	10061.5	\times		24		24	1	10166.1	\times		21.9		25.2	1
	9945.5	\times		\times		\times	1	10047.7	\times		\times		\times	1
		$bbb \otimes c\bar{n}$		$bbc \otimes b\bar{n}$			$bbb \otimes c\bar{s}$		$bbc \otimes b\bar{s}$					
J^P	Mass	$\Omega_{bbb}D^*$	$\Omega_{bbb}D$	$\Omega_{bbc}B^*$	$\Omega_{bbc}B$	$\Omega_{bbc}B_s^*$	$\Omega_{bbc}B_s$	Mass	$\Omega_{bbb}D_s^*$	$\Omega_{bbb}D_s$	$\Omega_{bbc}B_s^*$	$\Omega_{bbc}B_s$	$\Omega_{bbc}B_s^*$	$\Omega_{bbc}B_s$
$\frac{5}{2}^-$	16318.2*	\times		\times				16421.8*	\times		\times			
$\frac{3}{2}^-$	16537.8	0.005	1	3.3	3.5	1		16625.6	0.02	1	3.1	3.6	1	
	16318.2*	\times	1	\times	\times	\times		16421.8*	\times	1	\times	\times	\times	
$\frac{1}{2}^-$	16175.9*	\times	\times	\times	\times	\times		16276.8*	\times	\times	\times	\times	\times	
	16573.5	1		12		0.7	1	16663.2	1		12.7		0.8	1
	16522.8	1		0.003		2.1	1	16611.2	1		\times		2.0	1
	16315.2*	\times		\times		\times	\times	16418.3*	\times		\times		\times	\times
		$bbc \otimes c\bar{n}$		$ccb \otimes b\bar{n}$			$ccb \otimes c\bar{s}$		$ccb \otimes b\bar{s}$					
J^P	Mass	$\Omega_{bbc}D^*$	$\Omega_{bbc}D$	$\Omega_{bbc}D_s^*$	$\Omega_{bbc}D_s$	$\Omega_{ccb}B^*$	$\Omega_{ccb}B$	$\Omega_{ccb}B_s^*$	$\Omega_{ccb}B_s$	$\Omega_{ccb}B_s^*$	$\Omega_{ccb}B_s$	$\Omega_{ccb}B_s^*$	$\Omega_{ccb}B_s$	
$\frac{5}{2}^-$	13244.0	1				\times								
$\frac{3}{2}^-$	13382.7	1.7	18.7	1		1.1	0.7	1						
	13231.0	49	0.4	1		\times	\times	\times						
$\frac{1}{2}^-$	13220.5	0.04	0.15	1		\times	\times	\times						
	13099.6	\times	1	\times		\times	\times	\times						
	13413.9	12		3.7	1	0.04		0.004		1				
	13241.7	15		2.5	1	\times		\times		\times				
	13211.5	2.3		48	1	\times		\times		\times				
	13086.1	\times		\times	1	\times		\times		\times				
		$bbc \otimes c\bar{s}$		$ccb \otimes b\bar{s}$										
J^P	Mass	$\Omega_{bbc}D_s^*$	$\Omega_{bbc}D_s$	$\Omega_{bbc}D_s^*$	$\Omega_{bbc}D_s$	$\Omega_{ccb}B_s^*$	$\Omega_{ccb}B_s$	$\Omega_{ccb}B_s^*$	$\Omega_{ccb}B_s$	$\Omega_{ccb}B_s^*$	$\Omega_{ccb}B_s$	$\Omega_{ccb}B_s^*$	$\Omega_{ccb}B_s$	
$\frac{5}{2}^-$	13341.1	1				\times								
$\frac{3}{2}^-$	13469.5	3.3	22	1		1.1	0.7	1						
	13329.2	103	1.1	1		\times	\times	\times						
$\frac{1}{2}^-$	13319.3	0.002	0.1	1		\times	\times	\times						
	13200.3	\times	1	\times		\times	\times	\times						
	13501.8	14		4.3	1	3.6		0.4		1				
	13343.3	24		4.3	1	\times		\times		\times				
	13307.0	\times		40	1	\times		\times		\times				
	13186.7	\times		\times	1	\times		\times		\times				

TABLE XXVII. The stable states among the studied $qqqq\bar{Q}$, $qqq\bar{Q}\bar{q}$, $QQQQ\bar{q}$, $QQQQ\bar{Q}$, and $QQQq\bar{Q}$ systems in the modified CMI model in Eq. (4).

Systems	$I(J^P)$	Masses	Systems	$I(J^P)$	Masses
$nnnsc$	$1/2(1/2^-)$	2830.9	$nnss\bar{c}$	$0(3/2^-)$	3215.8
$nnns\bar{b}$	$1/2(1/2^-)$	6252.7	$nnnc\bar{n}$	$0(1/2^-)$	3025.8
$nnnc\bar{n}$	$0, 1(3/2^-)$	2539.8	$nnss\bar{b}$	$0(3/2^-)$	6526.5
$nnnb\bar{n}$	$0, 1(3/2^-)$	5853.0	$nnnb\bar{s}$	$0(1/2^-)$	6454.6
$nnnc\bar{s}$	$1/2(3/2^-)$	2906.1	$nnsb\bar{n}$	$1/2(3/2^-)$	6213.6
	$1/2(1/2^-)$	2779.5		$3/2(5/2^-)$	6702.3
$nnsc\bar{n}$	$1/2(3/2^-)$	2666.1	$nnsb\bar{n}$	$1/2(5/2^-)$	6702.3
	$1/2(1/2^-)$	2574.9		$1/2(3/2^-)$	5966.2
$nns\bar{s}$	$1/2(1/2^-)$	2404.5		$1/2(1/2^-)$	5726.5
	$1(3/2^-)$	3112.6	$nnsb\bar{s}$	$1(3/2^-)$	6396.7
	$0(3/2^-)$	3043.3		$0(3/2^-)$	6316.0
	$0(1/2^-)$	2929.0		$0(1/2^-)$	6281.0
$ssnbs$	$0(1/2^-)$	2780.9		$0(1/2^-)$	6166.0
	$1/2(1/2^-)$	6477.4	$ccbn\bar{c}$	$1/2(5/2^-)$	10012.4
$ccbb\bar{b}$	$0(5/2^-)$	17476.5	$ccbn\bar{c}$	$1/2(1/2^-)$	9830.7
	$0(3/2^-)$	17416.2	$ccbs\bar{b}$	$0(3/2^-)$	13191.3
$bbcnc$	$1/2(3/2^-)$	13165.4	$ccbs\bar{c}$	$0(5/2^-)$	10123.7
	$1/2(3/2^-)$	13161.4	$ccbs\bar{c}$	$0(1/2^-)$	9933.4
$bbcs\bar{b}$	$0(5/2^-)$	16523.0	$bbcn\bar{b}$	$1/2(5/2^-)$	16427.3
	$0(3/2^-)$	16459.1	$bbcn\bar{b}$	$1/2(3/2^-)$	16369.2

modify CMI model are over predicated, these narrow states have chances to be stable pentaquark states. For the $QQQQ\bar{Q}$ system, we only find two stable states, the $P_{c^2b^2\bar{b}}(17416.2, 0, 3/2^-)$ and $P_{c^2b^2\bar{b}}(17476.5, 0, 5/2^-)$ in the $ccb\bar{b}$ subsystem, we hope that LHCb can also search for such fully heavy pentaquark states.

The $QQQq\bar{Q}$ system is like the mirror structure of the $qqq\bar{Q}\bar{q}$ system. Firstly, after identifying scattering states, we find no ground $J^P = 5/2^-$ $cccq\bar{Q}$ and $bbbq\bar{Q}$ pentaquark state. Besides, we also do not find any stable state in the $cccq\bar{Q}$ and $bbbq\bar{Q}$ subsystems. On the contrary, the $cccq\bar{Q}$ and $bbbq\bar{Q}$ subsystems, the $ccbq\bar{Q}$ and $bcbq\bar{Q}$ subsystems have many stable states.

Among the studied $qqqq\bar{Q}$, $qqq\bar{Q}\bar{q}$, $QQQQ\bar{q}$, $QQQQ\bar{Q}$, and $QQQq\bar{Q}$ pentaquark states, most of them are explicit exotic states. If such pentaquark states are observed, their exotic nature can be easily identified. However, up to now, none of them is found. Our systematical study may provide theorists and experimentalists some preliminary understanding toward these pentaquark systems. More detailed dynamical investigations on these pentaquark systems are still needed. Besides, We hope that the present study may inspire the LHCb, ATLAS, CMS, BESIII, Belle II, JLAB, PANDA, EIC and other relative collaborations to search for these exotic states.

VIII. ACKNOWLEDGMENTS

This work is supported by the China National Funds for Distinguished Young Scientists under Grant No. 11825503, and the National Program for Support of Top-notch Young Professionals.

-
- [1] M. Gell-Mann, “A Schematic Model of Baryons and Mesons,” Phys. Lett. **8**, 214–215 (1964)
 - [2] G. Zweig, “An SU(3) model for strong interaction symmetry and its breaking. Version 1,” CERN-TH-401.
 - [3] G. Zweig, “An SU(3) model for strong interaction symmetry and its breaking. Version 2,” CERN-TH-412.
 - [4] S. K. Choi *et al.* [Belle Collaboration], “Observation of a narrow charmonium - like state in exclusive $B^{+-} \rightarrow K^{+-}\pi^+\pi^-J/\psi$ decays,” Phys. Rev. Lett. **91**, 262001 (2003) [hep-ex/0309032].
 - [5] D. Acosta *et al.* [CDF Collaboration], “Observation of the narrow state $X(3872) \rightarrow J/\psi\pi^+\pi^-$ in $\bar{p}p$ collisions at $\sqrt{s} = 1.96$ TeV,” Phys. Rev. Lett. **93**, 072001 (2004) [hep-ex/0312021].
 - [6] V. M. Abazov *et al.* [D0 Collaboration], “Observation and properties of the $X(3872)$ decaying to $J/\psi\pi^+\pi^-$ in $p\bar{p}$ collisions at $\sqrt{s} = 1.96$ TeV,” Phys. Rev. Lett. **93**, 162002 (2004) [hep-ex/0405004].
 - [7] E. S. Swanson, “The New heavy mesons: A Status report,” Phys. Rept. **429**, 243 (2006) [hep-ph/0601110].
 - [8] S. L. Zhu, “New hadron states,” Int. J. Mod. Phys. E **17** (2008) 283 [hep-ph/0703225].
 - [9] M. B. Voloshin, “Charmonium,” Prog. Part. Nucl. Phys. **61** (2008) 455 [arXiv:0711.4556 [hep-ph]].
 - [10] N. Drenska, R. Faccini, F. Piccinini, A. Polosa, F. Renga and C. Sabelli, “New Hadronic Spectroscopy,” Riv. Nuovo Cim. **33** (2010) 633 [arXiv:1006.2741 [hep-ph]].
 - [11] A. Esposito, A. L. Guerrieri, F. Piccinini, A. Pilloni and A. D. Polosa, “Four-Quark Hadrons: an Updated Review,” Int. J. Mod. Phys. A **30** (2015) 1530002 [arXiv:1411.5997 [hep-ph]].
 - [12] H. X. Chen, W. Chen, X. Liu and S. L. Zhu, “The hidden-charm pentaquark and tetraquark states,” Phys. Rept. **639** (2016) 1 [arXiv:1601.02092 [hep-ph]].
 - [13] R. Chen, X. Liu and S. L. Zhu, “Hidden-charm molecular pentaquarks and their charm-strange partners,” Nucl. Phys. A **954** (2016) 406 [arXiv:1601.03233 [hep-ph]].
 - [14] A. Hosaka, T. Iijima, K. Miyabayashi, Y. Sakai and S. Yasui, “Exotic hadrons with heavy flavors: X, Y, Z, and related states,” PTEP **2016** (2016) no.6, 062C01 [arXiv:1603.09229 [hep-ph]].
 - [15] J. M. Richard, “Exotic hadrons: review and perspectives,” Few Body Syst. **57** (2016) no.12, 1185 [arXiv:1606.08593 [hep-ph]].
 - [16] R. F. Lebed, R. E. Mitchell and E. S. Swanson, “Heavy-Quark QCD Exotica,” Prog. Part. Nucl. Phys. **93**, 143–194 (2017) [arXiv:1610.04528 [hep-ph]].

TABLE XXVIII. The estimated masses for the $QQQQ\bar{Q}$ ($Q = c, b$) system in units of MeV. The values in the second column are eigenvalues obtained with the CMI Hamiltonian in Eq. (2). The masses in the third and fourth columns are determined with meson-baryon thresholds in Eq. (3). The masses in the fifth column are determined with the modified CMI model in Eq. (4).

$cccc\bar{c}$			$cccb\bar{b}$						
J^P	Eigenvalue	$(\eta_c \Omega_{ccc})$	Mass	J^P	Eigenvalue	$(B_c \Omega_{ccb})$	Mass		
$\frac{3}{2}^-$	33.3	7861.2	7863.6	$\frac{3}{2}^-$	44.0	11130.9	11130.0		
$\frac{1}{2}^-$	118.1	7946.0	7948.8	$\frac{1}{2}^-$	96.8	11183.7	11177.2		
$bbbb\bar{c}$			$bbbb\bar{b}$						
J^P	Eigenvalue	$(B_c \Omega_{bbb})$	Mass	J^P	Eigenvalue	$(\eta_b \Omega_{bbb})$	Mass		
$\frac{3}{2}^-$	16.0	20639.0	20651.7	$\frac{3}{2}^-$	18.1	23758.8	23774.8		
$\frac{1}{2}^-$	68.8	20691.8	20698.8	$\frac{1}{2}^-$	64.5	23805.2	23820.7		
$cccb\bar{c}$			$cccb\bar{b}$						
J^P	Eigenvalue	$(B_c \Omega_{ccc})$	$(\eta_c \Omega_{ccb})$	Mass	J^P	Eigenvalue	$(\eta_b \Omega_{ccb})$	$(B_c \Omega_{ccb})$	Mass
$\frac{5}{2}^-$	59.0	11130.9	10915.5	11123.6	$\frac{5}{2}^-$	41.9	14246.5	14172.4	14245.9
$\frac{3}{2}^-$	$\begin{pmatrix} 59.0 \\ 23.6 \\ -45.2 \end{pmatrix}$	$\begin{pmatrix} 11145.9 \\ 11110.5 \\ 11041.7 \end{pmatrix}$	$\begin{pmatrix} 10930.5 \\ 10895.1 \\ 10826.4 \end{pmatrix}$	$\begin{pmatrix} 11136.8 \\ 11101.4 \\ 11037.7 \end{pmatrix}$	$\frac{3}{2}^-$	$\begin{pmatrix} 47.1 \\ 32.1 \\ -30.6 \end{pmatrix}$	$\begin{pmatrix} 14251.7 \\ 14236.7 \\ 14174.0 \end{pmatrix}$	$\begin{pmatrix} 14177.6 \\ 14162.6 \\ 14099.9 \end{pmatrix}$	$\begin{pmatrix} 14372.6 \\ 14245.7 \\ 14181.9 \end{pmatrix}$
$\frac{1}{2}^-$	$\begin{pmatrix} 101.3 \\ 61.2 \\ -26.2 \end{pmatrix}$	$\begin{pmatrix} 11188.2 \\ 11148.1 \\ 11060.7 \end{pmatrix}$	$\begin{pmatrix} 10972.9 \\ 10932.8 \\ 10845.4 \end{pmatrix}$	$\begin{pmatrix} 11174.7 \\ 11137.0 \\ 11047.6 \end{pmatrix}$	$\frac{1}{2}^-$	$\begin{pmatrix} 83.7 \\ 45.5 \\ -8.8 \end{pmatrix}$	$\begin{pmatrix} 14288.3 \\ 14250.1 \\ 14195.8 \end{pmatrix}$	$\begin{pmatrix} 14214.2 \\ 14176.1 \\ 14121.7 \end{pmatrix}$	$\begin{pmatrix} 14411.0 \\ 14356.9 \\ 14238.0 \end{pmatrix}$
$bbbc\bar{c}$			$bbcb\bar{b}$						
J^P	Eigenvalue	$(\eta_c \Omega_{bbb})$	$(B_c \Omega_{bbc})$	Mass	J^P	Eigenvalue	$(B_c \Omega_{bbb})$	$(\eta_b \Omega_{bbc})$	Mass
$\frac{5}{2}^-$	42.7	17406.7	17551.9	17406.6	$\frac{5}{2}^-$	32.0	20655.0	20658.9	20648.4
$\frac{3}{2}^-$	$\begin{pmatrix} 44.7 \\ 15.0 \\ -77.3 \end{pmatrix}$	$\begin{pmatrix} 17408.7 \\ 17379.0 \\ 17286.7 \end{pmatrix}$	$\begin{pmatrix} 17553.9 \\ 17524.2 \\ 17431.9 \end{pmatrix}$	$\begin{pmatrix} 17535.4 \\ 17406.3 \\ 17291.0 \end{pmatrix}$	$\frac{3}{2}^-$	$\begin{pmatrix} 34.0 \\ 19.4 \\ -47.0 \end{pmatrix}$	$\begin{pmatrix} 20657.0 \\ 20642.4 \\ 20576.0 \end{pmatrix}$	$\begin{pmatrix} 20661.0 \\ 20646.3 \\ 20579.9 \end{pmatrix}$	$\begin{pmatrix} 20653.8 \\ 20643.6 \\ 20577.6 \end{pmatrix}$
$\frac{1}{2}^-$	$\begin{pmatrix} 76.5 \\ 36.2 \\ -18.3 \end{pmatrix}$	$\begin{pmatrix} 17440.5 \\ 17400.2 \\ 17345.7 \end{pmatrix}$	$\begin{pmatrix} 17585.7 \\ 17545.4 \\ 17491.0 \end{pmatrix}$	$\begin{pmatrix} 17578.2 \\ 17522.6 \\ 17399.1 \end{pmatrix}$	$\frac{1}{2}^-$	$\begin{pmatrix} 67.5 \\ 29.6 \\ -18.7 \end{pmatrix}$	$\begin{pmatrix} 20690.5 \\ 20652.6 \\ 20604.3 \end{pmatrix}$	$\begin{pmatrix} 20694.4 \\ 20656.5 \\ 20608.3 \end{pmatrix}$	$\begin{pmatrix} 20691.1 \\ 20652.8 \\ 20606.5 \end{pmatrix}$
$ccbb\bar{c}$			$ccbb\bar{b}$						
J^P	Eigenvalue	$(B_c \Omega_{ccb})$	$(\eta_c \Omega_{bbc})$	Mass	J^P	Eigenvalue	$(\eta_b \Omega_{ccb})$	$(B_c \Omega_{bbc})$	Mass
$\frac{5}{2}^-$	41.9	14372.4	14292.1	14294.8	$\frac{5}{2}^-$	35.5	17483.7	17544.7	17476.5
$\frac{3}{2}^-$	$\begin{pmatrix} 52.2 \\ 20.7 \\ 16.9 \\ -63.0 \end{pmatrix}$	$\begin{pmatrix} 14382.7 \\ 14351.2 \\ 14347.5 \\ 14267.6 \end{pmatrix}$	$\begin{pmatrix} 14302.4 \\ 14270.9 \\ 14267.2 \\ 14187.3 \end{pmatrix}$	$\begin{pmatrix} 14374.9 \\ 14298.0 \\ 14274.4 \\ 14196.8 \end{pmatrix}$	$\frac{3}{2}^-$	$\begin{pmatrix} 39.5 \\ 24.0 \\ 13.1 \\ -40.1 \end{pmatrix}$	$\begin{pmatrix} 17487.7 \\ 17472.2 \\ 17461.3 \\ 17408.1 \end{pmatrix}$	$\begin{pmatrix} 17548.7 \\ 17533.2 \\ 17522.3 \\ 17469.1 \end{pmatrix}$	$\begin{pmatrix} 17554.2 \\ 17478.9 \\ 17457.4 \\ 17416.2 \end{pmatrix}$
$\frac{1}{2}^-$	$\begin{pmatrix} 87.4 \\ 46.5 \\ -19.1 \\ -69.6 \end{pmatrix}$	$\begin{pmatrix} 14417.9 \\ 14377.0 \\ 14311.5 \\ 14260.9 \end{pmatrix}$	$\begin{pmatrix} 14337.6 \\ 14296.7 \\ 14231.2 \\ 14180.6 \end{pmatrix}$	$\begin{pmatrix} 14405.8 \\ 14317.8 \\ 14252.8 \\ 14185.1 \end{pmatrix}$	$\frac{1}{2}^-$	$\begin{pmatrix} 73.9 \\ 35.8 \\ -15.5 \\ -49.0 \end{pmatrix}$	$\begin{pmatrix} 17522.1 \\ 17484.1 \\ 17432.7 \\ 17399.2 \end{pmatrix}$	$\begin{pmatrix} 17583.1 \\ 17545.1 \\ 17493.7 \\ 17460.2 \end{pmatrix}$	$\begin{pmatrix} 17575.8 \\ 17496.3 \\ 17437.4 \\ 17404.9 \end{pmatrix}$

- [17] A. Esposito, A. Pilloni and A. D. Polosa, “Multiquark Resonances,” Phys. Rept. **668**, 1-97 (2017) [arXiv:1611.07920 [hep-ph]].
- [18] A. Ali, J. S. Lange and S. Stone, “Exotics: Heavy Pentaquarks and Tetraquarks,” Prog. Part. Nucl. Phys. **97**, 123-198 (2017) [arXiv:1706.00610 [hep-ph]].
- [19] N. Brambilla, S. Eidelman, C. Hanhart, A. Nefediev, C. P. Shen, C. E. Thomas, A. Vairo and C. Z. Yuan, “The XYZ states: experimental and theoretical sta-
- tus and perspectives,” Phys. Rept. **873**, 1-154 (2020) [arXiv:1907.07583 [hep-ex]].
- [20] S. K. Choi *et al.* [Belle Collaboration], “Observation of a resonance-like structure in the $\pi^\pm \psi'$ mass distribution in exclusive $B \rightarrow K \pi^\pm \psi'$ decays,” Phys. Rev. Lett. **100** (2008) 142001 [arXiv:0708.1790 [hep-ex]].
- [21] R. Mizuk *et al.* [Belle Collaboration], “Dalitz analysis of $B \rightarrow K \pi^+ \psi'$ decays and the $Z(4430)^+$,” Phys. Rev. D **80**, 031104 (2009) [arXiv:0905.2869 [hep-ex]].

TABLE XXIX. The relative partial decay widths for the $cccc\bar{c}$, $cccc\bar{b}$, $bbbb\bar{c}$, $bbbb\bar{b}$, $cccb\bar{c}$, $cccb\bar{b}$, $bbbc\bar{c}$, $bbbc\bar{b}$, $ccb\bar{c}$, and $ccb\bar{b}$ pentaquark states. For each pentaquark state, we choose one channel as a reference channel, and the relative partial decay widths for the other channels are obtained in units of the reference channel. The masses are all in units of MeV. The scattering states and stable states in the modified CMI model are marked with “*” and “†”, respectively.

J^P	$cccc\bar{c}$ Mass	$ccc \otimes c\bar{c}$ $\Omega_{ccc}J/\psi \quad \Omega_{ccc}\eta_c$	$cccc\bar{b}$ Mass	$ccc \otimes c\bar{b}$ $\Omega_{ccc}B_c^* \quad \Omega_{ccc}B_c$		$bbbb\bar{c}$ Mass	$bbb \otimes b\bar{c}$ $\Omega_{bbb}B_c^* \quad \Omega_{bbb}B_c$	$bbbb\bar{b}$ Mass	$bbb \otimes b\bar{b}$ $\Omega_{bbb}\Upsilon \quad \Omega_{bbb}\eta_b$		
$\frac{3}{2}^-$	7863.6	\times 1	11130.0	\times 1		20651.7	0.4 1	23774.8	0.45 1		
$\frac{1}{2}^-$	7948.8	1	11177.2	1		20698.8	1	23820.7	1		
$ccc \otimes b\bar{c}$ $ccb \otimes c\bar{c}$											
J^P	$ccc \otimes b\bar{c}$ Mass	$\Omega_{ccc}B_c^* \quad \Omega_{ccc}B_c$	$ccb \otimes c\bar{c}$ $\Omega_{ccb}J/\psi \quad \Omega_{ccb}\eta_c$	$ccc \otimes b\bar{b}$ $\Omega_{ccc}\Upsilon \quad \Omega_{ccc}\eta_b$	$ccb \otimes c\bar{b}$ $\Omega_{ccb}B_c^* \quad \Omega_{ccb}B_c$	Mass	$\Omega_{ccb}\Upsilon \quad \Omega_{ccb}\eta_b$	$ccb \otimes c\bar{b}$ $\Omega_{ccb}B_c^* \quad \Omega_{ccb}B_c$	Mass	$\Omega_{ccb}\Upsilon \quad \Omega_{ccb}\eta_b$	
$\frac{5}{2}^-$	11123.6*	1	\times			14245.9*	1		\times		
$\frac{3}{2}^-$	11136.8	5 1	1 0.001	1		14372.6	0.1 1	3.3 3.7	1		
	11101.4	\times 1	\times 19	1		14245.7*	\times 1	\times \times	\times		
	11037.7	\times \times	\times 1	\times		14181.9*	\times \times	\times \times	\times		
$\frac{1}{2}^-$	11174.7	1	247	1 0.003		14411.0	1	31	4	1	
	11137.0	1	6.5	98 1		14356.9	1	\times	2.1	1	
	11047.6	\times	\times	\times 1		14238.0*	\times	\times \times	\times		
$bbb \otimes c\bar{c}$ $bbc \otimes b\bar{c}$											
J^P	$bbb \otimes c\bar{c}$ Mass	$\Omega_{bbb}J/\psi \quad \Omega_{bbb}\eta_c$	$bbc \otimes b\bar{c}$ $\Omega_{bbc}^*B_c^* \quad \Omega_{bbc}^*B_c$	$bbc \otimes b\bar{c}$ $\Omega_{bbc}^*B_c^* \quad \Omega_{bbc}^*B_c$	Mass	$bbb \otimes c\bar{b}$ $\Omega_{bbb}B_c^* \quad \Omega_{bbb}B_c$	$bbc \otimes b\bar{b}$ $\Omega_{bbc}^*B_c^* \quad \Omega_{bbc}^*B_c$	$bbc \otimes b\bar{b}$ $\Omega_{bbc}\Upsilon \quad \Omega_{bbc}\eta_b$	Mass	$bbc \otimes b\bar{b}$ $\Omega_{bbc}\Upsilon \quad \Omega_{bbc}\eta_b$	
$\frac{5}{2}^-$	17406.6*	\times	\times			20648.4*	1	\times			
$\frac{3}{2}^-$	17535.4	0.2 1	1 3.9	1		20653.8	2.8 1	\times 0.1	1		
	17406.3*	\times 1	\times \times	\times		20643.6	\times 1	\times 30	1		
	17291.0*	\times \times	\times \times	\times		20577.6*	\times \times	\times \times	\times		
$\frac{1}{2}^-$	17578.2	1	20	1.9 1		20691.1	1	532	2.3	1	
	17522.6	1	\times	1.9 1		20652.8	1	\times	145	1	
	17399.1*	\times	\times	\times \times		20606.5	\times	\times \times	\times	1	
$bbc \otimes c\bar{c}$ $ccb \otimes b\bar{c}$											
J^P	$bbc \otimes c\bar{c}$ Mass	$\Omega_{bbc}^*J/\psi \quad \Omega_{bbc}\eta_c$	$ccb \otimes b\bar{c}$ $\Omega_{ccb}^*B_c^* \quad \Omega_{ccb}^*B_c$	$ccb \otimes b\bar{c}$ $\Omega_{ccb}^*B_c^* \quad \Omega_{ccb}^*B_c$	Mass	$ccb \otimes b\bar{c}$ $\Omega_{ccb}\Upsilon \quad \Omega_{ccb}\eta_b$	$ccb \otimes b\bar{b}$ $\Omega_{ccb}\Upsilon \quad \Omega_{ccb}\eta_b$	Mass	$ccb \otimes b\bar{b}$ $\Omega_{ccb}\Upsilon \quad \Omega_{ccb}\eta_b$	Mass	
$\frac{5}{2}^-$	14294.8	1		\times							
$\frac{3}{2}^-$	14374.9	11.5 28	1			1 0.6	1				
	14298.0	1.1 0.04	1			\times 1	\times				
	14274.4	\times 0.17	1			\times \times	\times				
	14196.8	\times 1	\times			\times \times	\times				
$\frac{1}{2}^-$	14405.8	44.6 6.9	1	5.1		0.5	1				
	14317.8	158 41.3	1	\times		\times	\times 1				
	14252.8	\times	\times 1	\times		\times	\times				
	14185.1	\times	\times 1	\times		\times	\times				
$bbc \otimes c\bar{b}$ $ccb \otimes b\bar{b}$											
J^P	$bbc \otimes c\bar{b}$ Mass	$\Omega_{bbc}^*B_c^* \quad \Omega_{bbc}^*B_c$	$ccb \otimes b\bar{b}$ $\Omega_{ccb}^*\Upsilon \quad \Omega_{ccb}^*\eta_b$	$ccb \otimes b\bar{b}$ $\Omega_{ccb}\Upsilon \quad \Omega_{ccb}\eta_b$	Mass	$ccb \otimes b\bar{b}$ $\Omega_{ccb}\Upsilon \quad \Omega_{ccb}\eta_b$	Mass	$ccb \otimes b\bar{b}$ $\Omega_{ccb}\Upsilon \quad \Omega_{ccb}\eta_b$	Mass	$ccb \otimes b\bar{b}$ $\Omega_{ccb}\Upsilon \quad \Omega_{ccb}\eta_b$	
$\frac{5}{2}^-$	17476.5†	\times		\times							
$\frac{3}{2}^-$	17554.2	1.2 0.6	1	35 247	1						
	17478.9	\times 1	\times	\times 0.4	1						
	17457.4	\times \times	\times	\times 0.3	1						
	17416.2†	\times \times	\times	\times \times							
$\frac{1}{2}^-$	17575.8	5.6 0.5	1	48 7.3	1						
	17496.3	\times	\times 1	21.7 6.7	1						
	17437.4	\times	\times \times	\times \times							
	17404.9	\times	\times \times	\times \times							

- [22] K. Chilikin *et al.* [Belle Collaboration], “Observation of a new charged charmoniumlike state in $\bar{B}^0 \rightarrow J/\psi K^- \pi^+$ decays,” Phys. Rev. D **90**, no. 11, 112009 (2014) [arXiv:1408.6457 [hep-ex]].
- [23] R. Aaij *et al.* [LHCb Collaboration], “Observation of the resonant character of the $Z(4430)^-$ state,” Phys. Rev. Lett. **112**, no. 22, 222002 (2014) [arXiv:1404.1903 [hep-ex]].
- [24] R. Mizuk *et al.* [Belle Collaboration], “Observation of two resonance-like structures in the $\pi^+ \chi_{c1}$ mass distribution in exclusive $\bar{B}^0 \rightarrow K^- \pi^+ \chi_{c1}$ decays,” Phys. Rev. D **78**, 072004 (2008) [arXiv:0806.4098 [hep-ex]].
- [25] M. Ablikim *et al.* [BESIII Collaboration], “Observation of a Charged Charmoniumlike Structure in $e^+ e^- \rightarrow \pi^+ \pi^- J/\psi$ at $\sqrt{s} = 4.26$ GeV,” Phys. Rev. Lett. **110**, 252001 (2013) [arXiv:1303.5949 [hep-ex]].
- [26] Z. Q. Liu *et al.* [Belle Collaboration], “Study of $e^+ e^- \rightarrow \pi^+ \pi^- J/\psi$ and Observation of a Charged Charmoniumlike State at Belle,” Phys. Rev. Lett. **110**, 252002 (2013) [arXiv:1304.0121 [hep-ex]].
- [27] T. Xiao, S. Dobbs, A. Tomaradze and K. K. Seth, “Observation of the Charged Hadron $Z_c^\pm(3900)$ and Evidence for the Neutral $Z_c^0(3900)$ in $e^+ e^- \rightarrow \pi\pi J/\psi$ at $\sqrt{s} = 4170$ MeV,” Phys. Lett. B **727**, 366 (2013) [arXiv:1304.3036 [hep-ex]].
- [28] M. Ablikim *et al.* [BESIII Collaboration], “Observation of $Z_c(3900)^0$ in $e^+ e^- \rightarrow \pi^0 \pi^0 J/\psi$,” Phys. Rev. Lett. **115**, no. 11, 112003 (2015) [arXiv:1506.06018 [hep-ex]].
- [29] M. Ablikim *et al.* [BESIII Collaboration], “Observation of a charged $(D\bar{D}^*)^\pm$ mass peak in $e^+ e^- \rightarrow \pi D\bar{D}^*$ at $\sqrt{s} = 4.26$ GeV,” Phys. Rev. Lett. **112**, no. 2, 022001 (2014) [arXiv:1310.1163 [hep-ex]].
- [30] M. Ablikim *et al.* [BESIII Collaboration], “Confirmation of a charged charmoniumlike state $Z_c(3885)^\mp$ in $e^+ e^- \rightarrow \pi^\pm (D\bar{D}^*)^\mp$ with double D tag,” Phys. Rev. D **92**, no. 9, 092006 (2015) [arXiv:1509.01398 [hep-ex]].
- [31] M. Ablikim *et al.* [BESIII Collaboration], “Observation of a Neutral Structure near the $D\bar{D}^*$ Mass Threshold in $e^+ e^- \rightarrow (D\bar{D}^*)^0 \pi^0$ at $\sqrt{s} = 4.226$ and 4.257 GeV,” Phys. Rev. Lett. **115**, no. 22, 222002 (2015) [arXiv:1509.05620 [hep-ex]].
- [32] M. Ablikim *et al.* [BESIII Collaboration], “Observation of a Charged Charmoniumlike Structure $Z_c(4020)$ and Search for the $Z_c(3900)$ in $e^+ e^- \rightarrow \pi^+ \pi^- h_c$,” Phys. Rev. Lett. **111**, no. 24, 242001 (2013) [arXiv:1309.1896 [hep-ex]].
- [33] M. Ablikim *et al.* [BESIII Collaboration], “Observation of $e^+ e^- \rightarrow \pi^0 \pi^0 h_c$ and a Neutral Charmoniumlike Structure $Z_c(4020)^0$,” Phys. Rev. Lett. **113**, no. 21, 212002 (2014) [arXiv:1409.6577 [hep-ex]].
- [34] M. Ablikim *et al.* [BESIII Collaboration], “Observation of a charged charmoniumlike structure in $e^+ e^- \rightarrow (D^* \bar{D}^*)^\pm \pi^\mp$ at $\sqrt{s} = 4.26$ GeV,” Phys. Rev. Lett. **112**, no. 13, 132001 (2014) [arXiv:1308.2760 [hep-ex]].
- [35] M. Ablikim *et al.* [BESIII Collaboration], “Observation of a neutral charmoniumlike state $Z_c(4025)^0$ in $e^+ e^- \rightarrow (D^* \bar{D}^*)^0 \pi^0$,” Phys. Rev. Lett. **115**, no. 18, 182002 (2015) [arXiv:1507.02404 [hep-ex]].
- [36] M. Ablikim *et al.* [BESIII], Phys. Rev. D **96**, no. 3, 032004 (2017) doi:10.1103/PhysRevD.96.032004 [arXiv:1703.08787 [hep-ex]].
- [37] A. Bondar *et al.* [Belle Collaboration], “Observation of two charged bottomonium-like resonances in $\Upsilon(5S)$ decays,” Phys. Rev. Lett. **108**, 122001 (2012) [arXiv:1110.2251 [hep-ex]].
- [38] B. Aubert *et al.* [BaBar Collaboration], “Observation of a narrow meson decaying to $D_s^+ \pi^0$ at a mass of 2.32 GeV/c 2 ,” Phys. Rev. Lett. **90**, 242001 (2003) [hep-ex/0304021].
- [39] D. Besson *et al.* [CLEO Collaboration], “Observation of a narrow resonance of mass 2.46 GeV/c 2 decaying to $D_s^{*+} \pi^0$ and confirmation of the $D_{sJ}(2317)$ state,” Phys. Rev. D **68**, 032002 (2003) Erratum: [Phys. Rev. D **75**, 119908 (2007)] [hep-ex/0305100].
- [40] S. Godfrey and N. Isgur, “Mesons in a Relativized Quark Model with Chromodynamics,” Phys. Rev. D **32**, 189 (1985).
- [41] A. V. Evdokimov *et al.* [SELEX Collaboration], “First observation of a narrow charm-strange meson $D_{sJ}^+(2632) \rightarrow D_s^+ \eta$ and $D^0 K^+$,” Phys. Rev. Lett. **93**, 242001 (2004) [hep-ex/0406045].
- [42] R. Aaij *et al.* [LHCb], “A model-independent study of resonant structure in $B^+ \rightarrow D^+ D^- K^+$ decays,” [arXiv:2009.00025 [hep-ex]].
- [43] R. Aaij *et al.* [LHCb], “Amplitude analysis of the $B^+ \rightarrow D^+ D^- K^+$ decay,” [arXiv:2009.00026 [hep-ex]].
- [44] M. W. Hu, X. Y. Lao, P. Ling and Q. Wang, “The $X_0(2900)$ and its heavy quark spin partners in molecular picture,” [arXiv:2008.06894 [hep-ph]].
- [45] M. Z. Liu, J. J. Xie and L. S. Geng, “ $X_0(2866)$ as a $D^* \bar{K}^*$ molecular state,” [arXiv:2008.07389 [hep-ph]].
- [46] J. He and D. Y. Chen, “Molecular picture for $X_0(2900)$ and $X_1(2900)$,” [arXiv:2008.07782 [hep-ph]].
- [47] H. X. Chen, W. Chen, R. R. Dong and N. Su, “ $X_0(2900)$ and $X_1(2900)$: hadronic molecules or compact tetraquarks,” [arXiv:2008.07516 [hep-ph]].
- [48] M. Karliner and J. L. Rosner, “First exotic hadron with open heavy flavor: $cs\bar{u}\bar{d}$ tetraquark,” [arXiv:2008.05993 [hep-ph]].
- [49] X. G. He, W. Wang and R. Zhu, “Open-charm tetraquark X_c and open-bottom tetraquark X_b ,” [arXiv:2008.07145 [hep-ph]].
- [50] X. H. Liu, M. J. Yan, H. W. Ke, G. Li and J. J. Xie, “Triangle singularity as the origin of $X_0(2900)$ and $X_1(2900)$ observed in $B^+ \rightarrow D^+ D^- K^+$,” [arXiv:2008.07190 [hep-ph]].
- [51] Q. F. Lü, D. Y. Chen and Y. B. Dong, “Open charm and bottom tetraquarks in an extended relativized quark model,” [arXiv:2008.07340 [hep-ph]].
- [52] J. R. Zhang, “An open charm tetraquark candidate: note on $X_0(2900)$,” [arXiv:2008.07295 [hep-ph]].
- [53] S. S. Agaev, K. Azizi and H. Sundu, “New scalar resonance $X_0(2900)$ as a $\bar{D}^* K^*$ molecule: Mass and width,” [arXiv:2008.13027 [hep-ph]].
- [54] Y. Xue, X. Jin, H. Huang and J. Ping, “Tetraquarks with open charm flavor,” [arXiv:2008.09516 [hep-ph]].
- [55] Y. K. Chen, J. J. Han, Q. F. Lü, J. P. Wang and F. S. Yu, “Branching fractions of $B^- \rightarrow D^- X_{0,1}(2900)$ and their implications,” [arXiv:2009.01182 [hep-ph]].
- [56] F. S. Yu, H. Y. Jiang, R. H. Li, C. D. Lü, W. Wang and Z. X. Zhao, “Discovery Potentials of Doubly Charmed Baryons,” Chin. Phys. C **42**, no. 5, 051001 (2018) [arXiv:1703.09086 [hep-ph]].
- [57] R. Aaij *et al.* [LHCb Collaboration], “Observation of the doubly charmed baryon Ξ_{cc}^{++} ,” Phys. Rev. Lett. **119**, no. 11, 112001 (2017) [arXiv:1707.01621 [hep-ex]].

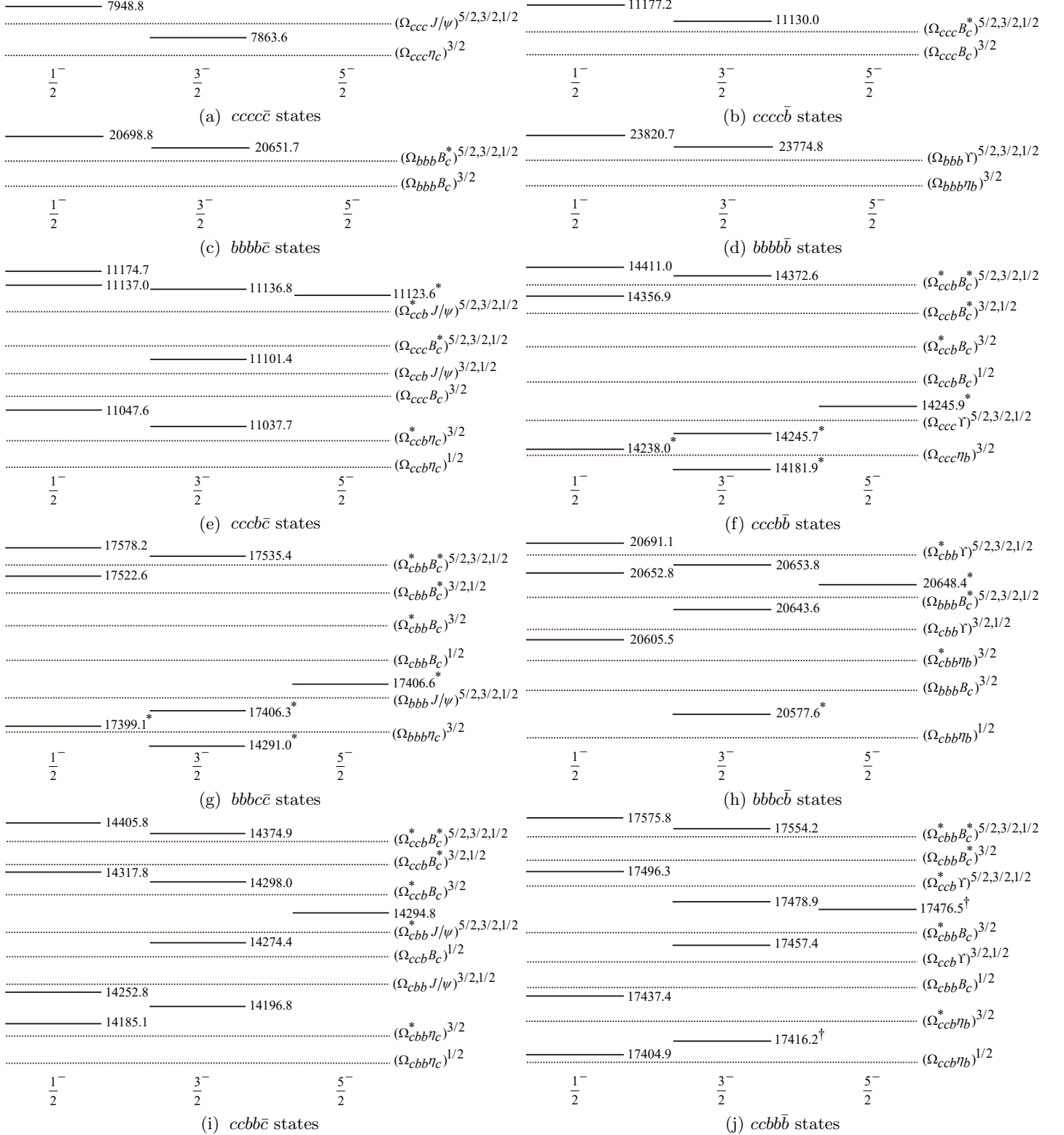


FIG. 6. Relative positions (units: MeV) for the $cccc\bar{c}$, $cccb\bar{b}$, $bbbc\bar{b}$, $bbbb\bar{b}$, $cccb\bar{c}$, $bbbc\bar{c}$, $bbbc\bar{b}$, $cccb\bar{c}$, and $ccbb\bar{b}$ pentaquark states labeled with solid lines. The dotted lines denote various baryon-meson thresholds. When the spin of an initial pentaquark state is equal to a number in the superscript of a baryon-meson state, its decay into that baryon-meson channel through S -wave is allowed by the angular momentum conservation. The scattering states and stable states in the modified CMI model are marked with “*” and “†”, respectively.

- [58] S. Q. Luo, K. Chen, X. Liu, Y. R. Liu and S. L. Zhu, “Exotic tetraquark states with the $qq\bar{Q}\bar{Q}$ configuration,” *Eur. Phys. J. C* **77**, no. 10, 709 (2017) [arXiv:1707.01180 [hep-ph]].
- [59] S. Q. Luo, K. Chen, X. Liu, Y. R. Liu and S. L. Zhu, “Exotic tetraquark states with the $qq\bar{Q}\bar{Q}$ configuration,” *Eur. Phys. J. C* **77**, no. 10, 709 (2017) [arXiv:1707.01180 [hep-ph]].
- [60] M. Karliner and J. L. Rosner, “Discovery of doubly-charmed Ξ_{cc} baryon implies a stable ($bb\bar{u}\bar{d}$) tetraquark,” *Phys. Rev. Lett.* **119**, no. 20, 202001 (2017) [arXiv:1707.07666 [hep-ph]].
- [61] E. J. Eichten and C. Quigg, “Heavy-quark symmetry implies stable heavy tetraquark mesons $Q_iQ_j\bar{q}_k\bar{q}_l$,” *Phys. Rev. Lett.* **119**, no. 20, 202002 (2017) [arXiv:1707.09575 [hep-ph]].
- [62] A. Ali, Q. Qin and W. Wang, “Discovery potential of stable and near-threshold doubly heavy tetraquarks at the LHC,” *Phys. Lett. B* **785**, 605-609 (2018) [arXiv:1806.09288 [hep-ph]].
- [63] W. Park, S. Noh and S. H. Lee, “Masses of the doubly heavy tetraquarks in a constituent quark model,” *Acta Phys. Polon. B* **50**, 1151-1157 (2019) [arXiv:1809.05257 [nucl-th]].
- [64] R. Aaij *et al.* [LHCb], “Observation of structure in the J/ψ -pair mass spectrum,” [arXiv:2006.16957 [hep-ex]].
- [65] K. Chen, X. Liu, J. Wu, Y. R. Liu and S. L. Zhu, “Triply heavy tetraquark states with the $QQ\bar{Q}\bar{q}$ configuration,” *Eur. Phys. J. A* **53**, no. 1, 5 (2017) [arXiv:1609.06117 [hep-ph]].
- [66] T. Nakano *et al.* [LEPS Collaboration], “Evidence for a narrow $S = +1$ baryon resonance in photoproduction from the neutron,” *Phys. Rev. Lett.* **91**, 012002 (2003) [hep-ex/0301020].
- [67] A. Martinez Torres and E. Oset, “A novel interpretation of the ‘ $\Theta^+(1540)$ pentaquark’ peak,” *Phys. Rev. Lett.* **105**, 092001 (2010) [arXiv:1008.4978 [nucl-th]].
- [68] T. Liu, Y. Mao and B. Q. Ma, “Present status on experimental search for pentaquarks,” *Int. J. Mod. Phys. A* **29**, no. 13, 1430020 (2014) [arXiv:1403.4455 [hep-ex]].
- [69] R. Aaij *et al.* [LHCb Collaboration], “Observation of $J/\psi p$ Resonances Consistent with Pentaquark States in $\Lambda_b^0 \rightarrow J/\psi K^- p$ Decays,” *Phys. Rev. Lett.* **115**, 072001 (2015) [arXiv:1507.03414 [hep-ex]].
- [70] R. Aaij *et al.* [LHCb Collaboration], “Model-independent evidence for $J/\psi p$ contributions to $\Lambda_b^0 \rightarrow J/\psi p K^-$ decays,” *Phys. Rev. Lett.* **117**, no. 8, 082002 (2016) [arXiv:1604.05708 [hep-ex]].
- [71] R. Aaij *et al.* [LHCb Collaboration], “Observation of a narrow pentaquark state, $P_c(4312)^+$, and of two-peak structure of the $P_c(4450)^+$,” *Phys. Rev. Lett.* **122**, no. 22, 222001 (2019) [arXiv:1904.03947 [hep-ex]].
- [72] J. J. Wu, R. Molina, E. Oset and B. S. Zou, “Prediction of narrow N^* and Λ^* resonances with hidden charm above 4 GeV,” *Phys. Rev. Lett.* **105**, 232001 (2010) [arXiv:1007.0573 [nucl-th]].
- [73] Z. C. Yang, Z. F. Sun, J. He, X. Liu and S. L. Zhu, “The possible hidden-charm molecular baryons composed of anti-charmed meson and charmed baryon,” *Chin. Phys. C* **36**, 6-13 (2012) [arXiv:1105.2901 [hep-ph]].
- [74] W. L. Wang, F. Huang, Z. Y. Zhang and B. S. Zou, “ $\Sigma_c\bar{D}$ and $\Lambda_c\bar{D}$ states in a chiral quark model,” *Phys. Rev. C* **84**, 015203 (2011) [arXiv:1101.0453 [nucl-th]].
- [75] J. Wu, Y. R. Liu, K. Chen, X. Liu and S. L. Zhu, “Hidden-charm pentaquarks and their hidden-bottom and B_c -like partner states,” *Phys. Rev. D* **95**, no. 3, 034002 (2017) [arXiv:1701.03873 [hep-ph]].
- [76] Q. S. Zhou, K. Chen, X. Liu, Y. R. Liu and S. L. Zhu, “Surveying exotic pentaquarks with the typical $QQq\bar{q}\bar{q}$ configuration,” *Phys. Rev. C* **98**, no. 4, 045204 (2018) [arXiv:1801.04557 [hep-ph]].
- [77] S. Y. Li, Y. R. Liu, Y. N. Liu, Z. G. Si and J. Wu, “Pentaquark states with the $QQQ\bar{q}\bar{q}$ configuration in a simple model,” *Eur. Phys. J. C* **79**, no. 1, 87 (2019) [arXiv:1809.08072 [hep-ph]].
- [78] H. T. An, Q. S. Zhou, Z. W. Liu, Y. R. Liu and X. Liu, “Exotic pentaquark states with the $qqQQ\bar{Q}$ configuration,” *Phys. Rev. D* **100**, no. 5, 056004 (2019) [arXiv:1905.07858 [hep-ph]].
- [79] Y. R. Liu, X. Liu and S. L. Zhu, “ $X(5568)$ and its partner states,” *Phys. Rev. D* **93**, no. 7, 074023 (2016) [arXiv:1603.01131 [hep-ph]].
- [80] J. Wu, Y. R. Liu, K. Chen, X. Liu and S. L. Zhu, “Heavy-flavored tetraquark states with the $QQ\bar{Q}\bar{Q}$ configuration,” *Phys. Rev. D* **97**, no. 9, 094015 (2018) [arXiv:1605.01134 [hep-ph]].
- [81] J. Wu, Y. R. Liu, K. Chen, X. Liu and S. L. Zhu, “ $X(4140)$, $X(4270)$, $X(4500)$ and $X(4700)$ and their $cs\bar{c}\bar{s}$ tetraquark partners,” *Phys. Rev. D* **94** (2016) no. 9, 094031 [arXiv:1608.07900 [hep-ph]].
- [82] J. Wu, X. Liu, Y. R. Liu and S. L. Zhu, “Systematic studies of charmonium-, bottomonium-, and B_c -like tetraquark states,” *Phys. Rev. D* **99**, no. 1, 014037 (2019) [arXiv:1810.06886 [hep-ph]].
- [83] H. Hagaasen, E. Kou, J. M. Richard and P. Sorba, “Isovector and hidden-beauty partners of the $X(3872)$,” *Phys. Lett. B* **732**, 97 (2014) [arXiv:1309.2049 [hep-ph]].
- [84] X. Z. Weng, X. L. Chen and W. Z. Deng, “Masses of doubly heavy-quark baryons in an extended chromomagnetic model,” *Phys. Rev. D* **97**, no. 5, 054008 (2018) [arXiv:1801.08644 [hep-ph]].
- [85] X. Z. Weng, X. L. Chen, W. Z. Deng and S. L. Zhu, “Hidden-charm pentaquarks and P_c states,” *Phys. Rev. D* **100**, no. 1, 016014 (2019) [arXiv:1904.09891 [hep-ph]].
- [86] J. B. Cheng and Y. R. Liu, “Understanding the structures of hidden-charm pentaquarks in a simple model,” *Nucl. Part. Phys. Proc.* **309-311**, 158-161 (2020) doi:10.1016/j.nuclphysbps.2019.11.027
- [87] J. B. Cheng and Y. R. Liu, “ $P_c(4457)^+$, $P_c(4440)^+$, and $P_c(4312)^+$: molecules or compact pentaquarks?,” *Phys. Rev. D* **100**, no. 5, 054002 (2019) [arXiv:1905.08605 [hep-ph]].
- [88] J. B. Cheng, S. Y. Li, Y. R. Liu, Y. N. Liu, Z. G. Si and T. Yao, “Spectrum and rearrangement decays of tetraquark states with four different flavors,” *Phys. Rev. D* **101**, no. 11, 114017 (2020) doi:10.1103/PhysRevD.101.114017 [arXiv:2001.05287 [hep-ph]].
- [89] J. B. Cheng, S. Y. Li, Y. R. Liu, Z. G. Si and T. Yao, “Double-heavy tetraquark states with heavy diquark-antiquark symmetry,” [arXiv:2008.00737 [hep-ph]].
- [90] B. Silvestre-Brac, “Systematics of Q^2 (anti- Q^2) systems with a chromomagnetic interaction,” *Phys. Rev. D* **46**, 2179 (1992). doi:10.1103/PhysRevD.46.2179
- [91] M. Karliner and J. L. Rosner, “Baryons with two heavy quarks: Masses, production, decays, and detection,”

TABLE XXX. The estimated masses for the $ccc\bar{q}\bar{Q}$ and $ccb\bar{q}\bar{Q}$ ($q = n, s; n = u, d; Q = c, b$) subsystems in units of MeV. The values in the second column are eigenvalues obtained with the CMI Hamiltonian in Eq. (2). The masses in the third, fourth, and fifth columns are determined with meson-baryon thresholds in Eq. (3). The masses in the sixth column are determined with the modified CMI model in Eq. (4).

$cccn\bar{c}$				$cccn\bar{b}$						
J^P	Eigenvalue	$(D\Omega_{ccc})$	$(\eta_c\Xi_{cc})$	Mass	J^P	Eigenvalue	$(B\Omega_{ccc})$	$(B_c\Xi_{cc})$	Mass	
$\frac{5}{2}^-$	61.6	6796.1	6785.6	6794.2	$\frac{5}{2}^-$	37.6	10109.9	10020.6	10110.3	
	$\begin{pmatrix} 63.9 \\ 37.6 \\ -94.8 \end{pmatrix}$	$\begin{pmatrix} 6798.4 \\ 6772.1 \\ 6639.8 \end{pmatrix}$	$\begin{pmatrix} 6787.8 \\ 6761.5 \\ 6629.2 \end{pmatrix}$	$\begin{pmatrix} 6797.2 \\ 6773.0 \\ 6638.0 \end{pmatrix}$	$\frac{3}{2}^-$	$\begin{pmatrix} 53.7 \\ 36.8 \\ -26.2 \end{pmatrix}$	$\begin{pmatrix} 10126.0 \\ 10109.1 \\ 10046.1 \end{pmatrix}$	$\begin{pmatrix} 10036.7 \\ 10019.8 \\ 9956.8 \end{pmatrix}$	10110.7	
	$\begin{pmatrix} 128.3 \\ 52.6 \\ -35.9 \end{pmatrix}$	$\begin{pmatrix} 6862.8 \\ 6787.2 \\ 6698.6 \end{pmatrix}$	$\begin{pmatrix} 6852.2 \\ 6776.6 \\ 6688.1 \end{pmatrix}$	$\begin{pmatrix} 6863.3 \\ 6788.6 \\ 6700.8 \end{pmatrix}$	$\frac{1}{2}^-$	$\begin{pmatrix} 100.2 \\ 29.0 \\ -27.5 \end{pmatrix}$	$\begin{pmatrix} 10172.5 \\ 10101.3 \\ 10044.8 \end{pmatrix}$	$\begin{pmatrix} 10083.2 \\ 10012.0 \\ 9955.5 \end{pmatrix}$	10131.3	
	$\begin{pmatrix} 62.1 \\ 63.1 \\ 41.5 \\ -97.4 \end{pmatrix}$	$\begin{pmatrix} 6896.8 \\ 6897.8 \\ 6876.2 \\ 6737.3 \end{pmatrix}$	$\begin{pmatrix} 6901.8 \\ 6902.8 \\ 6881.2 \\ 6742.3 \end{pmatrix}$	6897.7	$\frac{5}{2}^-$	38.7	10201.6	10137.4	10201.0	
	$\begin{pmatrix} 133.3 \\ 49.2 \\ -40.0 \end{pmatrix}$	$\begin{pmatrix} 6968.0 \\ 6883.9 \\ 6794.7 \end{pmatrix}$	$\begin{pmatrix} 6973.0 \\ 6888.9 \\ 6799.7 \end{pmatrix}$	$\begin{pmatrix} 6971.7 \\ 6888.7 \\ 6800.4 \end{pmatrix}$	$\frac{3}{2}^-$	$\begin{pmatrix} 57.4 \\ 36.7 \\ -30.3 \end{pmatrix}$	$\begin{pmatrix} 10220.3 \\ 10199.6 \\ 10132.6 \end{pmatrix}$	$\begin{pmatrix} 10156.1 \\ 10135.4 \\ 10068.4 \end{pmatrix}$	10202.4	
	$\begin{pmatrix} 24.4 \\ 24.0 \\ -8.2 \\ -42.7 \\ -102.5 \end{pmatrix}$	$\begin{pmatrix} 10002.5 \\ 10002.2 \\ 9969.9 \\ 9935.4 \\ 9875.7 \end{pmatrix}$	$\begin{pmatrix} 10007.4 \\ 10007.0 \\ 9974.7 \\ 9940.3 \\ 9880.5 \end{pmatrix}$	$\begin{pmatrix} 10046.4 \\ 10046.1 \\ 10013.8 \\ 9979.3 \\ 9919.6 \end{pmatrix}$	$\frac{1}{2}^-$	$\begin{pmatrix} 105.4 \\ 25.8 \\ -31.4 \end{pmatrix}$	$\begin{pmatrix} 10268.3 \\ 10188.7 \\ 10131.5 \end{pmatrix}$	$\begin{pmatrix} 10204.1 \\ 10124.5 \\ 10067.3 \end{pmatrix}$	10228.8	
$cccs\bar{c}$				$cccs\bar{b}$						
J^P	Eigenvalue	$(D_s\Omega_{ccc})$	$(\eta_c\Omega_{cc})$	Mass	J^P	Eigenvalue	$(B_s\Omega_{ccc})$	$(B_c\Omega_{cc})$	Mass	
$\frac{5}{2}^-$	62.1	6896.8	6901.8	6897.7	$\frac{5}{2}^-$	38.7	10201.6	10137.4	10201.0	
	$\begin{pmatrix} 63.1 \\ 41.5 \\ -97.4 \end{pmatrix}$	$\begin{pmatrix} 6897.8 \\ 6876.2 \\ 6737.3 \end{pmatrix}$	$\begin{pmatrix} 6902.8 \\ 6881.2 \\ 6742.3 \end{pmatrix}$	$\begin{pmatrix} 6899.3 \\ 6880.7 \\ 6738.1 \end{pmatrix}$	$\frac{3}{2}^-$	$\begin{pmatrix} 57.4 \\ 36.7 \\ -30.3 \end{pmatrix}$	$\begin{pmatrix} 10220.3 \\ 10199.6 \\ 10132.6 \end{pmatrix}$	$\begin{pmatrix} 10156.1 \\ 10135.4 \\ 10068.4 \end{pmatrix}$	10202.4	
	$\begin{pmatrix} 133.3 \\ 49.2 \\ -40.0 \end{pmatrix}$	$\begin{pmatrix} 6968.0 \\ 6883.9 \\ 6794.7 \end{pmatrix}$	$\begin{pmatrix} 6973.0 \\ 6888.9 \\ 6799.7 \end{pmatrix}$	$\begin{pmatrix} 6971.7 \\ 6888.7 \\ 6800.4 \end{pmatrix}$	$\frac{1}{2}^-$	$\begin{pmatrix} 105.4 \\ 25.8 \\ -31.4 \end{pmatrix}$	$\begin{pmatrix} 10268.3 \\ 10188.7 \\ 10131.5 \end{pmatrix}$	$\begin{pmatrix} 10204.1 \\ 10124.5 \\ 10067.3 \end{pmatrix}$	10228.8	
$ccb\bar{n}\bar{c}$				$ccb\bar{n}\bar{b}$						
J^P	Eigenvalue	$(D\Omega_{ccb})$	$(B_c\Xi_{cc})$	$(\eta_c\Xi_{bc}^*)$	Mass	J^P	Eigenvalue	$(B\Omega_{ccb})$	$(\eta_b\Xi_{cc})$	Mass
$\frac{5}{2}^-$	$\begin{pmatrix} 54.9 \\ 45.7 \end{pmatrix}$	$\begin{pmatrix} 10033.0 \\ 10023.9 \end{pmatrix}$	$\begin{pmatrix} 10037.8 \\ 10028.7 \end{pmatrix}$	$\begin{pmatrix} 10076.9 \\ 10067.8 \end{pmatrix}$	$\begin{pmatrix} 10071.7 \\ 10012.4 \end{pmatrix}$	$\frac{5}{2}^-$	$\begin{pmatrix} 45.7 \\ 29.4 \end{pmatrix}$	$\begin{pmatrix} 13361.6 \\ 13345.3 \end{pmatrix}$	$\begin{pmatrix} 13146.3 \\ 13130.1 \end{pmatrix}$	$\begin{pmatrix} 13327.1 \\ 13310.8 \end{pmatrix}$
	$\begin{pmatrix} 67.5 \\ 52.4 \end{pmatrix}$	$\begin{pmatrix} 10045.6 \\ 10030.6 \end{pmatrix}$	$\begin{pmatrix} 10050.4 \\ 10035.4 \end{pmatrix}$	$\begin{pmatrix} 10089.5 \\ 10074.5 \end{pmatrix}$	$\begin{pmatrix} 10075.7 \\ 10057.6 \end{pmatrix}$		$\begin{pmatrix} 50.0 \\ 38.6 \end{pmatrix}$	$\begin{pmatrix} 13366.0 \\ 13354.5 \end{pmatrix}$	$\begin{pmatrix} 13150.7 \\ 13139.3 \end{pmatrix}$	$\begin{pmatrix} 13331.5 \\ 13320.0 \end{pmatrix}$
	$\begin{pmatrix} 24.4 \\ 24.0 \end{pmatrix}$	$\begin{pmatrix} 10002.5 \\ 10002.2 \end{pmatrix}$	$\begin{pmatrix} 10007.4 \\ 10007.0 \end{pmatrix}$	$\begin{pmatrix} 10046.4 \\ 10046.1 \end{pmatrix}$	$\begin{pmatrix} 10045.0 \\ 10008.1 \end{pmatrix}$		$\begin{pmatrix} 28.1 \\ 2.0 \end{pmatrix}$	$\begin{pmatrix} 13344.1 \\ 13317.9 \end{pmatrix}$	$\begin{pmatrix} 13128.8 \\ 13102.7 \end{pmatrix}$	$\begin{pmatrix} 13309.6 \\ 13328.4 \end{pmatrix}$
	$\begin{pmatrix} -8.2 \\ -42.7 \end{pmatrix}$	$\begin{pmatrix} 9969.9 \\ 9935.4 \end{pmatrix}$	$\begin{pmatrix} 9974.7 \\ 9940.3 \end{pmatrix}$	$\begin{pmatrix} 9913.8 \\ 9979.3 \end{pmatrix}$	$\begin{pmatrix} 9981.0 \\ 9955.03 \end{pmatrix}$		$\begin{pmatrix} -13.8 \\ -24.1 \end{pmatrix}$	$\begin{pmatrix} 13302.1 \\ 13291.9 \end{pmatrix}$	$\begin{pmatrix} 13086.9 \\ 13076.6 \end{pmatrix}$	$\begin{pmatrix} 13267.6 \\ 13257.4 \end{pmatrix}$
	$\begin{pmatrix} -102.5 \\ 107.6 \end{pmatrix}$	$\begin{pmatrix} 9875.7 \\ 10085.7 \end{pmatrix}$	$\begin{pmatrix} 9880.5 \\ 10090.6 \end{pmatrix}$	$\begin{pmatrix} 9919.6 \\ 10129.6 \end{pmatrix}$	$\begin{pmatrix} 9874.0 \\ 10117.7 \end{pmatrix}$		$\begin{pmatrix} -39.8 \\ 82.7 \end{pmatrix}$	$\begin{pmatrix} 13276.1 \\ 13398.7 \end{pmatrix}$	$\begin{pmatrix} 13060.9 \\ 13183.4 \end{pmatrix}$	$\begin{pmatrix} 13241.6 \\ 13364.2 \end{pmatrix}$
	$\begin{pmatrix} 70.5 \\ 44.5 \end{pmatrix}$	$\begin{pmatrix} 10048.6 \\ 10022.7 \end{pmatrix}$	$\begin{pmatrix} 10053.4 \\ 10027.5 \end{pmatrix}$	$\begin{pmatrix} 10092.5 \\ 10066.6 \end{pmatrix}$	$\begin{pmatrix} 10079.7 \\ 10049.8 \end{pmatrix}$		$\begin{pmatrix} 49.2 \\ 22.8 \end{pmatrix}$	$\begin{pmatrix} 13365.1 \\ 13338.7 \end{pmatrix}$	$\begin{pmatrix} 13149.9 \\ 13123.5 \end{pmatrix}$	$\begin{pmatrix} 13330.6 \\ 13304.2 \end{pmatrix}$
	$\begin{pmatrix} 5.0 \\ -21.0 \end{pmatrix}$	$\begin{pmatrix} 9983.1 \\ 9957.1 \end{pmatrix}$	$\begin{pmatrix} 9987.9 \\ 9961.9 \end{pmatrix}$	$\begin{pmatrix} 10027.0 \\ 10001.0 \end{pmatrix}$	$\begin{pmatrix} 9988.2 \\ 9979.2 \end{pmatrix}$		$\begin{pmatrix} 2.2 \\ -15.2 \end{pmatrix}$	$\begin{pmatrix} 13318.1 \\ 13300.8 \end{pmatrix}$	$\begin{pmatrix} 13102.9 \\ 13085.5 \end{pmatrix}$	$\begin{pmatrix} 13283.6 \\ 13266.3 \end{pmatrix}$
	$\begin{pmatrix} -37.1 \\ -88.1 \end{pmatrix}$	$\begin{pmatrix} 9941.0 \\ 9890.0 \end{pmatrix}$	$\begin{pmatrix} 9945.8 \\ 9894.9 \end{pmatrix}$	$\begin{pmatrix} 9984.9 \\ 9933.9 \end{pmatrix}$	$\begin{pmatrix} 9966.3 \\ 9926.3 \end{pmatrix}$		$\begin{pmatrix} -29.6 \\ -57.4 \end{pmatrix}$	$\begin{pmatrix} 13286.3 \\ 13258.6 \end{pmatrix}$	$\begin{pmatrix} 13071.1 \\ 13043.3 \end{pmatrix}$	$\begin{pmatrix} 13251.8 \\ 13224.1 \end{pmatrix}$
	$\begin{pmatrix} -148.9 \\ 9829.2 \end{pmatrix}$	$\begin{pmatrix} 9834.0 \\ 10189.2 \end{pmatrix}$	$\begin{pmatrix} 9873.1 \\ 10209.5 \end{pmatrix}$	$\begin{pmatrix} 9830.7 \\ 10224.3 \end{pmatrix}$	$\begin{pmatrix} 9830.7 \\ 10213.9 \end{pmatrix}$		$\begin{pmatrix} -98.1 \\ 86.1 \end{pmatrix}$	$\begin{pmatrix} 13217.8 \\ 13492.6 \end{pmatrix}$	$\begin{pmatrix} 13002.5 \\ 13302.5 \end{pmatrix}$	$\begin{pmatrix} 13183.3 \\ 13459.0 \end{pmatrix}$
$ccbs\bar{c}$				$ccbs\bar{b}$						
J^P	Eigenvalue	$(D_s\Omega_{ccb})$	$(B_c\Omega_{cc})$	$(\eta_c\Omega_{bc}^*)$	Mass	J^P	Eigenvalue	$(B_s\Omega_{ccb})$	$(\eta_b\Omega_{cc})$	Mass
$\frac{5}{2}^-$	$\begin{pmatrix} 56.0 \\ 47.3 \end{pmatrix}$	$\begin{pmatrix} 10134.3 \\ 10125.6 \end{pmatrix}$	$\begin{pmatrix} 10154.7 \\ 10146.0 \end{pmatrix}$	$\begin{pmatrix} 10169.4 \\ 10160.8 \end{pmatrix}$	$\begin{pmatrix} 10163.7 \\ 10123.7 \end{pmatrix}$	$\frac{5}{2}^-$	$\begin{pmatrix} 48.3 \\ 29.9 \end{pmatrix}$	$\begin{pmatrix} 13454.8 \\ 13436.5 \end{pmatrix}$	$\begin{pmatrix} 13264.7 \\ 13246.3 \end{pmatrix}$	$\begin{pmatrix} 13421.1 \\ 13402.8 \end{pmatrix}$
	$\begin{pmatrix} 70.6 \\ 51.4 \end{pmatrix}$	$\begin{pmatrix} 10149.0 \\ 10129.7 \end{pmatrix}$	$\begin{pmatrix} 10169.3 \\ 10150.1 \end{pmatrix}$	$\begin{pmatrix} 10184.1 \\ 10164.9 \end{pmatrix}$	$\begin{pmatrix} 10173.0 \\ 10155.5 \end{pmatrix}$		$\begin{pmatrix} 53.4 \\ 39.9 \end{pmatrix}$	$\begin{pmatrix} 13459.9 \\ 13446.5 \end{pmatrix}$	$\begin{pmatrix} 13269.8 \\ 13256.3 \end{pmatrix}$	$\begin{pmatrix} 13426.2 \\ 13412.8 \end{pmatrix}$
	$\begin{pmatrix} 26.7 \\ 23.6 \end{pmatrix}$	$\begin{pmatrix} 10105.0 \\ 10101.9 \end{pmatrix}$	$\begin{pmatrix} 10125.4 \\ 10122.3 \end{pmatrix}$	$\begin{pmatrix} 10140.2 \\ 10137.1 \end{pmatrix}$	$\begin{pmatrix} 10137.2 \\ 10108.0 \end{pmatrix}$		$\begin{pmatrix} 28.3 \\ 1.5 \end{pmatrix}$	$\begin{pmatrix} 13434.8 \\ 13408.0 \end{pmatrix}$	$\begin{pmatrix} 13244.7 \\ 13217.9 \end{pmatrix}$	$\begin{pmatrix} 13401.1 \\ 13374.3 \end{pmatrix}$
	$\begin{pmatrix} -12.7 \\ -40.0 \end{pmatrix}$	$\begin{pmatrix} 10065.6 \\ 10038.3 \end{pmatrix}$	$\begin{pmatrix} 10086.0 \\ 10058.7 \end{pmatrix}$	$\begin{pmatrix} 10100.7 \\ 10073.5 \end{pmatrix}$	$\begin{pmatrix} 10083.9 \\ 10059.6 \end{pmatrix}$		$\begin{pmatrix} -15.9 \\ -24.1 \end{pmatrix}$	$\begin{pmatrix} 13390.7 \\ 13382.4 \end{pmatrix}$	$\begin{pmatrix} 13200.5 \\ 13192.3 \end{pmatrix}$	$\begin{pmatrix} 13357.0 \\ 13348.8 \end{pmatrix}$
	$\begin{pmatrix} -105.4 \\ 110.8 \end{pmatrix}$	$\begin{pmatrix} 9973.0 \\ 10189.2 \end{pmatrix}$	$\begin{pmatrix} 9993.3 \\ 10209.5 \end{pmatrix}$	$\begin{pmatrix} 10008.1 \\ 10224.3 \end{pmatrix}$	$\begin{pmatrix} 9975.2 \\ 10213.9 \end{pmatrix}$		$\begin{pmatrix} -43.2 \\ 86.1 \end{pmatrix}$	$\begin{pmatrix} 13363.3 \\ 13492.6 \end{pmatrix}$	$\begin{pmatrix} 13173.2 \\ 13302.5 \end{pmatrix}$	$\begin{pmatrix} 13329.7 \\ 13459.0 \end{pmatrix}$
	$\begin{pmatrix} 74.0 \\ 42.4 \end{pmatrix}$	$\begin{pmatrix} 10152.3 \\ 10120.7 \end{pmatrix}$	$\begin{pmatrix} 10172.7 \\ 10141.1 \end{pmatrix}$	$\begin{pmatrix} 10187.4 \\ 10155.9 \end{pmatrix}$	$\begin{pmatrix} 10181.6 \\ 10143.6 \end{pmatrix}$		$\begin{pmatrix} 53.0 \\ 20.6 \end{pmatrix}$	$\begin{pmatrix} 13459.5 \\ 13427.2 \end{pmatrix}$	$\begin{pmatrix} 13269.4 \\ 13237.0 \end{pmatrix}$	$\begin{pmatrix} 13425.8 \\ 13393.5 \end{pmatrix}$
	$\begin{pmatrix} 1.6 \\ -18.3 \end{pmatrix}$	$\begin{pmatrix} 10080.0 \\ 10060.0 \end{pmatrix}$	$\begin{pmatrix} 10100.3 \\ 10080.4 \end{pmatrix}$	$\begin{pmatrix} 10115.1 \\ 10095.1 \end{pmatrix}$	$\begin{pmatrix} 10090.7 \\ 10080.9 \end{pmatrix}$		$\begin{pmatrix} 4.6 \\ -17.9 \end{pmatrix}$	$\begin{pmatrix} 13411.1 \\ 13388.7 \end{pmatrix}$	$\begin{pmatrix} 13221.0 \\ 13198.5 \end{pmatrix}$	$\begin{pmatrix} 13377.4 \\ 13355.0 \end{pmatrix}$
	$\begin{pmatrix} -40.7 \\ -92.1 \\ -152.1 \end{pmatrix}$	$\begin{pmatrix} 10037.6 \\ 9986.3 \\ 9926.2 \end{pmatrix}$	$\begin{pmatrix} 10058.0 \\ 10006.6 \\ 9946.6 \end{pmatrix}$	$\begin{pmatrix} 10072.8 \\ 10021.1 \\ 9961.4 \end{pmatrix}$	$\begin{pmatrix} 10063.1 \\ 10019.0 \\ 9933.4 \end{pmatrix}$		$\begin{pmatrix} -32.7 \\ -61.0 \\ -103.0 \end{pmatrix}$	$\begin{pmatrix} 13373.8 \\ 13345.5 \\ 13303.6 \end{pmatrix}$	$\begin{pmatrix} 13183.7 \\ 13155.4 \\ 13113.4 \end{pmatrix}$	$\begin{pmatrix} 13340.1 \\ 13311.9 \\ 13269.9 \end{pmatrix}$

- Phys. Rev. D **90**, no. 9, 094007 (2014) [arXiv:1408.5877 [hep-ph]].
- [92] M. Karliner, S. Nussinov and J. L. Rosner, “ $QQ\bar{Q}\bar{Q}$ states: masses, production, and decays,” Phys. Rev. D **95**, no. 3, 034011 (2017) [arXiv:1611.00348 [hep-ph]].
- [93] Y. R. Liu, H. X. Chen, W. Chen, X. Liu and S. L. Zhu, “Pentaquark and Tetraquark states,” Prog. Part. Nucl. Phys. **107**, 237 (2019) [arXiv:1903.11976 [hep-ph]].
- [94] A. De Rujula, H. Georgi and S. L. Glashow, “Hadron Masses in a Gauge Theory,” Phys. Rev. D **12** (1975), 147-162 doi:10.1103/PhysRevD.12.147
- [95] F. Stancu, “Can $Y(4140)$ be a $c\bar{c}ss$ tetraquark?,” J. Phys. G **37**, 075017 (2010) Erratum: [J. Phys. G **46**, no. 1, 019501 (2019)] [arXiv:0906.2485 [hep-ph]].
- [96] W. Park, A. Park, S. Cho and S. H. Lee, “ $P_c(4380)$ in a constituent quark model,” Phys. Rev. D **95**, no. 5, 054027 (2017) [arXiv:1702.00381 [hep-ph]].
- [97] F. Stancu and S. Pepin, “Isoscalar factors of the permutation group,” Few Body Syst. **26**, 113 (1999).
- [98] W. Park, A. Park and S. H. Lee, “Dibaryons in a constituent quark model,” Phys. Rev. D **92**, no. 1, 014037 (2015) [arXiv:1506.01123 [nucl-th]].
- [99] A. Park, W. Park and S. H. Lee, “Dibaryons with two strange quarks and one heavy flavor in a constituent quark model,” Phys. Rev. D **94**, no. 5, 054027 (2016) [arXiv:1606.01006 [hep-ph]].
- [100] W. Park, A. Park and S. H. Lee, “Dibaryons with two strange quarks and total spin zero in a constituent quark model,” Phys. Rev. D **93**, no. 7, 074007 (2016) [arXiv:1602.05017 [hep-ph]].
- [101] M. Tanabashi *et al.* [Particle Data Group], “Review of Particle Physics,” Phys. Rev. D **98**, no. 3, 030001 (2018).
- [102] M. Genovese, J. M. Richard, F. Stancu and S. Pepin, “Heavy flavor pentaquarks in a chiral constituent quark model,” Phys. Lett. B **425**, 171-176 (1998) [arXiv:hep-ph/9712452 [hep-ph]].
- [103] J. M. Richard, A. Valcarce and J. Vijande, “Doubly-heavy baryons, tetraquarks, and related topics,” Bled Workshops Phys. **19**, 24 (2018) [arXiv:1811.02863 [hep-ph]].
- [104] E. M. Aitala *et al.* [E791], “Search for the pentaquark via the $P_0(\bar{c}s)$ decay,” Phys. Rev. Lett. **81**, 44-48 (1998) [arXiv:hep-ex/9709013 [hep-ex]].
- [105] E. M. Aitala *et al.* [E791], “Search for the pentaquark via the $P_0(\bar{c}s) \rightarrow K_0^* K^- p$ decay,” Phys. Lett. B **448**, 303-310 (1999).
- [106] I. W. Stewart, M. E. Wessling and M. B. Wise, “Stable heavy pentaquark states,” Phys. Lett. B **590**, 185-189 (2004) [arXiv:hep-ph/0402076 [hep-ph]].
- [107] R. L. Jaffe and F. Wilczek, “Diquarks and exotic spectroscopy,” Phys. Rev. Lett. **91**, 232003 (2003) [arXiv:hep-ph/0307341 [hep-ph]].
- [108] A. K. Leibovich, Z. Ligeti, I. W. Stewart and M. B. Wise, “Predictions for nonleptonic Lambda(b) and Theta(b) decays,” Phys. Lett. B **586**, 337-344 (2004) [arXiv:hep-ph/0312319 [hep-ph]].
- [109] Y. s. Oh, B. Y. Park and D. P. Min, “Pentaquark exotic baryons in the Skyrme model,” Phys. Lett. B **331**, 362-370 (1994) [arXiv:hep-ph/9405297 [hep-ph]].
- [110] W. Park, S. Cho and S. H. Lee, “Where is the stable pentaquark?,” Phys. Rev. D **99**, no. 9, 094023 (2019) [arXiv:1811.10911 [hep-ph]].
- [111] R. Aaij *et al.* [LHCb], “Search for weakly decaying b -flavored pentaquarks,” Phys. Rev. D **97**, no.3, 032010 (2018) [arXiv:1712.08086 [hep-ex]].
- [112] C. Gignoux, B. Silvestre-Brac and J. M. Richard, “Possibility of Stable Multi - Quark Baryons,” Phys. Lett. B **193**, 323 (1987).
- [113] H. J. Lipkin, “New Possibilities for Exotic Hadrons: Anticharmed Strange Baryons,” Phys. Lett. B **195**, 484-488 (1987) doi:10.1016/0370-2693(87)90055-4
- [114] J. Yamagata-Sekihara and T. Sekihara, “ $\bar{K}\bar{D}N$ molecular state as a “ $uuds\bar{c}$ pentaquark” in a three-body calculation,” Phys. Rev. C **100**, no.1, 015203 (2019) doi:10.1103/PhysRevC.100.015203 [arXiv:1809.08896 [nucl-th]].
- [115] P. Kroll, “Mixing of pseudoscalar mesons and isospin symmetry breaking,” Int. J. Mod. Phys. A **20**, 331 (2005) [hep-ph/0409141].
- [116] J. M. Richard, “About the $J/\psi J/\psi$ peak of LHCb: fully-charmed tetraquark?,” [arXiv:2008.01962 [hep-ph]].
- [117] Q. F. Lü, D. Y. Chen and Y. B. Dong, “Masses of fully heavy tetraquarks $QQ\bar{Q}\bar{Q}$ in an extended relativized quark model,” [arXiv:2006.14445 [hep-ph]].
- [118] G. Yang, J. Ping, L. He and Q. Wang, “A potential model prediction of fully-heavy tetraquarks $QQ\bar{Q}\bar{Q}$ ($Q = c, b$),” [arXiv:2006.13756 [hep-ph]].
- [119] H. X. Chen, W. Chen, X. Liu and S. L. Zhu, “Strong decays of fully-charm tetraquarks into di-charmonia,” [arXiv:2006.16027 [hep-ph]].
- [120] G. Aad *et al.* [ATLAS], “Measurement of the associated production of a Higgs boson decaying into b -quarks with a vector boson at high transverse momentum in pp collisions at $\sqrt{s} = 13$ TeV with the ATLAS detector,” [arXiv:2008.02508 [hep-ex]].
- [121] M. Karliner and J. L. Rosner, “Interpretation of structure in the di- J/ψ spectrum,” [arXiv:2009.04429 [hep-ph]].
- [122] J. F. Giron and R. F. Lebed, “The Simple Spectrum of $c\bar{c}c\bar{c}$ States in the Dynamical Diquark Model,” [arXiv:2008.01631 [hep-ph]].
- [123] R. Maciula, W. Schafer and A. Szczurek, “On the mechanism of $T_{4c}(6900)$ tetraquark production,” [arXiv:2009.02100 [hep-ph]].
- [124] J. Sonnenschein and D. Weissman, “Deciphering the recently discovered tetraquark candidates around 6.9 GeV,” [arXiv:2008.01095 [hep-ph]].

TABLE XXXI. The estimated masses for the $bbbq\bar{Q}$ and $bbcq\bar{Q}$ ($q = n, s; n = u, d; Q = c, b$) subsystems in units of MeV. The values in the second column are eigenvalues obtained with the CMI Hamiltonian in Eq. (2). The masses in the third, fourth, and fifth columns are determined with relevant thresholds in Eq. (3). The masses in the sixth column are determined with the modified CMI model in Eq. (4).

$bbbn\bar{c}$				$bbbn\bar{b}$							
J^P	Eigenvalue	$(D\Omega_{bbb})$	$(B_c\Xi_{bb})$	Mass	J^P	Eigenvalue	$(B\Omega_{bbb})$	$(\eta_c\Xi_{bb})$	Mass		
$\frac{5}{2}^-$	49.6	16320.2	16555.3	16318.2	$\frac{5}{2}^-$	25.6	19634.0	19649.0	19634.3		
$\frac{3}{2}^-$	$\begin{pmatrix} 52.9 \\ 8.1 \\ -95.6 \end{pmatrix}$	$\begin{pmatrix} 16323.5 \\ 16278.7 \\ 16175.0 \end{pmatrix}$	$\begin{pmatrix} 16558.6 \\ 16513.7 \\ 16410.0 \end{pmatrix}$	$\begin{pmatrix} 16538.8 \\ 16317.8 \\ 16175.8 \end{pmatrix}$	$\frac{3}{2}^-$	$\begin{pmatrix} 32.3 \\ 14.4 \\ -29.0 \end{pmatrix}$	$\begin{pmatrix} 19640.7 \\ 19622.8 \\ 19579.4 \end{pmatrix}$	$\begin{pmatrix} 19655.6 \\ 19637.7 \\ 19594.4 \end{pmatrix}$	$\begin{pmatrix} 19648.7 \\ 19628.7 \\ 19582.2 \end{pmatrix}$		
$\frac{1}{2}^-$	$\begin{pmatrix} 74.4 \\ 43.2 \\ -9.8 \end{pmatrix}$	$\begin{pmatrix} 16345.0 \\ 16313.8 \\ 16260.8 \end{pmatrix}$	$\begin{pmatrix} 16580.0 \\ 16548.8 \\ 16495.9 \end{pmatrix}$	$\begin{pmatrix} 16583.0 \\ 16535.5 \\ 16314.8 \end{pmatrix}$	$\frac{1}{2}^-$	$\begin{pmatrix} 57.9 \\ 32.5 \\ -15.4 \end{pmatrix}$	$\begin{pmatrix} 19666.3 \\ 19640.9 \\ 19593.0 \end{pmatrix}$	$\begin{pmatrix} 19681.3 \\ 19655.9 \\ 19608.0 \end{pmatrix}$	$\begin{pmatrix} 19679.0 \\ 19650.4 \\ 19604.5 \end{pmatrix}$		
$bbbs\bar{c}$				$bbbs\bar{s}$							
J^P	Eigenvalue	$(D_s\Omega_{bbb})$	$(B_c\Omega_{bb})$	Mass	J^P	Eigenvalue	$(B_s\Omega_{bbb})$	$(\eta_b\Omega_{bb})$	Mass		
$\frac{5}{2}^-$	50.1	16420.9	16644.8	16421.8	$\frac{5}{2}^-$	26.7	19725.7	19739.1	19725.1		
$\frac{3}{2}^-$	$\begin{pmatrix} 53.7 \\ 7.2 \\ -97.0 \end{pmatrix}$	$\begin{pmatrix} 16424.5 \\ 16378.0 \\ 16273.8 \end{pmatrix}$	$\begin{pmatrix} 16648.4 \\ 16601.9 \\ 16497.7 \end{pmatrix}$	$\begin{pmatrix} 16616.7 \\ 16420.7 \\ 16277.2 \end{pmatrix}$	$\frac{3}{2}^-$	$\begin{pmatrix} 33.1 \\ 13.2 \\ -31.3 \end{pmatrix}$	$\begin{pmatrix} 19732.1 \\ 19712.2 \\ 19667.7 \end{pmatrix}$	$\begin{pmatrix} 19745.5 \\ 19725.6 \\ 19681.1 \end{pmatrix}$	$\begin{pmatrix} 19736.5 \\ 19709.8 \\ 19670.5 \end{pmatrix}$		
$\frac{1}{2}^-$	$\begin{pmatrix} 73.8 \\ 44.0 \\ -8.7 \end{pmatrix}$	$\begin{pmatrix} 16444.6 \\ 16414.8 \\ 16362.1 \end{pmatrix}$	$\begin{pmatrix} 16668.5 \\ 16638.7 \\ 16586.0 \end{pmatrix}$	$\begin{pmatrix} 16660.5 \\ 16622.3 \\ 16418.9 \end{pmatrix}$	$\frac{1}{2}^-$	$\begin{pmatrix} 57.5 \\ 33.7 \\ -14.1 \end{pmatrix}$	$\begin{pmatrix} 19756.5 \\ 19732.7 \\ 19684.9 \end{pmatrix}$	$\begin{pmatrix} 19769.9 \\ 19746.1 \\ 19698.3 \end{pmatrix}$	$\begin{pmatrix} 19756.5 \\ 19740.9 \\ 19695.4 \end{pmatrix}$		
$bbcn\bar{c}$				$bbcn\bar{b}$							
J^P	Eigenvalue	$(D\Omega_{bbc})$	$(\eta_c\Xi_{bb})$	$(B_c\Xi_{bc}^*)$	Mass	J^P	Eigenvalue	$(B\Omega_{bbc})$	$(B_b\Xi_{bb})$	$(\eta_b\Xi_{bc}^*)$	Mass
$\frac{5}{2}^-$	$\begin{pmatrix} 50.8 \\ 39.4 \end{pmatrix}$	$\begin{pmatrix} 13207.7 \\ 13196.3 \end{pmatrix}$	$\begin{pmatrix} 13297.5 \\ 13286.1 \end{pmatrix}$	$\begin{pmatrix} 13332.3 \\ 13320.9 \end{pmatrix}$	$\begin{pmatrix} 13285.7 \\ 13195.8 \end{pmatrix}$	$\frac{5}{2}^-$	$\begin{pmatrix} 35.0 \\ 24.4 \end{pmatrix}$	$\begin{pmatrix} 16529.6 \\ 16519.0 \end{pmatrix}$	$\begin{pmatrix} 16540.7 \\ 16530.1 \end{pmatrix}$	$\begin{pmatrix} 16434.1 \\ 16423.5 \end{pmatrix}$	$\begin{pmatrix} 16572.3 \\ 16427.3 \end{pmatrix}$
$\frac{3}{2}^-$	$\begin{pmatrix} 60.6 \\ 44.4 \\ 27.0 \\ 14.2 \\ 3.9 \\ -66.7 \\ -105.6 \\ 89.6 \\ 53.2 \\ 37.4 \\ 6.9 \\ -12.9 \\ -34.9 \\ -70.0 \\ -151.8 \end{pmatrix}$	$\begin{pmatrix} 13217.4 \\ 13201.2 \\ 13183.8 \\ 13171.1 \\ 13160.8 \\ 13090.1 \\ 13051.3 \\ 13246.4 \\ 13210.0 \\ 13194.2 \\ 13163.7 \\ 13144.0 \\ 13121.9 \\ 13086.9 \\ 13005.0 \end{pmatrix}$	$\begin{pmatrix} 13307.3 \\ 13291.1 \\ 13273.7 \\ 13260.9 \\ 13250.6 \\ 13180.0 \\ 13141.1 \\ 13336.2 \\ 13299.9 \\ 13284.1 \\ 13253.3 \\ 13233.8 \\ 13211.8 \\ 13176.7 \\ 13094.9 \end{pmatrix}$	$\begin{pmatrix} 13342.0 \\ 13325.8 \\ 13308.4 \\ 13295.7 \\ 13285.4 \\ 13214.7 \\ 13175.9 \\ 13371.0 \\ 13334.6 \\ 13318.8 \\ 13288.3 \\ 13268.6 \\ 13246.5 \\ 13211.5 \\ 13129.6 \end{pmatrix}$	$\begin{pmatrix} 13337.5 \\ 13287.3 \\ 13272.2 \\ 13198.0 \\ 13165.4 \\ 13161.4 \\ 13054.9 \\ 13369.3 \\ 13309.5 \\ 13291.8 \\ 13262.3 \\ 13186.2 \\ 13157.2 \\ 13148.5 \\ 13018.0 \end{pmatrix}$	$\frac{3}{2}^-$	$\begin{pmatrix} 21.7 \\ 16.8 \\ -14.0 \\ -28.5 \\ -51.1 \\ 68.6 \\ 38.4 \\ 17.8 \\ -8.2 \\ -11.5 \\ -29.1 \\ -40.4 \\ -94.9 \end{pmatrix}$	$\begin{pmatrix} 16516.4 \\ 16511.4 \\ 16480.6 \\ 16466.1 \\ 16443.5 \\ 16563.2 \\ 16533.0 \\ 16512.4 \\ 16486.5 \\ 16483.2 \\ 16465.5 \\ 16454.3 \\ 16399.8 \end{pmatrix}$	$\begin{pmatrix} 16527.4 \\ 16522.4 \\ 16491.7 \\ 16477.1 \\ 16454.6 \\ 16574.3 \\ 16544.0 \\ 16523.4 \\ 16497.5 \\ 16494.2 \\ 16476.5 \\ 16453.0 \\ 16410.8 \end{pmatrix}$	$\begin{pmatrix} 16420.9 \\ 16415.9 \\ 16385.1 \\ 16370.6 \\ 16348.0 \\ 16584.9 \\ 16557.1 \\ 16503.9 \\ 16391.0 \\ 16387.7 \\ 16370.0 \\ 16358.8 \\ 16304.3 \end{math>$	$\begin{pmatrix} 16519.5 \\ 16432.5 \\ 16411.3 \\ 16374.5 \\ 16369.2 \\ 16584.9 \\ 16557.1 \\ 16503.9 \\ 16449.7 \\ 16397.0 \\ 16370.0 \\ 16363.3 \\ 16326.9 \end{pmatrix}$
$bbcs\bar{c}$				$bbcs\bar{b}$							
J^P	Eigenvalue	$(D_s\Omega_{bbc})$	$(\eta_c\Omega_{bb})$	$(B_c\Omega_{bc}^*)$	Mass	J^P	Eigenvalue	$(B_s\Omega_{bbc})$	$(B_c\Omega_{bb})$	$(\eta_b\Omega_{bc}^*)$	Mass
$\frac{5}{2}^-$	$\begin{pmatrix} 51.7 \\ 39.2 \end{pmatrix}$	$\begin{pmatrix} 13308.7 \\ 13296.3 \end{pmatrix}$	$\begin{pmatrix} 13387.4 \\ 13374.9 \end{pmatrix}$	$\begin{pmatrix} 13424.6 \\ 13412.1 \end{pmatrix}$	$\begin{pmatrix} 13364.5 \\ 13303.1 \end{pmatrix}$	$\frac{5}{2}^-$	$\begin{pmatrix} 36.3 \\ 24.2 \end{pmatrix}$	$\begin{pmatrix} 16621.5 \\ 16609.5 \end{pmatrix}$	$\begin{pmatrix} 16631.0 \\ 16618.9 \end{pmatrix}$	$\begin{pmatrix} 16526.9 \\ 16514.8 \end{pmatrix}$	$\begin{pmatrix} 16651.6 \\ 16523.0 \end{pmatrix}$
$\frac{3}{2}^-$	$\begin{pmatrix} 62.7 \\ 43.5 \\ 28.8 \\ 15.1 \\ 2.1 \\ -65.8 \\ -108.4 \\ 91.0 \\ 55.1 \\ 36.2 \\ 5.0 \\ -11.2 \\ -38.1 \\ -68.6 \\ -154.2 \end{pmatrix}$	$\begin{pmatrix} 13319.8 \\ 13300.5 \\ 13285.9 \\ 13272.1 \\ 13259.2 \\ 13191.3 \\ 13148.6 \\ 13348.0 \\ 13312.1 \\ 13293.3 \\ 13262.0 \\ 13245.9 \\ 13218.9 \\ 13188.4 \\ 13102.8 \end{pmatrix}$	$\begin{pmatrix} 13398.4 \\ 13379.2 \\ 13364.5 \\ 13350.8 \\ 13337.8 \\ 13269.9 \\ 13227.3 \\ 13426.7 \\ 13390.8 \\ 13371.9 \\ 13340.7 \\ 13324.5 \\ 13297.6 \\ 13267.1 \\ 13181.5 \end{pmatrix}$	$\begin{pmatrix} 13435.6 \\ 13416.3 \\ 13401.7 \\ 13387.9 \\ 13375.0 \\ 13307.1 \\ 13264.4 \\ 13463.8 \\ 13427.9 \\ 13409.1 \\ 13377.9 \\ 13361.7 \\ 13348.8 \\ 13304.3 \\ 13218.7 \end{pmatrix}$	$\begin{pmatrix} 13429.7 \\ 13369.4 \\ 13361.3 \\ 13296.9 \\ 13268.9 \\ 13250.1 \\ 13156.1 \\ 13460.0 \\ 13394.7 \\ 13380.2 \\ 13350.4 \\ 13285.4 \\ 13260.6 \\ 13245.0 \\ 13119.2 \end{pmatrix}$	$\frac{3}{2}^-$	$\begin{pmatrix} 41.5 \\ 27.5 \\ 22.7 \\ 18.3 \\ -15.0 \\ -29.6 \\ -53.4 \\ 70.0 \\ 40.6 \\ 16.4 \\ -7.9 \\ -11.7 \\ -32.1 \\ -39.2 \\ -98.0 \end{pmatrix}$	$\begin{pmatrix} 16626.8 \\ 16612.8 \\ 16607.9 \\ 16603.5 \\ 16570.3 \\ 16555.6 \\ 16531.9 \\ 16655.3 \\ 16625.8 \\ 16601.6 \\ 16577.4 \\ 16573.6 \\ 16553.1 \\ 16546.1 \\ 16487.2 \end{pmatrix}$	$\begin{pmatrix} 16636.2 \\ 16622.2 \\ 16617.4 \\ 16613.0 \\ 16579.7 \\ 16565.1 \\ 16541.3 \\ 16664.7 \\ 16635.3 \\ 16611.1 \\ 16586.8 \\ 16583.0 \\ 16562.6 \\ 16555.5 \\ 16496.7 \end{pmatrix}$	$\begin{pmatrix} 16656.2 \\ 16645.9 \\ 16600.6 \\ 16526.0 \\ 16509.2 \\ 16469.3 \\ 16437.2 \\ 16668.6 \\ 16641.4 \\ 16587.7 \\ 16543.0 \\ 16495.2 \\ 16480.9 \\ 16462.5 \\ 16417.7 \end{pmatrix}$	

TABLE XXXII. The relative partial decay widths for the $cccn\bar{c}$, $cccn\bar{b}$, $cccs\bar{c}$, $cccs\bar{b}$, $bbbn\bar{c}$, $bbbn\bar{b}$, $bbbs\bar{c}$, and $bbbs\bar{b}$ pentaquark states. For each pentaquark state, we choose one channel as a reference channel, and the relative partial decay widths for the other channels are obtained in units of the reference channel. The masses are all in units of MeV. The scattering states in the modified CMI model are marked with “*”, respectively.

J^P		$ccc \otimes n\bar{c}$						$ccn \otimes c\bar{c}$						$ccc \otimes n\bar{b}$						$ccn \otimes c\bar{b}$													
Mass		$\Omega_{ccc}D^*$	$\Omega_{ccc}D$	Ξ_{cc}^*J/ψ	$\Xi_{cc}^*\eta_c$	$\Xi_{cc}J/\psi$	$\Xi_{cc}\eta_c$	Mass		$\Omega_{ccc}B^*$	$\Omega_{ccc}B$	$\Xi_{cc}^*B_c^*$	$\Xi_{cc}^*B_c$	$\Xi_{cc}B_c^*$	$\Xi_{cc}B_c$	Mass		$\Omega_{ccc}B_s^*$	$\Omega_{ccc}B_s$	$\Omega_{cc}^*B_c^*$	$\Omega_{cc}^*B_c$	$\Omega_{cc}B_c^*$	$\Omega_{cc}B_c$										
$\frac{5}{2}^-$	6794.2*	x				1										10110.3*	x				1												
$\frac{3}{2}^-$	6797.2*	8.6	1	1	0.75	6.3										10110.7*	33.6	1	x	0.9	1												
	6773.0	x	1	x	66	1										10080.3	x	1	33	0.002	1												
	6638.0*	x	x	x	x	x										9999.3	x	x	x	1.6	1												
$\frac{1}{2}^-$	6863.3	1		2294		1	x									10131.3*	263.5		4.6	0.8	1												
	6788.6	x		x		27	1									10035.8	x		1.0	3.3	1												
	6700.8	x		x	x	1										9965.7	x		x	0.4	1												
J^P		$ccc \otimes s\bar{c}$						$ccs \otimes c\bar{c}$						$ccc \otimes s\bar{b}$						$ccs \otimes c\bar{b}$													
Mass		$\Omega_{ccc}D_s^*$	$\Omega_{ccc}D_s$	Ω_{cc}^*J/ψ	$\Omega_{cc}^*\eta_c$	$\Omega_{cc}J/\psi$	$\Omega_{cc}\eta_c$	Mass		$\Omega_{ccc}B_s^*$	$\Omega_{ccc}B_s$	$\Omega_{cc}^*B_c^*$	$\Omega_{cc}^*B_c$	$\Omega_{cc}B_c^*$	$\Omega_{cc}B_c$	Mass		$\Omega_{ccc}B_s^*$	$\Omega_{ccc}B_s$	$\Omega_{cc}^*B_c^*$	$\Omega_{cc}^*B_c$	$\Omega_{cc}B_c^*$	$\Omega_{cc}B_c$										
$\frac{5}{2}^-$	6897.7*	x		x												10201.0*	1				1												
$\frac{3}{2}^-$	6899.3*	13	1	x	0.2	1										10202.4*	15.2	1	0.02	1	0.9												
	6880.7	x	1	x	38	1										10173.7	x	1	200	1	0.03												
	6738.1*	x	x	x	x	x										10099.4	x	x	x	1.4	1												
$\frac{1}{2}^-$	6971.7	1		2048		1	x									10228.8	1		8.3	0.8	1												
	6888.7	x		x		23	1									10136.6	x		x	3.0	1												
	6800.4	x		x	x	1										10066.0	x		x	0.4	1												
J^P		$bbb \otimes n\bar{c}$						$bbn \otimes b\bar{c}$						$bbb \otimes n\bar{b}$						$bbn \otimes b\bar{b}$													
Mass		$\Omega_{bbb}D^*$	$\Omega_{bbb}D$	$\Xi_{bb}^*B_c^*$	$\Xi_{bb}^*B_c$	$\Xi_{bb}B_c^*$	$\Xi_{bb}B_c$	Mass		$\Omega_{bbb}B^*$	$\Omega_{bbb}B$	$\Xi_{bb}^*\Upsilon$	$\Xi_{bb}^*\eta_b$	$\Xi_{bb}\Upsilon$	$\Xi_{bb}\eta_b$	Mass		$\Omega_{bbb}B_s^*$	$\Omega_{bbb}B_s$	$\Omega_{bb}^*\Upsilon$	$\Omega_{bb}^*\eta_b$	$\Omega_{bb}\Upsilon$	$\Omega_{bb}\eta_b$										
$\frac{5}{2}^-$	16318.2*	x		x												19634.3*	x		x														
$\frac{3}{2}^-$	16538.8	0.6	1	3.2	4.1	1										19648.7	2.2	1	x	0.6	1												
	16317.8*	x	1	x	x	x										19628.7	0	1	x	1	x												
	16175.8*	x	x	x	x	x										19582.2*	x	x	x	x	x												
$\frac{1}{2}^-$	16583.0	1		18.4		2.1	1									19679.0	1		160	7.7	1												
	16535.5	1		0.03		1.6	1									19650.4	1		0.07	123	1												
	16314.8*	x		x	x	x										19604.5	x		x	x	x												
J^P		$bbb \otimes s\bar{c}$						$bbs \otimes b\bar{c}$						$bbb \otimes s\bar{b}$						$bbs \otimes b\bar{b}$													
Mass		$\Omega_{bbb}D_s^*$	$\Omega_{bbb}D_s$	$\Omega_{bb}^*B_c^*$	$\Omega_{bb}^*B_c$	$\Omega_{bb}B_c^*$	$\Omega_{bb}B_c$	Mass		$\Omega_{bbb}B_s^*$	$\Omega_{bbb}B_s$	$\Omega_{bb}^*\Upsilon$	$\Omega_{bb}^*\eta_b$	$\Omega_{bb}\Upsilon$	$\Omega_{bb}\eta_b$	Mass		$\Omega_{bbb}B_s^*$	$\Omega_{bbb}B_s$	$\Omega_{bb}^*\Upsilon$	$\Omega_{bb}^*\eta_b$	$\Omega_{bb}\Upsilon$	$\Omega_{bb}\eta_b$										
$\frac{5}{2}^-$	16421.8*	x		x												19725.1*	x		x														
$\frac{3}{2}^-$	16616.7	1.9	1	3.7	4.7	1										19736.5	9.5	1	1.2	0.05	1												
	16420.7*	x	1	x	x	x										19709.8	x	1	x	1	x												
	16277.2*	x	x	x	x	x										19670.5*	x	x	x	x	x												
$\frac{1}{2}^-$	16660.5	1		23		3.2	1									19756.5	1		255	19	1												
	16622.3	1		0.08		1.5	1									19740.9	1		0.05	635	1												
	16418.9*	x		x	x	x										19695.4	x		x	x	x												

IX. APPENDIX

A. Appendix A: Color wave functions

Three color singlets for the studied pentaquark systems are

$$\begin{aligned}
 |C_1\rangle &= \begin{array}{|c|c|} \hline 1 & 2 \\ \hline 3 & 4 \\ \hline 3 & 4 \\ \hline 3 & 4 \\ \hline \end{array} \otimes (5)_3 \\
 &= \frac{1}{4\sqrt{3}} \left[(2bbgr - 2bbrg + gbrb - gbbr + bgrb - bgbr) \bar{b} + (2rrbg - 2rrgb + rgbr - rgbr + grbr + rbgr - rbrg) \bar{r} + (2ggbr - 2ggbg + rgbg - rgbg + grgb - grbg) \bar{g} \right], \quad (114)
 \end{aligned}$$

$$\begin{aligned}
 |C_2\rangle &= \begin{array}{|c|c|} \hline 1 & 3 \\ \hline 2 & 4 \\ \hline 4 & 3 \\ \hline \end{array} \otimes (5)_3 \\
 &= \frac{1}{12} \left[(3bgbr - 3gbbr - 3brbg + 3rbbg - rbgb - 2rgbb + 2grbb + brgb + gbrb - bgrb) \bar{b} + (3grrb - 3rgrb - 3brrg + 3rbrg - rbgr - 2gbrr + 2bgrr - grbr + rgbr + brgr) \bar{r} + (3grgb - 3rggb + 3bggr - 3gbgr - grbg + rgbg + 2rbgg - 2brgg + gbrg - bgrg) \bar{g} \right], \quad (115)
 \end{aligned}$$

TABLE XXXIII. The relative partial decay widths for the $b\bar{b}c s\bar{c}$ and $b\bar{b}c s\bar{b}$ pentaquark states. For each pentaquark state, we choose one channel as a reference channel, and the relative partial decay widths for the other channels are obtained in units of the reference channel. The masses are all in units of MeV. The scattering states and stable states in the modified CMI model are marked with “*” and “†”, respectively.

J^P	Mass	$b\bar{b}c \otimes s\bar{c}$				$b\bar{b}s \otimes c\bar{c}$				$c\bar{b}s \otimes b\bar{c}$					
		$\Omega_{bbc}^* D_s^*$	$\Omega_{bbc}^* D_s$	$\Omega_{bbc}^* D_s^*$	$\Omega_{bbc}^* D_s$	$\Omega_{bb}^* J/\psi$	$\Omega_{bb}^* \eta_c$	$\Omega_{bb}^* J/\psi$	$\Omega_{bb}^* \eta_c$	$\Omega_{cb}^* B_c^*$	$\Omega_{cb}^* B_c$	$\Omega_{cb}^* B_c^*$	$\Omega_{cb}^* B_c$		
$\frac{5}{2}^-$	13364.5*	1				1				x					
	13303.1*	x				x				x					
$\frac{3}{2}^-$	13429.7	9.5	1	3.9		1.3	1.6	1		0.2	1	2.4	1.2		
	13369.4	19	1	2.2		0.08	0.0	1		x	1	x	1.3		
	13361.3	0.2	1	39		x	0.0	1		x	1	x	5.6		
	13296.9	x	0.0	1		x	1	x		x	x	x	x		
	13268.9	x	1	x		x	1	x		x	x	x	x		
	13250.1	x	1	x		x	x	x		x	x	x	x		
	13156.1*	x	x	x		x	x	x		x	x	x	x		
$\frac{1}{2}^-$	13460.0	0.0		1	30	0.2		1	135	5.3	0.7	0.5	1	2.7	
	13394.7	0.007		1	9.0	2.1		1	176	x	2.2	1.0	19	1	
	13380.2	1		55	0.05	0.0		1.5	1	x	x	1.2	0.4	1	
	13350.4	1		5.7	1.1	x		x	1	x	x	1.3	0.003	1	
	13285.4	x		7.2	1	x		x	1	x	x	x	x	1	
	13260.6	x		x	1	x		x	1	x	x	x	x	x	
	13245.0	x		x	1	x		x	1	x	x	x	x	x	
	13119.2*	x		x	x	x		x	x	x	x	x	x	x	
J^P	Mass	$b\bar{b}c \otimes s\bar{b}$				$b\bar{b}s \otimes c\bar{b}$				$c\bar{b}s \otimes b\bar{b}$					
		$\Omega_{bbc}^* B_s^*$	$\Omega_{bbc}^* B_s$	$\Omega_{bbc}^* B_s^*$	$\Omega_{bbc}^* B_s$	$\Omega_{bb}^* B_c^*$	$\Omega_{bb}^* B_c$	$\Omega_{bb}^* B_c^*$	$\Omega_{bb}^* B_c$	$\Omega_{cb}^* \Upsilon$	$\Omega_{cb}^* \eta_b$	$\Omega_{cb}^* \Upsilon$	$\Omega_{cb}^* \eta_b$	$\Omega_{cb}^* \Upsilon$	$\Omega_{cb}^* \eta_b$
$\frac{5}{2}^-$	16651.6	1				1				1					
	16523.0†	x				x				x					
$\frac{3}{2}^-$	16656.2	1	1.2	9.5		3.9	4.1	1		40	1	0.9		5.1	
	16645.9	1	1.9	0.8		1	0.7	1775		208	1	0.02		98	
	16600.6	x	7.2	1		x	324	1		40	1	0.2		7.3	
	16526.0	x	x	x		x	x	x		0.1	1	19		25	
	16509.2	x	x	x		x	x	x		x	1	0.6		1.0	
	16469.3	x	x	x		x	x	x		x	1	x		x	
	16459.1†	x	x	x		x	x	x		x	x	x	x	x	
$\frac{1}{2}^-$	16668.6	16.9	41	1	33		65	1	1.6	12	1	0.005	0.01		
	16641.4	21	40	1	0.9		1.0	4.2	2.6		1	6.3	0.0	0.005	
	16587.7	x	66	1	x		x	1	11		10	4.3	9.4	1	
	16543.0	x	x	1	x		x	1	14		1.2	25	0.1	1	
	16495.2	x	x	x	x		x	x	x		x	0.3	0.7	1	
	16480.9	x	x	x	x		x	x	x		x	1.4	0.03	1	
	16462.5	x	x	x	x		x	x	x		x	0.1	x	1	
	16417.2	x	x	x	x		x	x	x		x	x	x	x	1

and

B. Appendix B

$$\begin{aligned}
 |C_3\rangle &= \begin{array}{|c|c|}\hline 1 & 4 \\ \hline 2 & \\ \hline 3 & 3 \\ \hline \end{array} \otimes (5)_{\bar{3}} \\
 &= \frac{1}{3\sqrt{2}} \left[(grbb - rgbb + rbgb - brgb + bgrb - gbrb)\bar{b} \right. \\
 &\quad \left. + (grbr - rgbr + rbgr - brgr + bgrr - gbrr)\bar{r} \right. \\
 &\quad \left. + (grbg - rgbg + rbgg - brgg + bgrg - gbrg)\bar{g} \right]. \tag{116}
 \end{aligned}$$

In this appendix, we present all the possible Young-Yamanouchi color \otimes spin bases in Eq. (117), which are obtained from the Young tableaus in Eqs. (13-17).

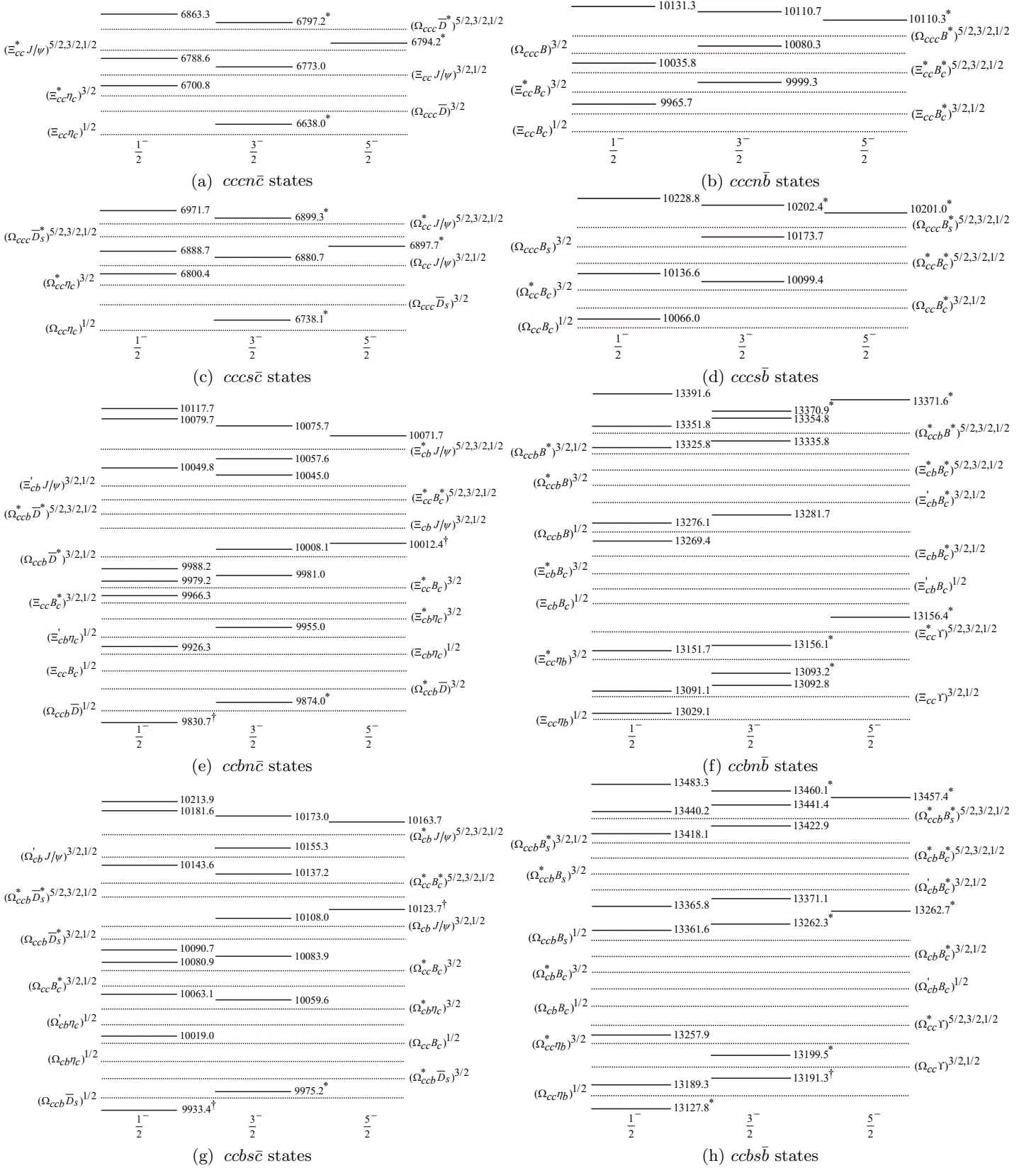


FIG. 7. Relative positions (units: MeV) for the $cccn\bar{c}$, $cccn\bar{b}$, $cccs\bar{c}$, $cccs\bar{b}$, $ccbn\bar{c}$, $ccbn\bar{b}$, $ccbs\bar{c}$, and $ccbs\bar{b}$ pentaquark states labeled with solid lines. The dotted lines denote various baryon-meson thresholds. When the spin of an initial pentaquark state is equal to a number in the superscript of a baryon-meson state, its decay into that baryon-meson channel through S -wave is allowed by the angular momentum conservation. The scattering states and stable states in the modified CMI model are marked with “*” and “†”, respectively.

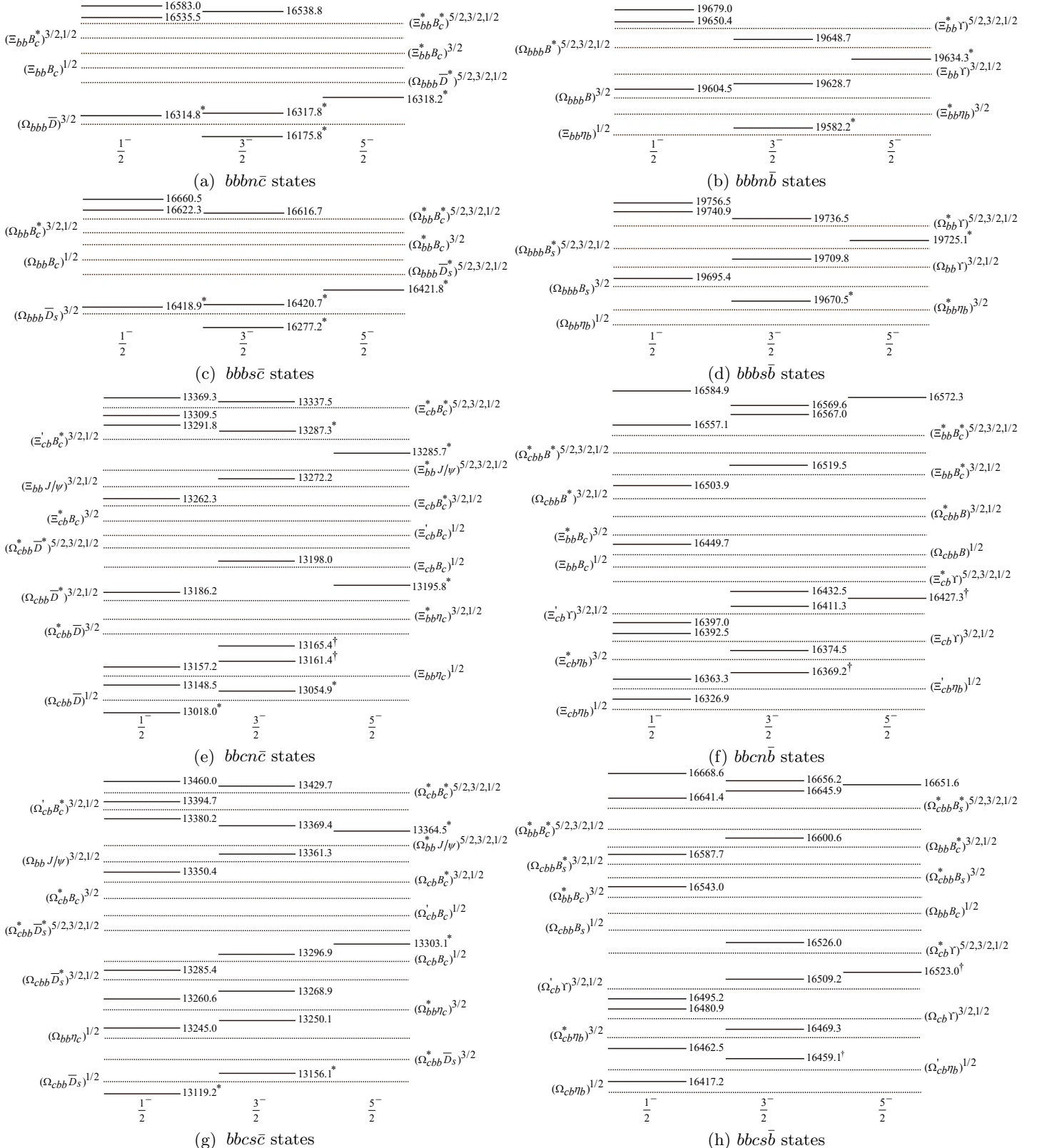


FIG. 8. Relative positions (units: MeV) for the $bbbn\bar{c}$, $bbbn\bar{b}$, $bbbs\bar{c}$, $bbbs\bar{b}$, $bbcn\bar{c}$, $bbcn\bar{b}$, $bbcs\bar{c}$, and $bbcs\bar{b}$ pentaquark states labeled with solid lines. The dotted lines denote various baryon-meson thresholds. When the spin of an initial pentaquark state is equal to a number in the superscript of a baryon-meson state, its decay into that baryon-meson channel through S -wave is allowed by the angular momentum conservation. The scattering states and stable states are marked with “*” and “†”, respectively.

TABLE XXXIV. The relative partial decay widths for the $ccbn\bar{c}$, $ccbn\bar{b}$, and $ccbs\bar{c}$ pentaquark states. For each pentaquark state, we choose one channel as a reference channel, and the relative partial decay widths for the other channels are obtained in units of the reference channel. The masses are all in units of MeV. The scattering states and stable states in the modified CMI model are marked with “*” and “†”, respectively.

J^P	Mass	$ccb \otimes n\bar{c}$				$ccn \otimes b\bar{c}$				$cbn \otimes c\bar{c}$			
		$\Omega_{ccb}^* D^*$	$\Omega_{ccb}^* D$	$\Omega_{ccb}^* D^*$	$\Omega_{ccb} D$	$\Xi_{cc}^* B_c^*$	$\Xi_{cc}^* B_c$	$\Xi_{cc}^* B_c^*$	$\Xi_{cc} B_c$	$\Xi_{cb}^* J/\psi$	$\Xi_{cb}^* \eta_c$	$\Xi_{cb}^* J/\psi$	$\Xi_{cb}^* \eta_c$
$\frac{5}{2}^-$	10071.7	1				1				1			
	10012.4 [†]	×				×				×			
$\frac{3}{2}^-$	10075.7	6.7	1	0.002		0.5	1	3.8		1.6	1	256	351
	10057.6	11	1	116		6.0	1	5.9		0	1	1.7	0.001
	10045.0	1.0	1	8.2		0.09	1	0.8		0	1	0.03	0.7
	10008.1	×	1	7.9		×	1	510		×	1	×	×
	9981.0	×	1	×		×	1	6.4		×	1	×	×
	9955.0	×	1	×		×	×	×		×	×	×	×
	9874.0*	×	×	×		×	×	×		×	×	×	×
$\frac{1}{2}^-$	10117.7	0.005		0.2	1	0.03		1	2.3	4.0	4.1	1	0.003
	10079.7	0.05		2.7	1	0.06		1	58	2.7	1.4	1	0.02
	10049.8	0.1		6.9	1	0.02		1	0.4	0	0.2	1	0.006
	9988.2	×		×	1	×		1	3	×	1	×	14.4
	9979.2	×		×	1	×		1	14	×	1	×	0.7
	9966.3	×		×	1	×		1	5.4	×	1	×	0.13
	9926.3	×		×	×	×		1	1	1	1	1	1
	9830.7 [†]	×		×	1	1		1	1	1	1	1	1
J^P	Mass	$ccb \otimes nb$				$ccn \otimes bb$				$cbn \otimes cb$			
		$\Omega_{ccb}^* B^*$	$\Omega_{ccb}^* B$	$\Omega_{ccb}^* B^*$	$\Omega_{ccb} B$	$\Xi_{cc}^* \Upsilon$	$\Xi_{cc}^* \eta_b$	$\Xi_{cc}^* \Upsilon$	$\Xi_{cc} \eta_b$	$\Xi_{cb}^* B_c^*$	$\Xi_{cb}^* B_c$	$\Xi_{cb}^* B_c^*$	$\Xi_{cb}^* B_c$
$\frac{5}{2}^-$	13371.6*	1				1				1			
	13156.4*	×				×				×			
$\frac{3}{2}^-$	13370.9*	0.004	0.02	1		191	1	0.4		12.8	6.1	0.002	1
	13354.8	2.7	34	1		192	1	0.001		1.2	0.08	9.3	1
	13335.8	×	4.4	1		88	1	6.7		2.3	0.3	0.7	1
	13281.7	×	×	×		13.5	1	0.2		1	7.0	1	1
	13156.1*	×	×	×		1	0.0	1		1	1	1	1
	13093.2*	×	×	×		1	1	1		1	1	1	1
	13092.8	×	×	1		1	1	1		1	1	1	1
$\frac{1}{2}^-$	13391.6	0.9		1	20	0.0003		5.0	1	0.7	11.8	1.4	1
	13351.8	1		1	4.3	0.004		40	1	2.3	0.004	35	1
	13325.8	×		4.2	1	0.2		1	67	6.8	12.5	21.9	1
	13276.1	×		1		0.002		1	4.6	1	3.6	1	7.0
	13269.4	×		1		1.1		1	19	1	0.14	1	0.6
	13151.7	×		1		1		1	5.2	1	1	1	1
	13091.1	×		1		1		1	5.4	1	1	1	1
	13029.1*	×		1		1		1	1	1	1	1	1
J^P	Mass	$ccb \otimes sc$				$ccs \otimes bc$				$cbs \otimes cc$			
		$\Omega_{ccb}^* D_s^*$	$\Omega_{ccb}^* D_s$	$\Omega_{ccb}^* D_s^*$	$\Omega_{ccb} D_s$	$\Omega_{cc}^* B_c^*$	$\Omega_{cc}^* B_c$	$\Omega_{cc}^* B_c^*$	$\Omega_{cc} B_c$	$\Omega_{cb}^* J/\psi$	$\Omega_{cb}^* \eta_c$	$\Omega_{cb}^* J/\psi$	$\Omega_{cb}^* \eta_c$
$\frac{5}{2}^-$	10163.7	1				1				1			
	10123.7 [†]	×				1				1			
$\frac{3}{2}^-$	10173.0	13	1	2.0		0.014	1	8.7		7.6	1	242	512
	10155.5	0.003	1	20		3.2	1	1.2		1	1	208	91
	10137.2	0.2	1	12		1	1	1.2		1	1	1	0.7
	10108.0	×	1	1.9		1	1	50.6		1	1	1	0.008
	10083.9	×	1	1		1	1	4.0		1	1	1	1
	10059.6	×	1	1		1	1	1		1	1	1	1
	9975.2*	×	1	1		1	1	1		1	1	1	1
$\frac{1}{2}^-$	10213.9	0.02		1	6.2	0.02		1	1.9	453	564	98	0.2
	10181.6	0.03		2.2	1	0.07		1	85.9	136	43	54	0.6
	10143.6	0.007		2.0	1	0.005		1	0.5	1	1	105.1	1
	10090.7	×		1		1		1	2.9	1	1	1	6.9
	10080.9	×		1		1		1	0.0	1	1	2.9	1
	10063.1	×		1		1		1	1	1	1	1.4	1
	10019.0	×		1		1		1	1	1	1	1	1
	9933.4 [†]	×		1		1		1	1	1	1	1	1

TABLE XXXV. The relative partial decay widths for the $ccbs\bar{b}$, $bbcn\bar{c}$, and $bbcn\bar{b}$ pentaquark states. For each pentaquark state, we choose one channel as a reference channel, and the relative partial decay widths for the other channels are obtained in units of the reference channel. The masses are all in units of MeV. The scattering states and stable states in the modified CMI model are marked with “*” and “†”, respectively.

J^P	Mass	$ccb \otimes sb$				$ccs \otimes bb$				$cbs \otimes cb$			
		$\Omega_{ccb}^* B_s^*$	$\Omega_{ccb}^* B_s$	$\Omega_{ccb}^* B_s$	$\Omega_{ccb}^* B_s$	$\Omega_{cc}^* \Upsilon$	$\Omega_{cc}^* \eta_b$	$\Omega_{cc}^* \Upsilon$	$\Omega_{cc}^* \eta_b$	$\Omega_{cb}^* B_c^*$	$\Omega_{cb}^* B_c$	$\Omega_{cb}^* B_c^*$	$\Omega_{cb}^* B_c$
$\frac{5}{2}^-$	13457.4*	1				1				1			
	13262.7*	×				1				×			
$\frac{3}{2}^-$	13460.1*	0.008	0.04	1		115	1	0.8		25	14	0.4	1
	13441.4	0.9	16	1		240	1	0.002		1.1	0.1	7.6	1
	13422.9	×	15.5	1		18	0.03	1		1.4	0.3	0.6	1
	13371.1	×	×	×		84	6.6	1		×	6.9	×	1
	13262.3*	×	×	×		×	0.0	1		×	×	×	×
	13199.5*	×	×	×		×	×	1		×	×	×	×
	13191.3†	×	×	×		×	×	×		×	×	×	×
$\frac{1}{2}^-$	13483.3	0.8		1	31	0.0007		4.3	1	0.8	13.4	1.6	1
	13440.2	0.7		1	4.2	0.002		1486	1	0.7	0.002	17.6	1
	13418.1	×		3.8	1	1		0.3	704	17.7	21.3	50	1
	13365.8	×		×	1	1		13	39	×	×	0.6	1
	13361.6	×		×	1	1		15	67	×	×	2.3	1
	13257.9	×		×	×	×		1	6.8	×	×	×	×
	13189.3	×		×	×	×		1	1	1	1	1	1
	13127.8*	×		×	×	1		1	1	1	1	1	1
J^P		$bbc \otimes n\bar{c}$				$bbn \otimes c\bar{c}$				$cbn \otimes b\bar{c}$			
		$\Omega_{bbc}^* D^*$	$\Omega_{bbc}^* D$	$\Omega_{bbc}^* D^*$	$\Omega_{bbc}^* D$	$\Xi_{bb}^* J/\psi$	$\Xi_{bb}^* \eta_c$	$\Xi_{bb}^* J/\psi$	$\Xi_{bb}^* \eta_c$	$\Xi_{cb}^* B_c^*$	$\Xi_{cb}^* B_c$	$\Xi_{cb}^* B_c^*$	$\Xi_{cb}^* B_c$
$\frac{5}{2}^-$	13285.7*	1				1				1			
	13195.8*	×				1				1			
$\frac{3}{2}^-$	13337.5	13	1	1.4		1	2.1	1.6		0.14	1	2.5	1.2
	13287.3*	12	1	0.04		1	0.003	249		1	1	0.008	2.4
	13272.2	67	1	70		1	1	950		1	1	1	13
	13198.0	×	0.0	1		1	1	1		1	1	1	1
	13165.4†	×	×	1		1	1	1		1	1	1	1
	13161.4†	×	1	1		1	1	1		1	1	1	1
	13054.9*	1	1	1		1	1	1		1	1	1	1
$\frac{1}{2}^-$	13369.3	0.001		1	20.6	0.1		1	92	2.4	0.4	0.14	0.4
	13309.5	0.01		1	3.6	7.2		1	529	14	70	239	1
	13291.8	4.1		135	1	0.002		1	2.3	1.2	0.9	0.5	1
	13262.3	1.1		1.0	1	1		1	1	1	1.4	0.003	1
	13186.2	1		11	1	1		1	1	1	1	1	1
	13157.2	1		1	1	1		1	1	1	1	1	1
	13148.5	1		1	1	1		1	1	1	1	1	1
	13018.0*	1		1	1	1		1	1	1	1	1	1
J^P		$bbc \otimes nb$				$bbn \otimes cb$				$cbn \otimes bb$			
		$\Omega_{bbc}^* B^*$	$\Omega_{bbc}^* B$	$\Omega_{bbc}^* B^*$	$\Omega_{bbc}^* B$	$\Xi_{bb}^* B_c^*$	$\Xi_{bb}^* B_c$	$\Xi_{bb}^* B_c^*$	$\Xi_{bb}^* B_c$	$\Xi_{cb}^* \Upsilon$	$\Xi_{cb}^* \eta_b$	$\Xi_{cb}^* \Upsilon$	$\Xi_{cb}^* \eta_b$
$\frac{5}{2}^-$	16572.3	1				1				1			
	16427.3†	1				1				1			
$\frac{3}{2}^-$	16569.6	0.7	1	2.6		0.7	1	1.8		3.4	1	0.2	0.03
	16567.0	0.6	1	3.0		0.7	1	19		677	1	0.2	298
	16519.5	1	1	0.1		1	1	0.002		71	1	0.04	17
	16432.5	1	1	1		1	1	1		1	1	15	12
	16411.3	1	1	1		1	1	1		1	1	0.4	2.0
	16374.5	1	1	1		1	1	1		1	1	1	1
	16369.2†	1	1	1		1	1	1		1	1	1	1
$\frac{1}{2}^-$	16584.9	17		38	1	14		30	1	0.7	4.2	1	0.0
	16557.1	1		1.7	0.0	1.7		2.8	1	1.3	1	3.3	0.0
	16503.9	1		578	1	1		1	2.8	7.4	1	4.5	0.9
	16449.7	1		1	1	1		1	14	1	25	0.2	1.3
	16397.0	1		1	1	1		1	1	1	1	0.7	0.8
	16392.5	1		1	1	1		1	1	1	1	1	0.008
	16363.3	1		1	1	1		1	1	1	1	0	8.1
	16326.9	1		1	1	1		1	1	1	1	1	1

(117)

C. Appendix C

In the $nnnn\bar{Q}$ pentaquark subsystem, to find the isospin \otimes color \otimes spin wave function with fully antisymmetric $\{1234\}$ property, we need to combine the isospin bases with color \otimes spin bases represented in Young tableaus in Eqs. (13-17).

We use the notation $|[I^i CS^j]_k\rangle$ to denote the symmetry allowed isospin \otimes color \otimes spin pentaquark wave function. Here, i denotes the isospin quantum number of the $nnnn\bar{Q}$ pentaquark subsystem, j denotes the total spin quantum number, and k denotes the k -th symmetry allowed pentaquark wave function. We also adopt this notation in Appendix D and E. Here, we present the complete Young-Yamanouchi bases for the $nnnn\bar{Q}$ subsystem in Eq. (118).

Let us take the pentaquark wave functions with $I = 1$, $S = 1/2$ as an example to briefly describe our construction process. We combine the isospin bases obtained from Young tableau [3,1] in Eq. (6) with color \otimes spin bases obtained from Young tableau [2,1,1] in Eq. (16) or Eq. (17) to form the pentaquark wave functions with $\{1234\}$ symmetry, and finally we find two $\{1234\}$ symmetry isospin \otimes color \otimes spin pentaquark wave functions.

$$\begin{aligned}
 I = 2; S = \frac{3}{2} : \quad & |[I^2 CS^{3/2}]_1\rangle = \boxed{1 \ 2 \ 3 \ 4}_{I_1} \otimes \begin{array}{c} 1 \\ 2 \\ 3 \\ 4 \\ \hline CS_1 \end{array} . \\
 I = 2; S = \frac{1}{2} : \quad & |[I^2 CS^{1/2}]_1\rangle = \boxed{1 \ 2 \ 3 \ 4}_{I_1} \otimes \begin{array}{c} 1 \\ 2 \\ 3 \\ 4 \\ \hline CS_1 \end{array} . \\
 I = 1; S = \frac{5}{2} : \quad & |[I^1 CS^{5/2}]_1\rangle = \frac{1}{\sqrt{3}} \boxed{\begin{array}{c} 1 \ 3 \ 4 \\ 2 \end{array}}_{I_2} \otimes \begin{array}{c} 1 \ 2 \\ 3 \\ 4 \\ \hline CS_1 \end{array} - \frac{1}{\sqrt{3}} \boxed{\begin{array}{c} 1 \ 2 \ 4 \\ 3 \end{array}}_{I_3} \otimes \begin{array}{c} 1 \ 3 \\ 2 \\ 4 \\ \hline CS_2 \end{array} + \frac{1}{\sqrt{3}} \boxed{\begin{array}{c} 1 \ 2 \ 3 \\ 4 \end{array}}_{I_4} \otimes \begin{array}{c} 1 \ 4 \\ 2 \\ 3 \\ \hline CS_3 \end{array} . \\
 I = 1; S = \frac{3}{2} : \quad & |[I^1 CS^{3/2}]_1\rangle = \frac{1}{\sqrt{3}} \boxed{\begin{array}{c} 1 \ 3 \ 4 \\ 2 \end{array}}_{I_2} \otimes \begin{array}{c} 1 \ 2 \\ 3 \\ 4 \\ \hline CS_2 \end{array} - \frac{1}{\sqrt{3}} \boxed{\begin{array}{c} 1 \ 2 \ 4 \\ 3 \end{array}}_{I_3} \otimes \begin{array}{c} 1 \ 3 \\ 2 \\ 4 \\ \hline CS_4 \end{array} + \frac{1}{\sqrt{3}} \boxed{\begin{array}{c} 1 \ 2 \ 3 \\ 4 \end{array}}_{I_4} \otimes \begin{array}{c} 1 \ 4 \\ 2 \\ 3 \\ \hline CS_3 \end{array} ; \\
 & |[I^1 CS^{3/2}]_2\rangle = \frac{1}{\sqrt{3}} \boxed{\begin{array}{c} 1 \ 3 \ 4 \\ 2 \end{array}}_{I_2} \otimes \begin{array}{c} 1 \ 2 \\ 3 \\ 4 \\ \hline CS_{10} \end{array} - \frac{1}{\sqrt{3}} \boxed{\begin{array}{c} 1 \ 2 \ 4 \\ 3 \end{array}}_{I_3} \otimes \begin{array}{c} 1 \ 3 \\ 2 \\ 4 \\ \hline CS_{12} \end{array} + \frac{1}{\sqrt{3}} \boxed{\begin{array}{c} 1 \ 2 \ 3 \\ 4 \end{array}}_{I_4} \otimes \begin{array}{c} 1 \ 4 \\ 2 \\ 3 \\ \hline CS_{11} \end{array} . \\
 I = 1; S = \frac{1}{2} : \quad & |[I^1 CS^{1/2}]_1\rangle = \frac{1}{\sqrt{3}} \boxed{\begin{array}{c} 1 \ 3 \ 4 \\ 2 \end{array}}_{I_2} \otimes \begin{array}{c} 1 \ 2 \\ 3 \\ 4 \\ \hline CS_2 \end{array} - \frac{1}{\sqrt{3}} \boxed{\begin{array}{c} 1 \ 2 \ 4 \\ 3 \end{array}}_{I_3} \otimes \begin{array}{c} 1 \ 3 \\ 2 \\ 4 \\ \hline CS_4 \end{array} + \frac{1}{\sqrt{3}} \boxed{\begin{array}{c} 1 \ 2 \ 3 \\ 4 \end{array}}_{I_4} \otimes \begin{array}{c} 1 \ 4 \\ 2 \\ 3 \\ \hline CS_3 \end{array} ; \\
 & |[I^1 CS^{1/2}]_2\rangle = \frac{1}{\sqrt{3}} \boxed{\begin{array}{c} 1 \ 3 \ 4 \\ 2 \end{array}}_{I_2} \otimes \begin{array}{c} 1 \ 2 \\ 3 \\ 4 \\ \hline CS_{10} \end{array} - \frac{1}{\sqrt{3}} \boxed{\begin{array}{c} 1 \ 2 \ 4 \\ 3 \end{array}}_{I_3} \otimes \begin{array}{c} 1 \ 3 \\ 2 \\ 4 \\ \hline CS_{12} \end{array} + \frac{1}{\sqrt{3}} \boxed{\begin{array}{c} 1 \ 2 \ 3 \\ 4 \end{array}}_{I_4} \otimes \begin{array}{c} 1 \ 4 \\ 2 \\ 3 \\ \hline CS_{11} \end{array} . \\
 I = 0; S = \frac{3}{2} : \quad & |[I^0 CS^{3/2}]_1\rangle = \frac{1}{\sqrt{2}} \boxed{\begin{array}{c} 1 \ 2 \\ 3 \ 4 \end{array}}_{I_6} \otimes \begin{array}{c} 1 \ 3 \\ 2 \ 4 \\ \hline CS_6 \end{array} - \frac{1}{\sqrt{2}} \boxed{\begin{array}{c} 1 \ 3 \\ 2 \ 4 \end{array}}_{I_5} \otimes \begin{array}{c} 1 \ 2 \\ 3 \ 4 \\ \hline CS_5 \end{array} . \\
 I = 0; S = \frac{1}{2} : \quad & |[I^0 CS^{1/2}]_1\rangle = \frac{1}{\sqrt{2}} \boxed{\begin{array}{c} 1 \ 2 \\ 3 \ 4 \end{array}}_{I_6} \otimes \begin{array}{c} 1 \ 3 \\ 2 \ 4 \\ \hline CS_6 \end{array} - \frac{1}{\sqrt{2}} \boxed{\begin{array}{c} 1 \ 3 \\ 2 \ 4 \end{array}}_{I_5} \otimes \begin{array}{c} 1 \ 2 \\ 3 \ 4 \\ \hline CS_5 \end{array} . \tag{118}
 \end{aligned}$$

D. Appendix D

After introducing the SU(3) breaking effect, in the $nnns\bar{Q}$ subsystem, the s quark is different from the first three n ($n = u, d$) quarks. We only need to consider that the total wave function of the first three n quarks should be fully antisymmetric. So we construct the isospin \otimes color \otimes spin wave function with the $\{123\}$ symmetry.

For example, for $I = 1/2$, $S = 3/2$ pentaquark

states, we combine the isospin bases obtained from Young tableau [2,1] in Eq. (7) with color \otimes spin bases obtained from Young tableau [2,1,1], [2,2], and [3,1] in Eq. (14) or Young tableau [2,1,1] in Eq. (15) to form the pentaquark bases with $\{123\}$ symmetry. Finally, we find four isospin \otimes color \otimes spin pentaquark states with $\{123\}$ symmetry. Here, we present the complete Young-Yamanouchi bases for the $nnns\bar{Q}$ subsystem in Eq. (119).

$$\begin{aligned}
I = \frac{3}{2}; S = \frac{5}{2} : \quad & |[I^{3/2}CS^{5/2}]_1\rangle = \boxed{1 \ 2 \ 3}_{I_1} \otimes \begin{array}{c} 1 \ 4 \\ 2 \\ 3 \\ 4 \end{array}_{CS_3} ; \\
I = \frac{3}{2}; S = \frac{3}{2} : \quad & |[I^{3/2}CS^{3/2}]_1\rangle = \boxed{1 \ 2 \ 3}_{I_1} \otimes \begin{array}{c} 1 \\ 2 \\ 3 \\ 4 \end{array}_{CS_1} ; \\
& |[I^{3/2}CS^{3/2}]_2\rangle = \boxed{1 \ 2 \ 3}_{I_1} \otimes \begin{array}{c} 1 \ 4 \\ 2 \\ 3 \end{array}_{CS_3} ; \\
& |[I^{3/2}CS^{3/2}]_3\rangle = \boxed{1 \ 2 \ 3}_{I_1} \otimes \begin{array}{c} 1 \ 4 \\ 2 \\ 3 \end{array}_{CS_{11}} ; \\
I = \frac{3}{2}; S = \frac{1}{2} : \quad & |[I^{3/2}CS^{1/2}]_1\rangle = \boxed{1 \ 2 \ 3}_{I_1} \otimes \begin{array}{c} 1 \\ 2 \\ 3 \\ 4 \end{array}_{CS_1} ; \\
& |[I^{3/2}CS^{1/2}]_2\rangle = \boxed{1 \ 2 \ 3}_{I_1} \otimes \begin{array}{c} 1 \ 4 \\ 2 \\ 3 \end{array}_{CS_3} ; \\
& |[I^{3/2}CS^{1/2}]_3\rangle = \boxed{1 \ 2 \ 3}_{I_1} \otimes \begin{array}{c} 1 \ 4 \\ 2 \\ 3 \end{array}_{CS_{11}} ; \\
I = \frac{1}{2}; S = \frac{5}{2} : \quad & |[I^{1/2}CS^{5/2}]_1\rangle = \frac{1}{\sqrt{2}} \boxed{1 \ 2}_{I_2} \otimes \begin{array}{c} 1 \ 3 \\ 2 \\ 4 \end{array}_{CS_2} - \frac{1}{\sqrt{2}} \boxed{1 \ 3}_{I_3} \otimes \begin{array}{c} 1 \ 2 \\ 3 \\ 4 \end{array}_{CS_1} ; \\
I = \frac{1}{2}; S = \frac{3}{2} : \quad & |[I^{1/2}CS^{3/2}]_1\rangle = \frac{1}{\sqrt{2}} \boxed{1 \ 2}_{I_2} \otimes \begin{array}{c} 1 \ 3 \\ 2 \\ 4 \end{array}_{CS_4} - \frac{1}{\sqrt{2}} \boxed{1 \ 3}_{I_3} \otimes \begin{array}{c} 1 \ 2 \\ 3 \\ 4 \end{array}_{CS_2} ; \\
& |[I^{1/2}CS^{3/2}]_2\rangle = \frac{1}{\sqrt{2}} \boxed{1 \ 2}_{I_2} \otimes \begin{array}{c} 1 \ 3 \\ 2 \ 4 \end{array}_{CS_6} - \frac{1}{\sqrt{2}} \boxed{1 \ 3}_{I_3} \otimes \begin{array}{c} 1 \ 2 \\ 3 \ 4 \end{array}_{CS_5} ; \\
& |[I^{1/2}CS^{3/2}]_3\rangle = \frac{1}{\sqrt{2}} \boxed{1 \ 2}_{I_2} \otimes \begin{array}{c} 1 \ 3 \ 4 \\ 2 \end{array}_{CS_7} - \frac{1}{\sqrt{2}} \boxed{1 \ 3}_{I_3} \otimes \begin{array}{c} 1 \ 2 \ 4 \\ 3 \end{array}_{CS_8} ; \\
& |[I^{1/2}CS^{3/2}]_4\rangle = \frac{1}{\sqrt{2}} \boxed{1 \ 2}_{I_2} \otimes \begin{array}{c} 1 \ 3 \\ 2 \\ 4 \end{array}_{CS_{12}} - \frac{1}{\sqrt{2}} \boxed{1 \ 3}_{I_3} \otimes \begin{array}{c} 1 \ 2 \\ 3 \\ 4 \end{array}_{CS_{10}} ; \\
I = \frac{1}{2}; S = \frac{1}{2} : \quad & |[I^{1/2}CS^{1/2}]_1\rangle = \frac{1}{\sqrt{2}} \boxed{1 \ 2}_{I_2} \otimes \begin{array}{c} 1 \ 3 \\ 2 \\ 4 \end{array}_{CS_4} - \frac{1}{\sqrt{2}} \boxed{1 \ 3}_{I_3} \otimes \begin{array}{c} 1 \ 2 \\ 3 \\ 4 \end{array}_{CS_2} ; \\
& |[I^{1/2}CS^{1/2}]_2\rangle = \frac{1}{\sqrt{2}} \boxed{1 \ 2}_{I_2} \otimes \begin{array}{c} 1 \ 3 \\ 2 \ 4 \end{array}_{CS_6} - \frac{1}{\sqrt{2}} \boxed{1 \ 3}_{I_3} \otimes \begin{array}{c} 1 \ 2 \\ 3 \ 4 \end{array}_{CS_5} ; \\
& |[I^{1/2}CS^{1/2}]_3\rangle = \frac{1}{\sqrt{2}} \boxed{1 \ 2}_{I_2} \otimes \begin{array}{c} 1 \ 3 \ 4 \\ 2 \end{array}_{CS_7} - \frac{1}{\sqrt{2}} \boxed{1 \ 3}_{I_3} \otimes \begin{array}{c} 1 \ 2 \ 4 \\ 3 \end{array}_{CS_8} ; \\
& |[I^{1/2}CS^{1/2}]_4\rangle = \frac{1}{\sqrt{2}} \boxed{1 \ 2}_{I_2} \otimes \begin{array}{c} 1 \ 3 \\ 2 \\ 4 \end{array}_{CS_{12}} - \frac{1}{\sqrt{2}} \boxed{1 \ 3}_{I_3} \otimes \begin{array}{c} 1 \ 2 \\ 3 \\ 4 \end{array}_{CS_{10}} ; \\
& |[I^{1/2}CS^{1/2}]_5\rangle = \frac{1}{\sqrt{2}} \boxed{1 \ 2}_{I_2} \otimes \begin{array}{c} 1 \ 3 \ 4 \\ 2 \end{array}_{CS_{13}} - \frac{1}{\sqrt{2}} \boxed{1 \ 3}_{I_3} \otimes \begin{array}{c} 1 \ 2 \ 4 \\ 3 \end{array}_{CS_{14}} .
\end{aligned}$$

(119)

E. Appendix E

For the $nnss\bar{Q}$ subsystem, we have two pairs of identical light quarks, i.e., nn and ss . So we construct the isospin \otimes color \otimes spin pentaquark wave function with $\{12\} \{34\}$ symmetry property. Here, we present the complete Young-Yamanouchi bases for the $nnss\bar{Q}$ subsystem in Eq. (120).

$$\begin{aligned}
I = 1; S = \frac{5}{2} : \quad & |[I^1 CS^{5/2}]_1\rangle = \sqrt{\frac{2}{3}} \boxed{1 \boxed{2}}_{I_1} \otimes \begin{array}{c} 1 \boxed{3} \\ 2 \\ 4 \end{array}_{CS_2} - \sqrt{\frac{1}{3}} \boxed{1 \boxed{2}}_{I_1} \otimes \begin{array}{c} 1 \boxed{4} \\ 2 \\ 3 \end{array}_{CS_3} . \\
I = 1; S = \frac{3}{2} : \quad & |[I^1 CS^{3/2}]_1\rangle = \boxed{1 \boxed{2}}_{I_1} \otimes \begin{array}{c} 1 \\ 2 \\ 3 \\ 4 \end{array}_{CS_1} ; \\
& |[I^1 CS^{3/2}]_2\rangle = \sqrt{\frac{2}{3}} \boxed{1 \boxed{2}}_{I_1} \otimes \begin{array}{c} 1 \boxed{3} \\ 2 \\ 4 \end{array}_{CS_4} - \sqrt{\frac{1}{3}} \boxed{1 \boxed{2}}_{I_1} \otimes \begin{array}{c} 1 \boxed{4} \\ 2 \\ 3 \end{array}_{CS_3} ; \\
& |[I^1 CS^{3/2}]_3\rangle = \boxed{1 \boxed{2}}_{I_1} \otimes \begin{array}{c} 1 \boxed{3} \\ 2 \boxed{4} \end{array}_{CS_6} ; \\
& |[I^1 CS^{3/2}]_4\rangle = \sqrt{\frac{2}{3}} \boxed{1 \boxed{2}}_{I_1} \otimes \begin{array}{c} 1 \boxed{3} \\ 2 \\ 4 \end{array}_{CS_{12}} - \sqrt{\frac{1}{3}} \boxed{1 \boxed{2}}_{I_1} \otimes \begin{array}{c} 1 \boxed{4} \\ 2 \\ 3 \end{array}_{CS_{11}} . \\
I = 1; S = \frac{1}{2} : \quad & |[I^1 CS^{1/2}]_1\rangle = \boxed{1 \boxed{2}}_{I_1} \otimes \begin{array}{c} 1 \\ 2 \\ 3 \\ 4 \end{array}_{CS_1} ; \\
& |[I^1 CS^{1/2}]_2\rangle = \sqrt{\frac{2}{3}} \boxed{1 \boxed{2}}_{I_1} \otimes \begin{array}{c} 1 \boxed{3} \\ 2 \\ 4 \end{array}_{CS_4} - \sqrt{\frac{1}{3}} \boxed{1 \boxed{2}}_{I_1} \otimes \begin{array}{c} 1 \boxed{4} \\ 2 \\ 3 \end{array}_{CS_3} ; \\
& |[I^1 CS^{3/2}]_3\rangle = \boxed{1 \boxed{2}}_{I_1} \otimes \begin{array}{c} 1 \boxed{3} \\ 2 \boxed{4} \end{array}_{CS_6} ; \\
& |[I^1 CS^{3/2}]_4\rangle = \sqrt{\frac{2}{3}} \boxed{1 \boxed{2}}_{I_1} \otimes \begin{array}{c} 1 \boxed{3} \\ 2 \\ 4 \end{array}_{CS_{12}} - \sqrt{\frac{1}{3}} \boxed{1 \boxed{2}}_{I_1} \otimes \begin{array}{c} 1 \boxed{4} \\ 2 \\ 3 \end{array}_{CS_{11}} . \\
I = 0; S = \frac{5}{2} : \quad & |[I^0 CS^{5/2}]_1\rangle = \begin{array}{c} 1 \\ 2 \end{array}_{I_2} \otimes \begin{array}{c} 1 \boxed{2} \\ 3 \\ 4 \end{array}_{CS_1} . \\
I = 0; S = \frac{3}{2} : \quad & |[I^0 CS^{3/2}]_1\rangle = \begin{array}{c} 1 \\ 2 \end{array}_{I_2} \otimes \begin{array}{c} 1 \boxed{2} \\ 3 \\ 4 \end{array}_{CS_2} ; \\
& |[I^0 CS^{3/2}]_2\rangle = -\sqrt{\frac{1}{3}} \begin{array}{c} 1 \\ 2 \end{array}_{I_2} \otimes \begin{array}{c} 1 \boxed{2} \boxed{4} \\ 3 \end{array}_{CS_8} + \sqrt{\frac{2}{3}} \begin{array}{c} 1 \\ 2 \end{array}_{I_2} \otimes \begin{array}{c} 1 \boxed{2} \boxed{3} \\ 4 \end{array}_{CS_9} ; \\
& |[I^0 CS^{3/2}]_3\rangle = \begin{array}{c} 1 \\ 2 \end{array}_{I_1} \otimes \begin{array}{c} 1 \boxed{2} \\ 3 \\ 4 \end{array}_{CS_{10}} .
\end{aligned}$$

$$\begin{aligned}
I = 0; S = \frac{1}{2} : \quad & |[I^0 CS^{1/2}]_1\rangle = \left| \begin{array}{c} 1 \\ 2 \end{array} \right|_{I_2} \otimes \left| \begin{array}{cc} 1 & 2 \\ 3 & \end{array} \right|_{CS_2}; \\
& |[I^0 CS^{1/2}]_2\rangle = -\sqrt{\frac{1}{3}} \left| \begin{array}{c} 1 \\ 2 \end{array} \right|_{I_2} \otimes \left| \begin{array}{ccc} 1 & 2 & 4 \\ 3 & \end{array} \right|_{CS_8} + \sqrt{\frac{2}{3}} \left| \begin{array}{c} 1 \\ 2 \end{array} \right|_{I_2} \otimes \left| \begin{array}{ccc} 1 & 2 & 3 \\ 4 & \end{array} \right|_{CS_9}; \\
& |[I^0 CS^{1/2}]_3\rangle = \left| \begin{array}{c} 1 \\ 2 \end{array} \right|_{I_1} \otimes \left| \begin{array}{cc} 1 & 2 \\ 3 & \end{array} \right|_{CS_{10}}. \\
& |[I^0 CS^{1/2}]_4\rangle = -\sqrt{\frac{1}{3}} \left| \begin{array}{c} 1 \\ 2 \end{array} \right|_{I_2} \otimes \left| \begin{array}{ccc} 1 & 2 & 4 \\ 3 & \end{array} \right|_{CS_{14}} + \sqrt{\frac{2}{3}} \left| \begin{array}{c} 1 \\ 2 \end{array} \right|_{I_2} \otimes \left| \begin{array}{ccc} 1 & 2 & 3 \\ 4 & \end{array} \right|_{CS_{15}}.
\end{aligned} \tag{120}$$

F. Appendix F

In the $nnsQ\bar{q}$ subsystem, only the first two light quarks are identical. Thus, the less symmetry constrain leads to more symmetrical allowed pentaquark bases.

Here, we show completely all possible the Young-Yamanouchi bases of the color \otimes spin coupling (117), with different isospin and spin quantum numbers for the $nnsQ\bar{q}$ pentaquark subsystem in Table XXXVI.

TABLE XXXVI. The CMI Hamiltonian for the $nnsQ\bar{n}$ ($n = u, d; Q = c, d$) subsystem. The I (S) represents the isospin (spin) of the $nnsQ\bar{n}$ pentaquark states.

I	S	The color \otimes spin Young-Yamanouchi bases
$I = 1$	$S = 5/2$	$\left \begin{array}{cc} 1 & 4 \\ 2 & \end{array} \right _{CS_3} \left \begin{array}{cc} 1 & 3 \\ 2 & \end{array} \right _{CS_2}$
	$S = 3/2$	$\left \begin{array}{c} 1 \\ 2 \\ 3 \\ 4 \end{array} \right _{CS_1} \left \begin{array}{cc} 1 & 4 \\ 2 & \end{array} \right _{CS_3} \left \begin{array}{cc} 1 & 3 \\ 2 & \end{array} \right _{CS_4} \left \begin{array}{cc} 1 & 3 \\ 2 & 4 \end{array} \right _{CS_6} \left \begin{array}{cc} 1 & 3 \\ 2 & 4 \end{array} \right _{CS_7} \left \begin{array}{cc} 1 & 4 \\ 2 & \end{array} \right _{CS_{11}} \left \begin{array}{cc} 1 & 3 \\ 2 & \end{array} \right _{CS_{12}}$
	$S = 1/2$	$\left \begin{array}{c} 1 \\ 2 \\ 3 \\ 4 \end{array} \right _{CS_1} \left \begin{array}{cc} 1 & 4 \\ 2 & \end{array} \right _{CS_3} \left \begin{array}{cc} 1 & 3 \\ 2 & \end{array} \right _{CS_4} \left \begin{array}{cc} 1 & 3 \\ 2 & 4 \end{array} \right _{CS_5} \left \begin{array}{cc} 1 & 3 \\ 2 & 4 \end{array} \right _{CS_8} \left \begin{array}{cc} 1 & 4 \\ 2 & \end{array} \right _{CS_{11}} \left \begin{array}{cc} 1 & 3 \\ 2 & \end{array} \right _{CS_{12}} \left \begin{array}{cc} 1 & 3 \\ 2 & 4 \end{array} \right _{CS_{13}}$
	$S = 5/2$	$\left \begin{array}{c} 1 \\ 2 \\ 3 \\ 4 \end{array} \right _{CS_1} \left \begin{array}{cc} 1 & 2 \\ 3 & \end{array} \right _{CS_1}$
	$S = 3/2$	$\left \begin{array}{c} 1 \\ 2 \\ 3 \\ 4 \end{array} \right _{CS_2} \left \begin{array}{cc} 1 & 2 \\ 3 & \end{array} \right _{CS_5} \left \begin{array}{cc} 1 & 2 & 4 \\ 3 & \end{array} \right _{CS_8} \left \begin{array}{cc} 1 & 2 & 3 \\ 4 & \end{array} \right _{CS_9} \left \begin{array}{cc} 1 & 2 \\ 3 & \end{array} \right _{CS_{10}}$
	$S = 1/2$	$\left \begin{array}{c} 1 \\ 2 \\ 3 \\ 4 \end{array} \right _{CS_2} \left \begin{array}{cc} 1 & 2 \\ 3 & 4 \end{array} \right _{CS_5} \left \begin{array}{cc} 1 & 2 & 4 \\ 3 & \end{array} \right _{CS_8} \left \begin{array}{cc} 1 & 2 & 3 \\ 4 & \end{array} \right _{CS_9} \left \begin{array}{cc} 1 & 2 \\ 3 & \end{array} \right _{CS_{10}} \left \begin{array}{cc} 1 & 2 & 4 \\ 3 & \end{array} \right _{CS_{14}} \left \begin{array}{cc} 1 & 2 & 3 \\ 4 & \end{array} \right _{CS_{15}}$
	$S = 5/2$	
	$S = 3/2$	
	$S = 1/2$	

G. Appendix G

The expressions of CMI Hamiltonian for $nnns\bar{Q}$ ($I = 3/2, 1/2$), $nnss\bar{Q}$ ($I = 1, 0$), and $nnsQ\bar{n}$ ($I_{nn} = 1, 0$) pentaquark states are presented in Tables XXXVII, XXXVIII, and XXXIX, respectively.

TABLE XXXVII. The expressions of CMI Hamiltonian for $nnns\bar{Q}$ and $nnss\bar{Q}$ with $I = 1$ ($n = u, d$; $Q = c, d$) pentaquark subsystems. The I (S) represents the isospin (spin) of the pentaquark states.

I	S	The expressions of CMI Hamiltonian for $nnns\bar{Q}$ subsystems			
$I=3/2$	S=5/2	$8C_{nn} + \frac{16}{3}C_{s\bar{Q}}$	$\left(\begin{array}{l} \left(\frac{28}{3}C_{nn} + \frac{28}{3}C_{ns} \right) \\ -4C_{n\bar{Q}} - \frac{4}{3}C_{s\bar{Q}} \end{array} \right)$	$\left(\begin{array}{l} -\frac{2\sqrt{2}}{3}C_{nn} + \frac{2\sqrt{2}}{3}C_{ns} \\ +\frac{2\sqrt{2}}{3}C_{n\bar{Q}} - \frac{2\sqrt{2}}{3}C_{s\bar{Q}} \end{array} \right)$	$-\frac{8\sqrt{5}}{3}C_{n\bar{Q}} + \frac{8\sqrt{5}}{3}C_{s\bar{Q}}$
	S=3/2	$\left(\begin{array}{l} -\frac{2\sqrt{2}}{3}C_{nn} + \frac{2\sqrt{2}}{3}C_{ns} \\ +\frac{2\sqrt{2}}{3}C_{n\bar{Q}} - \frac{2\sqrt{2}}{3}C_{s\bar{Q}} \end{array} \right)$	$\left(\begin{array}{l} \frac{26}{3}C_{nn} - 6C_{ns} \\ +\frac{2}{3}C_{n\bar{Q}} - 2C_{s\bar{Q}} \end{array} \right)$	$\frac{4\sqrt{10}}{3}C_{s\bar{Q}} + \frac{8\sqrt{10}}{3}C_{s\bar{Q}}$	$8C_{nn} - 8C_{s\bar{Q}}$
	S=1/2	$\left(\begin{array}{l} \left(\frac{28}{3}C_{nn} + \frac{28}{3}C_{ns} \right) \\ +8C_{n\bar{Q}} + \frac{8}{3}C_{s\bar{Q}} \end{array} \right)$	$\left(\begin{array}{l} \frac{4\sqrt{10}}{3}C_{n\bar{Q}} + \frac{8\sqrt{10}}{3}C_{s\bar{Q}} \\ -\frac{2\sqrt{2}}{3}C_{n\bar{Q}} + \frac{4\sqrt{2}}{3}C_{s\bar{Q}} \end{array} \right)$	$\frac{2\sqrt{2}}{3}C_{n\bar{Q}} - \frac{2\sqrt{2}}{3}C_{s\bar{Q}}$	$8C_{nn} - 8C_{s\bar{Q}}$
	S=1/2	$\left(\begin{array}{l} -\frac{2\sqrt{2}}{3}C_{nn} + \frac{2\sqrt{2}}{3}C_{ns} \\ -\frac{4\sqrt{2}}{3}C_{n\bar{Q}} + \frac{4\sqrt{2}}{3}C_{s\bar{Q}} \end{array} \right)$	$\left(\begin{array}{l} \frac{26}{3}C_{nn} - 6C_{ns} \\ -\frac{4}{3}C_{n\bar{Q}} + 4C_{s\bar{Q}} \end{array} \right)$	$-\frac{26}{3}C_{n\bar{Q}} + \frac{2}{3}C_{s\bar{Q}}$	$10C_{nn} - 10C_{ns}$
$I=\frac{1}{2}$	S=5/2	$8C_{nn} + \frac{16}{3}C_{s\bar{Q}}$	$\left(\begin{array}{l} \left(-\frac{7}{3}C_{nn} + 5C_{ns} \right) \\ -\frac{11}{6}C_{n\bar{Q}} + \frac{1}{2}C_{s\bar{Q}} \end{array} \right)$	$\left(\begin{array}{l} -\frac{\sqrt{2}}{3}C_{nn} + \frac{\sqrt{2}}{3}C_{ns} \\ -\frac{3\sqrt{2}}{3}C_{n\bar{Q}} + \frac{3\sqrt{2}}{3}C_{s\bar{Q}} \end{array} \right)$	$-\frac{23\sqrt{5}}{3\sqrt{2}}C_{n\bar{Q}} + \frac{\sqrt{5}}{3\sqrt{2}}C_{s\bar{Q}}$
	S=3/2	$\left(\begin{array}{l} -\frac{\sqrt{2}}{3}C_{nn} + \frac{\sqrt{2}}{3}C_{ns} \\ -\frac{7}{3}C_{n\bar{Q}} + \frac{7}{3}C_{s\bar{Q}} \end{array} \right)$	$\left(\begin{array}{l} -\frac{8}{3}C_{nn} - \frac{8}{3}C_{ns} \\ +5C_{n\bar{Q}} + \frac{5}{3}C_{s\bar{Q}} \end{array} \right)$	$-\frac{\sqrt{5}}{3}C_{n\bar{Q}} + \frac{\sqrt{5}}{3}C_{s\bar{Q}}$	$-\frac{\sqrt{5}}{3}C_{n\bar{Q}} + \frac{\sqrt{5}}{3}C_{s\bar{Q}}$
	S=1/2	$\left(\begin{array}{l} \frac{5}{3}C_{nn} - \frac{5}{3}C_{ns} \\ +\frac{5}{3}C_{n\bar{Q}} - \frac{5}{3}C_{s\bar{Q}} \end{array} \right)$	$\left(\begin{array}{l} \frac{5\sqrt{2}}{3}C_{nn} - \frac{5\sqrt{2}}{3}C_{ns} \\ +\frac{5}{\sqrt{6}}C_{n\bar{Q}} - \frac{5}{\sqrt{6}}C_{s\bar{Q}} \end{array} \right)$	$-\frac{\sqrt{5}}{6}C_{n\bar{Q}} + \frac{31}{17}C_{s\bar{Q}}$	$-\frac{\sqrt{5}}{\sqrt{6}}C_{n\bar{Q}} + \frac{\sqrt{5}}{\sqrt{6}}C_{s\bar{Q}}$
	S=1/2	$\left(\begin{array}{l} -\frac{23\sqrt{5}}{3\sqrt{2}}C_{n\bar{Q}} + \frac{\sqrt{5}}{3\sqrt{2}}C_{s\bar{Q}} \\ -\frac{\sqrt{5}}{3}C_{n\bar{Q}} + \frac{\sqrt{5}}{3}C_{s\bar{Q}} \end{array} \right)$	$\left(\begin{array}{l} -\frac{\sqrt{5}}{6}C_{n\bar{Q}} + \frac{\sqrt{5}}{6}C_{s\bar{Q}} \\ -\frac{\sqrt{5}}{6}C_{n\bar{Q}} + \frac{\sqrt{5}}{6}C_{s\bar{Q}} \end{array} \right)$	$\left(\begin{array}{l} 2C_{nn} + 6C_{ns} \\ -9C_{n\bar{Q}} + C_{s\bar{Q}} \end{array} \right)$	$\left(\begin{array}{l} 2C_{nn} + 6C_{ns} \\ -9C_{n\bar{Q}} + C_{s\bar{Q}} \end{array} \right)$
The expressions of CMI Hamiltonian for $nnss\bar{Q}$ ($I = 1$) subsystems					
$I=1$	S=5/2	$\frac{8}{3}C_{nn} + \frac{8}{3}C_{ss} + \frac{8}{3}C_{ns} + \frac{8}{3}C_{n\bar{Q}} + \frac{8}{3}C_{s\bar{Q}}$	$\left(\begin{array}{l} \left(\frac{28}{9}C_{nn} + \frac{28}{9}C_{ss} + \frac{112}{9}C_{ns} \right) \\ -\frac{8}{3}C_{n\bar{Q}} - \frac{8}{3}C_{s\bar{Q}} \end{array} \right)$	$\left(\begin{array}{l} \frac{2}{3}\sqrt{\frac{2}{3}}C_{nn} - \frac{2}{3}\sqrt{\frac{2}{3}}C_{ss} \\ -\frac{4}{3}\sqrt{\frac{2}{3}}C_{n\bar{Q}} + \frac{4}{3}\sqrt{\frac{2}{3}}C_{s\bar{Q}} \end{array} \right)$	$-\frac{2}{9}\sqrt{2}C_{nn} - \frac{2}{9}\sqrt{2}C_{ss}$
	S=3/2	$2\sqrt{10}C_{n\bar{Q}} + 2\sqrt{10}C_{s\bar{Q}}$	$\left(\begin{array}{l} \frac{2}{3}\sqrt{\frac{2}{3}}C_{nn} + \frac{2}{3}\sqrt{\frac{2}{3}}C_{ss} \\ -\frac{4}{3}\sqrt{\frac{2}{3}}C_{n\bar{Q}} + \frac{4}{3}\sqrt{\frac{2}{3}}C_{s\bar{Q}} \end{array} \right)$	$\left(\begin{array}{l} -\frac{2}{3}\sqrt{3}C_{nn} + \frac{2}{3}\sqrt{3}C_{ss} \\ -\frac{14}{3}\sqrt{\frac{2}{3}}C_{n\bar{Q}} + \frac{14}{3}\sqrt{\frac{2}{3}}C_{s\bar{Q}} \end{array} \right)$	$2\sqrt{10}C_{n\bar{Q}} + 2\sqrt{10}C_{s\bar{Q}}$
	S=1/2	$-\frac{2}{3}\sqrt{\frac{10}{3}}C_{n\bar{Q}} + \frac{2}{3}\sqrt{\frac{10}{3}}C_{s\bar{Q}}$	$\left(\begin{array}{l} -\frac{2}{3}\sqrt{3}C_{nn} + \frac{2}{3}\sqrt{3}C_{ss} \\ -\frac{14}{3}\sqrt{\frac{2}{3}}C_{n\bar{Q}} + \frac{14}{3}\sqrt{\frac{2}{3}}C_{s\bar{Q}} \end{array} \right)$	$\left(\begin{array}{l} \frac{26}{9}C_{nn} + \frac{26}{9}C_{ss} - \frac{100}{9}C_{ns} \\ +\frac{10}{3}C_{n\bar{Q}} + \frac{10}{3}C_{s\bar{Q}} \end{array} \right)$	$-\frac{2}{3}\sqrt{\frac{10}{3}}C_{n\bar{Q}} + \frac{2}{3}\sqrt{\frac{10}{3}}C_{s\bar{Q}}$
	S=1/2	$\left(\begin{array}{l} \frac{8}{3}C_{nn} + \frac{8}{3}C_{ss} + \frac{8}{3}C_{ns} \\ -4C_{n\bar{Q}} - 4C_{s\bar{Q}} \end{array} \right)$	$\left(\begin{array}{l} \frac{2}{3}\sqrt{\frac{2}{3}}C_{nn} - \frac{2}{3}\sqrt{\frac{2}{3}}C_{ss} \\ +\frac{8}{3}\sqrt{\frac{2}{3}}C_{n\bar{Q}} - \frac{8}{3}\sqrt{\frac{2}{3}}C_{s\bar{Q}} \end{array} \right)$	$\left(\begin{array}{l} -\frac{2}{9}\sqrt{2}C_{nn} - \frac{2}{9}\sqrt{2}C_{ss} \\ -\frac{4}{9}\sqrt{2}C_{ns} \end{array} \right)$	$-\frac{4}{3}\sqrt{\frac{2}{3}}C_{n\bar{Q}} + \frac{4}{3}\sqrt{\frac{2}{3}}C_{s\bar{Q}}$
$I=1$	S=3/2	$-4C_{n\bar{Q}} - 4C_{s\bar{Q}}$	$\left(\begin{array}{l} \frac{2}{3}\sqrt{\frac{2}{3}}C_{nn} - \frac{2}{3}\sqrt{\frac{2}{3}}C_{ss} \\ +\frac{8}{3}\sqrt{\frac{2}{3}}C_{n\bar{Q}} - \frac{8}{3}\sqrt{\frac{2}{3}}C_{s\bar{Q}} \end{array} \right)$	$\left(\begin{array}{l} -\frac{2}{3}\sqrt{3}C_{nn} + \frac{2}{3}\sqrt{3}C_{ss} \\ +\frac{28}{3}\sqrt{\frac{2}{3}}C_{n\bar{Q}} - \frac{28}{3}\sqrt{\frac{2}{3}}C_{s\bar{Q}} \end{array} \right)$	$-4C_{n\bar{Q}} - 4C_{s\bar{Q}}$
	S=1/2	$\frac{28}{3\sqrt{3}}C_{n\bar{Q}} - \frac{28}{3\sqrt{3}}C_{s\bar{Q}}$	$\left(\begin{array}{l} -\frac{2}{3}\sqrt{3}C_{nn} + \frac{2}{3}\sqrt{3}C_{ss} \\ -\frac{4}{3}\sqrt{\frac{2}{3}}C_{n\bar{Q}} + \frac{4}{3}\sqrt{\frac{2}{3}}C_{s\bar{Q}} \end{array} \right)$	$\left(\begin{array}{l} \frac{26}{9}C_{nn} + \frac{26}{9}C_{ss} - \frac{100}{9}C_{ns} \\ -\frac{20}{3}C_{n\bar{Q}} - \frac{20}{3}C_{s\bar{Q}} \end{array} \right)$	$\frac{28}{3\sqrt{3}}C_{n\bar{Q}} - \frac{28}{3\sqrt{3}}C_{s\bar{Q}}$
	S=1/2	$\frac{8}{3}C_{nn} + \frac{8}{3}C_{ss} - \frac{16}{3}C_{ns}$	$\left(\begin{array}{l} -\frac{2}{3}\sqrt{3}C_{nn} + \frac{2}{3}\sqrt{3}C_{ss} \\ -\frac{4}{3}\sqrt{\frac{2}{3}}C_{n\bar{Q}} + \frac{4}{3}\sqrt{\frac{2}{3}}C_{s\bar{Q}} \end{array} \right)$	$\left(\begin{array}{l} \frac{26}{9}C_{nn} + \frac{26}{9}C_{ss} - \frac{100}{9}C_{ns} \\ -\frac{20}{3}C_{n\bar{Q}} - \frac{20}{3}C_{s\bar{Q}} \end{array} \right)$	$\frac{8}{3}C_{nn} + \frac{8}{3}C_{ss} - \frac{16}{3}C_{ns}$

TABLE XXXVIII. The expressions of CMI Hamiltonian for $mssQ$ with $I = 0$ and $mssQ\bar{n}$ with $I_{nn} = 0$ ($n = u, d; Q = c, d$) pentaquark subsystems. The I (S) represents the isospin (spin) of the pentaquark states.

S	The expressions of CMI Hamiltonian for $mns\bar{Q}$ ($I_{nn} = 0$) subsystems
S=5/2	$\begin{aligned} & \left(\begin{pmatrix} -\frac{14}{3}C_{nn} + \frac{8}{3}C_{ss} + \frac{14}{3} \\ C_{ns} - \frac{7}{3}C_{n\bar{Q}} + C_{s\bar{Q}} \\ -\frac{10}{3}C_{nn} + \frac{10}{3}C_{ns} \\ -\frac{5}{3}C_{n\bar{Q}} + \frac{5}{3}C_{s\bar{Q}} \end{pmatrix} \begin{pmatrix} -\frac{10}{3}C_{nn} + \frac{10}{3}C_{ns} \\ -\frac{5}{3}C_{n\bar{Q}} + \frac{5}{3}C_{s\bar{Q}} \end{pmatrix} \begin{pmatrix} \frac{11\sqrt{10}}{3}C_{n\bar{Q}} + \frac{\sqrt{10}}{3}C_{s\bar{Q}} \\ \frac{11\sqrt{10}}{3}C_{n\bar{Q}} + \frac{\sqrt{10}}{3}C_{s\bar{Q}} \end{pmatrix} \right) \\ & \left(\begin{pmatrix} -\frac{14}{3}C_{nn} + \frac{8}{3}C_{ss} + \frac{14}{3} \\ C_{ns} + \frac{14}{3}C_{n\bar{Q}} - 2C_{s\bar{Q}} \\ -\frac{10}{3}C_{nn} + \frac{10}{3}C_{ns} \\ +\frac{10}{3}C_{n\bar{Q}} - \frac{10}{3}C_{s\bar{Q}} \end{pmatrix} \begin{pmatrix} -\frac{14}{3}C_{nn} + \frac{8}{3}C_{ss} - \frac{34}{3} \\ C_{ns} + \frac{17}{3}C_{n\bar{Q}} + C_{s\bar{Q}} \end{pmatrix} \begin{pmatrix} \frac{\sqrt{10}}{3}C_{n\bar{Q}} - \frac{\sqrt{10}}{3}C_{s\bar{Q}} \\ \frac{\sqrt{10}}{3}C_{n\bar{Q}} - \frac{\sqrt{10}}{3}C_{s\bar{Q}} \end{pmatrix} \right) \\ & \left(\begin{pmatrix} -\frac{10}{3}C_{nn} + \frac{10}{3}C_{ns} \\ +\frac{10}{3}C_{n\bar{Q}} - \frac{10}{3}C_{s\bar{Q}} \end{pmatrix} \begin{pmatrix} -\frac{10}{3}C_{nn} + \frac{10}{3}C_{ns} \\ +\frac{10}{3}C_{n\bar{Q}} - \frac{10}{3}C_{s\bar{Q}} \end{pmatrix} \begin{pmatrix} -\frac{4}{3}C_{nn} + \frac{8}{3}C_{ss} + \frac{10}{3} \\ C_{ns} - 10C_{n\bar{Q}} + 2C_{s\bar{Q}} \end{pmatrix} \right) \end{aligned}$
S=3/2	$\begin{aligned} & \left(\begin{pmatrix} -\frac{14}{3}C_{nn} + \frac{8}{3}C_{ss} + \frac{14}{3} \\ C_{ns} + \frac{14}{3}C_{n\bar{Q}} - 2C_{s\bar{Q}} \\ -\frac{10}{3}C_{nn} + \frac{10}{3}C_{ns} \\ +\frac{10}{3}C_{n\bar{Q}} - \frac{10}{3}C_{s\bar{Q}} \end{pmatrix} \begin{pmatrix} -\frac{10}{3}C_{nn} + \frac{10}{3}C_{ns} \\ +\frac{10}{3}C_{n\bar{Q}} - \frac{10}{3}C_{s\bar{Q}} \end{pmatrix} \begin{pmatrix} -\frac{4}{3}C_{nn} + \frac{4}{3}C_{s\bar{Q}} \\ -\frac{4}{3}C_{n\bar{Q}} - \frac{20}{3}C_{s\bar{Q}} \end{pmatrix} \right) \\ & \left(\begin{pmatrix} -\frac{4}{3}C_{n\bar{Q}} - \frac{20}{3}C_{s\bar{Q}} \\ -\frac{4}{\sqrt{3}}C_{n\bar{Q}} + \frac{4}{\sqrt{3}}C_{s\bar{Q}} \end{pmatrix} \begin{pmatrix} \frac{16}{3}C_{n\bar{Q}} - \frac{16}{3}C_{s\bar{Q}} \\ \frac{16}{\sqrt{3}}C_{n\bar{Q}} + \frac{8}{\sqrt{3}}C_{s\bar{Q}} \end{pmatrix} \begin{pmatrix} -\frac{4}{3}C_{n\bar{Q}} - \frac{20}{3}C_{s\bar{Q}} \\ -\frac{4}{\sqrt{3}}C_{n\bar{Q}} + \frac{4}{\sqrt{3}}C_{s\bar{Q}} \end{pmatrix} \right) \end{aligned}$
S=1/2	$\begin{aligned} & \left(\begin{pmatrix} \frac{2}{3}(2C_{nn} + C_{\bar{s}\bar{n}} + 4C_{sc}) + \frac{10}{3}(C_{ns} + C_{nc} + 2C_{n\bar{n}}) \\ \frac{5}{6\sqrt{3}}(C_{sn} + 3C_{Qn} + 2C_{n\bar{Q}}) + 2C_{ns} + 4C_{nn} \end{pmatrix} \begin{pmatrix} \frac{5}{3}\sqrt{\frac{2}{3}}(2C_{n\bar{n}} - 2) \\ C_{nn} - C_{n\bar{n}} + C_{s\bar{n}} \end{pmatrix} \right) \\ & \left(\begin{pmatrix} \frac{2}{3}\sqrt{\frac{2}{3}}(C_{sn} + 2C_{Qn} - C_{n\bar{Q}} - 2C_{s\bar{Q}}) \\ C_{Qn} + 2C_{n\bar{n}} - \frac{14}{3}(C_{sQ} + C_{nn}) \end{pmatrix} \begin{pmatrix} \frac{10}{3\sqrt{3}}(C_{nn} - C_{ns} + C_{nQ}) \\ +2C_{n\bar{n}} - \frac{5}{3\sqrt{6}}(C_{sn} + 3C_{Qn}) \end{pmatrix} \right) \\ & \left(\begin{pmatrix} \frac{5}{3}\sqrt{\frac{2}{3}}(C_{sn} + 2C_{Qn} - C_{n\bar{Q}} + \frac{9\pi}{9}) \\ +2C_{n\bar{n}} - \frac{14}{3}(C_{sn} + 3C_{Qn}) \end{pmatrix} \begin{pmatrix} \frac{22\sqrt{2}}{9}(C_{sn} - C_{sQ}) \\ C_{n\bar{n}} - \frac{29}{20}C_{sQ} - \frac{5}{18}C_{sn} + \frac{17}{6}C_{Qn} \end{pmatrix} \right) \\ & \left(\begin{pmatrix} \frac{10}{3\sqrt{3}}(C_{nn} - C_{ns} + C_{nQ}) \\ +C_{n\bar{n}} - C_{sQ} - C_{s\bar{n}} \end{pmatrix} \begin{pmatrix} -\frac{3}{4}(C_{nn} + 2C_{ns}) + \frac{22}{9}(C_{sn} + \\ +\frac{\pi}{9}(C_{sn} - C_{n\bar{n}}) \end{pmatrix} \begin{pmatrix} 2C_{n\bar{n}} + \frac{2}{9}(C_{sn} - 3C_{Qn} + 2C_{nQ}) \\ +C_{n\bar{n}} - C_{sQ} - C_{s\bar{n}} \end{pmatrix} \right) \\ & \left(\begin{pmatrix} \frac{1}{3}\sqrt{\frac{2}{3}}(C_{sn} + C_{Qn}) \\ +11\frac{\sqrt{10}}{3}C_{n\bar{n}} \end{pmatrix} \begin{pmatrix} \frac{\sqrt{5}}{3}(C_{Qn} - C_{sn}) \\ -\frac{1}{3}\sqrt{\frac{10}{3}}C_{n\bar{n}} \end{pmatrix} \right) \\ & \left(\begin{pmatrix} \frac{7}{3}(C_{ns} - 2C_{nn} + C_{nQ} - C_{n\bar{n}}) \\ +\frac{8}{3}C_{sQ} + \frac{1}{2}(C_{s\bar{n}} + C_{Q\bar{n}}) \end{pmatrix} \begin{pmatrix} \frac{\sqrt{2}}{3}(C_{sn} - C_{ns}) - \\ \frac{7}{3}\sqrt{2}(C_{Q\bar{n}} - C_{s\bar{n}}) \end{pmatrix} \begin{pmatrix} \frac{5}{3}\sqrt{(-C_{sn} + 3C_{Qn} - 2)} \\ \frac{7}{3}\sqrt{2}(C_{Q\bar{n}} - C_{s\bar{n}}) \end{pmatrix} \right) \\ & \left(\begin{pmatrix} 2(C_{ns} + C_{nQ}) - \frac{10}{3}(C_{s\bar{n}} + C_{Q\bar{n}}) \\ +2C_{n\bar{n}} - \frac{14}{3}(C_{sQ} + C_{nn}) \end{pmatrix} \begin{pmatrix} \frac{10}{3}\sqrt{\frac{2}{3}}(C_{nn} - C_{ns} + C_{nQ}) \\ -2C_{n\bar{n}} - C_{sQ} + 2C_{s\bar{n}} \end{pmatrix} \right) \\ & \left(\begin{pmatrix} \frac{5}{3}\sqrt{(-C_{sn} + 3C_{Qn} - 2C_{n\bar{n}})} \\ -3C_{n\bar{n}} + C_{ns} + 2C_{Qn} \end{pmatrix} \begin{pmatrix} \frac{22\sqrt{2}}{9}(C_{sn} - C_{sQ}) \\ C_{n\bar{n}} - \frac{14}{3}C_{sQ} + \frac{73}{9}C_{sn} - \frac{74}{9}C_{Qn} \end{pmatrix} \right) \\ & \left(\begin{pmatrix} \frac{10}{3}\sqrt{(-C_{sn} - C_{ns} + C_{nQ})} \\ +C_{n\bar{n}} - C_{sQ} + 2C_{s\bar{n}} \end{pmatrix} \begin{pmatrix} -\frac{14}{9}\sqrt{2}(C_{sn} + 2C_{ns}) - \\ \frac{2}{3}C_{Qn} + 6C_{Qn} + 2C_{nQ} \end{pmatrix} \right) \\ & \left(\begin{pmatrix} \frac{8}{3}\sqrt{(-C_{sn} - C_{ns} + C_{nQ})} \\ C_{s\bar{n}} + 3C_{Q\bar{n}} \end{pmatrix} \begin{pmatrix} \frac{16}{9}\sqrt{2}(C_{sn} - C_{s\bar{n}}) \\ C_{sn} - 3C_{Q\bar{n}} \end{pmatrix} \right) \\ & \left(\begin{pmatrix} \frac{4}{3}\sqrt{(-C_{sn} - C_{ns} + C_{nQ})} \\ -2C_{n\bar{n}} - C_{sQ} + 2C_{s\bar{n}} \end{pmatrix} \begin{pmatrix} \frac{16}{9}\sqrt{2}(C_{sn} - C_{s\bar{n}}) \\ -\frac{8}{9}\sqrt{3}(2C_{n\bar{n}} + \\ +C_{ns} - C_{n\bar{n}}) \end{pmatrix} \right) \\ & \left(\begin{pmatrix} \frac{5}{3}\sqrt{(-C_{sn} - C_{ns} + C_{nQ})} \\ C_{s\bar{n}} + 3C_{Q\bar{n}} \end{pmatrix} \begin{pmatrix} \frac{16}{9}\sqrt{2}(C_{sn} - C_{s\bar{n}}) \\ C_{sn} - 3C_{Q\bar{n}} \end{pmatrix} \right) \\ & \left(\begin{pmatrix} \frac{8}{3}\sqrt{(-C_{sn} - C_{ns} + C_{nQ})} \\ C_{s\bar{n}} + 3C_{Q\bar{n}} \end{pmatrix} \begin{pmatrix} \frac{4}{3}\sqrt{(-C_{sn} - C_{ns} + C_{nQ})} \\ C_{sn} - 3C_{Q\bar{n}} \end{pmatrix} \right) \\ & \left(\begin{pmatrix} \frac{4}{3}\sqrt{(-C_{sn} - C_{ns} + C_{nQ})} \\ C_{s\bar{n}} + 3C_{Q\bar{n}} \end{pmatrix} \begin{pmatrix} \frac{4}{3}\sqrt{(-C_{sn} - C_{ns} + C_{nQ})} \\ C_{sn} - 3C_{Q\bar{n}} \end{pmatrix} \right) \end{aligned}$

TABLE XXXIX. The expressions of CMI Hamiltonian for $mnsQ\bar{n}$ with $I_{nn} = 1$ ($n = u, d; Q = c, d$) pentaquark subsystem. The I (S) represents the isospin (spin) of the pentaquark states.

TABLE XL. The eigenvectors of the $nnns\bar{c}$, $nnns\bar{b}$, $sssn\bar{c}$, $sssn\bar{b}$, $nnss\bar{c}$, and $nnss\bar{b}$ pentaquark subsystems. The masses are all in units of MeV.

$nnns\bar{c}$		$nnn \otimes s\bar{c}$				$nns \otimes n\bar{c}$				$nnns\bar{b}$		$nnn \otimes s\bar{b}$				$nns \otimes n\bar{b}$			
$I(J^P)$	Mass	$\Delta\bar{D}_s^*$	$\Delta\bar{D}_s$	$\Sigma^*\bar{D}^*$	$\Sigma^*\bar{D}$	$\Sigma\bar{D}^*$	$\Sigma\bar{D}$	$\Lambda\bar{D}^*$	$\Lambda\bar{D}$	Mass	ΔB_s^*	ΔB_s	Σ^*B^*	Σ^*B	ΣB^*	ΣB	ΛB^*	ΛB	
$\frac{3}{2}(\frac{5}{2}^-)$	3352.1*	1.000		0.333						6655.3*	1.000	0.333							
$\frac{3}{2}(\frac{3}{2}^-)$	3500.4	0.248	-0.291	0.508	-0.360	-0.088				6861.9	0.297	-0.257	0.496	-0.375	-0.081				
	3343.3*	0.966	0.145	-0.191	-0.150	0.259				6641.6*	0.906	0.380	-0.225	-0.187	0.193				
	3177.4*	-0.072	0.946	0.042	0.264	0.270				6579.1	-0.302	0.889	-0.003	-0.216	-0.323				
$\frac{3}{2}(\frac{1}{2}^-)$	3603.2	-0.442		0.613	-0.046	-0.043				6895.2	-0.411		0.619	-0.044	-0.059				
	3352.9	-0.580		-0.100	0.566	-0.049				6657.2	-0.288		-0.041	0.607	-0.216				
	3246.4	0.684		0.149	0.220	-0.467				6601.0	0.865		-0.152	0.415	0.001				
		$\bar{N}\bar{D}_s^*$	$N\bar{D}_s$								NB_s^*	NB_s							
$\frac{1}{2}(\frac{5}{2}^-)$	3405.4			0.666						6723.1			0.667						
$\frac{1}{2}(\frac{3}{2}^-)$	3376.4	0.159		-0.580	-0.238	-0.069		0.197		6702.4	0.072		-0.507	-0.421	-0.032		0.090		
	3208.5	0.127		-0.056	0.360	0.352		0.427		6599.5	-0.201		-0.298	0.454	-0.105		-0.358		
	3198.9	-0.266		0.087	-0.437	0.4700		0.035		6515.0	-0.263		0.026	0.029	0.583		0.282		
	3022.3*	0.942		-0.072	0.110	0.275		-0.236		6323.7*	0.941		0.077	0.072	0.271		0.254		
$\frac{1}{2}(\frac{1}{2}^-)$	3308.7	0.316	0.108	0.486	0.166	0.044	0.346	0.147		6617.5	0.207	0.157	0.525	0.111	0.072	0.265	0.243		
	3172.2	0.274	-0.332	-0.234	0.260	-0.113	0.328	-0.374		6530.5	0.375	-0.271	-0.109	0.269	-0.129	0.401	-0.334		
	3081.9	-0.219	0.293	0.027	0.377	0.446	0.165	0.175		6472.9	0.053	0.261	0.029	0.293	0.502	-0.175	0.228		
	2999.8	-0.879	-0.208	-0.035	0.263	-0.177	-0.139	-0.227		6307.5	0.876	0.278	-0.063	-0.004	0.343	0.107	0.173		
	2830.9	-0.071	0.866	-0.054	-0.093	0.379	-0.064	0.184		6252.7	-0.217	0.869	0.063	0.164	-0.340	0.071	0.160		
$sssn\bar{c}$		$sss \otimes n\bar{c}$		$ssn \otimes s\bar{c}$						$sssn\bar{b}$		$sss \otimes n\bar{b}$		$ssn \otimes s\bar{b}$					
		$\Omega\bar{D}^*$	$\Omega\bar{D}$	$\Xi^*\bar{D}_s^*$	$\Xi^*\bar{D}_s$	$\Xi\bar{D}_s^*$	$\Xi\bar{D}_s$			ΩB^*	ΩB	$\Xi^*B_s^*$	Ξ^*B_s	ΞB_s^*	ΞB_s				
$\frac{1}{2}(\frac{5}{2}^-)$	3680.3*	1.000		0.333						6996.3*	1.000	0.333							
$\frac{1}{2}(\frac{3}{2}^-)$	3723.6	0.627	-0.349	0.386	-0.345	0.068				7078.5	0.571	-0.404	0.410	-0.331	0.061				
	3655.1	0.772	0.396	-0.375	-0.041	0.226				6976.3	0.733	0.642	0.290	0.179	-0.109				
	3482.5	-0.102	0.849	-0.080	0.319	0.304				6878.1	-0.368	0.653	0.209	-0.285	-0.364				
$\frac{1}{2}(\frac{1}{2}^-)$	3829.0	-0.648		-0.551	-0.025	-0.025				7113.5	-0.681		-0.536	-0.030	-0.042				
	3600.5	-0.676		-0.293	0.427	0.150				6899.2	0.714		0.339	-0.311	-0.250				
	3465.0	0.638		-0.136	-0.433	0.446				6813.0	0.163		0.071	0.522	-0.397				
$nnss\bar{c}$		$nns \otimes s\bar{c}$		$ssn \otimes n\bar{c}$						$nnss\bar{b}$		$nns \otimes s\bar{b}$		$ssn \otimes n\bar{b}$					
		$\Sigma^*\bar{D}_s^*$	$\Sigma^*\bar{D}_s$	$\Sigma\bar{D}_s^*$	$\Sigma\bar{D}_s$	$\Xi^*\bar{D}^*$	$\Xi^*\bar{D}$	$\Xi\bar{D}^*$	$\Xi\bar{D}$	$\Sigma^*B_s^*$	Σ^*B_s	ΣB_s^*	ΣB_s	Ξ^*B^*	Ξ^*B	ΞB^*	ΞB		
$1(\frac{5}{2}^-)$	3519.7	-0.577		-0.577						6829.4	-0.577		-0.577						
$1(\frac{3}{2}^-)$	3613.5	0.298	-0.316	-0.052	0.575	-0.360	0.122			6971.7	0.344	-0.290	-0.049	0.542	-0.396	0.108			
	3505.4	0.612	0.051	0.151	-0.369	-0.239	-0.272			6813.0	-0.532	-0.243	-0.090	-0.410	-0.338	-0.185			
	3367.6	0.006	-0.330	-0.367	0.074	0.266	-0.589			6747.3	-0.244	0.508	-0.101	-0.060	0.366	-0.448			
	3325.2	0.093	-0.453	0.533	-0.021	0.397	0.101			6650.1	0.105	-0.125	0.651	-0.084	0.108	0.444			
$1(\frac{1}{2}^-)$	3715.5	0.497		-0.030	-0.025	-0.643	-0.045	-0.051		7005.1	0.468		-0.029	-0.036	-0.661	-0.051	-0.076		
	3474.5	0.493		0.035	0.065	0.320	0.408	0.158		6772.2	-0.250		0.245	-0.077	-0.317	-0.342	-0.287		
	3349.5	-0.250		0.393	-0.334	0.187	-0.331	0.441		6706.9	0.141		-0.470	0.299	-0.090	0.412	-0.399		
	3219.5	-0.061		0.283	-0.548	0.067	-0.288	-0.441		6609.2	-0.106		-0.295	-0.563	0.099	-0.268	-0.412		
		$\Lambda\bar{D}_s^*$	$\Lambda\bar{D}_s$								ΛB_s^*	ΛB_s							
$0(\frac{5}{2}^-)$	3555.2			0.817						6874.5			-0.817						
$0(\frac{3}{2}^-)$	3523.9	-0.189		-0.706	-0.305	0.198				6853.5	0.082		-0.612	-0.527	0.086				
	3350.8	-0.186		0.128	-0.674	-0.402				6743.1	-0.282		-0.060	0.366	-0.448				
	3215.8	0.513		-0.021	0.397	0.101				6526.5	0.497		-0.121	0.115	-0.626				
$0(\frac{1}{2}^-)$	3451.2	-0.354	-0.140	0.592		-0.386	-0.148			6759.3	-0.245	-0.213	-0.638	0.297	0.257				
	3312.0	0.280	-0.392	0.294		0.473	-0.353			6667.3	0.386	-0.318	-0.138	-0.517	0.360				
	3213.1	0.609	-0.062	-0.027		-0.515	-0.161			6513.0	0.567	0.078	0.097	0.520	0.244				
	3025.8	0.095	-0.489	0.080		-0.033	0.641			6454.6	0.230	-0.514	0.094	-0.114	0.572				

TABLE XLI. The values of $k \cdot |c_i|^2$ for the $nnns\bar{c}$, $nnns\bar{b}$, $sssn\bar{c}$, $sssn\bar{b}$, $nnss\bar{c}$, and $nnss\bar{b}$ pentaquark subsystems. The masses are all in units of MeV.

$nnns\bar{c}$		$nnn \otimes s\bar{c}$					$nns \otimes n\bar{c}$					$nnns\bar{b}$		$nnn \otimes s\bar{b}$					$nns \otimes n\bar{b}$				
$I(J^P)$	Mass	$\Delta\bar{D}_s^*$	$\Delta\bar{D}_s$	$\Sigma^*\bar{D}^*$	$\Sigma^*\bar{D}$	$\Sigma\bar{D}^*$	$\Sigma\bar{D}$	$\Lambda\bar{D}^*$	$\Lambda\bar{D}$	Mass	ΔB_s^*	ΔB_s	Σ^*B^*	Σ^*B	ΣB^*	ΣB	ΛB^*	ΛB					
$\frac{3}{2}(\frac{5}{2}^-)$	3352.1*	111.0		0.0						6655.3*	126.1		0.0										
$\frac{3}{2}(\frac{3}{2}^-)$	3500.4	30.8	58.7	108.7	82.9	5.3				6861.9	59.5	49.6	145.3	94.9	5.6								
	3343.3*	0.0	9.9	0.0	8.6	31.2				6641.6*	0.0	42.5	0.0	0.0	18.6								
	3177.4*	0.0	0.0	0.0	0.0	0.0				6579.1	0.0	0.0	0.0	0.0	36.5								
$\frac{3}{2}(\frac{1}{2}^-)$	3603.2	127.1		223.9		1.7	1.7			6895.2	123.0		251.2		1.7	3.3							
	3352.9	39.2			0.0	154.0	1.2			6657.2	11.6		0.0	196.1	28.7								
	3246.4	0.0			0.0	12.4	55.9			6601.0	0.0		0.0	70.4	0.0								
		$N\bar{D}_s^*$	$N\bar{D}_s$								NB_s^*	NB_s											
$\frac{1}{2}(\frac{5}{2}^-)$	3405.4			60.7						6723.1			80.1										
$\frac{1}{2}(\frac{3}{2}^-)$	3376.4	17.2		0.0	25.3	2.5		23.9		6702.4	4.1		0.0	52.3	0.6		5.8						
	3208.5	7.5		0.0	0.0	11.4		63.3		6599.5	26.5		0.0	0.0	4.5		71.1						
	3198.9	31.7		0.0	0.0	0.0		0.4		6515.0	36.2		0.0	0.0	0.0		29.8						
	3022.3*	0.0		0.0	0.0	0.0		0.0		6323.7*	0.0		0.0	0.0	0.0		0.0						
$\frac{1}{2}(\frac{1}{2}^-)$	3308.7	59.8	8.8	0.0		11.1	1.2	62.5	15.0	6617.5	29.2	18.4	0.0		5.5	2.8	40.9	39.0					
	3172.2	30.3	66.2	0.0		0.0	5.2	27.8	72.9	6530.5	77.3	45.9	0.0		11.6	5.7	66.5	56.9					
	3081.9	9.7	41.5	0.0		0.0	33.7	0.0	11.4	6472.9	1.3	36.4	0.0		0.0	11.1	7.5	19.9					
	2999.8	0.0	15.1	0.0		0.0	0.0	0.0	7.3	6307.5	0.0	4.7	0.0		0.0	0.0	0.0	0.0					
	2830.9	0.0	0.0	0.0		0.0	0.0	0.0	0.0	6252.7	0.0	0.0	0.0		0.0	0.0	0.0	0.0					
$sssn\bar{c}$		$sss \otimes n\bar{c}$					$ssn \otimes s\bar{c}$					$ssn\bar{b}$		$sss \otimes n\bar{b}$					$ssn \otimes s\bar{b}$				
		$\Omega\bar{D}^*$	$\Omega\bar{D}$	$\Xi^*\bar{D}_s^*$	$\Xi^*\bar{D}_s$	$\Xi\bar{D}_s^*$	$\Xi\bar{D}_s$			ΩB^*	ΩB	$\Xi^*B_s^*$	Ξ^*B_s	ΞB_s^*	ΞB_s								
$\frac{1}{2}(\frac{5}{2}^-)$	3680.3*	0		28.2						6996.3*	0		38.2										
$\frac{1}{2}(\frac{3}{2}^-)$	3723.6	107.6	69.9	56.4	75.1	3.8				7078.5	149.4	93.6	95.4	73.0	3.3								
	3655.1	0	70.6	19.8	0.9	31.7				6976.3	0	103.0	22.3	13.9	31.2								
	3482.5	0	0	0	0	27.8				6878.1	0	0	0	0	75.4								
$\frac{1}{2}(\frac{1}{2}^-)$	3829.0	219.2		176.4		0.5	0.6			7113.5	254.9		184.0		0.8	1.8							
	3600.5	0		0		98.1	16.3			6899.2	0		0		59.0	43.5							
	3465.0	0		0		46.6	108.2			6813.0	0		0		115.1	84.3							
$nns\bar{c}$		$nns \otimes s\bar{c}$					$ssn \otimes n\bar{c}$					$nns\bar{b}$		$nns \otimes s\bar{b}$					$ssn \otimes n\bar{b}$				
		$\Sigma^*\bar{D}_s^*$	$\Sigma^*\bar{D}_s$	$\Sigma\bar{D}_s^*$	$\Sigma\bar{D}_s$	$\Xi^*\bar{D}^*$	$\Xi^*\bar{D}$	$\Xi\bar{D}^*$	$\Xi\bar{D}$	$\Sigma^*B_s^*$	Σ^*B_s	ΣB_s^*	ΣB_s	Ξ^*B^*	Ξ^*B	ΞB^*	ΞB						
$1(\frac{5}{2}^-)$	3519.7	66.5				0.0				6829.4	86.3		0.0										
$1(\frac{3}{2}^-)$	3613.5	39.8	66.5	1.9		117.1	78.7	10.3		6971.7	74.4	60.1	2.1		155.6	98.4	10.1						
	3505.4	47.2	1.3	12.9		0.0	24.1	40.2		6813.0	49.6	22.0	5.3		0.0	7.7	21.1						
	3367.6	0.0	17.4	41.9		0.0	0.0	90.4		6747.3	0.0	0.0	5.4		0.0	0.0	96.9						
	3325.2	0.0	0.0	50.2		0.0	0.0	0.0		6650.1	0.0	0.0	122.3		0.0	0.0	29.4						
$1(\frac{1}{2}^-)$	3715.5	152.4	0.7	0.6	230.0		1.6	2.5		7005.1	151.0		0.8	1.3	263.6		2.4	5.6					
	3474.5	0.0		65.2	3.0	0.0		82.2	17.1	6772.2	0.0		34.8	3.9	0.0		62.8	51.5					
	3349.5	0.0		40.5	60.1	0.0		21.6	99.5	6706.9	0.0		98.5	48.9	0.0		64.5	78.6					
	3219.5	0.0		0.0	89.1	0.0		0.0	45.3	6609.2	0.0		4.2	99.4	0.0		0.0	30.2					
		$\Lambda\bar{D}_s^*$	$\Lambda\bar{D}_s$								ΛB_s^*	ΛB_s											
$0(\frac{5}{2}^-)$	3555.2					100.8				6874.5					69.0								
$0(\frac{3}{2}^-)$	3523.9	24.3				0.0	167.7	22.4		6853.5	5.4		0.0	88.5	5.1								
	3350.8	14.9				0.0	0.0	32.7		6743.1	51.4		0.0	0.0	95.0								
	3215.8	0.0				0.0	0.0	0.0		6526.5	0.0		0.0	0.0	0.0								
$0(\frac{1}{2}^-)$	3451.2	73.3	14.7			0.0		67.4	14.4	6759.3	40.3	33.8	0.0		45.0	39.7							
	3312.0	27.7	89.7			0.0		0.0	55.9	6667.3	40.7	60.7	0.0		64.8	51.3							
	3213.1	0.0	1.7			0.0		0.0	5.5	6513.0	0.0	1.4	0.0		0.0	0.0	0.0						
	3025.8	0.0	0.0			0.0		0.0	0.0	6454.6	0.0	0.0	0.0		0.0	0.0	0.0						

TABLE XLII. The eigenvectors of the $nnnc\bar{n}$, $nnnb\bar{n}$, $nnnc\bar{s}$, $nnnb\bar{s}$, $sssc\bar{n}$, $sssb\bar{n}$, $sssc\bar{s}$, and $sssb\bar{s}$ pentaquark subsystems. The masses are all in units of MeV.

$I_{nnn} = 3/2$		$nnn \otimes c\bar{n}$						$nnc \otimes n\bar{n}$						$nnn \otimes b\bar{n}$						$nnb \otimes n\bar{n}$					
J^P	Mass	ΔD^*	ΔD	$\Sigma_c^*\rho(\omega)$	$\Sigma_c^*\pi(\eta)$	$\Sigma_c\rho(\omega)$	$\Sigma_c\pi(\eta)$	$\Lambda_c\rho(\omega)$	$\Lambda_c\pi(\eta)$	Mass	ΔB^*	ΔB	$\Sigma_b^*\rho(\omega)$	$\Sigma_b^*\pi(\eta)$	$\Sigma_b\rho(\omega)$	$\Sigma_b\pi(\eta)$	$\Lambda_b\rho(\omega)$	$\Lambda_b\pi(\eta)$							
$\frac{5}{2}^-$	3248.5*	1.000		0.333						6564.6*	1.000		0.333												
$\frac{3}{2}^-$	3399.7	-0.670	-0.349	-0.438	0.050	0.245				6741.3	-0.630	-0.422	-0.450	0.045	0.220										
	3176.6	0.658	-0.688	-0.264	0.145	-0.228				6537.6*	-0.622	0.776	0.186	-0.021	0.911										
	2937.5	0.344	0.636	0.188	-0.446	-0.191				6288.5	0.465	0.468	-0.247	0.467	0.142										
$\frac{1}{2}^-$	3560.0	0.230		0.606		-0.243	-0.013			6880.1	0.073		-0.570		0.343	0.005									
	3425.0	-0.752		0.103		0.495	-0.021			6753.0	0.768		0.231		0.440	-0.034									
	2943.1	0.617			0.171	0.258	-0.471			6285.6	0.636		0.170		0.245	-0.470									
$I_{nnn} = 1/2$		ND^*	ND																NB^*	NB					
$\frac{5}{2}^-$	3294.6*			0.943							6612.8*			0.943											
$\frac{3}{2}^-$	3305.8	-0.107		0.810	0.106	0.031		0.000		6624.1	-0.074		0.786	0.099	-0.072							0.000			
	3239.1*	-0.045		0.103	-0.022	0.904		0.000		6595.8*	-0.004		-0.186	0.021	-0.911							0.000			
	3007.6*	0.917		-0.188	-0.139	0.180		0.000		6331.8*	0.916		-0.225	-0.153	0.128							0.000			
	2539.8	-0.382		0.039	0.864	-0.026		0.000		5853.0	-0.394		0.041	0.863	-0.021							0.000			
$\frac{1}{2}^-$	3281.2	0.134	0.070	-0.536		-0.518	-0.079	0.557	0.038	6615.6	0.019	0.060	-0.476		-0.598	-0.093	0.541	0.012							
	3114.3	-0.723	-0.228	0.421		-0.547	-0.031	0.039	-0.166	6452.1	-0.693	-0.317	0.518		-0.450	-0.012	0.001	-0.177							
	2939.4	-0.405	0.770	0.171		0.258	-0.471	-0.461	0.135	6308.8	0.429	-0.797	0.212		0.192	0.177	-0.478	0.044							
	2631.4	0.530	0.367	-0.195		0.202	0.171	0.092	0.704	5968.0	0.554	0.335	-0.227		0.180	0.062	0.031	0.721							
	2445.9	-0.122	0.465	0.039		0.007	0.835	0.150	-0.113	5824.7	-0.168	0.386	0.034		0.026	0.857	0.182	-0.044							
$I_{nnn} = 3/2$		$sss \otimes c\bar{n}$						$ssc \otimes s\bar{n}$						$sss \otimes b\bar{n}$						$ssb \otimes s\bar{n}$					
J^P	Mass	ΩD^*	ΩD	$\Omega_c^*\rho(\omega)$	$\Omega_c^*\pi(\eta)$	$\Omega_c\rho(\omega)$	$\Omega_c\pi(\eta)$			Mass	ΩB^*	ΩB	$\Omega_b^*\rho(\omega)$	$\Omega_b^*\pi(\eta)$	$\Omega_b\rho(\omega)$	$\Omega_b\pi(\eta)$									
$\frac{5}{2}^-$	3680.3*	1.000		0.333						6996.3*	1.000		0.333												
$\frac{3}{2}^-$	3741.4	0.776	0.294	-0.384	-0.001	0.260				7075.5	0.744	0.388	0.395	0.015	-0.231										
	3613.0	0.585	-0.666	0.341	-0.193	0.171				6966.9	-0.540	0.829	0.221	-0.035	0.261										
	3431.9	0.236	0.686	-0.181	0.430	0.226				6769.8	0.394	0.404	0.302	-0.470	-0.163										
$\frac{1}{2}^-$	3837.6	0.491		-0.598			0.078	-0.001		7114.5	0.175		0.589		-0.295	0.001									
	3749.8	-0.686		0.120		-0.522	-0.028			7086.1	0.825		0.141		0.444	0.023									
	3434.8	0.537		0.187		0.303	-0.471			6772.6	0.538		0.201		0.293	-0.471									
$I_{nnn} = 3/2$		$nnn \otimes c\bar{s}$						$nnc \otimes n\bar{s}$						$nnn \otimes b\bar{s}$						$nnb \otimes n\bar{s}$					
J^P	Mass	ΔD_s^*	ΔD_s	$\Sigma_c^*\rho(\omega)$	$\Sigma_c^*\pi(\eta)$	$\Sigma_c\rho(\omega)$	$\Sigma_c\pi(\eta)$	$\Lambda_c\rho(\omega)$	$\Lambda_c\pi(\eta)$	Mass	ΔB_s^*	ΔB_s	$\Sigma_b^*\rho(\omega)$	$\Sigma_b^*\pi(\eta)$	$\Sigma_b\rho(\omega)$	$\Sigma_b\pi(\eta)$	$\Lambda_b\rho(\omega)$	$\Lambda_b\pi(\eta)$							
$\frac{5}{2}^-$	3352.0*	1.000		0.333						6655.3*	1.000		0.333												
$\frac{3}{2}^-$	3482.1	-0.534	-0.301	0.487	-0.139	-0.250				6816.9	-0.507	-0.345	0.495	-0.137	-0.235										
	3309.4	0.820	-0.420	-0.241	0.261	-0.194				6630.5	0.723	-0.668	0.189	-0.111	0.270										
	3151.7	0.204	0.861	-0.035	0.367	0.218				6524.6	0.468	0.659	-0.125	0.437	0.141										
$\frac{1}{2}^-$	3635.8	0.207		0.611		-0.237	-0.028			6957.4	0.062		-0.572		0.341	0.011									
	3497.7	0.671		0.123		0.523	-0.078			6824.8	-0.646		-0.257		-0.475	0.116									
	3199.0	0.712		-0.137		-0.203	0.464			6531.4	0.761		0.119		0.169	-0.457									
$I_{nnn} = 1/2$		ND_s^*	ND_s																NB_s^*	NB_s					
$\frac{5}{2}^-$	3414.9*			0.943							6734.8*			0.943											
$\frac{3}{2}^-$	3407.2	-0.095		-0.816	-0.132	-0.183		0.000		6727.3	-0.052		0.771	0.096	0.399							0.000			
	3354.4	-0.027		-0.037	-0.049	0.887		0.000		6712.3	0.024		-0.238	-0.087	0.822							0.000			
	3113.8	0.808		-0.188	-0.327	0.177		0.000		6432.8	0.784		-0.224	-0.369	0.127							0.000			
	2906.1	-0.580		-0.034	0.807	0.016		0.000		6213.6	-0.618		-0.044	0.791	0.020							0.000			
$\frac{1}{2}^-$	3376.8	0.119	0.054	0.539		0.517	0.092	0.555	0.055	6713.1	-0.019	-0.044	0.476		0.598	0.115	0.538	0.018							
	3204.4	-0.577	-0.201	0.472		-0.563	-0.041	0.053	-0.310	6539.0	-0.541	-0.254	0.562		-0.472	-0.017	-0.006	0.334							
	3068.8	0.461	-0.573	-0.268		-0.170	-0.403	-0.477	0.196	6415.3	-0.402	0.639	-0.199		-0.198	-0.406	-0.511	0.067							
	2907.5	0.662	0.274	0.082		-0.103	-0.390	0.133	0.600	6230.4	-0.728	-0.274	-0.102		0.074	0.243	0.054	0.638							
	2779.5	-0.054	0.744	-0.023		-0.075	0.673	0.002	-0.242	6174.4	-0.122	0.671	0.014		0.064	-0.735	0.046	-0.179							
$I_{nnn} = 3/2$		$sss \otimes c\bar{s}$						$ssc \otimes s\bar{s}$						$sss \otimes b\bar{s}$						$ssb \otimes s\bar{s}$					
J^P	Mass	ΩD_s^*	ΩD_s	$\Omega_c^*\phi$	$\Omega_c^*\eta'$	$\Omega_c\phi$	$\Omega_c\eta'$			Mass	ΩB_s^* </														

TABLE XLIII. The eigenvectors of the $nns\bar{c}n$ and $ssnc\bar{n}$ pentaquark subsystems. The masses are all in units of MeV.

$I_{nn} = 1$ J^P	$nns \otimes c\bar{n}$				$nn\bar{c} \otimes s\bar{n}$				$nsc \otimes n\bar{n}$						
	Mass	$\Sigma^* D^*$	$\Sigma^* D$	ΞD^*	ΞD	$\Sigma_c^* K^*$	$\Sigma_c^* K$	$\Sigma_c K^*$	$\Sigma_c K$	$\Xi_c^* \rho(\omega)$	$\Xi_c^* \pi(\eta)$	$\Xi_c' \rho(\omega)$	$\Xi_c' \pi(\eta)$	$\Xi_c \rho(\omega)$	$\Xi_c \pi(\eta)$
$\frac{5}{2}^-$	3408.1*	0.444				0.993				0.274					
	3397.3	-0.896				-0.120				0.508					
$\frac{3}{2}^-$	3515.6	0.698	0.332	-0.041		-0.312	0.032	0.226		-0.466	0.030	-0.383		0.028	
	3452.3	0.179	0.053	-0.135		0.806	0.167	-0.136		0.368	0.015	-0.269		0.001	
	3356.7*	0.185	-0.170	0.130		0.303	-0.054	0.910		0.048	0.040	0.017		0.387	
	3326.1	-0.596	0.666	0.019		-0.276	0.199	0.037		0.287	-0.127	0.303		0.149	
	3223.9*	-0.031	0.054	-0.904		0.094	0.161	-0.203		-0.109	-0.017	-0.173		-0.175	
	3126.0	0.269	0.621	0.209		-0.242	0.661	0.227		-0.146	0.290	-0.533		-0.167	
	2832.0	-0.138	-0.160	0.319		0.134	0.682	-0.088		0.043	-0.560	-0.002		0.367	
$\frac{1}{2}^-$	3641.4	0.326		-0.011	0.010	0.593		-0.190	-0.005	-0.621		0.184	0.011	0.020	0.009
	3535.6	0.743		-0.030	0.027	0.001		0.485	0.018	0.030		0.518	-0.006	-0.051	0.004
	3433.6	-0.104		-0.231	-0.102	-0.577		-0.455	-0.120	0.282		0.224	0.001	-0.470	-0.034
	3321.2	0.025		-0.761	-0.215	-0.336		0.578	0.062	0.149		-0.306	0.002	0.076	-0.080
	3165.3	0.229		-0.276	0.665	-0.158		0.059	-0.483	-0.218		-0.196	0.086	-0.389	0.077
	3112.6	0.503		0.240	-0.462	-0.329		-0.329	0.493	0.060		0.176	-0.349	-0.120	0.063
	2817.7	-0.076		0.481	0.223	-0.214		0.275	0.273	-0.128		0.085	0.222	0.092	0.586
	2737.5	0.139		0.001	0.488	0.152		0.023	0.656	-0.013		0.072	-0.487	-0.111	0.236
$I_{nn} = 0$	ΛD^*	ΛD				$\Lambda_c K^*$	$\Lambda_c K$								
$\frac{5}{2}^-$	3427.3									0.816					
$\frac{3}{2}^-$	3416.4	0.132				-0.336				0.705	0.081	0.184		0.254	
	3361.3	-0.032				0.286				0.051	0.034	-0.758		0.216	
	3192.8	-0.599				0.220				0.148	0.096	-0.140		-0.642	
	3174.0	-0.710				-0.830				0.070	0.036	-0.099		0.232	
	2666.1	-0.344				-0.259				-0.043	-0.752	0.027		0.077	
$\frac{1}{2}^-$	3387.5	-0.177	-0.068			-0.471	-0.047			0.477		0.413	0.059	0.367	0.026
	3248.0	0.715	0.194			0.032	0.166			0.339		-0.493	-0.025	-0.109	0.089
	3188.9	0.101	-0.047			-0.679	-0.014			0.049		0.131	0.059	-0.638	-0.012
	3114.3	-0.430	0.751			0.508	-0.221			-0.283		-0.093	-0.137	0.154	-0.084
	2905.4	-0.479	-0.477			0.121	0.799			-0.135		0.177	0.097	-0.055	-0.222
	2574.9	0.149	-0.397			-0.206	0.071			-0.027		-0.030	-0.740	0.059	-0.006
	2404.5	-0.100	-0.078			0.013	-0.527			-0.030		0.024	-0.009	0.008	-0.720
J^P	$ssn \otimes c\bar{n}$				$ssc \otimes n\bar{n}$				$nsc \otimes s\bar{n}$						
	Mass	$\Xi^* D^*$	$\Xi^* D$	ΞD^*	ΞD	$\Omega_c^* \rho(\omega)$	$\Omega_c^* \pi(\eta)$	$\Omega_c \rho(\omega)$	$\Omega_c \pi(\eta)$	$\Xi_c^* K^*$	$\Xi_c^* K$	$\Xi_c' K^*$	$\Xi_c' K$	$\Xi_c K^*$	$\Xi_c K$
$\frac{5}{2}^-$	3547.2	0.749				-0.375				0.562					
	3538.5*	0.662				-0.927				0.132					
$\frac{3}{2}^-$	3628.3	-0.751	-0.318	-0.059		0.387	-0.019	-0.242		0.400	-0.001	-0.259		0.031	
	3541.8	-0.044	-0.014	-0.165		0.848	0.063	0.112		0.385	0.086	0.065		-0.352	
	3483.8	0.389	-0.398	-0.091		-0.151	0.062	0.598		-0.211	0.135	-0.467		-0.208	
	3468.7	-0.476	0.549	-0.058		-0.248	0.108	-0.667		0.258	-0.152	-0.107		-0.202	
	3372.5*	0.033	-0.069	-0.913		0.173	0.044	-0.301		0.025	0.091	-0.082		0.413	
	3285.3	0.246	0.650	-0.186		-0.125	0.239	0.189		-0.207	0.510	0.225		0.025	
	2865.1*	0.101	0.110	0.300		0.013	0.960	-0.009		-0.096	-0.317	0.058		-0.193	
$\frac{1}{2}^-$	3734.5	0.425		0.000	-0.021	0.593		-0.120	-0.008	-0.614		0.127	-0.000	-0.010	0.006
	3643.0	0.719		0.033	-0.025	0.062		-0.493	-0.003	-0.062		0.529	0.029	0.268	0.021
	3519.6	-0.033		0.280	0.076	-0.600		-0.415	-0.034	0.282		0.189	0.055	-0.486	-0.053
	3413.1	-0.011		-0.725	-0.161	0.290		-0.667	-0.020	0.146		-0.284	-0.045	0.097	-0.114
	3316.4	-0.255		-0.308	0.620	0.408		0.231	-0.043	0.041		-0.139	0.348	0.343	-0.156
	3274.6	-0.470		0.291	-0.436	-0.065		0.162	-0.311	-0.253		-0.271	0.426	-0.135	0.133
	3114.0	0.045		0.445	0.512	-0.171		0.216	0.124	-0.067		0.128	0.015	0.106	0.598
	2776.2*	0.119		0.131	-0.360	0.010		0.004	0.940	0.059		0.082	0.329	0.154	-0.042

TABLE XLIV. The eigenvectors of the $nnsb\bar{n}$ and $ssnb\bar{n}$ pentaquark subsystems. The masses are all in units of MeV.

$I_{nn} = 1$ J^P	Mass	$nns \otimes b\bar{n}$				$nnb \otimes s\bar{n}$				$nsb \otimes n\bar{n}$					
		$\Sigma^* B^*$	$\Sigma^* B$	ΞB^*	ΣB	$\Sigma_b^* K^*$	$\Sigma_b^* K$	$\Sigma_b K^*$	$\Sigma_b K$	$\Xi_b^* \rho(\omega)$	$\Xi_b^* \pi(\eta)$	$\Xi_b' \rho(\omega)$	$\Xi_b' \pi(\eta)$	$\Xi_b \rho(\omega)$	$\Xi_b \pi(\eta)$
$\frac{5}{2}^-$	6730.5*	0.684				0.916				0.116					
	6702.3	-0.729				-0.402				0.566					
$\frac{3}{2}^-$	6853.5	0.670	0.423	-0.062		0.430	0.002	-0.215		-0.428	0.028	0.222		0.047	
	6766.3	0.076	0.030	-0.107		-0.731	-0.161	0.207		0.401	0.009	-0.107		-0.429	
	6709.4*	0.286	-0.356	0.014		0.363	-0.033	0.916		0.051	0.018	0.266		0.053	
	6682.1	0.526	-0.708	0.011		0.055	-0.033	-0.170		0.229	-0.032	0.454		0.039	
	6546.9*	0.009	0.015	-0.906		0.116	0.196	-0.075		-0.161	-0.008	0.087		-0.441	
	6474.1	0.404	0.417	0.239		-0.333	0.682	0.180		-0.214	0.319	0.125		-0.045	
	6138.4	-0.150	-0.134	0.327		0.145	0.684	-0.073		0.046	-0.559	-0.024		-0.174	
$\frac{1}{2}^-$	6947.7	0.096		0.012	0.011	0.579		-0.328	-0.001	0.573		-0.335	-0.005	0.001	-0.008
	6865.8	0.794		-0.036	0.043	-0.185		-0.412	-0.008	0.217		0.443	-0.019	-0.062	0.001
	6761.0	0.109		0.022	0.090	-0.477		-0.597	-0.150	-0.252		-0.293	-0.006	0.451	0.010
	6664.8	0.002		-0.751	-0.331	0.482		-0.431	-0.021	-0.240		0.234	-0.002	-0.002	0.091
	6522.7	-0.058		0.393	-0.784	-0.139		-0.072	-0.271	-0.149		-0.158	0.003	-0.428	0.029
	6468.0	-0.558		-0.152	0.258	0.247		0.328	-0.644	0.132		0.206	-0.338	0.008	0.014
	6136.3	-0.052		0.505	0.231	-0.259		0.250	0.168	-0.139		0.087	0.142	0.052	0.619
	6117.0	-0.174		0.049	-0.381	0.151		0.070	0.678	-0.003		0.062	-0.531	-0.153	0.156
$I_{nn} = 0$		ΛB^*	ΛB			$\Lambda_b K^*$	$\Lambda_b K$								
$\frac{5}{2}^-$	6731.7									0.816					
$\frac{3}{2}^-$	6723.8	-0.054				-0.197				-0.576	-0.042	-0.541		-0.138	
	6713.3	-0.038				-0.409				-0.387	-0.068	0.574		-0.315	
	6510.0	-0.518				0.321				-0.169	-0.097	0.104		0.657	
	6506.9	-0.776				-0.792				-0.125	-0.056	0.075		-0.165	
	5966.2	-0.353				-0.252				0.044	0.751	-0.023		-0.074	
$\frac{1}{2}^-$	6708.9	0.027	0.050			-0.475	-0.012			-0.409		-0.510	-0.073	-0.345	-0.007
	6578.7	-0.710	-0.276			0.006	0.171			0.438		-0.401	-0.015	0.019	0.097
	6512.2	0.031	-0.104			-0.644	-0.015			0.080		0.070	0.060	-0.662	0.003
	6481.9	-0.410	0.816			0.551	-0.064			-0.203		-0.144	0.114	0.143	-0.028
	6251.3	-0.535	-0.356			0.032	0.831			-0.190		0.154	0.029	-0.015	-0.232
	5945.1	0.170	-0.337			-0.235	0.034			0.029		0.038	0.748	-0.070	-0.009
	5726.5	-0.105	-0.075			-0.000	0.524			0.032		-0.023	0.016	-0.004	0.721
		$ssn \otimes b\bar{n}$				$ssb \otimes n\bar{n}$				$nsb \otimes s\bar{n}$					
J^P	Mass	$\Xi^* B^*$	$\Xi^* B$	ΞB^*	ΞB	$\Omega_b^* \rho(\omega)$	$\Omega_b^* \pi(\eta)$	$\Omega_b \rho(\omega)$	$\Omega_b \pi(\eta)$	$\Xi_b^* K^*$	$\Xi_b^* K$	$\Xi_b' K^*$	$\Xi_b' K$	$\Xi_b K^*$	$\Xi_b K$
$\frac{5}{2}^-$	6866.1*	0.904				-0.102				0.503					
	6829.7*	0.428				-0.995				0.284					
$\frac{3}{2}^-$	6965.5	-0.710	-0.413	-0.071		0.353	-0.018	-0.204		-0.435	-0.017	0.231		-0.012	
	6841.5	0.404	-0.566	-0.046		-0.253	-0.034	-0.354		0.326	-0.012	0.468		-0.057	
	6835.0	-0.153	0.204	-0.042		-0.786	-0.043	0.202		0.249	0.090	-0.177		-0.449	
	6818.8	-0.377	0.542	-0.010		-0.255	0.028	-0.863		0.069	-0.013	-0.158		-0.117	
	6699.3*	-0.009	-0.019	-0.923		0.297	0.043	-0.184		0.035	0.122	-0.037		0.402	
	6628.5	0.394	0.407	-0.214		-0.202	0.271	0.119		-0.313	0.541	0.169		0.024	
	6154.2*	-0.109	-0.095	-0.307		0.014	0.960	-0.007		0.101	0.317	-0.050		0.188	
$\frac{1}{2}^-$	7026.3	-0.130		0.026	0.022	0.548		-0.308	-0.005	0.598		-0.321	0.000	-0.004	-0.008
	6976.7	0.818		0.041	-0.049	-0.166		-0.404	0.009	-0.180		-0.448	-0.023	-0.026	-0.001
	6830.4	-0.034		0.042	0.043	-0.501		-0.603	-0.047	-0.211		-0.272	-0.078	0.480	0.011
	6746.5	0.001		-0.754	-0.248	0.491		-0.499	-0.009	0.223		-0.201	-0.023	-0.029	-0.121
	6672.1	0.068		0.350	-0.814	-0.325		-0.232	-0.038	-0.067		0.017	-0.178	-0.390	0.054
	6625.9	-0.538		0.152	-0.247	0.096		0.191	-0.292	-0.223		-0.301	0.523	-0.014	0.028
	6455.6	0.020		0.510	0.351	-0.254		0.195	0.037	-0.116		0.107	-0.004	0.024	0.631
	6140.2*	0.133		0.147	-0.297	0.011		0.010	0.954	0.063		0.088	0.324	0.177	-0.014

TABLE XLV. The eigenvectors of the $nns c\bar{s}$ and $ssn c\bar{s}$ pentaquark subsystems. The masses are all in units of MeV.

$I = 1$		$nns \otimes c\bar{s}$				$nnc \otimes s\bar{s}$				$nsc \otimes n\bar{s}$					
J^P	Mass	$\Sigma^* D_s^*$	$\Sigma^* D_s$	ΞD_s^*	ΞD_s	$\Sigma_c^* \phi$	$\Sigma_c^* \eta'$	$\Sigma_c \phi$	$\Sigma_c \eta'$	$\Xi_c^* K^*$	$\Xi_c^* K$	$\Xi_c' K^*$	$\Xi_c' K$	$\Xi_c K^*$	$\Xi_c K$
$\frac{5}{2}^-$	3534.6*	0.216				0.993				0.388					
	3501.4*	-0.976				0.122				0.427					
$\frac{3}{2}^-$	3600.2	0.592	0.296	-0.013		-0.298	0.106	0.232		-0.531	0.096	0.259		0.110	
	3550.4	-0.201	-0.078	0.128		-0.858	-0.142	0.063		-0.327	-0.034	-0.048		0.380	
	3481.8*	0.292	-0.163	0.096		0.251	-0.099	0.903		-0.011	0.088	0.344		0.188	
	3451.2	-0.694	0.444	0.015		0.274	-0.264	-0.161		-0.267	0.228	-0.325		-0.117	
	3324.7	0.026	-0.022	0.883		0.138	0.207	-0.210		-0.102	-0.076	0.138		-0.434	
	3296.9	0.195	0.823	0.092		-0.124	0.458	0.234		0.042	-0.338	-0.220		0.025	
	3112.6	-0.058	-0.077	0.431		0.043	0.798	-0.041		0.001	0.476	0.003		0.149	
$\frac{1}{2}^-$	3730.1	0.282		-0.006	0.004	-0.585		0.191	0.022	-0.631		0.194	0.027	0.017	0.020
	3614.7	0.700		-0.019	0.016	-0.035		-0.487	0.025	-0.064		-0.542	0.045	0.049	-0.009
	3530.5	-0.117		-0.193	-0.078	-0.577		-0.465	-0.106	-0.274		-0.222	0.007	0.180	0.053
	3403.4	0.048		-0.678	-0.198	0.406		-0.593	-0.069	-0.170		0.302	-0.012	-0.072	0.173
	3330.9	-0.634		-0.008	-0.045	0.163		0.305	-0.553	0.157		0.211	-0.417	0.100	-0.016
	3269.5	-0.094		-0.441	0.665	-0.337		-0.152	-0.241	-0.029		-0.164	-0.092	0.627	0.032
	3104.6	-0.036		0.554	0.291	-0.139		0.204	0.369	-0.057		0.077	0.216	0.126	0.547
	2996.5	0.050		-0.027	0.652	0.050		-0.036	0.695	-0.004		0.033	-0.395	-0.041	0.224
$I = 0$		ΛD_s^*	ΛD_s			$\Lambda_c \phi$	$\Lambda_c \eta'$								
$\frac{5}{2}^-$	3547.0									0.816					
$\frac{3}{2}^-$	3531.4	-0.109				-0.304				-0.699	-0.111	-0.231		-0.244	
	3478.0	0.030				0.293				0.094	0.053	-0.746		0.236	
	3300.7	-0.338				0.421				-0.132	-0.158	0.112		0.683	
	3277.1	-0.800				-0.768				-0.111	-0.147	0.130		-0.038	
	3043.3	-0.483				-0.235				0.017	-0.722	-0.004		0.029	
$\frac{1}{2}^-$	3498.2	-0.154	-0.051			-0.455	-0.051			-0.472		-0.423	-0.077	-0.375	-0.035
	3343.1	0.618	0.189			0.065	0.243			0.383		-0.486	-0.031	-0.137	0.154
	3299.9	0.107	-0.018			-0.679	0.007			-0.029		-0.164	-0.092	0.627	0.032
	3232.2	-0.490	0.605			0.525	-0.253			-0.263		-0.111	-0.262	0.162	-0.130
	3084.2	-0.572	-0.427			0.202	0.649			-0.070		0.127	0.271	-0.064	-0.286
	2929.0	-0.112	0.641			-0.106	0.172			0.014		0.046	-0.653	-0.002	-0.077
	2780.9	0.044	0.030			0.021	-0.651			-0.014		0.011	-0.003	-0.014	0.673
$I = 0$		$ssn \otimes c\bar{s}$				$ssc \otimes n\bar{s}$				$nsc \otimes s\bar{s}$					
J^P	Mass	$\Xi^* D_s^*$	$\Xi^* D_s$	ΞD_s^*	ΞD_s	$\Omega_c^* K^*$	$\Omega_c^* K$	$\Omega_c K^*$	$\Omega_c K$	$\Xi_c^* \phi$	$\Xi_c^* \eta'$	$\Xi_c' \phi$	$\Xi_c' \eta'$	$\Xi_c \phi$	$\Xi_c \eta'$
$\frac{5}{2}^-$	3666.8	-0.325				0.783				-0.554					
	3644.5*	-0.946				0.622				0.162					
$\frac{3}{2}^-$	3718.9	-0.685	-0.297	-0.030		0.432	-0.066	-0.242		-0.432	0.055	0.270		-0.016	
	3660.4	-0.016	-0.036	-0.130		0.823	0.104	0.139		-0.409	-0.078	-0.081		0.352	
	3606.2	-0.435	0.324	0.074		-0.200	0.115	0.586		-0.203	0.184	-0.770		0.148	
	3589.5	0.551	-0.392	0.056		-0.248	0.188	-0.673		0.243	-0.208	-0.146		-0.195	
	3470.5	0.022	-0.060	-0.897		-0.181	-0.127	0.275		-0.064	-0.106	0.092		-0.420	
	3438.1	0.188	0.802	-0.120		-0.043	0.308	0.224		-0.113	0.424	0.233		0.001	
	3208.3*	0.053	0.067	0.393		0.004	0.909	-0.006		0.036	0.374	-0.029		0.177	
$\frac{1}{2}^-$	3834.0	-0.359	0.006	0.012		0.609		-0.149	-0.022	-0.619		0.150	0.016	-0.004	-0.002
	3733.4	0.711	0.017	-0.013		0.025		-0.501	0.021	-0.004		0.536	-0.001	-0.002	-0.003
	3636.0	0.011		-0.237	-0.054	-0.583		-0.455	-0.047	0.278		0.194	0.062	-0.492	-0.056
	3512.7	-0.015		-0.681	-0.175	0.348		-0.643	-0.028	-0.178		0.288	0.044	-0.082	0.168
	3466.1	0.590		0.026	-0.083	0.211		0.246	-0.353	-0.145		-0.275	0.517	0.097	-0.030
	3414.1	0.115		-0.476	0.645	-0.337		-0.088	-0.292	-0.201		-0.092	-0.036	-0.354	0.246
	3271.8	0.031		0.489	0.494	-0.098		0.194	0.277	-0.047		0.113	0.109	0.156	0.558
	3102.6	0.054		0.117	-0.547	-0.001		-0.029	0.842	-0.021		-0.015	-0.362	-0.094	0.113

TABLE XLVI. The eigenvectors of the $nnsb\bar{s}$ and $ssnb\bar{s}$ pentaquark subsystems. The masses are all in units of MeV.

$I = 1$	J^P	Mass	$nns \otimes b\bar{s}$				$nnb \otimes s\bar{s}$				$nsb \otimes n\bar{s}$					
			$\Sigma^* B_s^*$	$\Sigma^* B_s$	ΞB_s^*	ΣB_s	$\Sigma_b^* \phi$	$\Sigma_b^* \eta'$	$\Sigma_b \phi$	$\Sigma_b \eta'$	$\Xi_b^* K^*$	$\Xi_b^* K$	$\Xi_b' K^*$	$\Xi_b' K$	$\Xi_b K^*$	$\Xi_b K$
$\frac{5}{2}^-$	6858.8*	0.116					0.975				0.429					
	6714.4*	-0.993					0.222				0.386					
$\frac{3}{2}^-$	6903.1	0.423	0.293	-0.022			-0.318	0.188	0.165		-0.580	0.168	0.263		0.138	
	6873.5	0.156	0.117	-0.074			-0.880	-0.091	0.119		0.262	0.065	0.022		-0.416	
	6843.4*	0.098	-0.037	-0.006			-0.177	0.024	-0.944		0.107	-0.007	0.415		0.125	
	6691.8	-0.761	0.613	-0.002			0.174	-0.160	0.182		-0.187	0.120	-0.307		-0.031	
	6614.1	0.401	0.667	0.188			-0.045	0.630	0.100		0.091	-0.262	-0.155		0.201	
	6575.7	-0.202	-0.266	-0.734			-0.244	-0.195	0.154		-0.109	-0.319	0.024		-0.409	
	6396.7	-0.081	-0.083	0.648			0.010	0.704	-0.002		-0.034	0.447	0.021		0.032	
$\frac{1}{2}^-$	7049.6	0.044		0.009	0.006		-0.556		0.337	0.009	-0.571		0.357	0.012	-0.003	0.020
	6910.5	0.547		-0.022	0.018		0.156		0.313	-0.162	-0.328		-0.539	0.152	0.146	-0.000
	6867.0	0.211		0.003	0.057		-0.522		-0.699	-0.083	0.164		0.169	0.056	-0.447	-0.016
	6708.1	-0.026		0.537	0.259		-0.579		0.469	0.026	0.271		-0.230	0.007	0.006	-0.290
	6622.6	-0.782		0.013	-0.064		-0.077		-0.151	0.599	0.102		0.124	-0.352	0.122	-0.009
	6560.6	-0.187		-0.392	0.600		-0.203		-0.215	-0.347	-0.092		-0.104	-0.294	-0.424	0.056
	6382.2	-0.064		0.732	-0.014		-0.099		0.074	0.447	-0.045		0.006	0.278	0.032	0.456
	6354.1	0.060		0.143	0.752		-0.042		0.074	-0.535	-0.004		-0.047	0.320	-0.013	-0.347
$I = 0$	ΛB_s^*	ΛB_s					$\Lambda_b \phi$	$\Lambda_b \eta'$								
$\frac{5}{2}^-$	6864.0										0.816					
$\frac{3}{2}^-$	6855.3	-0.026					-0.116				-0.489	-0.039	-0.642		-0.079	
	6839.0	-0.021					-0.426				0.487	0.104	-0.458		0.343	
	6633.6	-0.007					-0.685				-0.085	-0.090	0.052		0.643	
	6544.8	-0.740					-0.569				-0.200	-0.365	0.112		0.213	
	6316.0	-0.672					-0.106				-0.065	0.656	0.030		0.021	
$\frac{1}{2}^-$	6833.4	0.018	0.024				-0.459	-0.014			-0.400		-0.516	-0.099	-0.352	-0.009
	6646.5	0.447	0.205				0.088	-0.384			-0.487		0.413	0.030	-0.085	-0.228
	6636.4	-0.053	-0.045				-0.674	-0.061			0.126		0.021	0.082	-0.641	0.028
	6528.8	-0.383	0.592				0.566	-0.066			-0.166		-0.174	-0.397	0.199	-0.031
	6365.2	-0.779	-0.340				-0.054	-0.657			-0.031		0.018	0.157	-0.012	-0.250
	6281.0	-0.197	0.697				-0.061	0.149			0.046		0.067	-0.619	-0.029	-0.031
	6116.0	0.070	0.063				-0.005	0.625			-0.017		0.010	0.016	-0.004	0.683
			$ssn \otimes b\bar{s}$				$ssb \otimes n\bar{s}$				$nsb \otimes s\bar{s}$					
J^P	Mass		$\Xi^* B_s^*$	$\Xi^* B_s$	ΞB_s^*	ΞB_s	$\Omega_b^* K^*$	$\Omega_b^* K$	$\Omega_b K^*$	$\Omega_b K$	$\Xi_b^* \phi$	$\Xi_b^* \eta'$	$\Xi_b' \phi$	$\Xi_b' \eta'$	$\Xi_b \phi$	$\Xi_b \eta'$
$\frac{5}{2}^-$	6972.5	-0.597					-0.597				0.577					
	6937.8	-0.802					-0.802				0.816					
$\frac{3}{2}^-$	7047.1	-0.652	-0.369	-0.044			-0.375	0.073	0.214		-0.475	0.040	0.248		0.013	
	6959.9	0.182	-0.216	-0.038			-0.596	-0.057	-0.520		-0.353	-0.023	-0.390		0.185	
	6953.1	-0.112	0.155	-0.001			-0.561	-0.050	0.569		0.151	0.091	-0.331		-0.432	
	6916.6	-0.585	0.711	0.000			-0.288	0.072	-0.558		-0.169	0.076	-0.085		0.041	
	6798.3	0.394	0.494	0.247			-0.255	0.278	0.194		-0.194	0.510	0.128		0.181	
	6784.7	0.167	0.197	-0.875			-0.204	-0.280	0.105		-0.176	0.080	0.115		-0.366	
	6496.8*	-0.065	-0.063	-0.412			-0.001	0.910	-0.001		0.041	0.366	-0.024		0.165	
$\frac{1}{2}^-$	7130.0	-0.085		0.026	0.016		0.552		-0.332	-0.010	0.586		-0.334	-0.006	-0.006	0.000
	7057.6	0.762		0.027	-0.031		-0.205		-0.417	0.056	0.229		0.462	-0.028	0.262	0.008
	6950.4	-0.020		0.039	0.020		-0.492		-0.607	-0.067	0.209		0.274	0.078	-0.483	-0.012
	6837.6	-0.023		-0.685	-0.234		0.518		-0.503	-0.006	0.251		-0.207	-0.040	-0.032	-0.189
	6801.1	-0.632		0.038	0.032		0.181		0.199	-0.362	0.158		0.261	-0.515	-0.074	0.003
	6759.4	-0.083		0.398	-0.780		-0.281		-0.179	-0.245	-0.139		-0.088	-0.073	-0.394	0.083
	6608.4	0.020		0.582	0.382		-0.177		0.153	0.100	-0.092		0.091	0.031	0.046	0.610
	6477.4	0.074		0.171	-0.435		0.002		-0.012	0.889	-0.026		-0.028	-0.369	-0.139	0.048

TABLE XLVII. The eigenvectors of the $cccc\bar{n}$, $cccc\bar{s}$, $bbbb\bar{n}$, $bbbb\bar{s}$, $cccb\bar{n}$, $cccb\bar{s}$, $bbbc\bar{n}$, $bbbc\bar{s}$, $ccb\bar{b}$, and $ccb\bar{s}$ pentaquark subsystems. The masses are all in units of MeV.

J^P	Mass	$ccc \otimes c\bar{n}$		$ccc \otimes c\bar{s}$			$bbb \otimes b\bar{n}$		$bbb \otimes b\bar{s}$					
		$\Omega_{ccc}D^*$	$\Omega_{ccc}D$	Mass	$\Omega_{ccc}D_s^*$	$\Omega_{ccc}D_s$	Mass	$\Omega_{bbb}B^*$	$\Omega_{bbb}B$					
$\frac{3}{2}^-$	6761.4	0.456	-0.354	6863.7	0.456	-0.354		19647.2	0.456	-0.354	19736.2	0.456	-0.354	
$\frac{1}{2}^-$	6867.4	-0.577		6971.5	0.577			19681.1	-0.577		19772.6	0.577		
J^P	Mass	$ccc \otimes b\bar{n}$			$ccb \otimes c\bar{n}$			$ccc \otimes b\bar{s}$			$ccb \otimes c\bar{s}$			
		$\Omega_{ccc}B^*$	$\Omega_{ccc}B$	$\Omega_{ccb}^*D^*$	Ω_{ccb}^*D	$\Omega_{ccb}D^*$	$\Omega_{ccb}D$	Mass	$\Omega_{ccc}B_s^*$	$\Omega_{ccc}B_s$	$\Omega_{ccb}^*D_s^*$	$\Omega_{ccb}^*D_s$	$\Omega_{ccb}D_s^*$	$\Omega_{ccb}D_s$
$\frac{5}{2}^-$	10110.3*	1.000			0.333			10201.0*	1.000			0.333		
$\frac{3}{2}^-$	10117.6*	0.950	0.188	0.217	0.140	-0.255		10209.5*	0.939	0.197	0.234	0.127	-0.258	
	10078.2*	-0.261	0.917	0.333	-0.019	0.174		10167.7	-0.289	0.895	0.345	-0.043	0.169	
	9961.3	0.172	0.352	0.372	-0.450	-0.230		10062.0	0.184	0.399	0.350	-0.452	-0.231	
$\frac{1}{2}^-$	10134.4*	0.914		-0.333		-0.201	-0.121	10228.3	0.891		-0.365		-0.188	-0.106
	10061.5	-0.246		0.498		-0.415	-0.064	10166.1	-0.290		0.477		-0.430	-0.065
	9945.5	0.323		0.220		0.397	-0.451	10047.7	0.349		0.217		0.387	-0.455
J^P	Mass	$bbb \otimes c\bar{n}$			$bbc \otimes b\bar{n}$			$bbb \otimes c\bar{s}$			$bbc \otimes b\bar{s}$			
		$\Omega_{bbb}D^*$	$\Omega_{bbb}D$	$\Omega_{bbc}^*B^*$	Ω_{bbc}^*B	$\Omega_{bbc}B^*$	$\Omega_{bbc}B$	Mass	$\Omega_{bbb}D_s^*$	$\Omega_{bbb}D_s$	$\Omega_{bbc}^*B_s^*$	$\Omega_{bbc}^*B_s$	$\Omega_{bbc}B_s^*$	$\Omega_{bbc}B_s$
$\frac{5}{2}^-$	16318.2*	1.000		0.333				16421.8*	1.000		0.333			
$\frac{3}{2}^-$	16537.8	-0.004	-0.052	0.508	-0.375	-0.213		16625.6	-0.009	-0.056	0.509	-0.373	-0.213	
	16318.2*	0.999	-0.001	0.053	0.217	-0.139		16421.8*	0.999	-0.001	0.051	0.218	-0.140	
	16175.9*	0.001	0.999	0.189	0.187	0.204		16276.8*	0.001	0.998	0.187	0.188	0.204	
$\frac{1}{2}^-$	16573.5	-0.085		-0.634		0.135	0.146	16663.2	-0.092		-0.634		0.139	0.141
	16522.8	-0.074		0.045		0.580	-0.323	16611.2	-0.086		0.052		0.580	-0.321
	16315.2*	0.994		0.054		0.127	-0.130	16418.3*	0.992		0.049		0.121	0.315
J^P	Mass	$bbc \otimes c\bar{n}$				$ccb \otimes b\bar{n}$								
		$\Omega_{bbc}^*D^*$	Ω_{bbc}^*D	$\Omega_{bbc}D^*$	$\Omega_{bbc}D$	$\Omega_{ccb}^*B^*$	Ω_{ccb}^*B	$\Omega_{ccb}B^*$	$\Omega_{ccb}B$					
$\frac{5}{2}^-$	13244.0	-0.577				-0.577								
$\frac{3}{2}^-$	13382.7	-0.018	-0.052	-0.013		0.566	-0.372	0.452						
	13231.0	0.621	0.033	-0.072		-0.077	-0.454	-0.251						
	13220.5	-0.155	-0.167	-0.586		-0.319	-0.040	0.410						
	13099.6	0.250	-0.620	0.310		0.209	0.265	-0.096						
$\frac{1}{2}^-$	13413.9	-0.099		0.053	0.024	-0.710		-0.222	-0.317					
	13241.7	0.641		0.220	-0.107	-0.124		0.385	0.180					
	13211.5	0.197		-0.535	0.052	-0.078		-0.271	0.510					
	13086.1	0.310		0.155	0.634	0.173		-0.301	-0.155					
J^P	Mass	$bbc \otimes c\bar{s}$				$ccb \otimes b\bar{s}$								
		$\Omega_{bbc}^*D_s^*$	$\Omega_{bbc}^*D_s$	$\Omega_{bbc}D_s^*$	$\Omega_{bbc}D_s$	$\Omega_{ccb}^*B_s^*$	$\Omega_{ccb}^*B_s$	$\Omega_{ccb}B_s^*$	$\Omega_{ccb}B_s$					
$\frac{5}{2}^-$	13341.1	-0.577				-0.577								
$\frac{3}{2}^-$	13469.5	-0.025	-0.056	-0.013		0.569	-0.366	0.453						
	13329.2	0.647	0.041	0.051		-0.122	-0.448	-0.167						
	13319.3	-0.041	-0.142	-0.596		-0.292	0.052	0.448						
	13200.3	-0.226	0.626	-0.293		0.218	0.282	-0.104						
$\frac{1}{2}^-$	13501.8	-0.109		0.057	0.025	-0.713		-0.220	-0.308					
	13343.3	0.648		0.232	-0.085	-0.108		0.380	0.172					
	13307.0	0.201		-0.531	0.055	-0.069		-0.265	0.515					
	13186.7	0.286		0.150	0.637	-0.177		0.313	0.164					

TABLE XLVIII. The eigenvectors of the $cccc\bar{c}$, $cccc\bar{b}$, $bbbb\bar{c}$, $bbbb\bar{b}$, $cccb\bar{c}$, $cccb\bar{b}$, $bbbc\bar{c}$, $bbbc\bar{b}$, $ccb\bar{c}$, and $ccb\bar{b}$ pentaquark subsystems. The masses are all in units of MeV.

$cccc\bar{c}$		$ccc \otimes c\bar{c}$		$cccc\bar{b}$		$ccc \otimes c\bar{b}$			$bbbb\bar{c}$		$bbb \otimes b\bar{c}$		$bbbb\bar{b}$		$bbb \otimes b\bar{b}$			
J^P	Mass	$\Omega_{ccc}J/\psi$	$\Omega_{ccc}\eta_c$	Mass	$\Omega_{ccc}B_c^*$	$\Omega_{ccc}B_c$	Mass	$\Omega_{bbb}B_c^*$	$\Omega_{bbb}B_c$	Mass	$\Omega_{bbb}\Upsilon$	$\Omega_{bbb}\eta_b$	Mass	$\Omega_{bbb}\Upsilon$	$\Omega_{bbb}\eta_b$	Mass	$\Omega_{bbb}\Upsilon$	$\Omega_{bbb}\eta_b$
$\frac{3}{2}^-$	7863.6	0.456	-0.354	11130.0	0.456	-0.354	20651.7	0.456	-0.354	23774.8	0.456	-0.354	20698.8	-0.577	23820.7	0.577		
$\frac{1}{2}^-$	7948.8	-0.577		11177.2	0.577													
		$ccc \otimes b\bar{c}$		$ccb \otimes c\bar{c}$		$ccc \otimes b\bar{b}$		$ccb \otimes c\bar{b}$										
J^P	Mass	$\Omega_{ccc}B_c^*$	$\Omega_{ccc}B_c$	Ω_{ccb}^*J/ψ	$\Omega_{ccb}\eta_c$	$\Omega_{ccb}J/\psi$	$\Omega_{ccb}\eta_c$	Mass	$\Omega_{ccc}\Upsilon$	$\Omega_{ccc}\eta_b$	$\Omega_{ccb}^*B_c^*$	$\Omega_{ccb}^*B_c$	$\Omega_{ccb}B_c^*$	$\Omega_{ccb}B_c$				
$\frac{5}{2}^-$	11123.6*	1.000		0.333				14245.9*	1.000		0.333							
$\frac{3}{2}^-$	11136.8	0.812	0.236	-0.361	-0.008	0.275		14372.6	-0.046	-0.120	0.521	-0.352	-0.209					
	11101.4	0.569	-0.524	0.396	-0.279	0.102		14245.7*	0.999	-0.016	0.030	0.229	-0.242					
	11037.7	0.130	0.818	0.095	-0.380	-0.250		14181.9*	0.011	0.993	0.154	0.214	0.215					
$\frac{1}{2}^-$	11174.7	-0.543		-0.587		0.034	-0.001	14411.0	0.130		-0.626		0.199	0.087				
	11137.0	-0.657		0.172		-0.519	-0.039	14356.9	-0.206		0.126		0.571	-0.297				
	11047.6	0.523		0.180		0.316	-0.470	14238.0*	0.969		0.004		0.068	0.355				
		$bbb \otimes c\bar{c}$		$bbc \otimes b\bar{c}$		$bbb \otimes c\bar{b}$		$bbc \otimes b\bar{b}$										
J^P	Mass	$\Omega_{bbb}J/\psi$	$\Omega_{bbb}\eta_c$	$\Omega_{bbc}^*B_c^*$	$\Omega_{bbc}^*B_c$	$\Omega_{bbc}B_c^*$	$\Omega_{bbc}B_c$	Mass	$\Omega_{bbb}B_c^*$	$\Omega_{bbb}B_c$	$\Omega_{bbc}^*\Upsilon$	$\Omega_{bbc}^*\eta_b$	$\Omega_{bbc}\Upsilon$	$\Omega_{bbc}\eta_b$				
$\frac{5}{2}^-$	17406.6*	1.000		0.333				20648.4*	1.000		0.333							
$\frac{3}{2}^-$	17535.4	-0.045	-0.093	0.517	-0.358	-0.214		20653.8	0.689	0.225	0.429	-0.079	-0.281					
	17406.3*	0.999	-0.009	-0.031	-0.231	0.240		20643.6	0.724	-0.248	0.333	-0.362	0.084					
	17291.0*	0.005	0.996	-0.168	-0.203	-0.211		20577.6*	0.026	0.942	0.038	0.291	0.249					
$\frac{1}{2}^-$	17578.2	-0.133		-0.631		0.169	0.106	20691.1	-0.505		0.598		-0.034	-0.019				
	17522.6	-0.187		0.092		0.580	-0.296	20652.8	-0.662		-0.156		0.522	0.033				
	17399.1*	0.973		0.010		0.073	0.351	20606.5	0.554		-0.158		-0.311	0.470				
		$bbc \otimes c\bar{c}$		$ccb \otimes b\bar{c}$		$ccb \otimes c\bar{b}$												
J^P	Mass	Ω_{bbc}^*J/ψ	$\Omega_{bbc}\eta_c$	Ω_{bbc}^*J/ψ	$\Omega_{bbc}\eta_c$	$\Omega_{ccb}^*B_c^*$	$\Omega_{ccb}^*B_c$	$\Omega_{ccb}B_c^*$	$\Omega_{ccb}B_c$									
$\frac{5}{2}^-$	14294.8	-0.577				-0.577												
$\frac{3}{2}^-$	14374.9	-0.070	-0.088	-0.019		0.592	-0.316	0.450										
	14298.0	0.631	-0.057	0.370		-0.138	-0.325	0.056										
	14274.4	-0.251	0.126	0.507		-0.224	0.242	0.471										
	14196.8	-0.074	0.624	-0.225		0.229	0.390	-0.128										
$\frac{1}{2}^-$	14405.8	0.202		-0.074	-0.025	-0.722		-0.200	-0.242									
	14317.8	0.666		0.277	0.033	-0.008		-0.348	-0.156									
	14252.8	0.225		-0.505	0.120	-0.012		0.273	-0.522									
	14185.1	0.146		0.155	0.633	0.184		-0.354	-0.248									
		$bbc \otimes c\bar{b}$		$ccb \otimes b\bar{b}$		$ccb \otimes c\bar{b}$												
J^P	Mass	$\Omega_{bbc}^*B_c^*$	$\Omega_{bbc}^*B_c$	$\Omega_{bbc}^*B_c^*$	$\Omega_{bbc}B_c$	$\Omega_{ccb}^*\Upsilon$	$\Omega_{ccb}^*\eta_b$	$\Omega_{ccb}\Upsilon$	$\Omega_{ccb}\eta_b$									
$\frac{5}{2}^-$	17476.5 [†]	-0.577				-0.577												
$\frac{3}{2}^-$	17554.2	0.601	-0.308	0.440		-0.052	-0.117	-0.008										
	17478.9	-0.082	-0.289	-0.051		0.669	-0.166	0.315										
	17457.4	0.265	-0.123	-0.492		-0.144	0.193	0.530										
	17416.2 [†]	-0.184	-0.472	0.076		0.043	0.581	-0.253										
$\frac{1}{2}^-$	17575.8	-0.723		-0.195	-0.226	0.219		-0.080	-0.026									
	17496.3	0.038		0.317	0.150	0.675		0.281	0.088									
	17437.4	0.069		-0.365	0.438	-0.224		0.458	-0.277									
	17404.9	-0.164		0.300	0.389	0.036		0.257	0.576									

TABLE XLIX. The eigenvectors of the $cccn\bar{c}$, $cccn\bar{b}$, $cccs\bar{c}$, $cccn\bar{b}$, $bbbn\bar{c}$, $bbbn\bar{b}$, $bbbs\bar{c}$, and $bbbs\bar{b}$ pentaquark subsystems. The masses are all in units of MeV.

J^P	$ccc \otimes n\bar{c}$						$ccn \otimes c\bar{c}$						$ccc \otimes n\bar{b}$						$ccn \otimes c\bar{b}$						
	Mass	$\Omega_{ccc}D^*$	$\Omega_{ccc}D$	Ξ_{cc}^*J/ψ	$\Xi_{cc}^*\eta_c$	$\Xi_{cc}J/\psi$	$\Xi_{cc}\eta_c$	Mass	$\Omega_{ccc}B^*$	$\Omega_{ccc}B$	$\Xi_{cc}^*B_c^*$	$\Xi_{cc}^*B_c$	$\Xi_{cc}B_c^*$	$\Xi_{cc}B_c$	Mass	$\Omega_{ccc}B_s^*$	$\Omega_{ccc}B_s$	$\Omega_{cc}^*B_c^*$	$\Omega_{cc}^*B_c$	$\Omega_{cc}B_c^*$	$\Omega_{cc}B_c$				
$\frac{5}{2}^-$	6794.2*	1.000		0.333				10110.3*	1.000		0.333														
$\frac{3}{2}^-$	6797.2*	0.938	0.099	-0.239	-0.090	0.288		10110.7*	0.995	-0.055	-0.004	-0.235	0.240												
	6773.0	0.347	-0.314	0.487	-0.362	-0.050		10080.3	0.083	0.899	0.412	0.002	0.057												
	6638.0*	0.017	0.944	0.041	0.288	0.250		9999.3	-0.047	0.434	0.356	-0.408	0.295												
$\frac{1}{2}^-$	6863.3	-0.588		-0.574		-0.010	0.000	10131.3*	0.900		-0.371		-0.134	-0.138											
	6788.6	-0.651		0.231		-0.494	-0.075	10035.8	0.388		-0.499		0.344	0.164											
	6700.8	0.480		0.158		0.355	-0.465	9965.7	0.200		-0.144		-0.484	0.420											
J^P	$ccc \otimes s\bar{c}$						$ccn \otimes c\bar{c}$						$ccc \otimes s\bar{b}$						$ccn \otimes c\bar{b}$						
	Mass	$\Omega_{ccc}D_s^*$	$\Omega_{ccc}D_s$	Ω_{cc}^*J/ψ	$\Omega_{cc}^*\eta_c$	$\Omega_{cc}J/\psi$	$\Omega_{cc}\eta_c$	Mass	$\Omega_{ccc}B_s^*$	$\Omega_{ccc}B_s$	$\Omega_{cc}^*B_c^*$	$\Omega_{cc}^*B_c$	$\Omega_{cc}B_c^*$	$\Omega_{cc}B_c$	Mass	$\Omega_{ccc}B_s^*$	$\Omega_{ccc}B_s$	$\Omega_{cc}^*B_c^*$	$\Omega_{cc}^*B_c$	$\Omega_{cc}B_c^*$	$\Omega_{cc}B_c$				
$\frac{5}{2}^-$	6897.7*	1.000		0.333				10201.0*	1.000		0.333														
$\frac{3}{2}^-$	6899.3*	0.958	0.085	-0.208	-0.115	0.283		10202.4*	0.983	-0.102	0.042	-0.252	0.231												
	6880.7	0.287	-0.320	0.502	-0.356	-0.068		10173.7	0.167	0.837	0.449	-0.026	0.004												
	6738.1*	0.011	0.943	-0.039	-0.287	-0.252		10099.4	-0.072	0.538	0.305	-0.397	-0.308												
$\frac{1}{2}^-$	6971.7	0.589		-0.573		-0.011	-0.000	10228.8	0.858		-0.416		-0.112	-0.115											
	6888.7	-0.655		0.234		-0.490	-0.080	10136.6	0.465		0.464		-0.357	-0.173											
	6800.4	0.473		0.156		0.360	-0.465	10066.0	0.219		-0.138		-0.480	0.423											
J^P	$bbb \otimes n\bar{c}$						$bbn \otimes b\bar{c}$						$bbb \otimes n\bar{b}$						$bbn \otimes b\bar{b}$						
	Mass	$\Omega_{bbb}D^*$	$\Omega_{bbb}D$	$\Xi_{bb}^*B_c^*$	$\Xi_{bb}^*B_c$	$\Xi_{bb}B_c^*$	$\Xi_{bb}B_c$	Mass	$\Omega_{bbb}B^*$	$\Omega_{bbb}B$	$\Xi_{bb}^*\Upsilon$	$\Xi_{bb}^*\eta_b$	$\Xi_{bb}\Upsilon$	$\Xi_{bb}\eta_b$	Mass	$\Omega_{bbb}B_s^*$	$\Omega_{bbb}B_s$	$\Omega_{bb}^*B_c^*$	$\Omega_{bb}^*B_c$	$\Omega_{bb}B_c^*$	$\Omega_{bb}B_c$				
$\frac{5}{2}^-$	16318.2*	1.000		0.333				19634.3*	1.000		0.333														
$\frac{3}{2}^-$	16538.8	-0.046	-0.053	0.510	-0.365	-0.223		19648.7	-0.540	-0.256	0.483	-0.150	-0.263												
	16317.8*	0.999	-0.006	0.031	0.231	-0.239		19628.7	0.839	-0.236	0.248	-0.330	0.145												
	16175.8*	0.004	0.999	0.188	0.188	0.203		19582.2*	0.064	0.937	0.035	0.302	0.241												
$\frac{1}{2}^-$	16583.0	0.064		-0.626		0.195	0.116	19679.0	0.364		0.620		-0.119	-0.036											
	16535.5	-0.102		0.112		0.565	-0.330	19650.4	0.660		-0.026		0.545	-0.035											
	16314.8*	0.993		0.060		0.113	0.316	19604.5	0.658		-0.148		-0.242	0.469											
J^P	$bbb \otimes s\bar{c}$						$bbs \otimes b\bar{c}$						$bbb \otimes s\bar{b}$						$bbs \otimes b\bar{b}$						
	Mass	$\Omega_{bbb}D_s^*$	$\Omega_{bbb}D_s$	$\Omega_{bb}^*B_c^*$	$\Omega_{bb}^*B_c$	$\Omega_{bb}B_c^*$	$\Omega_{bb}B_c$	Mass	$\Omega_{bbb}B_s^*$	$\Omega_{bbb}B_s$	$\Omega_{bb}^*\Upsilon$	$\Omega_{bb}^*\eta_b$	$\Omega_{bb}\Upsilon$	$\Omega_{bb}\eta_b$	Mass	$\Omega_{bbb}B_s^*$	$\Omega_{bbb}B_s$	$\Omega_{bb}^*B_c^*$	$\Omega_{bb}^*B_c$	$\Omega_{bb}B_c^*$	$\Omega_{bb}B_c$				
$\frac{5}{2}^-$	16421.8*	1.000		0.333				19725.1*	1.000		0.333														
$\frac{3}{2}^-$	16616.7	-0.074	-0.047	0.509	-0.360	-0.231		19736.5	0.764	0.163	0.388	-0.048	-0.297												
	16420.7*	0.997	-0.008	0.017	0.241	-0.233		19709.8	0.639	-0.328	0.381	-0.351	0.067												
	16277.2*	0.005	0.999	-0.191	-0.186	-0.202		19670.5*	0.091	0.930	0.029	0.311	0.235												
$\frac{1}{2}^-$	16660.5	0.045		-0.619		0.224	0.105	19756.5	0.328		0.619		-0.156	-0.028											
	16622.3	-0.109		-0.142		-0.556	0.334	19740.9	0.712		0.006		0.525	-0.015											
	16418.9*	0.993		0.069		0.107	0.315	19695.4	0.621		0.027		-0.210	-0.551											

H. Appendix H

TABLE L. The eigenvectors of the $ccbn\bar{c}$, $ccbn\bar{b}$, and $ccbs\bar{c}$ pentaquark subsystems. The masses are all in units of MeV.

J^P	Mass	$ccb \otimes n\bar{c}$				$ccn \otimes b\bar{c}$				$cbn \otimes c\bar{c}$					
		$\Omega_{ccb}^* D^*$	$\Omega_{ccb}^* D$	$\Omega_{ccb}^* D^*$	$\Omega_{ccb} D$	$\Xi_{cc}^* B_c^*$	$\Xi_{cc}^* B_c$	$\Xi_{cc}^* B_c^*$	$\Xi_{cc} B_c$	$\Xi_{cb}^* J/\psi$	$\Xi_{cb}^* \eta_c$	$\Xi_{cb}^* J/\psi$	$\Xi_{cb}^* \eta_c$	$\Xi_{cb}^* J/\psi$	$\Xi_{cb}^* \eta_c$
$\frac{5}{2}^-$	10071.7	-0.549				-0.605				0.577					
	10012.4	-0.836				-0.796				0.020					
$\frac{3}{2}^-$	10075.7	-0.663	-0.180	0.009		-0.244	-0.281	-0.534		0.070	0.026	-0.593		-0.597	
	10057.6	-0.238	0.045	0.637		0.676	0.199	-0.469		-0.392	-0.013	0.258		0.004	
	10045.0	0.222	0.122	-0.474		0.126	0.266	-0.235		-0.330	0.211	-0.169		0.242	
	10008.1	-0.482	0.076	-0.419		0.509	-0.027	0.568		0.042	0.432	-0.131		0.153	
	9981.0	-0.287	-0.210	-0.402		-0.032	0.139	0.291		0.530	-0.028	-0.066		0.301	
	9955.0	0.337	-0.014	-0.177		-0.137	0.858	-0.067		0.098	0.354	-0.034		0.311	
	9874.0*	-0.162	0.949	-0.025		-0.434	0.231	0.166		-0.385	0.242	0.055		0.002	
$\frac{1}{2}^-$	10117.7	0.056	0.323	-0.681		0.083	0.409	-0.574		-0.455		0.415	0.163	0.010	0.015
	10079.7	-0.094		-0.605	-0.331	-0.015	0.047	0.316		-0.418		-0.216	-0.129	0.018	-0.017
	10049.8	-0.062		-0.400	-0.130	-0.149		-0.692	-0.379	0.209		0.352	-0.354	-0.037	0.021
	9988.2	-0.169		0.456	-0.156	-0.081		0.384	-0.500	-0.272		-0.086	-0.124	0.374	-0.429
	9979.2	0.075		0.049	0.458	-0.264		0.107	0.279	-0.017		-0.486	-0.388	0.220	0.297
	9966.3	-0.216		-0.257	0.273	0.296		-0.147	-0.189	-0.335		0.130	-0.482	-0.290	-0.151
	9926.3	0.343		0.249	0.313	0.705		0.227	0.219	0.109		0.301	-0.242	0.320	0.286
	9830.7	-0.887		0.180	0.047	-0.557		0.346	0.123	-0.032		-0.121	0.287	0.200	-0.196
J^P	Mass	$ccb \otimes n\bar{b}$				$ccn \otimes b\bar{b}$				$cbn \otimes c\bar{b}$					
		$\Omega_{ccb}^* B^*$	$\Omega_{ccb}^* B$	$\Omega_{ccb}^* B^*$	$\Omega_{ccb} B$	$\Xi_{cc}^* \Upsilon$	$\Xi_{cc}^* \eta_b$	$\Xi_{cc} \Upsilon$	$\Xi_{cc} \eta_b$	$\Xi_{cb}^* B_c^*$	$\Xi_{cb}^* B_c$	$\Xi_{cb}^* B_c^*$	$\Xi_{cb}^* B_c$	$\Xi_{cb}^* B_c^*$	$\Xi_{cb}^* B_c$
$\frac{5}{2}^-$	13371.6*	0.940				-0.009				0.474					
	13156.4*	0.342				-0.999				-0.329					
$\frac{3}{2}^-$	13370.9*	0.071	0.122	-0.945		-0.565	0.038	0.025		0.485	-0.280	0.005		-0.117	
	13354.8	0.261	0.585	0.108		-0.782	-0.053	-0.002		0.210	0.044	-0.523		-0.158	
	13335.8	0.213	0.541	0.092		0.074	-0.007	-0.018		0.513	-0.139	-0.229		-0.255	
	13281.7	-0.138	-0.464	-0.034		-0.247	0.061	0.024		0.109	-0.455	0.322		0.192	
	13156.1*	-0.604	0.217	0.031		-0.020	0.009	-0.999		-0.298	-0.229	-0.042		-0.518	
	13093.2*	0.487	-0.189	-0.177		-0.006	0.995	0.007		-0.225	-0.205	-0.171		-0.389	
	13092.8	-0.510	0.230	-0.232		0.050	0.033	0.003		0.120	0.125	-0.107		0.255	
$\frac{1}{2}^-$	13391.6	0.119		0.109	-0.437	0.006		-0.719	0.306	-0.173		0.643	0.196	-0.177	0.012
	13351.8	0.226		0.141	0.240	-0.007		-0.606	-0.091	-0.167		-0.006	0.487	0.090	-0.219
	13325.8	0.614		0.320	-0.104	0.042		0.079	-0.609	-0.334		-0.352	0.368	0.088	0.038
	13276.1	0.417		0.117	0.715	-0.014		0.305	0.611	-0.091		-0.070	-0.348	0.249	0.442
	13269.4	0.463		0.173	-0.470	0.103		0.088	0.356	-0.091		0.184	-0.107	-0.433	0.200
	13151.7	-0.308		0.752	0.044	-0.001		0.073	-0.141	-0.530		0.179	-0.333	0.162	-0.293
	13091.1	-0.136		0.245	-0.062	0.000		0.062	0.087	-0.398		-0.248	-0.231	-0.211	-0.215
	13029.1*	0.237		-0.444	-0.059	-0.994		0.008	0.005	0.005		-0.198	-0.017	-0.221	0.012
J^P	Mass	$ccb \otimes s\bar{c}$				$ccs \otimes b\bar{c}$				$cbs \otimes c\bar{c}$					
		$\Omega_{ccb}^* D_s^*$	$\Omega_{ccb}^* D_s$	$\Omega_{ccb}^* D_s^*$	$\Omega_{ccb} D_s$	$\Omega_{cc}^* B_c^*$	$\Omega_{cc}^* B_c$	$\Omega_{cc}^* B_c^*$	$\Omega_{cc} B_c$	$\Omega_{cb}^* J/\psi$	$\Omega_{cb}^* \eta_c$	$\Omega_{cb}^* J/\psi$	$\Omega_{cb}^* \eta_c$	$\Omega_{cb}^* J/\psi$	$\Omega_{cb}^* \eta_c$
$\frac{5}{2}^-$	10163.7	-0.504				-0.646				0.575					
	10123.7	-0.864				-0.763				0.050					
$\frac{3}{2}^-$	10173.0	0.717	0.136	-0.243		-0.036	-0.232	-0.675		-0.111	0.022	-0.482		-0.572	
	10155.5	0.010	-0.106	-0.619		-0.722	-0.268	0.283		-0.412	-0.018	0.432		0.183	
	10137.2	0.124	0.106	-0.524		0.078	0.292	-0.305		0.358	-0.238	0.149		-0.254	
	10108.0	0.396	-0.121	0.354		0.508	-0.082	0.557		-0.129	-0.361	0.142		-0.110	
	10083.9	-0.390	-0.205	-0.379		-0.077	0.121	0.202		0.473	-0.053	-0.074		0.282	
	10059.6	-0.387	0.100	0.117		-0.117	0.861	0.006		-0.124	-0.382	0.057		-0.327	
	9975.2*	-0.109	0.945	-0.025		0.440	-0.166	-0.143		-0.377	0.283	0.053		0.036	
$\frac{1}{2}^-$	10213.9	0.045		0.329	-0.671	-0.070		-0.440	0.546	-0.438		0.453	0.149	0.006	0.014
	10181.6	-0.075		-0.614	-0.320	-0.013		0.037	0.307	-0.435		-0.205	-0.165	0.021	-0.020
	10143.6	-0.030		-0.345	-0.169	-0.100		-0.673	-0.417	0.225		0.359	-0.390	-0.050	0.020
	10090.7	-0.193		0.439	-0.202	0.109		-0.399	0.478	-0.262		-0.113	-0.169	0.387	-0.394
	10080.9	-0.031		0.171	0.338	-0.168		0.001	0.236	-0.110		-0.406	-0.493	0.068	0.251
	10063.1	-0.260		-0.281	0.370	0.433		-0.100	-0.255	0.302		-0.281	0.322	0.308	0.228
	10019.0	0.311		0.266	0.353	0.680		0.257	0.254	0.137		0.245	-0.220	0.348	0.317
	9933.4	0.888		-0.154	-0.046	-0.543		0.342	0.138	-0.042		-0.125	0.289	0.207	-0.212

TABLE LI. The eigenvectors of the $ccbs\bar{b}$, $bbcn\bar{c}$ and $bbcn\bar{b}$ pentaquark subsystems. The masses are all in units of MeV.

J^P	Mass	$ccb \otimes sb$				$ccs \otimes b\bar{b}$				$cbs \otimes cb$					
		$\Omega_{ccb}^* B_s^*$	$\Omega_{ccb}^* B_s$	$\Omega_{ccb}^* B_s^*$	$\Omega_{ccb} B_s$	$\Omega_{cc}^* \Upsilon$	$\Omega_{cc}^* \eta_b$	$\Omega_{cc} \Upsilon$	$\Omega_{cc} \eta_b$	$\Omega_{cb}^* B_c^*$	$\Omega_{cb}^* B_c$	$\Omega'_{cb} B_c^*$	$\Omega'_{cb} B_c$	$\Omega_{cb} B_c^*$	$\Omega_{cb} B_c$
$\frac{5}{2}^-$	13457.4*	0.947				0.011				0.468					
	13262.7*	0.322				-0.999				-0.339					
$\frac{3}{2}^-$	13460.1*	0.102	0.169	-0.933		-0.536	0.047	0.043		0.449	-0.278	0.053		-0.076	
	13441.4	0.241	0.549	0.152		0.794	0.047	0.002		0.224	0.058	-0.536		-0.171	
	13422.9	0.203	0.517	0.156		0.043	-0.002	-0.010		-0.545	0.137	0.241		0.260	
	13371.1	-0.155	-0.521	-0.026		-0.277	0.069	0.026		0.132	-0.446	0.285		0.184	
	13262.3*	-0.604	0.214	0.014		-0.029	0.014	-0.999		-0.285	-0.235	-0.041		-0.519	
	13199.5*	-0.497	0.179	0.169		0.005	0.994	0.010		0.217	0.212	0.173		0.389	
	13191.3	-0.504	0.232	-0.229		0.049	0.041	0.004		-0.114	-0.132	0.106		-0.261	
$\frac{1}{2}^-$	13483.3	0.098		0.096	-0.469	0.010		-0.694	0.319	-0.170		0.644	0.194	-0.163	0.023
	13440.2	0.241		0.153	0.253	0.001		-0.619	-0.015	-0.124		-0.006	0.465	0.118	-0.231
	13418.1	0.524		0.290	-0.100	-0.029		-0.015	0.671	0.362		0.323	-0.380	-0.057	-0.055
	13365.8	0.111		-0.005	0.832	-0.069		0.220	0.350	-0.046		-0.185	-0.267	0.436	0.281
	13361.6	0.690		0.249	-0.049	-0.082		-0.277	-0.542	0.095		-0.152	0.287	0.251	-0.375
	13257.9	-0.310		0.751	0.055	-0.001		0.068	-0.151	-0.526		0.187	-0.328	0.156	-0.299
	13189.3	-0.141		0.244	-0.067	-0.005		0.064	0.092	0.402		0.241	0.220	0.214	0.225
	13127.8*	0.230		-0.445	-0.061	-0.994		0.001	0.003	0.003		-0.197	-0.016	-0.223	0.009
J^P	Mass	$bbc \otimes n\bar{c}$				$bbn \otimes c\bar{c}$				$cbn \otimes b\bar{c}$					
		$\Omega_{bbc}^* D^*$	$\Omega_{bbc}^* D$	$\Omega_{bbc} D^*$	$\Omega_{bbc} D$	$\Xi_{bb}^* J/\psi$	$\Xi_{bb}^* \eta_c$	$\Xi_{bb} J/\psi$	$\Xi_{bb} \eta_c$	$\Xi_{cb}^* B_c^*$	$\Xi_{cb}^* B_c$	$\Xi'_{cb} B_c^*$	$\Xi'_{cb} B_c$	$\Xi_{cb} B_c^*$	$\Xi_{cb} B_c$
$\frac{5}{2}^-$	13285.7*	-0.320				0.999				0.340					
	13195.8*	-0.947				0.014				0.467					
$\frac{3}{2}^-$	13337.5	-0.155	-0.036	-0.047		-0.094	-0.102	-0.111		-0.162	-0.319	0.581		0.367	
	13287.3*	-0.717	0.161	-0.038		0.118	-0.002	0.967		0.243	0.266	0.054		0.450	
	13272.2	0.428	-0.039	0.395		0.217	0.003	-0.209		-0.292	-0.072	0.162		-0.302	
	13198.0	0.378	-0.002	-0.833		-0.366	0.605	-0.002		-0.524	0.124	-0.131		-0.083	
	13165.4	-0.125	-0.135	-0.304		-0.793	-0.458	0.067		-0.031	0.207	0.234		0.229	
	13161.4	0.326	-0.022	0.231		-0.106	0.604	0.015		-0.247	0.374	0.016		0.369	
	13054.9*	0.120	0.976	-0.019		-0.395	0.223	0.064		-0.449	0.203	0.183		0.025	
$\frac{1}{2}^-$	13369.3	-0.006		0.203	-0.811	-0.034		-0.103	0.826	-0.430		0.155	0.083	0.150	0.213
	13309.5	0.041		-0.345	-0.554	-0.059		0.019	-0.314	0.359		0.071	0.114	0.242	-0.013
	13291.8	-0.134		0.715	-0.051	0.020		0.335	0.340	0.132		-0.456	0.216	-0.189	0.212
	13262.3	-0.053		0.045	0.035	-0.016		0.040	-0.295	0.474		0.186	0.426	0.045	0.320
	13186.2	-0.025		0.487	0.076	-0.638		0.482	0.009	-0.020		-0.610	-0.041	0.272	0.008
	13157.2	-0.160		0.051	0.031	-0.141		-0.544	0.108	0.237		-0.053	-0.463	-0.094	0.374
	13148.5	0.184		0.281	0.159	-0.686		-0.479	-0.052	0.065		-0.111	-0.311	0.416	0.182
	13018.0*	0.958		0.086	-0.014	0.311		-0.343	-0.053	0.090		0.223	-0.385	-0.204	0.224
J^P	Mass	$bbc \otimes nb$				$bbn \otimes cb$				$cbn \otimes bb$					
		$\Omega_{bbc}^* B^*$	$\Omega_{bbc}^* B$	$\Omega_{bbc} B^*$	$\Omega_{bbc} B$	$\Xi_{bb}^* B_c^*$	$\Xi_{cc}^* B_c$	$\Xi_{cc} B_c^*$	$\Xi_{cc} B_c$	$\Xi_{cb}^* \Upsilon$	$\Xi_{cb}^* \eta_b$	$\Xi_{cb}' \Upsilon$	$\Xi_{cb}' \eta_b$	$\Xi_{cb} \Upsilon$	$\Xi_{cb} \eta_b$
$\frac{5}{2}^-$	16572.3	0.804				0.828				0.012					
	16427.3	-0.594				-0.560				0.577					
$\frac{3}{2}^-$	16569.6	-0.386	0.383	-0.648		-0.321	0.303	-0.459		0.125	-0.063	-0.030		-0.012	
	16567.0	-0.265	0.291	0.529		-0.161	0.150	0.749		0.676	0.023	-0.011		0.414	
	16519.5	0.441	-0.593	-0.224		-0.563	0.662	0.043		-0.293	0.031	0.007		-0.127	
	16432.5	-0.346	-0.255	-0.128		-0.335	-0.281	-0.143		-0.263	-0.133	0.653		0.486	
	16411.3	-0.295	-0.217	0.301		-0.259	-0.154	0.220		-0.175	0.180	-0.211		0.273	
	16374.5	-0.612	-0.551	-0.014		-0.168	-0.125	-0.385		-0.221	0.481	0.015		0.261	
	16369.2	-0.065	0.035	-0.378		-0.589	-0.574	0.098		-0.040	0.361	0.022		0.242	
$\frac{1}{2}^-$	16584.9	0.320		-0.435	0.064	0.290		-0.395	0.062	-0.276		0.665	-0.303	-0.004	-0.023
	16557.1	0.118		-0.133	-0.002	-0.096		0.110	0.054	0.440		0.366	0.611	-0.005	0.021
	16503.9	0.601		-0.554	0.016	0.633		-0.575	0.001	-0.095		-0.142	-0.046	0.104	-0.042
	16449.7	-0.151		-0.090	0.718	-0.128		0.094	0.743	-0.419		0.087	0.348	0.038	0.075
	16397.0	0.297		0.375	-0.347	-0.483		-0.528	-0.122	-0.213		0.001	0.127	-0.145	-0.101
	16392.5	-0.423		-0.388	-0.313	-0.040		-0.142	0.418	0.102		0.267	-0.154	0.021	-0.139
	16363.3	0.298		0.361	0.458	0.328		0.355	0.428	0.284		-0.048	-0.229	0.321	0.517
	16326.9	-0.379		-0.240	0.229	-0.384		-0.259	0.263	0.184		0.173	-0.167	-0.529	0.333

TABLE LII. The eigenvectors of the $bbcs\bar{c}$ and $bbcs\bar{b}$ pentaquark subsystems. The masses are all in units of MeV.

J^P	Mass	$bbc \otimes s\bar{c}$				$bbs \otimes c\bar{c}$				$cbs \otimes b\bar{c}$					
		$\Omega_{bbc}^* D_s^*$	$\Omega_{bbc}^* D_s$	$\Omega_{bbc}^* D_s^*$	$\Omega_{bbc} D_s$	$\Omega_{bb}^* J/\psi$	$\Omega_{bb}^* \eta_c$	$\Omega_{bb} J/\psi$	$\Omega_{bb} \eta_c$	$\Omega_{cb}^* B_c^*$	$\Omega_{cb}^* B_c$	$\Omega_{cb}^{'} B_c^*$	$\Omega_{cb}^{'} B_c$	$\Omega_{cb} B_c^*$	$\Omega_{cb} B_c$
$\frac{5}{2}^-$	13364.5*	-0.297				0.999				0.351					
	13303.1*	-0.955				0.037				0.458					
$\frac{3}{2}^-$	13429.7	-0.137	-0.036	-0.083		-0.107	-0.091	-0.090		0.189	0.316	-0.577		-0.357	
	13369.4	-0.830	0.142	-0.255		0.262	0.001	0.744		0.054	0.207	0.142		0.259	
	13361.3	0.025	0.045	0.338		-0.146	0.001	0.651		0.374	0.182	-0.107		0.488	
	13296.9	0.311	-0.002	-0.883		-0.415	0.401	0.020		0.549	-0.230	0.123		-0.011	
	13268.9	-0.121	0.1333	0.118		0.710	0.034	-0.089		-0.106	0.043	-0.178		0.021	
	13250.1	-0.418	-0.131	-0.141		0.283	0.862	-0.040		0.121	-0.395	-0.182		-0.438	
	13156.1*	0.076	0.970	-0.019		-0.377	0.295	0.069		-0.451	0.174	0.167		-0.009	
$\frac{1}{2}^-$	13460.0	0.001		-0.173	0.820	-0.036		-0.086	0.833	-0.414		0.138	0.097	0.151	0.222
	13394.7	0.020		-0.220	-0.544	-0.063		-0.041	-0.382	-0.333		-0.135	-0.054	-0.271	0.049
	13380.2	0.109		-0.739	-0.017	-0.003		-0.411	-0.216	-0.145		0.490	-0.191	0.122	-0.153
	13350.4	0.057		-0.120	-0.041	0.013		0.025	0.301	0.497		0.130	0.455	0.045	0.328
	13285.4	-0.028		0.486	-0.088	-0.542		0.477	0.004	0.016		0.605	0.127	-0.326	-0.037
	13260.6	0.114		-0.199	-0.054	0.089		-0.439	0.146	-0.259		0.037	0.500	0.031	-0.424
	13245.0	0.254		0.284	0.133	0.755		0.539	0.010	-0.003		-0.001	-0.207	0.390	0.078
	13119.2*	0.952		0.059	-0.016	-0.350		0.333	0.049	0.086		0.215	-0.379	-0.210	0.217
J^P	Mass	$bbc \otimes s\bar{b}$				$bbs \otimes c\bar{b}$				$cbs \otimes b\bar{b}$					
		$\Omega_{bbc}^* B_s^*$	$\Omega_{bbc}^* B_s$	$\Omega_{bbc}^* B_s^*$	$\Omega_{bbc} B_s$	$\Omega_{bb}^* B_c^*$	$\Omega_{bb}^* B_c$	$\Omega_{bb} B_c^*$	$\Omega_{bb} B_c$	$\Omega_{cb}^* \Upsilon$	$\Omega_{cb}^* \eta_b$	$\Omega_{cb}^{'} \Upsilon$	$\Omega_{cb}^{'} \eta_b$	$\Omega_{cb} \Upsilon$	$\Omega_{cb} \eta_b$
$\frac{5}{2}^-$	16651.6	0.831				0.801				0.015					
	16523.0	-0.556				-0.598				0.577					
$\frac{3}{2}^-$	16656.2	-0.294	0.265	-0.791		-0.363	0.305	-0.177		0.348	-0.050	-0.052		0.113	
	16645.9	-0.358	0.391	0.273		-0.021	0.014	0.846		-0.591	-0.038	0.005		-0.373	
	16600.6	-0.433	0.610	0.266		-0.605	0.636	0.071		-0.327	0.044	0.024		-0.122	
	16526.0	-0.301	-0.202	-0.147		-0.278	-0.283	-0.181		-0.260	-0.104	0.612		0.535	
	16509.2	-0.355	-0.270	0.283		-0.304	-0.211	0.202		-0.126	0.185	-0.307		0.193	
	16469.3	-0.618	-0.525	-0.062		-0.228	-0.201	-0.388		-0.217	0.527	0.013		0.305	
	16459.1	0.005	0.127	-0.351		-0.529	-0.581	0.154		-0.007	-0.296	-0.009		-0.204	
$\frac{1}{2}^-$	16668.6	0.280		-0.392	0.055	0.319		-0.437	0.046	0.211		-0.710	0.235	0.014	0.018
	16641.4	-0.134		0.155	-0.021	-0.041		0.042	0.068	0.464		0.279	0.639	-0.003	0.017
	16587.7	0.609		-0.584	0.044	-0.623		0.555	0.045	-0.136		-0.124	-0.069	0.108	-0.031
	16543.0	-0.163		-0.061	0.699	-0.081		-0.097	0.742	0.424		-0.102	-0.363	-0.028	-0.067
	16495.2	-0.384		-0.434	0.319	-0.481		-0.545	-0.016	-0.178		0.050	0.077	-0.147	-0.126
	16480.9	-0.378		-0.309	-0.364	0.074		-0.047	0.425	0.140		0.267	-0.165	0.031	-0.116
	16462.5	0.282		0.364	0.474	-0.351		-0.358	-0.418	0.280		-0.044	-0.217	0.338	0.504
	16417.2	-0.370		-0.246	0.216	-0.377		-0.251	0.292	0.193		0.159	-0.165	-0.517	0.356